Romanian Journal of
MINERAL DEPOSITS

continuation of

DARI DE SEAMA ALE SEDINTELOR INSTITUTULUI DE GEOLOGIE SI GEOFIZICA
COMPTES RENDUS DES SÉANCES DE L'INSTITUT DE GÉOLOGIE ET GÉOPHYSIQUE
(2. Zacaminte)

Founded 1910 by the Geological Institute of Romania

ISSN 1220-5648

VOL. 87
No. 1

CONTENT

Gheorghe C. POPESCU, Antonela NEACȘU
The odyssey of minerals resources *vs.* necessities, possibilities and requirements **1**

Sorin Silviu UDUBAȘA, Gheorghe UDUBAȘA
Keeping alive the mining tradition/heritage: the museum mines and geoparks in Romania **7**

Mircea GEORGESCU
The sustainable development in mining **11**

Gheorghe ILINCA
Contact metamorphism and mineralization related to Late Cretaceous magmatism in Romania **15**

A. Feyzi BİNGÖL, Mesut ANIL, Melahat BEYARSLAN
Chromite deposits in Turkey **21**

Nicolae ANASTASIU, Mihai BRÂNZILĂ
Slate formations with gas potential in the Eastern Carpathians **25**

Sorin TAMAS-BADESCU, Gabriela TAMAS-BADESCU
A GIS mineral potential modeling in the Skellefte District (Sweden) **31**

Sylejman HYSENI, Bedri. DURMISHAJ, Ahmet BYTYQI
Cost benefit analysis in vermince limestone deposit Republic of Kosovo **37**

Grigore BUIA, Csaba LORINȚ, Monica RĂDULESCU
Considerations about economic outlook of Jiu Valley hard coal deposit, Romania **41**

Ion BERBELEAC, Sorin Silviu UDUBAȘA, Elena-Luisa IATAN, Mădălina VIȘAN
Geological and structural constraints on the localization of Neogene porphyry– epithermal related
Cu-Au (Mo), and epigenetic hydrothermal deposits/prospects from South Apuseni, Mts., Romania **47**

- continued on the back cover -

Geological Institute of Romania
Society of Economic Geology of Romania

Bucureşti – 2014

DIRECTORS

Dr. Marcel Mărunțiu, General Director of the Geological Institute of Romania

Prof. Dr. Gheorghe Damian, President of the Society of Economic Geology of Romania

Editor in Chief: Sorin Silviu Udubaşa (University of Bucharest).

Editorial Secretary: Monica Macovei (University of Bucharest)

Editorial board

Gheorghe Udubaşa, Romanian Academy; University of Bucharest
Gheorghe Popescu, University of Bucharest,
Essaid Bilal, Ecole des Mines, Saint Etienne, France
Georgios Christofides, Aristotle University of Thessaloniki, Greece
Peter Andráš, Geological Institute of the Slovak Academy of Science
Radu Jude, University of Bucharest
Gheorghe Damian, Technical Univ. Cluj-Napoca – North Center Baia Mare,
Floarea Damian, Technical Univ. Cluj-Napoca – North Center Baia Mare
Grigore Buia, University of Petrosani
Marian Lupulescu, New York State Museum, USA
János Földessy, Miskolc University, Hungary
Ovidiu Gabriel Iancu, "Alexandru Ioan Cuza" University, Iaşi
Anne-Sylvie Andre-Mayer, Université de Lorraine, Nancy, France
Ferenc Molnar, Geological Survey of Finland
M.S. Pandian, Pondicherry University, India
Vasilios Melfos, Aristotle University of Thessaloniki, Greece
Gheorghe Ilinca, University of Bucharest
Mihai Marinescu, University of Bucharest
Marcel Mărunţiu, Geological Institute of Romania, Bucharest
Ioan Pintea, Geological Institute of Romania
Mircea Ţicleanu, Geological Institute of Romania, Bucharest
Nicolae Buzgar, "Alexandru Ioan Cuza" University, Iaşi
Marian Munteanu, Geological Institute of Romania
Ioan Seghedi, Institute of Geodynamics of the Romanian Academy, Bucharest
Dan Stumbea, "Alexandru Ioan Cuza" University, Iaşi
Sorin Silviu Udubaşa, University of Bucharest
Antonela Neacsu, University of Bucharest
Călin Tămaş, Babeş-Bolyai University, Cluj-Napoca
George Tudor, Geological Institute of Romania, Bucharest

Rom . J. Mineral Deposits is also the Bulletin of the Society of Economic Geology of Romania

The authors are responsible for the ideas presented in the papers.

ISSN 1220-5648

Geological Institute of Romania
Society of Economic Geology of Romania

Romanian Journal of MINERAL DEPOSITS

ISSN 1220-5648

VOL. 87 / 2014
No. 1

Volume dedicated to *Univ. Prof. Dr. Gheorghe C. Popescu*
(Honorary President of SGER)
on the occasion of his 75th Anniversary

CONTENT

Gheorghe C. POPESCU, Antonela NEACŞU
The odyssey of minerals resources *vs.* necessities, possibilities and requirements ……...…..... **1**

Sorin Silviu UDUBAŞA, Gheorghe UDUBAŞA
Keeping alive the mining tradition/heritage: the museum mines and geoparks in Romania …….. **7**

Mircea GEORGESCU
The sustainable development in mining …….…..... **11**

Gheorghe ILINCA
Contact metamorphism and mineralization related to Late Cretaceous magmatism in Romania …... **15**

A. Feyzi BİNGÖL, Mesut ANIL, Melahat BEYARSLAN
Chromite deposits in Turkey …….……..... **21**

Nicolae ANASTASIU, Mihai BRÂNZILĂ
Slate formations with gas potential in the Eastern Carpathians …….. **25**

Sorin TAMAS-BADESCU, Gabriela TAMAS-BADESCU
A GIS mineral potential modeling in the Skellefte District (Sweden) ……...……..... **31**

Sylejman HYSENI, Bedri. DURMISHAJ, Ahmet BYTYQI
Cost benefit analysis in vermince limestone deposit Republic of Kosovo ……..... **37**

Grigore BUIA, Csaba LORINŢ, Monica RĂDULESCU
Considerations about economic outlook of Jiu Valley hard coal deposit, Romania **41**

Ion BERBELEAC, Sorin Silviu UDUBAŞA, Elena-Luisa IATAN, Mădălina VIŞAN
Geological and structural constraints on the localization of Neogene porphyry– epithermal related Cu-Au (Mo), and epigenetic hydrothermal deposits/prospects from South Apuseni Mts., Romania ……. **47**

Paulina HÎRTOPANU, Robert J. FAIRHURST
Mineralogy of the Grădiştea de Munte rare element minerals occurrence, Sebeş Mts., South Carpathians, Romania. Part I: oxides and carbonates …….. **53**

Paulina HÎRTOPANU, Robert J. FAIRHURST
Mineralogy of the Grădiştea de Munte rare element minerals occurrence, Sebeş Mts., South Carpathians, Romania. Part II: phosphates and silicates ……..…. **57**

Ingrid TURISOVÁ, Tomáš ŠTRBA, Peter ANDRÁŠ, Štefan ASCHENBRENNER
Floristic composition on the abandoned copper heaps in Central Slovakia ……. **61**

Giuseppe BUCCHERI, Peter ANDRÁŠ, Maria Luisa ASTOLFI, Silvia CANEPARI, Mara CIUCCI, Alessandra MARINO
Heavy metal contamination in water at Libiola abandoned copper mine, Italy ……...……. **65**

Paulina HÎRTOPANU, Sorin Silviu UDUBAŞA
Detailed mineralogy of blastfurnace slag samples from Galați metalurgical plant, Romania …….. **71**

Teodor VELEA, Andreea MITU, Andreea GRĂDINARU, Georgiana MOISE, Luminiţa MARA, Cornel FRAȚILĂ, Mihai GHIȚĂ, Valentin DRĂGUȚ
Research on methods of treating mine water generated from exploitation of Roşia Poieni, Romania . **75**

Ioan PINTEA
Magmatic and hydrothermal features of the fluid and melt inclusions from the quartz xenoliths, fragments and phenocrysts from Săpânţa Valley (Igniş Mountains, Romania) ……. **79**

Igor V. CHERNYSHEV, Vladimir A. KOVALENKER, Andrei CHUGAEV, Gheorghe DAMIAN, Floarea DAMIAN, Luisa Elena IATAN, Ioan SEGHEDI
New high-precision lead isotope analyses of galena from Romanian ore districts and a review …... **83**

Olga Yu. PLOTINSKAYA, Gheorghe DAMIAN, Floarea DAMIAN
Sphalerite assemblages and composition in the Baia Mare region, Eastern Carpathians, Romania (preliminary data) ……. **87**

Ioan SEGHEDI, Zoltan PÉCSKAY, Paraschiva ONESCU
Petrography, geochemistry and geochronology of selected samples from two Banatite intrusions near Gladna Montană, Poiana Ruscă Mountains, Romania ……...……... **91**

Călin G. TĂMAŞ, Béatrice CAUUET, Jean MILOT
Mineralogy of precious metals ore from Les Fouilloux Gaul mine, Limousin (France) from metals traceability perspective ……... **95**

Réka DÉNES, István MÁRTON, Gabriella B. KISS, Paul IVĂŞCANU, Zsolt VERESS
Additional data regarding the petrography and geochemistry of the magmatic phases and hydrothermal vein types from Bolcana porphyry Cu-Au mineralization (Apuseni Mts., Romania) .. **99**

Laura TUŞA, Călin G. TĂMAŞ, Paul IVĂŞCANU, Zsolt KULCSAR, Laurenţiu IGNA
The Teascu epithermal gold deposit (Metaliferi Mountains): first data on the alteration and mineralization ……... **105**

Alexandru LĂZĂREAN, Paul IVĂŞCANU, Horia POPESCU, Călin TĂMAŞ
Preliminary mineralogical and petrographical investigations on Muncelul Mic deposit, Poiana Ruscă Mountains, Romania ……. **109**

Rom. J. Mineral Deposits, vol. 87 (2014), No. 1, p. 1-6

THE ODYSSEY OF MINERALS RESOURCES *VS.* NECESSITIES, POSSIBILITIES AND REQUIREMENTS

Gheorghe C.POPESCU*, Antonela NEACŞU**

Dept of Mineralogy, Faculty of Geology and Geophysics, University of Bucharest, 1, N. Bălcescu Blvd., 010041 Bucharest,
**ghpop@geo.edu.ro, **antonela.neacsu@gmail.com*

Abstract. Mineral resources have been the basis of the progress of human civilization. The relationship between man and mineral resources has developed under auspices of the interaction between the needs, possibilities and requirements. At first, man used stone, most likely for defense and hunting, thus acting alone. Then, by appreciating other benefits of rarer materials, humans began to use metals such as gold, copper, tin, iron, *etc*. Owing to the genetic association between copper and tin in several metallogenic districts – e.g. Erzgebirge or Cornwall, the primitive man has probably accidentally „produced" *bronze* – a copper and tin alloy which marked an entire epoch of the human history. In fact, owing to the poor quality of pure iron which was soft and oxidable, the new metal was also an alloy of iron and carbon, most probably obtained accidentally through contamination with charcoal. The iron ore naturally contains other metals. For example, the laterites formed on ultramafic rocks, contain small quantities of Cr and Ni, whereas laterites formed on siderites, contain Mn. Thus, man has used chemical elements long before he actually knew them. Until the beginning of the 19th century the self-taught prospectors and encyclopaedists have managed to met the requirements for new mineral resources to supply the metal craftsmanship. In the beginning the search for ores conformed the expression **„ore deposits are found where they exist"**; empirical research followed, involving a step by step search of the deposits, according to the *centrifugal* principle **„ore deposits are found near other ore deposits"**. But, the classical saying „**if you want to fiind ore deposits, go for the mountains"** has emerged. This kind of thinking had a guiding role in the discovery of ore deposits and has been fundamenting for a long time the exploration activities. Ever since its foundation at the beginning of the 20th century, several crises occurred in the Economic Geology. One of the crises was triggered by the Club of Rome Report in 1972, which stated the intense consumption of metal by emerging industries *vs.* the limited amount of ore deposits in the Earth's crust. With the advent of the global tectonics concept, at the beginning of the 70's, exploration works were spectacularly stimulated. The new discoveries have grown the reserves to such an extent that in 2003 the dead line envisaged by the Club of Rome Report was considerably delayed. The last crisis faced by the mineral resource industry was of ecological nature. The negative impact over the environment may be directly related both to the actual mining and to supporting activities which ensure the mining logistics. In the present days, a special attention must be given to this issue by the geologists, miners, processing engineers, economists and more recently, by the ecologists. Based on their expertise, and by virtue of the constitutional provisions stating that the mineral resources belong to the state, the governmental factors have to decide on the viability of the exploration projects.

Keywords: mineral resources, possibilities and requirements, metals in the human society, stones, bronze, alloy of iron, philosophy of mineral resource, crises of modern Economic Geology.

Introduction.

Ever since the dawn of mankind, mineral resources have been the basis of the progress of human civilization. These were the first materials used by the primitive man to obtain food through hunting and agriculture. At the same time such mineral resources often satisfied aesthetic needs (colors for drawing and painting, ornaments, *etc.*).

The relationship between man and mineral resources has developed under auspices of the interaction between the needs, possibilities and requirements. These factors have acted in a historical succession: necessity, imposed by the feeding and protection requirements of the primitive man, followed by the possibilities of obtaining resources and ultimately, by the modern demands and limits according to which society had to take into account the natural framework (Fig. 1).

Raising requirements have imposed an extension of the interaction between humans and minerals. At first, man used stone, most likely for defense and hunting, thus acting alone. Then, by appreciating

other benefits of rarer materials, humans began to use metals such as gold, copper (tin, *etc*.) iron, which, certainly, required a collective will and action for discovering, mining and processing.

In this context, man has certainly noticed the minerals with aesthetic features, which he used as adornments and in magic; later, the useful properties of such minerals were understood and man's life witnessed a significant improvement. Besides, the name "mineral" comes from *minera* = ore, which underlines that ever since the beginning, man has regarded minerals from an utilitarian point of view.

The most of the tools and weapons used by prehistoric man were manufactured from broken and later chiseled flint. This signified the exercise of a choice, the knowledge of properties yielded by certain stones, from the many occurring on Earth's surface. After „testing" other stones such as granite, quartzite, hard limestone etc., the prehistoric man noticed the advantages of flint and started to look for it, that is they *surveyed* and exercised for the first time *economic geology*. The extraction of flint followed by means digging galleries and pits, thus putting the man in the posture of „mining". These activities developed over a long period, until approximately 2500 B.C. Later, metals began to be used on a current basis. The primitive „geologists" and miners – embodied by the same persons have surveyed and extracted ores wherefrom copper was firstly obtained, followed by bronze and eventually by iron.

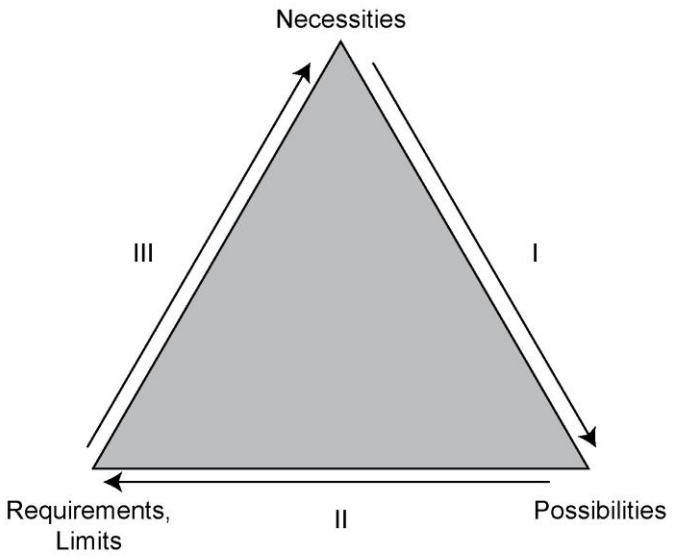

Fig. 1. Diagram of interactions between necessities, possibilities and requirements in the process of usage of mineral resources. I – the primary stage when necessities determined the usage of unprocessed or slightly modified raw materials; II – the secondary stage when resources were processed without inflicting a bad influence over the environment; III – the tertiary stage when resource processing and consumption tend to overcome the supportability of nature. For this reason, the resource consumption needs to be rationalized.

Metals in the human society.

The first metal observed and used by man – mainly due to its native color, was gold. Owing to its remarkable malleability and ductility, gold was easy to distinguish from hard and brittle stones. Gold could easily be processed and shaped, turned into thin toils and wires, which helped in developing a specific processing technique long before its extraction from ores. Its unique properties conferred gold a value which surpassed the simple status of a raw material and has often been assigned with mystical properties, qualifying it as a symbol of wealth and power; however, gold has not left its sign over an entire epoch of the human history as other metals (copper-bronze, iron, aluminum) did.

In native and unoxidized form, copper was equally shinning as gold, but harder and more abundant and has been intensely used for manufacturing tools and weapons. For this reason, copper was heavily extracted especially from the oxidation zones of superficial ore deposits, which drew attention by their vivid colors. The extraction of copper was made possible only by the use of fire. Owing to the genetic association between copper and tin in several metallogenic districts – e.g. Erzgebirge or Cornwall, the primitive man has probably accidentally „produced" *bronze* – a copper and tin alloy (Popescu, 2002, Laznicka, 2006) which marked an entire epoch of the human history.

The manufacturing of tools from metals or alloys represented an obvious technical progress. Such tools were more durable than those created of stone. Metal weapons also proved to be more efficient both in hunting and war. On the other hand, metals were rare and difficult to get, hence very expensive; as a matter of fact, the word „metal" derives from Greek and means „to search", suggesting what it took to obtain such materials. For this reason, metals were often used to manufacture luxury objects. Thus, for a long time, farmers and craftsmen have continued to use stone tools and objects. Eventually, bronze has won due to its low melting point which allowed casting and processing and to its oxidation resistance. Bronze was most durable than stone and began to be used for large scale production of tools and weapons. Even before 3000 B.C. the metal production raised to several tons of Cu (Sn) per year and several kilograms of Au per year. A special situation occurred on the present day territory of Romania where tin was absent. Thus, tin was „imported" from Erzgebirge area (Macovei, 2011, Macovei & Popescu, 2011). Little by little, bronze has replaced stone, and the Bronze Age took the place of the Stone Age.

In the early times, iron was as rare as copper, or even rarer, due to the difficulties raised by its extraction. Iron was obtained through ore melting in clay furnaces with air bellows. In fact, owing to the poor quality of pure iron which was soft and oxidable, the new metal was also an alloy of iron and carbon, most probably obtained accidentally through contamination with charcoal. In time, man has learned how to obtain cast iron and steel and a new occupation of blacksmithing has emerged.

The iron ore naturally contains other metals. For example, the laterites formed on ultramafic rocks, contain small quantities of Cr and Ni, whereas laterites formed on siderites, contain Mn. Thus, man has used chemical elements long before he actually knew them. Moreover, manganese was discovered in 1774, whereas nickel and chromium in 1751 and 1797, respectively. The conscious use of such elements for obtaining special sorts of steel, occurred several decades later: manganese in 1839, chrome in 1850 and nickel in 1880. Besides, starting with 1751 and until the end of the 19th century, 49 new elements were added to the Mendeleev Table, while during the 20th century only two new elements were added: hafnium in 1922 and rhenium in 1925 ((Laznicka, 2006). In this context, aluminum – which was discovered in 1808 by Davy, was only used in 1880 when the industrial demand for this metal raised considerably, qualifying it as the second industrial metal after iron. Uranium is another example of a large time interval between its discovery and industrial use. Uranium was discovered in 1789 by Klaproth, but it began to be used only after 1890, when its radioactivity was firstly observed and allowed its usage in energetics and weaponry.

The present metal demands refer mainly to the major industrial elements – iron, aluminum, copper and gold – which recorded a production of over 10 billion USD/year, followed by zinc, nickel, lead, PGE, silver, manganese, cobalt, magnesium, tin, uranium and molybdenum, with a production of over 1 billion USD/year. Finally, some metals which became of strategic importance in the last ten years, especially for the top industries such as IT, aeronautics and defense: lithium, beryllium, REE, niobium, tantalum, germanium, cadmium, gallium, tellurium, rubidium, yttrium, hafnium. Their annual output ranges from several millions USD/year to zero in some countries (Laznicka, 2006).

A present feature of the industrial metal production is that more than 95% of them are mined in giant ore deposits. A clinching example is that of gold, with over 30% of the production is owned by five

global mining corporations (Barrick, Newmont, Anglo Gold, Placer Dome and Kinross Gold). In the last decades, mining facilities have grown to huge proportions and focused especially on open pit mining.

The philosophy of mineral resource.

Until the beginning of the 19th century the self-taught prospectors and encyclopaedists have managed to met the requirements for new mineral resources to supply the metal craftsmanship. However, during the industrial revolution, the empirical approach of ore deposit surveying could no longer meet the demands.

In the beginning the search for ores conformed the expression **„ore deposits are found where they exist"**; empirical research followed, involving a step by step search of the deposits, according to the *centrifugal* principle **„ore deposits are found near other ore deposits"**. The mineral, rock and fossils collector could not possibly support this kind of research. One could at most get marveled by the odd objects the Earth produced. On the other hand, the miner was so preoccupied by ores and by the signs of its presence or by its association with certain rocks, that he could not have an explanation of ore's genesis and history, the less so of Earth's structure and past evolution.

A.v. Humboldt was the first scientist who presented observation data on the link between igneous rocks and metallic concentrations. Such observations were later explained by Elie de Beaumont in his theory regarding the volcanic and metallic emanations. In fact, his theory materialized two principles which govern the modern metallogeny: **the actualism-uniformitarianism principle** (*as long as metals occur in the modern volcanic terrains, especially in the form of sulfides, the old time ore deposits must have formed in the same way*) and **the similarity principle** *(the rocks and ores have formed through the same geological processes*).

Such considerations were consistent with the distribution of metallic deposits, most often found in volcanic rocks. From this, the classical saying „**if you want to fiind ore deposits, go for the mountains"** has emerged. This kind of thinking had a guiding role in the discovery of ore deposits and has been fundamenting for a long time the exploration activities.

In our country, in Metaliferi Mts., the gold ore deposits have become more numerous over the time, owing to the discovery of new ore veins near the known ones, or of new ore deposits near the already mined ones. An example is that of Roșia Montană where this kind of discoveries have maintained one of the longest mining activities known in Europe. Moreover, during the 70's, the porphyry copper deposit of Roșia Poieni was uncovered in the vicinity of the gold ore deposits. This is just an example of the many "pairs" of Au-Cu deposits in Metaliferi Mts.: Roșia Montană – Roșia Poieni, Bucium – Tarnița, Musariu Vechi – Musariu Nou, Troița – Bolcana *etc.* In the Baia Mare district, the eastern extension of the main vein of Baia Sprie, outlines the gold ore deposit of Șuior.

The crises of modern Economic Geology.

Ever since its foundation at the beginning of the 20th century (Skinner, 2005), several crises occurred in the Economic Geology (Popescu, 1981; Neacșu, Popescu, 2009).

One of the crises was triggered by the Club of Rome Report in 1972, which stated the intense consumption of metal by emerging industries *vs.* the limited amount of ore deposits in the Earth's crust. The report has alerted the governments and suggested an imminent crisis of metallic and energetic raw materials. The solution from the geological point of view came quickly stating that there exist a direct correlation between crustal abundance of the elements and the reserves (McKelvey, 1973). For example, in 1973 the gold reserves were estimated at 0.002 metric tons, with 0.0086 metric tons of potential resources (Erickson, 1973). The resource/reserve ratio was therefore of 4.3 which equaled the odds of

discovering new ore deposits. For the entire Earth's crust (minus USA), the reserves amounted 0.0011 metric tons and the resources, 0.15 metric tons, thus yielding a resource/reserve ratio (i.e. ore deposits discovery odds) of 14 (table 1). **Thus, the lower the geological knowledge, the greater the chance of discovering new ore deposits.** With the advent of the global tectonics concept, at the beginning of the 70's, exploration works were spectacularly stimulated. The new discoveries have grown the reserves to such an extent that in 2003 the dead line envisaged by the Club of Rome Report was considerably delayed. For example, the degree of coverage for Ni was extended to 131 years, for Zn, to 53 years, for Cu, to 48 years and for Au, to 32 years (Schode, 2003 in Popescu et al., 2007).

Table 1. *Resources/reserves ratio for some elements (Popescu, 1974)*

Elements	USA crust	Eart's crust
Pb	1	10
Mo	1	23
Cu	1,6	10
Ag	3,2	18
Au	4,1	14
Zn	6,3	42
Sb	11	5
Hg	15	30
U	20	11
Th	31	22
W	37	4
Ni	830	3
Sn	Very high	12

The last crisis faced by the mineral resource industry was of ecological nature. The exploration and mining activities have a major impact over the environment. In the absence of appropriate prevention methods, the mining activity could damage severely the natural environment, especially by modifying the relief, by affecting the quality of underground waters, the wilde life habitats, by degrading the soils, *etc.* The negative impact over the environment may be directly related both to the actual mining and to supporting activities which ensure the mining logistics.

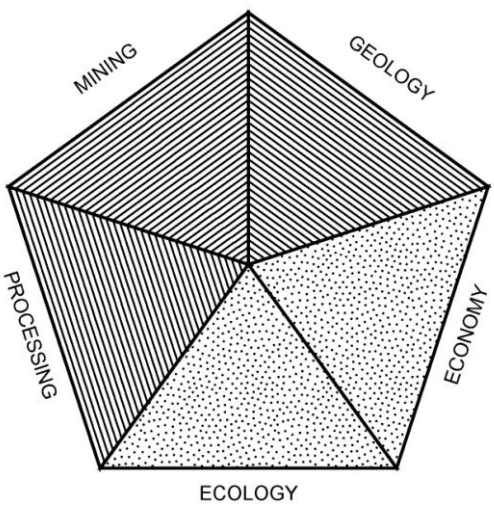

Fig. 2. Diagram of the specific activities involved in the extraction of mineral resources

The mineral *resources* represent *geological entities* formed as a result of geological processes. **"The issue of how and where ore deposits can be found, may only be solved on the basis of geological principles and by exercising geological sagacity"(Brobst & Pratt, 1973**). However, in the present days, a special attention must be given to this issue by the geologists, miners, processing engineers, economists and more recently, by the ecologists (Fig.2, and see fig. 1). Based on their expertise, and by virtue of the constitutional provisions stating that the mineral resources belong to the state, the governmental factors have to decide on the viability of the exploration projects

References

Brobst, D. A. & Pratt W. P., 1973. Introduction in United States Mineral Resources US Geol. Survey, Prof. Paper, 820

Erickson, R. L., 1973. Crustal abundance of elements and mineral reserves and resources in United States Mineral Resources US Geol. Surv. Prof. Paper, 820

Laznicka, P. 2006. Giant Metallic Deposits, Future Sources of Industrial Metals, Springer-Verlag Berlin, Heidelberg, Germany, 732 p

McKelvey, V. E. 1973. Mineral resource estimates an public policy in US Mineral Resources & US Geol. Survey Prof. Paper, 820

Neacșu, A., Popescu, Gh., C., 2009. Metalogenie aplicată şi prognoză geologică, Ediţie revizuită și adăugită, Editura Universităţii Bucureşti, 2009 , 210 p

Macovei, M., 2011. Cercetări mineralogice, fizico-chimice şi geochimice comparative asupra „bronzurilor" din siturile arheologice Arad, Şpălnaca (Jud. Alba), Drajna (Jud. Prahova) şi a minereurilor din ariile potenţiale sursă, PhD Thesis, University of Bucharest, 125 p.

Macovei, M., Popescu, Gh. C., 2011. Metallographic and chemical data and possible sources of ore on two bronze age metal ingots from Şpălnaca Co. Alba, (RO) and Arad, Co.(RO), Mining Historical Science and Heritage Landscape, Research Methodology, Valuation and Positioning of ancient Mining Relics, Valkenburg a/d Geul, Netherlands, p. 31-37.

Popescu, Gh., C., 1974. Potenţialul metalogenetic al crustei terestre , Bul. Geol. al MMPG, 14-23

Popescu, Gh., C., 1981. Metalogenie aplicată şi prognoză geologică, Tip. Univ. Bucureşti, 136 p

Popescu, Gh., C., 2003. Geology and mining relationship, Societatea de Geologie Economică a României, 1 SEGR Series, Ed. Focus, Petroșani, 47 p

Popescu, Gh., C., Tămaş-Bădescu, S., Bogatu, L., Tămaş-Bădescu, G., Neacşu, A., 2007. Geologia economică a aurului, Ed. Aeternitas, Alba Iulia, 536 p.

Skinner, B., J., 2005. Introduction: A Century of Excellence. Economic Geology 100th Anniversary Volume, p. 1-4.

Rom. J. Mineral Deposits, vol. 87 (2014), No. 1, p. 7-10

KEEPING ALIVE THE MINING TRADITION/HERITAGE: THE MUSEUM MINES AND GEOPARKS IN ROMANIA

Sorin Silviu UDUBAȘA*, Gheorghe UDUBAȘA**

University of Bucharest, Faculty of Geology and Geophysics, 1, N. Bălcescu Blv., 010041, Bucharest, Romania; *sorin.udubasa@gmail.com; **udubasa@geo.edu.ro

Abstract: After cessation of the mining activity many remnants are occurring such as waste dumps, galleries and many mining machineries and tools. Parts of them could be used to create mining museums or museum mines as a touristic successors of the minig activity as well as an attempt to keep alive the mining tradition. Several hundreds of mines have existed in Romania until 1998 when a political decision has been taken to close all the mines, except some coal and uranium ones. It is not too late to transform some of the mines into museum mines (either underground or open pit) as shown already some years ago by one of the authors. The investment for creating museum mines by using the abandoned galleries or open pits could be relatively easy to recover by a smart touristic management. Examples from Germany, Austria, Slovakia, Switzerland or even from Australia and South Africa should be taken into consideration. Such museum mines could contribute to keep alive the mining tradition and to create conditions for better environment conservation, as well as for sustainable development of local communities.

Key words: museum mines, selection criteria, geoparks, type localities

Introduction

The geological heritage as a part of the georesources (Christmann, 2008) should probably include also its most "perishable" part, i.e. the mining heritage. In many countries, Romania included, the mining industry was an important component of the industrial progress until last years. Whatever the reason for the uneven development of mining industry in Romania would be, its role in the development of the country cannot be ruled out. The fact is that the mining industry left a lot of "objects" which should be taken into consideration as geological/mining heritage. It is the mines which should be first considered, then several quarries and even outcrops.

The number of mines in Romania is of several thousands. Of course only a limited number of mines could be selected to become part of a mining heritage. Several criteria are to be fulfilled:

a) the geographic accessibility of the mine;
b) the conservation grade of the places organised to be visited (anyhow they should be over the hydrostatic level)
c) the attractiveness of the ores, which should bear well developed mineral crystals and/or rare minerals. If the mines involved represent also type localities of different minerals this is the ideal situation.
d) the existence of mining machineries and tools as supplementary points of attractiveness.

The mining industry (MI) in general and especially in Romania is clearly in decline. "The perception that the MI is conservative, traditional and resistant to change was true in the past but the today's realities suggest that the MI may partly overcome the general decline by using better technologies" (Bartos, 2008). In addition, the conservation of some mines may supplement the chance of saving the mining tradition.

The Museum mines

The museum mines in Romania as previously suggested (Udubasa, 2003) could become a reality. There are numerous examples of such mines in Europe, either traditional (agate mines in the Pfalz, Germany) or relatively recently settled up, such as Rammelsberg in Germany, some gold mines in the Austrian Alps (e.g. Schellgaden), Lengenbach in Switzerland etc. Rammelsberg was until the year of 2000 the biggest copper mine in Germany but it was decided to transform it in a big museum, exhibiting not only parts of the ore bodies but also old mining machineries. By using smart methods of advertisement the Rammelsberg museum mine is now a well-known point of tourist attraction.

Such museum mines exist also in other parts of the world, such as Kalgoorlie in Australia or Kimberley in South Africa, to mention only a few. The Big Hole (1 km deep) at Kimberley is now half filled with water and around it a very impressive museum has been developed, including of course an exhibition of diamonds recovered by De Beers. A very interesting point to be underlined is also the

following. Several tables have been crudely installed, on which fragments of kimberlites (diamond-bearing rocks) are exposed. There are many visitors wishing to check their luck to eventually find a diamond or at least a small fragment of it.

In Romania also there are several places (Fig. 1) where some mines can easily be transformed into museums (of course part of them, fulfilling the above mentioned criteria). The Baia Mare mining district could provide the greatest number of potential museum mines (Table 1), i.e. Herja, Baia Sprie, Cavnic, Dealul Crucii, Nistru, Băiţa, Săsar, etc. In the Apuseni Mts. there are also some examples: Băiţa Bihor, Săcărâmb, Roşia Poieni, Roşia Montană, Baia de Arieş, to mention only few.

The Herja mine is by far the most modern, with a huge potential of exhibiting parts of the veins with beautiful minerals such as black sphalerite, quartz, calcite, siderite etc.; the Baia Sprie mine (the upper horizons) with thick veins rich in sphalerite, galena, quartz, calcite. By chance visitors could find small pieces with stibnite, "plumosite", barite etc. Baia Sprie is also the type locality of some minerals such as felsöbanyaite, dietrichite, semseyite, andorite etc. However, how big should be the luck to find such rare to very rare minerals is difficult to answer. But the possibility exists (the hope is the last to die)! The Cavnic mine is another potential museum mine: beautiful rhodochrosite (first described here in 1716) samples, as a rule decorated with sulfides, have been found within all the veins existing here; barite with various colors, calcite, sphalerite etc. Supplementary arguments for a Baia Mare Geopark have been presented by Bud et al. (2006), Iştvan and Minghiraş (2004), Fülöp and Kovacs (2006) and Kovacs and Fülöp (2009).

Other candidates for becoming museum mines exist also in the Apuseni Mts., i.e. the Săcărâmb mine (type locality of many tellurides), the Băiţa Bihor mines (type locality of several Bi-sulfosalts), this last one still partly active (Table 1). Some ore deposits mined in open pits may also provide attraction due to the uncommon rich mineral assemblages such as the Răzoare Mn-Fe deposits in the Preluca Mts. Easy

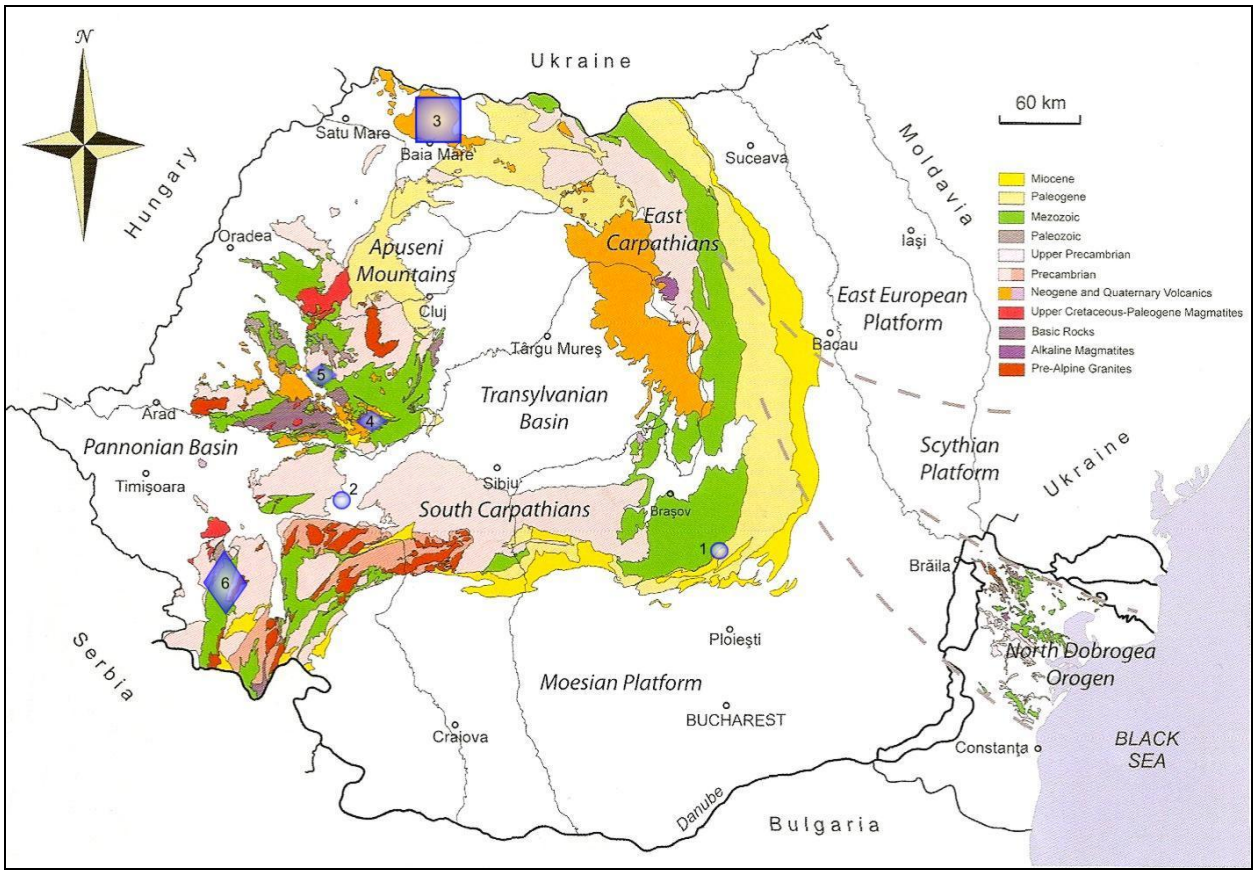

Figure 1. Localization of existing geoparks and possible museum mines in Romania (geological map from Ilinca, 2010, modified after the geological map compiled by the Geological Insitute of Romania).
Already established Geoparks: 1. Buzău, and 2. Haţeg;
3. Baia Mare Geological and Mining Park as proposed by Kovacs and Fülöp (2009);
Possible geological and mining parks: 4. Metaliferi Mountains Geopark, 5. North Apuseni Geopark, and 6. Banat Geopark.

Table 1. Type localities of minerals or outstanding mineral associations (in brackets) of the above-mentioned mines (after Udubasa, 2002, with completions).

Type locality	**Minerals or mineral associations**
Baia Sprie	andorite, dietrichite, felsöbanyaite, klebelsbergite, semseyite, szmikite;
Băiţa Bihor	kotoite (co-type locality), makovickyite, paderaite, szaibélyite, *graţianite* (recently discovered by Brugger et al., 2013);
Cavnic	rhodochrosite, rhodonite (?), whewellite (?);
Herja	fizelyite;
Răzoare	[rare minerals: nearly all the members of the manganese humite group, manganoan fayalite, pyroxmangite, jacobsite, Mn-ferrosilite, etc.]
Săcărâmb	alabandite, krautite, krennerite, museumite, muthmanite, nagyagite, petzite, stützite.
Roşia Montană	*alburnite* (recently discovered by Tămaş et al., 2013);
Baia de Arieş	sylvanite

accessible, this place has the advantage to provide good samples of relatively big dimensions, which can be brought near the main road in a kind of a free air museum for people not wishing or not having the physical strength to climb up the quarry (near 1 km far away from the road). In addition, some minerals from the nearby situated pegmatite bodies (feldspar, limpid quartz crystals, blue-green apatite crystals) may represent supplementary attractions for the potential visitors.

Shops with small mineral pieces, photographs and booklets on the history and mineral development of individual mines are commonplace in all the museum mines one of the authors had visited worldwide. We are sure that mining tourism could represent a successful investment in the near future in Romania and in keeping alive the mining tradition/heritage. The already existing salt mines acting as museums offer an excellent example: Slănic Prahova, Praid, Ocnele Mari, Turda, Slănic Moldova, Ocna Şugatag, etc. even if in some places mining is still active.

The dream of museum mines could therefore become a reality if the local authorities are wishing to make minimal investments and to organize provoking and appropriate advertising. The Museum of Mineralogy in Baia Mare, the Gold Museum in Brad and other places of public interest are or could become important attractors for development of such a mining tourism. Otherwise the rich mining tradition in Romania will be very soon completely lost.

The Geoparks

Establishing Geoparks, as shown by Kovacs & Fülöp (2009), represents a development alternative for the communities in the former mining centres. In addition to the Baia Mare Geological and Mining Park proposed by Kovacs & Fülöp (2009), similar parks could be imagined in the Apuseni Mts., where not only old mines (potential museum mines) do exist but also many other localities with either natural issues (e.g. Detunata basalt columns, some 20 m in height, many caves or picturesque geological landscapes), or existing museums (e.g. Roşia Montană – old and new museums; Gold Museum in Brad, Roman Stairways – Ruda Valley, etc).

In the Baia Mare Geopark museum mines could be located in the former mines of Herja, Baia Sprie, Cavnic, Dealul Crucii etc.

In the North Apuseni Geopark the possible museum mines could be at Băița Bihor, Valea Leucii (zeolites) and the open pit at Moneasa (red marbles), as well as several caves.

The Metaliferi Mts. Geopark could contain museum mines at Săcărâmb, Roșia Montană, Brad/Gurabarza, etc. as well as the important museums at Brad – Gold Museum, and Roșia Montană – Roman Galleries and Cătălina Monulescu gallery. Also in the Brad zone, another point of interest could be revitalised – the Roman Stairways (Ruda Valley), or private collections could be included in the circuit of visited museums, as the Calcedony Museum of Doru Toda in Crișcior.

In Banat area, the Geopark could include museum mines as Ocna de Fier, Dognecea, Sasca Montană, Oravița etc., those being among the first kind of skarn-related ore deposits in history, described in 1864 by Bernhard von Cotta. Another important point of interest is the ”Gruescu Museum” of minerals in Ocna de Fier.

These mentioned zones could take the example of already established geoparks (Fig. 1) as for example the Buzău County Geopark, with the well-known Mud Volcanoes from Pâclele and Amber Museum in Colți, as well as the Hațeg Country Geopark, world-wide known for its "dwarf dinosaurs" from the end of Cretaceous, 72-65 million years ago.

Conclusions

The solutions to overcome the social shortcomings produced by cessation of the minig related activities are quite difficult and vary from place to place; they are very difficult in areas with mining as sole activity (as in the Jiu Valley) and less difficult in areas with much more other possibilities to work. Alternative to cessation of the mining activity may be surely related to utilization of mine "remnants" to create museum either inside or outside the mines. The touristic value of such museum mines may be enhanced by combination with possibilities to use local capabilities to attract the potential tourists: special geologic issues, archaeological sites (if exist), manufactured objects, etc. all of them could represent a sound basis for creating also Geoparks and at the same time to facilitate investments for the future. Developing in the future the mining in the old production sites implies re-opening of some old mines, a fact enabling museum mines to be easier established. The two activities are in no way of exclusion but merely of reciprocal help. The lesson of the salt mines (with simultaneous extraction activity and museum activity) should be followed up by other mines too, which presumably will be active in the future.

References:

Bartos P.J., 2008. How does the mining industry rate? A look at innovation and productivity advance. SEG Newsletter, 75 (October Issue), 1, p. 8-12.

Brugger J., Ciobanu C.L., Mills S.J., Cook N.J., Damian G., Damian F., Elliott P., 2013. Grațianite, $MnBi_2S_4$, IMA 2013-076. CNMNC Newsletter No. 18, December 2013, page 3252; Mineralogical Magazine, 77, 3249-3258.

Bud I., Duma S, Iştvan D., Jurje M., Kacso C., Pop L., Pop S., 2006. Study on the potential regarding the mining industrial heritage of Maramureş county and its opportunities to be valued for touristic purposes. Maramureş County Council Archives, Baia Mare, 158 p. (in Romanian).

Christmann P., 2008. What's the point of geologists? Research*eu - The Magazine of European Research Area, Special issue, September 2008, p. 7-8.

Fülöp A. and Kovacs M., 2006. Geoturisn in Gutâi Mountains, Eastern Carpathians. Environment & Progress, 6, 187-192 (in Romanian).

Iştvan D. and Minghiraş T., 2004. Middle Age gallery from Dealul Crucii. Pro Unione, VII (1-2), 127-129 (in Romanian).

Kovacs M. and Fülöp A., 2009. Baia Mare Geological and Minig Park – a potential new Geopark in the northwestern part of Romania. Studia Universitatis Babes-Bolyai, Geologia, 54 (1), 27-32.

Tămaş C.G., Grobety B., Bailly L., Bernhardt H.-J., Minuţ A., 2013. Alburnite, $Ag_8GeTe_2S_4$, a new mineral species from the Roşia Montana Au-Ag epithermal deposit, Apuseni Mountains, Romania. American Mineralogist, Vol. 99, p. 57–64.

Udubasa G., 2002. Mineralogical regions – Romania. In: Minerals of the Carpathians, Szakall S. (Ed.). Granit Publ. House, Prague, p. 52-84.

Udubasa G., 2003. Museum mines in Romania: a dream? (abs.) The 5th Symposium of Baia Mare branch of the Geological Society of Romania, 6-7 Nov. 2003, Baia Mare. Anuarul Institutului Geologic al Romaniei, 73, Special issue, p. 6.

Rom. J. Mineral Deposits, vol. 87 (2014), No. 1, p. 11-14

THE SUSTAINABLE DEVELOPMENT IN MINING

Mircea GEORGESCU*

University of Petrosani, 20, Universitatii str., 332006, Petrosani, Romania
**mirgeorgescu@gmail.com*, Tel.0722514766

Abstract: Issues related to sustainable development of natural resources are becoming increasingly accepted as secondary targets through mining. This is due to differences between the local population and environmentalists, on the one hand, and the interests of the shareholders of mining companies, on the other hand. Therefore policies on sustainable development in mining must know, in the near future, significant changes to create the necessary balance between economic, social and environmental.

Keywords: sustainable development, mining zones, SWOT analysis, mining policies

1.Introduction

Nothing could be more controversial than ever circulated a concept that anyway by anyone, which is taken orally almost empirically, without paying attention to the meaning and content, using and when and when not. It is, of course, the concept of sustainable development.

The concept of sustainable development was originally introduced as a micro economic concept in forestry meaning a strategy aimed at providing the world continuously without wiping the forest. Since the mid-1980s, however it has been accepted and in others (Moore, J., 1996).

At the 1992 United Nation Conference on Environment and Development (UNCED) in Rio de Janeiro more than 300 pages of recommendation for sustainable development were collected and published as Agenda 21(UN,1993).

The objective of sustainable development is fundamentally grounded in ethics. The welfare of future generation is a basic ethical concern, and such welfare embodies both human and environmental values. The most agreed upon and oft-quoted definition is derived from Brundtland report "Development that meets the needs of the present without compromising the ability of the future generations to meet their own needs".

2. Sustainability as a Working Concept

The fundamental concerns that must be on the table in any discussion of sustainable development are human welfare, the environment, and the future. The ultimate goal must be to maintain both the productivity of nature and the environment, as well as material gains in their utility. Given today's economic structure, the goal is distant. Neither in the area of energy utilization nor in the consumption of nonrenewable resources, it is imaginable that we continue with today's production techniques and rates of utilization over the long term. But today it is possible, and would be sensible for developing ways and strategies of coursing closer to the common good. The pertinent working definition today is like the following.

Sustainability is achieved when the capital of material resources is preserved to the extent that to quality of life available for future generation will not be inferior to the quality of life of the present generation.

On the basis of the above, are proposed (Renn, O., Goble,R, 1998) the following five principles using the themes as pointers towards sustainability:

(a) Acknowledgement of absolute limits with respect to the carrying capacity of the earth

Although utilization rates of the carrying capacity for human purposes depends on the nature and productivity of an economy, the world's resources are limited and critical loads have already been reached in many parts of the world. Future economic activity must use natural resources more efficiently. That requires growth in the stock of artificial capital as the only way of keeping welfare of a country at least constant. As said earlier, the growth in the stock of artificial would mean safer, efficient, multi-modal, less resource incentive machines and production processes.

(b) Acknowledgement of the limits of substitution between natural and artificial capital

In traditional economic theory, the monetary value of any goods determines the rate at which it can be discharged for the goods. The production and consumption of such goods incurs high external costs that infinite compensation of those damaged would be needed to make the transaction economically efficient.

For this reason, the natural cycles necessary for mankind's survival must be identified and appropriately protected by political measures.

(c) Focus on the resilience of anthropogenic ecosystems

Renewable resources would appear to be utilizable for the long term, since they regenerate themselves. Their regeneration capacity lasts, however, only as long as they remain invulnerable to changes in their natural and anthropogenic environments. Monoculture or ecosystems intensified so as to produce a maximum yield may have high vulnerability to natural or human caused stresses. A sustainable economy must assess the resilience of economic activity and incorporate resilient strategies into its decision-making framework on the basis of common welfare and equity.

(d) Incorporation of social values in man's relationship to the environment and nature

In addition to the ecological and economic consequences associated with human use of the environment, society link social and cultural values to nature and its inhabitants. Typical examples are the protection of animals and plants and beyond their economic utility and the aesthetic pleasure derived from preserving bio-diversity (even far from one's region). Any concept of sustainability needs to acknowledge the intrinsic value and benefits provided by nature and must design polices that are in line with the prevailing social preferences for environmental change — an important aspect of reform environmentalism.

(e) Aversion of risk from ignorance and shock

Many truths about the nature of interactions between environment, economy and society are yet unknown. Also in an open market economy where the richest and the poorest, and regional and local economies would participate in the sustainability goals cannot be uniform. Applying similar environment management principles will not be effective in all situations. There is also a possibility of social and economic damage arising from low margins of resilience to external shocks like market upheavals and political collapse energy indefinitely. However, there is much room for improvement over business as usual and these improvements are the most accessible present day opportunity for approaching sustainability.

3. Sustainable Development in Mining

From the perspective of sustainable development of mining communities, the fundamental element consists of natural capital, made from natural and aesthetic resources, and potential services that can be offered to support ecosystem structure.

Therefore a mono-industrial mining area , as most mining areas in Romania , is a special case when analyzed in terms of sustainable development and mining community in the area should support the extent that efficiently use natural resources they extract .

Fortunately, the solution "mining" among other sustainable solutions must be found. The conclusion should be that for many years from now, will be sustainable mining in Romania.

Analysis between concept and reality of economic sustainability is an important step that should combine theoretical considerations on sustainable development with a detailed analysis of the social reality of the economic and environmental analysis, which is, in fact, the three objectives of sustainable development.

Ways of achieving this goal can be by constructive policies based on existing links positive by interrupting negative links and removing obstacles.

In order to ensure consistency of the reconstruction of the area and to develop its business plan, should be pretty thorough analysis of the main sectors covered in this area: the primary sector of agriculture mountainous secondary sector mining industry, energy, manufacturing (wood, textiles), buildings and tertiary sector whit tourism and trade.

Starting from the concept of economic rehabilitation and knowing very well the current situation in the area, define priorities, objectives and actions to be taken to achieve this goal.

As much importance should be given to environmental issues in the area, recommending actions that contribute to sustainability and the environment.

To see the future of the need to conduct a SWOT analysis of this complex, establishing the more discerning strengths, weaknesses, opportunities and threats related activities in the area.

The concepts of sustainable minerals development are at the nascent stage. In fact, it has just made a humble beginning(Georgescu M. et al.,2009).

The Department of Environment, UK (1994) charted the aims of its sustainable minerals strategy as the following:

- to conserve minerals as far as possible, whilst ensuring an adequate supply to meet the needs of the society for minerals.
- to minimize production of wastes and to encourage efficient use of minerals, including appropriate

use of high quality materials, and recycling of wastes.

- to encourage sensitive working practices during minerals extraction and to preserve or enhance the overall quality of environment once extraction has ceased.
- to protect designated areas of critical landscape or nature conservation quality from the development, other than in exceptional circumstances where it has been demonstrated that development is in the public interest.

This strategy is however not exactly in keeping with the principles of sustainability. For example, the phrase "... ensuring an adequate supply of to meet the needs of the society for minerals" does not stop at saying that the minerals will not use or their use will be reduced over a time frame. The use will be carried on as long as the supply is available from sources other than those in the country. It also presupposes that sufficient minerals are available in the market and so, it is necessary not to produce but to consume. The phrase in the fourth point "... other than in exceptional circumstances where ... public interest" is also not very straight forward; it reads like a compromise because it does not include "within the regenerative capacity of the nature" after the word "development"—leaving room for such scopes in the future. An important implication of strong sustainability is that demands for a range of good and services must be tempered if meeting them would breach environmental capacities. There is a potential conflict with policies based on the premise that projected demands constitute legitimate needs, the satisfaction of which is "essential" in some social or economic sense. As long as choices of national mineral development can be deferred by locating developments offshore where there is willingness, compulsion or supposedly sufficient environmental capacity that has to be deferred from a mature economy. An example of such rationale as a marketable concept is the much publicized "pollution trading". The combination of structural and spatial measures judged to be effective and politically acceptable any one time links the intra-generational distribution of activities (what goes where now) and the inter-generational distribution of resources. So in minerals planning the importance of changing practices of mineral extraction and restoration in determining the acceptability of minerals development, whether it breaches capacity constraints or denies future generations of critical natural material, cannot be undermined.

Four case studies made by Cragg and McAllister (Cragg, A.W., 1998) on Canadian mining projects suggested that mining industry faces certain negative public perception.

The usual view of resource use companies, including mining companies, is that their development proposals and their approach are self-serving and oriented to profit maximization. What follows from the view is that concern of the extraction companies for other stakeholders and for the environment is inevitably minimal. This kind of perspective is reinforced in the public mind by pictures of abandoned mine sites, unsightly tailing ponds and slagheaps.

For most of the mining and minerals companies, the cost means total financial cost. The usual strategy is "least cost planning". Wherever the cost could be externalized it would be either passed onto the government or quietly dismissed. The local communities carried the externalized costs. The result has been a legacy of grievances and mistrust.

The plan to open a mine even supported with the works of the government was to be greeted with deep skepticism. What lay behind the conflict was the belief that economic and the environmental objectives being advocated were incompatible.

In the transition of economies towards post-industrial modern technological era the intelligentsia and talented young people distanced themselves from the industry.

On the basis of the above public perception and experience, articulating a clear and defensible vision of values that lie at the heart of resource extraction projects is crucial to building public confidence in mining industry. Commitment to the principles of sustainable development has an important role to play in building the basis for communication, reducing conflict, and building public confidence and trust.

Like most of the streams of production and manufacturing the sustainable mineral planning process would have to evolve. Needless to say in almost all mineral producing countries of the world, the government action points to the withdrawal and termination of mining work instead of helping the industry to chart its ways toward a sustainability path. The other production and manufacturing industries, on the other hand are being supported by arrays of regulations which are uniformly changing each industry segment. This support is non-existent in the minerals industry because of the inherent lack of public support for the industry as well as the governments of the developed economies who no longer believe minerals of strategic importance in terms of supply side security.

However, if the minerals industry has to take a sustainability course, the following strategies will work as the initial framework:

(a) Ethics,
(b) Maintenance and growth of natural capital,
(c) Regarding environmental capacity,
(d) Market behaviour,
(e) Technological options,
(f) Uniform extraction standards,
(g) Alliance with government, NGO and indigenous peoples.

Assessing the impacts of a mineral development on the characteristics of the local and indigenous groups bring out several important factors:

- Social and cultural impacts are largely irreversible and the largest changes take place in the traditional value systems.
- Conflicts arise because the process of change is rapid but the capacity to change is slow. Greatest conflicts arise between the tribalists and the develop mentalists.
- Wherever compensation is given, lack of knowledge and cultural inadequacies prevent local and indigenous people to accrue sustainable benefits from the capital.

  Central to achieving effective and sustainable benefits for the affected people is the requirement that the traditional government — industry alliance of the past becomes a government- industry-indigenous people-NGO alliance of the future.

(h) Sustaining Mining and Minerals Business — As we observed that qualitative growth does not confront the scheme of development there are certain requirements of change for the long-term sustenance of the minerals industry to make it a more flexible business proposition than what it is today (Bhattacharya, J., 2000).

4. Conclusions

Applying the concept of sustainable development in mining, especially in mining areas, where activities are, generally, monoindustrials is difficult because deposits are non-renewable resources and therefore, sooner or later, they will run out.

Therefore, these areas should be a profitable mining, allowing further development, or parallel, to other activities.

Not is a solution for today's conservation of natural resources for creation of wealth for future generations.

Natural sustainability in the mining projects will be synonymous with the overall growth and sustenance of mining business. International acceptance of such development is urgently necessary. Application of sustainability principles in the mining business will depend much on the uniform business practices and standards.

Sustainability is an evolutionary process. Global mining industry at best is at the beginning of it by adopting broad environmental principles of pollution control. It needs to get into an overdrive on pollution prevention and conservation, not merely pollution control that is soon going to be passé in other industries.

References

Bhattacharya, J., 2000. Sustainable development of natural resources implications for mining of minerals. Mineral Resources Engineering, vol.9, no.4 , pg.451-464, Imperial College Press, London.

Cragg, A.W., 1998. Sustainable development and mining: Opportunity or threat to industry, CIM Bull, September, pg.45-50.

Georgescu M., Dunca E., Ciolea D.I.,2009. The peculiarities of sustainable development in mining activity.Proc.3rd International Seminar ECOMINING, Milos Island,Greece, pg. 37-43.

Moore, J., 1996.The death of competition, New York, Harper Business.

Renn, O., Goble,R.and Kastenholz., 1998.How to apply the concept of sustainability to a region, Technological Forecasting and Social Change 58, pg.63-81.

Wils, A., 1998. Finding technologies for sustainable natural resource use, Proc.5th Biennial Meeting Int.Soc.Ecological Economics, Santiago Chile.

Rom. J. Mineral Deposits, vol. 87 (2014), No. 1, p. 15-20

CONTACT METAMORPHISM AND MINERALIZATION RELATED TO LATE CRETACEOUS MAGMATISM IN ROMANIA

Gheorghe ILINCA*

University of Bucharest, Department of Mineralogy, Bd. N. Balcescu, 1, RO-010041, Bucharest),
* *ilinca@gg.unibuc.ro*

Abstract: The paper overviews contact phenomena and mineralization related to the Banatitic Magmatic and Metallogenic Belt (BMMB, Berza et al. 1998) which represents a series of discontinuous magmatic and metallogenic occurrences of Late Cretaceous age, discordant over mid-Cretaceous nappe structures (Cioflica and Vlad, 1973; Ciobanu et al., 2002.) The subvolcanic/plutonic rocks belonging to the BMMB are known under the collective name of "banatites" and have been recognized since the 19th century, when von Cotta (1864) was the first to describe a series of cogenetic magmatic rocks occurring as either shallow intrusions or subvolcanic bodies, older than Jurassic and mid-Cretaceous sedimentary formations. Banatites are overviewed with regard to their extension, geodynamic setting, petrology and age. Contact metamorphic rocks of either isochemical or metasomatic nature and related mineralization are described. A general depositional scheme of metallic mineral phases in the skarn deposits is given, suggesting a single mineralizing fluid rather than random polyscendant waves of mineralization.

Key words: Banatites, skarns, hornfels, skarn deposit, mineralization

The BMMB has drawn considerable interest in petrology, age, structural-tectonic significance and in the contained skarn, porphyry-copper and hydrothermal ore deposits, with a vast amount of literature published to date. Owing to the space constraints, only selected citations were therefore included in this abstract.

Regional extension and geodynamic setting of the BMMB. The strictly lineamental part of BMMB is exposed over approximately 900 km in length and around 30 to 70 km in width. The belt has a north-east to south-west trend over Apuseni Mts. and Southern Carpathians, it aligns to a north-south direction over eastern Serbia (Timok and Ridanji-Krepoljin zones), and bends widely to the east, through the Srednogorie area, reaching the shores of the Black Sea (Figure 1). However, various other occurences of Late Cretaceous igneous rocks have been identified recently outside this lineament, adding more than 200 km to the north-western end of the BMMB.

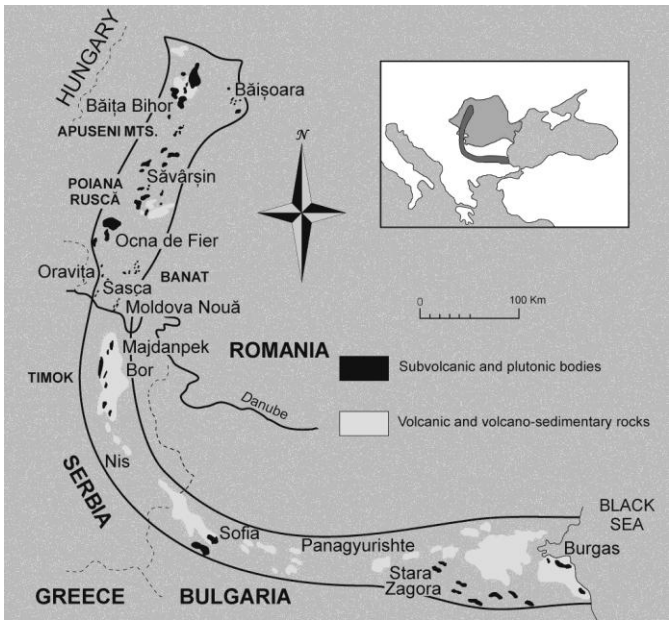

Fig. 1. The extension of the Banatitic Magmatic and Metallogenic Belt over Romania, Eastern Serbia and Bulgaria (with dark gray in the inset and with heavy outline in the map). Simplified after Cioflica and Vlad (1973).

Numerous models have been published in the last decades to explain the formation and the geodynamic significance of the BMMB. *Subduction models* have used the two major ocean sutures within the Carpathian-Balkan orogen: the Vardar Ocean with its Mureş Zone (and Transylvanian?) extension,

and the Severin Ocean with remnants preserved in Măgura, Ceahlău, Severin and Trojan nappes. Both the dominant calc-alkaline geochemical trend of the igneous rocks and the metallogenic features of the associated ore deposits were extensively used in support of the Cretaceous subduction models. However, major disagreement exists among these models, especially in what concerns the direction and timing of subduction.

Comprehensive overviews of such subduction related models are given by Berza et al. (1998), Ciobanu et al. (2002) and Zimmermann et al. (2008) and will be summarized during the presentation.

Authors such as Popov et al. (2000), Berza et al. (1998) and Neubauer (2002) have considered that the banatitic magmas where generated in an *extensional regime* caused by orogenic collapse affecting the upper crust. Mantle delamination due to slab break-off in the Late Cretaceous has followed the Jurassic and Lower Cretaceous northwards directed Vardar-Axios Ocean subduction.

Slab-rollback models postulate that in the Late Cretaceous, the subducting Vardar oceanic slab began to roll back and steepened, thus leading to extension in the upper crustal block and favoring the access of melts to high crustal levels, ultimately leading to volcanism. The slab-tear model (Neubauer, 2002; Neubauer et al., 2003) predicts that in a post-subduction, post-collisional regime, the subducting slab breaks from its continental counterpart and initiates asthenospheric upwelling into the slab window created as the tectonic units separate.

Based on the paleomagnetic data from the Carpathian and Pannonian areas, Panaiotu et al. (2005) suggested a two-step rotation model, to explain the up to 90° declinations measured on banatites in the Apuseni Mountains and in the Southern Carpathians. The Late Cretaceous paleoaltitude calculated for banatites by Panaiotu et al. (2005) is 24°N ± 4°. At the time of their emplacement, the banatites of the BMMB had an east-west spatial trend, and continued to the east with the alignments of the Western and Eastern Pontides (Figure 2).

Petrology and geochronological summary of the banatites. The BMMB is characterized by an extreme petrographic diversity, and many of the individual outcropping massifs encompass a significant part of this variety.

Effusive banatites encompass a wide range of compositions from rhyolites (Vlădeasa), to alkali basalts (Poiana Ruscă Mountains), but medium and high-K andesites and dacites prevail in all volcanic complexes of the Romanian portion of the BMMB. Intrusive banatites range from gabbros to leucogranites, but the most widespread are (quartz) diorites, granodiorites and (quartz) monzodiorites (Berza et al., 1998).

A compilation of radiometric dating for banatites was published by Ciobanu et al. (2002), pointing to a maximum of K-Ar age frequencies in the 65-95 Ma interval (Turonian–Maastrichtian) – a time span confirmed by later Ar-Ar, U-Pb and Re-Os dating.

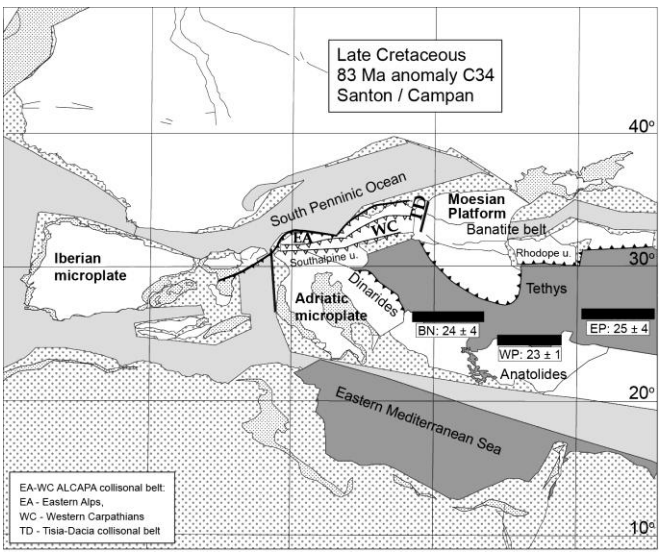

Fig 2. The position of banatites (BN), western Pontides (WP) and eastern Pontides (EP) on the basis of paleomagnetic data, compared with the paleogeographic reconstructions of Neubauer et al. (2003); (after Panaiotu et al., 2005).

Re-Os ages published by Zimmerman et al. (2008) for 50 banatite (molybdenite bearing) samples, from throughout the BMMB (Romania, Serbia, Bulgaria), indicate a time interval of 72.2-92.4 Ma. The Re-Os ages measured on molybdenite bearing samples by Zimmermann et al. (2008) for various segments of the BMMB, distribute as follows: Apuseni Mountains (Băița Bihor): 78.7-80.6 Ma; Poiana Ruscă (Calova, Valea Căprişoara, Tincova): 72.2-76.6 Ma; Banat (Ocna de Fier, Bocşa, Oravița, Ciclova, Moldova Nouă): 72.4-82.7 Ma; Timok (Majdanpek, Crni Vrh, Veliki Krivelj, Bor): 80.7-87.9; Panagyurishte (Elatsite, Chelopech, Medet, Assarel, Vlaykov Vruh-Elshitsa): 86.8-92.4 Ma.

Contact metamorphism related to BMMB. The main effect of the banatitic emplacement was the thermal and metasomatic transformation of the surrounding rocks. The metasomatic processes had an endomorphous character, affecting to different degrees the intrusive bodies themselves or extended over the pre-intrusion host formations, including crystalline schists, detrital sedimentary and carbonate rocks.

Isochemical transformations include recrystallization, prograde reactions without major implication of fluid phases, combinations of both, and subordinately, irreversible devolatilization (pyrolysis). The later process is often responsible for the discoloration of recrystallized carbonate rocks in the close vicinity of magmatic sources (*e.g.* Dognecea – Vlad, 1974), followed by the removal of organic carbon traces.

Recrystallization products are widespread within the contact aureoles, especially in areas where pure carbonate rocks prevail: calcitic or dolomitic marbles, often zoned, with rougher textures in the vicinity of the magmatic bodies (Vlad, 1974; Ionescu, 1996b). Carbonate rocks with silicate alloclasts, argillaceous or arenaceous limestones, marls, detrital rocks or crystalline schists are also transformed under the heat flow and may result in ”hardening”, ”hornfelsing”, ”softening” of the rocks – as named by various authors, or in textural transformations obliterating initial stratification or schistosity. Recrystallization commonly resulted in micro- or mesoblastic calcic or dolomitic marbles and relatively homogeneous, medium-grained calc-silicate hornfels with grossular + calcite or diopside + calcite. Siliceous and aluminous hornfels with biotite- or quartz-dominant assemblages or with andalusite + cordierite ± corundum and actinolite + chlorite + epidote ± zoisite are also present, yet at least in part, they might point to superposed hydrothermal alteration.

Prograde reaction products are much more diversified and reflect the complex nature of the premetamorphic rocks. In some cases, the prograde reactions are weak and only singular metamorphic mineral phases are identified against an unchanged background (*e.g.* ”biotite in gneisses”, ”cordierite in porphyritic rocks”, ”andalusite in biotite-bearing gneisses”). Sometimes, the thermal effects are inferred from *the loss* of certain mineral phases from the initial paragenesis (*e.g.* loss of biotite from thermally affected gneisses).

The most typical products of *allochemical transformations* in the contact aureoles of banatites are skarns and hydrothermal alterations. Cases of large scale Ca ⇔ Mg transfer reactions resulting in dolomitization of limestones (*e.g.* Ocna de Fier-Dognecea – Vlad, 1974) or in dedolomitization (*e.g.* Antoniu metasomatic body, Băița Bihor – Cioflica et al., 1992) have also been recorded.

Skarns have also been classified or referred to according to a multitude of criteria: (1) dominant chemical character (”calcic skarns”, ”magnesian skarns”); (2) mineralogical composition (skarns with various Ca, Mg, Al silicates); (3) the nature of the carbonate paleosome (”skarns formed on limestones”, ”skarns formed on dolostones”; (4) the passive or active role of the paleosome *vs.* the mineralizing fluids (”exoskarns”, ”endoskarns”, ”periskarns”); (5) position with regard to the magmatic contact (”proximal skarns”, ”distal skarns”); (6) evolution stage of magmatic bodies (”magmatic skarns”, ”post-magmatic skarns”); (7) thermal character of fluids (”pyro-metasomatites”, ”hydro-metasomatites”, ”pseudo skarns”).

Calcic skarns prevail in all banatite occurrences located nearby carbonate sedimentary formations. Subordinately, in several massifs from Bihor and Banat, magnesian skarns occur, with assemblages including forsterite + chondrodite + diopside ± phlogopite (clinochlore) + tremolite. At Băița Bihor, Budureasa, Pietroasa, Cacova Ierii, Ocna de Fier, skarns contain endogenous borates, such as ludwigite, kotoite, suanite or szaibelyite (*e.g.*, Ionescu, 1996a,b; Marincea, 2006). Other chemical types may also be present, such as Mn-rich skarns at Dognecea (*e.g.*, Vlad, 1974). Skarns unusually rich in aluminum occur in Valea Țiganilor, Ciclova and at Sasca Montană. The main Al-rich phase is vesuvianite which forms monomineralic concentrations, with crystals reaching up to 5-10 cm. Commonly, vesuvianite replaces diopside, wollastonite and garnet and points rather to a significant Al-mobility towards the late phases of metamorphism than to an Al-rich host rock.

Exoskarns are predominant in the banatitic contact aureoles, but well developed endoskarn assemblages have also been described. At Ciclova, the outer parts of a monzodiorite body have been

transformed in endoskarns with grossular + vesuvianite + Fe-diopside + phlogopite, locally accompanied by periskarns with Fe-augite + orthoclase + titanite + grossular (Cioflica et al., 1980). At Surduc, Marincea and Russo-Săndulescu (1996) described calcic endoskarns with prehnite + andradite + Ca-rich plagioclase + diopside, formed on bodies of basic magmatites of the Coniacian – Maastrichtian cycle.

High-temperature skarn assemblages with spurrite-tilleyite-gehlenite, or diopside-gehlenite occur at Cornet Hill-Măgureaua Vaței, Apuseni Mountains (Marincea et al., 2001, Pascal et al., 2001) and Ogaşul Crişenilor-Oravița (Constantinescu et al., 1988, Katona et al., 2003) where they are related to quartz monzonite-monzodiorites, or diorite-gabbros.

A continuum between skarns and hydrothermal alterations is specific to all skarns occurrences in BMMB, but the effects of hydro-metasomatism are usually extended beyond the limits of skarn zones. Hydrothermal retrograde reactions affecting garnets and vesuvianite, commonly result in epidote + chlorite ± carbonates, quartz whereas pyroxenes breakdown to form tremolite - actinolite + serpentine + talc. High temperature hydrothermal assemblages with tourmaline + quartz ± orthoclase, magnetite were described in relation to porphyritic granodiorite intrusions from Oravița and from Sasca Montană (Constantinescu, 1980).

More abundant are the hydrothermal assemblages containing a) K-feldspar + biotite ± quartz, muscovite (potassic alteration), b) epidote + actinolite + chlorite + quartz + calcite (propylitic alteration), and c) illite + quartz ± chlorite, calcite, pyrite (phyllic alteration) which are frequently related to ore deposits. Rich epithermal alteration with zeolites (laumontite, stilbite, thomsonite, chabasite etc.), gypsum, anhydrite, and crypto-crystalline silica are also present.

Types of mineral deposits in the BMMB. The studies of von Cotta (1864) upon the Fe-Cu-Pb-Zn skarn deposits of Dognecea, Ocna de Fier and other mines in Banat are the first widely cited papers to define a class of "contact-deposits" found at the contact of igneous intrusions and limestones. Since then, more than 50 mineral deposits have been discovered, and pending of a given historical epoch, they were of some economic interest. The mineralization related to the BMMB is represented mainly by porphyry copper, massive sulphide, skarn and vein (epithermal and mesothermal) deposits (Berza et al., 1998).

Copper metallogeny is predominant and distinguishes the BMMB in the context of the larger Alpine–Balkan–Carpathian–Dinarides belt (Ciobanu et al., 2002). Copper ores are commonly associated with Pb-Zn, Au-Ag, and subordinately with Mo, Bi, W, Fe, Co, Ni and B. Mineral deposits within the BMMB are strongly differentiated with respect to host rock types and depth of magma emplacement. Shallower hypabyssal bodies are hosts for porphyry copper ores with Cu ± Au, Ag, Mo: *e.g.* Moldova Nouă, Majdanpek, Cerovo, Veliki Krivelj, Bor (Timok Massif, Serbia), Elatsite, Chelopech, Assarel (Panagyurishte district, Bulgaria). High-sulphidation epithermal deposits are sometimes spatially associated with larger porphyry copper systems (*e.g.* at Bor and Majdanpek – Ciobanu et al., 2002). Subeconomic porphyry copper (± Mo) accumulations are also present at Oravița, but hydrothermal alteration is far less pervasive than at Moldova Nouă. Large shallow porphyry-style systems with pyrite halos (and/or skarn halos) extend only south of Poiana Ruscă but they lack economic mineralization: *e.g.* Tincova-Ruschița, Şopot-Teregova-Lăpuşnicel areas.

Copper and base metal skarn deposits form the most widespread metal accumulations across the BMMB. Some occurrences are set apart by prominent Fe metallogeny (*e.g..*, Ocna de Fier, Maşca Băişoara). Ocna de Fier is considered typical for fluid plume mineralization in a proximal skarn setting (Cook and Ciobanu, 2001). Forsterite skarns host a magnetite – chalcopyrite – bornite mineralization which represents the inner Cu-Fe core of the deposit (Cook and Ciobanu, 2001). Scheelite forms significant concentrations in the Cu-Mo mineralization of Băița Bihor and Oravița. Bismuth sulphosalts are minor but ubiquitous components of many skarn deposits. Extremely rich and diverse bismuth sulphosalt assemblages have been described at Băița Bihor, Valea Seacă, Ocna de Fier and Oravița-Ciclova.

Regional zoning of skarn deposits in correlation with Upper Cretaceous subduction settings was summarized by Berza et al. (1998) who distinguished two major metallogenic segments within the BMMB (Apuseni Mountains and Southern Carpathians), each one still amenable of division into further units (sub-belts, zones and districts). Local zoning is well expressed for numerous ore environments in the BMMB. At Băița Bihor, the areas closest to the magmatic sources are enriched in molybdenite. Towards the external zones, Mo-rich ores grade into Mo-W-Bi-Te (in calcic skarns) or Cu-W-Bi (in magnesian skarns), Pb-Zn (in magnesian skarns and sedimentary schists) and finally into boron mineralization overlapping dedolomitization zones. At Dognecea-Ocna de Fier, Ciobanu and Cook (2000) described a Cu-Fe → Fe → Pb-Zn metal zoning around a single granodiorite core in the deepest part of the deposit.

The polyascendant character of skarn deposits in the BMMB has either been asserted (*e.g.*, Popescu and Constantinescu, 1977; Cioflica and Vlad, 1981) or argued against (Ilinca, 1998). Extensive sampling and detailed investigation of ore paragenesis over numerous skarn deposits in the BMMB, plead for coeval and isochronous mineralization, most probably formed from the differentiation of a single fluid. Moreover, apart from several cases of prominent metallogeny (*e.g.* Fe at Ocna de Fier), the overall paragenetic sequence for virtually all mineral deposits in the BMMB is roughly the same, both as mineral phases and deposition sequence. Ilinca (1998) separated the following ore deposition sequences:

- Stage 1 (”siderophile” - Fe ± Co, Ni, As, Mn) - iron oxides and sulphides, Co, Ni, Fe arsenides and sulpharsenides, with subordinate Fe-Mn calcic silicates. The stage signifies the highest deposition temperatures and a continuous decrease of oxygen fugacity (e.g. hematite → magnetite, magnesioferrite) *vs.* increase of sulphur fugacity (pyrrhotite → pyirite ± nickeline, rammelsbergite, cobaltite, gersdorfite, Co-pentlandite, linnaeite, bravoite, siegenite, millerite).
- Stage 2 (Pb,Zn ± Ag, Bi, Fe) – forms the bulk of the mineralization in numerous occurrences across the BMMB. The stage is represented by galena (with up to 10 mol% matildite) and sphalerite usually with 14-15 mol% FeS). Invariably, the direct contact between galena and siderophiles, shows the late character of the Pb-Zn phases.
- Stage 3 (Pb, Bi ± Ag, Sb, Te, Cu) – contains Pb–(Ag)/Bi sulphosalts – lillianite homologues, cosalite, cannizzarite, galenobismutite and Bi (±Pb) tellurides. Some Pb-Bi sulphosalts are formed on older galena, most probably belonging to the previous stage. Stage 3 members often substitute galena and siderophile sulphides likely to belong to previous stages.
- Stage 4 (”copper metasomatosis” (CM) – Cu, Bi ± Pb, Ag, Au, Mo, W) – is distinguished by an increase of Cu content in sulphides and sulphosalts. Massive deposition of chalcopyrite, cubanite, bornite and fahlore minerals (tetrahedrite-tennantite, enargite, luzonite) occur in this stage, most frequently on Fe, Zn, Sb, As phases of earlier stages. ”Chalcopyrite disease” phenomena, *i.e.* chalcopyrite (± bornite, mackinawite) DIS in sphalerite are widespread. Bi-sulphosalts are particularly sensitive to CM transformations. First Bi phases show an increased Bi_2S_3/PbS ratio compared to previous stages and grade towards decreasing Bi/Cu ratio: proudite, lillianite (with up to 2.9 at.% Cu), felbertalite, (high Cu)cosalite, cuproneyite, junoite, nuffieldite, bismuthinite derivatives. In antimony dominated assemblages, bournonite is formed. The highest Cu contents are embodied by (cupro)makovickyite, paderaite, hodrushite and kupčikite and pure Cu-Bi sulphosalts such as emplectite and wittichenite.

References

Berza, T., Constantinescu, E., Vlad, S.N., 1998. Upper Cretaceous magmatic series and associated mineralisation in the Carpathian-Balkan Orogen. Resource Geology, Tokyo, 48/4: 281-306.

Ciobanu, C.L., Cook, N.J., 2000. Intergrowths of bismuth sulphosalts from the Ocna de Fier Fe–skarn deposit, Banat, Southwest Romania. European Journal of Mineralogy, 12: 899–917.

Ciobanu, C.L., Cook, N.J., Stein, H., 2002. Regional setting and geochronology of the Late Cretaceous Banatitic Magmatic and Metallogenetic Belt. Mineralium Deposita, 37: 541–567.

Cioflica, G., Vlad, Ş., 1973. The correlation of the Laramian metallogenic events belonging to the Carpatho – Balkan area. Revue Roumaine de Géologie, Géophysique, Géographie, s. Géologie, 17: 217–214.

Cioflica, G., Vlad, Ş.N., 1981. The copper mineralization of Ciclova. Analele Universităţii Bucureşti, XXX: 3–17 (in Romanian).

Cioflica, G., Jude, R., Lupulescu, M, 1992. Cupriferous metallization processes associated with Upper Cretaceous–Eocene magmatites from Romania. Romanian Journal of Mineralogy 76: 1–16.

Constantinescu, E, 1980. Mineralogy and genesis of the skarn deposit at Sasca Montană. Edit. Academiei R.S. Romania, Bucharest, 158 p. (in Romanian).

Constantinescu, E., Ilinca, Gh., Ilinca, A, 1988. Contributions to the study of the Oravița – Ciclova skarn occurrence, south-western Banat. Dări de Seamă ale Şedinţelor Institutul de Geologie şi Geofizică, 72–73 (2): 27–45.

Cook, N.J., Ciobanu, C.L, 2001. Paragenesis of Cu–Fe ores from Ocna de Fier–Dognecea (Romania), typifying fluid plume mineralization in a proximal skarn setting. Mineralogical Magazine, 65: 351–372.

Ilinca, G, 1998. Crystal chemistry of bismuth sulphosalts from the Banatitic province. PhD Thesis, University of Bucharest, Romania, 356 p.

Ionescu, C, 1996a. The metallogenetic study of the banatitic massifs from Budureasa and Pietroasa (Bihor Mts.). Ph.D. Thesis, Babeş-Bolyai University Cluj-Napoca (in Romanian), 180 p. (in Romanian).

Ionescu, C, 1996b. Stage relations between the postmagmatic processes from the contact aureoles of the Budureasa and Pietroasa banatitic massifs (Bihor Mts.). Studia Universitatis Babeş-Bolyai, Geologia, 41 (1): 127–135.

Katona, I., Pascal, M–L., Fonteilles, M., Verkaeren, J, 2003. The melilite (Gh_{50}) skarns of Oraviţa, Banat, Romania: Transition to gehlenite (Gh_{85}) and to vesuvianite. The Canadian Mineralogist, 41: 1255–1270.

Marincea, Şt, 2006. Suanite in two boron–bearing magnesian skarns from Romania: data on a longtime ignored mineral species. Neues Jahrbuch für Mineralogie – Abhandlungen, 182: 183–192.

Marincea, Şt., Russo–Săndulescu, D, 1996. Prehnite in calcic endoskarns from Surduc: A look on a neglected mineral species in Romania. Romanian Journal of Mineralogy, 77: 55–71.

Marincea, Şt., Bilal, E., Verkaeren, J., Pascal, M–L., Fonteilles, M, 2001. Superposed parageneses in the spurrite–, tilleyite and gehlenite–bearing skarns from Cornet Hill, Apuseni Mountains, Romania. The Canadian Mineralogist, 39: 1435–1453.

Neubauer, F, 2002. Contrasting Late Cretaceous with Neogene ore provinces in the Alpine–Balkan–Carpathian–Dinaride collision belt. In Blundell, D., Neubauer, F., von Quadt, A. (eds.): The timing and location of major ore deposits in an evolving orogen. Geological Society (London) Special Publication, 204: 81–102.

Neubauer, F., Heinrich, C., GEODE working group incl. Tomek, C., Lips, A., Nakov, R., Quadt, A. V., Peytcheva, I., Handler, R. Bonev, I., Ivăşcanu, P., Roşu, E., Ivanov, Z., Kaiser-Rohrmeier, M. *et al*, 2003. Late Cretaceous and Tertiary geodynamics and ore deposit evolution of the Alpine-Balkan-Carpathian-Dinaride orogen. In Eliopoulos, D. et al. (eds.): Mineral Exploration and sustainable development. Rotterdam: Millpress, 1133–1136.

Pamic, J., Belak, M., Bullen, T.D., Lanphere, M.A., McKee, E.H., (2000) Geochemistry and geodynamics of a Late Cretaceous bimodal volcanic association from the southern part of the Pannonian Basin in Slavonija (Northern Croatia). Mineralogy and Petrology, 68(4), 271-296.

Panaiotu, C.G., Panaiotu E.C., Nedelcu, A, 2005) Studiul paleomagnetic al banatitelor din România si Serbia (raport de cercetare grant). Rev. Pol. St. Sci - 2005, 8p.

Pascal, M-L., Fonteilles, M., Verkaeren, J., Piret, R., Marincea, Şt, 2001. The melilite-bearing high-temperature skarns of the Apuseni Mountains, Carpathians, Romania. The Canadian Mineralogist, 39: 1405-1434.

Poller, U., Uher, P., Janak, M., Plasienka, D., Kohut, M, 2001) Late Cretaceous age of the Rochovce Granite, Western Carpathians, constrained by U-Pb single-zircon dating in combination with cathodoluminescence imaging. Geologica Carpathica, 52: 41–47.

Popescu, Gh., Constantinescu, E, 1977. Mineralogical observations on the skarns and mineralization in Oraviţa region. Analele Universităţii Bucureşti, XXVI: 45–58 (in Romanian).

Popov, P.N., Berza, T., Grubić, A, 2000. Upper Cretaceous Apuseni–Banat–Timok–Srednogorie (ABTS) Magmatic and Metallogenic Belt in the Carpathian–Balkan Orogen. In ABCD–GEODE workshop Abstracts volume, Borovets, Bulgaria, 69–70.

Vlad, Ş.N, 1974. Mineralogy and genesis of the skarn deposit at Dognecea. Bucharest: Editura Academiei, 119 p. (in Romanian).

von Cotta, B, 1864. Erzlagerstätten im Banat und in Serbien. Wien: Braumüller, 108 p.

Zimmermann, A., Stein, H., Hannah, J., Koželj, D., Bogdanov, K., Berza T, 2008. Tectonic configuration of the Apuseni–Banat—Timok–Srednogorie belt, Balkans–South Carpathians, constrained by high precision RE–OS molybdenite ages. Mineralium Deposita, 43: 1–21.

Rom. J. Mineral Deposits, vol. 87 (2014), No. 1, p. 21-24

CHROMITE DEPOSITS IN TURKEY

A. Feyzi BİNGÖL[1*], Mesut ANIL[2], Melahat BEYARSLAN[1]

[1] Firat University, Department of Geological Engineering, Elazig /Turkey
[2] Çukurova University, Department of Mining engineering, Adana / Turkey
*afbingol@gmail.com Tel: +90 4242370000/5973 Fax: +904242411226

Abstract: Chromite deposits hosted by Mesozoic ophiolites of the Western Mediterranean Tethys play a relevant role as a major source of chromium, and are considered a potential target for platinum group elements (PGE) exploration. Important chromite deposits have been extensively exploited in the former Yugoslavia, Albania, Greece, Cyprus and Turkey. More than 2000 chromitite deposits are known in Turkey, most of which are mined presently, Turkey is one of the world's largest chromite producers, rated as the 3rd largest producer after South Africa and Kazakhstan. The majority of Turkey's chromite production has been utilized by the ferrochromium industry. The capacity of seventeen main Turkish chromite concentration plants is approximately 800,000-850,000 t/y. However demand has decreased for Turkish chromite, based on decreased demand from China and the closure of ferrochrome capacity in Europe. Chromite output has increased significantly in recent years, and production is up to 1.6Mt. Most of the chromite deposits are podiform and occur in the mantle sequence of the ophiolite. Only a few of them are found in the transition zone of the ophiolite sequence. The major podiform Turkish chromite deposits are relatively larger deposits (average size is 20,000 metric tons) inside the mantle peridotites which are always surrounded by dunite envelopes. In most locations, the podiform chromite deposits appear to be randomly distributed within the ultramafic rocks, which makes exploration difficult. Chromite can have many types of textures, such as massive aggregates, nodular, orbicular, banded, and graded layers. According to their chemical composition, Turkish chromite ores have been classified into metallurgical, refractory, and chemical ores. Metallurgical ore in which contents of Cr_2O_3 up to 46wt% and Al_2O_3 is low. Refractory ore and chemical ore in which the Cr_2O_3 content can be lower than in metalurgical ore (30-46 wt%).

Turkey's total export of chromite was US$ 465,3 million with a 3,4% decrease in 2011. Major markets were China (%82), Russia (%5), Sweden (%2) and India (%2). The most important ferrochromium markets for Turkey were the Netherlands, Italy and Belgium.

Key words : podiform chromite, ophiolite, Tethys, Turkey

1. Introduction

Chromian spinel (chromite hereafter) is a ubiquitous accessory mineral and is a primary chromium reservoir in the mantle peridotites. Chromite deposits play a relevant role as a major source of chromium, and are considered a potential target for platinum group elements (PGE) exploration There are two types of chromite deposits (chromitite)-namely, stratiform and podiform chromitites (Thayer,1960). The stratiform chromitite is of great economic importance, and lies within stratified igneous complexes, such as Bushveld, Muskox, Great Dyke, and Stillwater (e.g. Jackson, 1969; Irvine, 1977). In contrast, podiform chromitite tyrically occurs in ophiolites as lenticular or pod-shaped bodies. Podiform chromitite is not, however, equally distributed among the ophiolites. Boudier and Nicolas (1985) divided ophiolites into two subtypes in terms of the peridotite sections: the lherzolite ophiolite type (LOT) and the harzburgite ophiolite type (HOT). Chromitite is generally common in the HOT that was formed in supra-subduction zone settings (SSZ) and tectonically emplaced as ophiolites along continental margins, but is almost absent or found in small, if any, amounts in the LOT. According to their chemical composition, chromite ores have been classified into metallurgical, refractory, and chemical ores.

2. Geological Setting

The Turkish ophiolites belong to the The Tethyan ophiolite belt, extending from Spain to the Himalayas, is one of the longest ophiolite belts in the world. They are mainly located in five zones; these are from North to South: a)Pontide ophiolites, b)Anatolian ophiolite belt, c)Taurid ophiolite Belt, d) southeast ophiolite Belt and e) Peri-Arabian ophiolites (Robertson, 2002). The Turkish ophiolites consist of mantle peridotites, cumulates, sheeted dykes and basalts. Due to the intense tectonic activities, most of the ophiolitic massifs were dismembred and, therefore, it is not possibly to see the full sequence. The major podiform Turkish chromite deposits are relatively larger deposits (average size is 20,000 metric

tons) inside the mantle peridotites. The mantle peridotites are mostly composed of harzburgite and less dunite. More than 2000 chromitite deposits are known in Turkey. Only a few of them are found in the transition zone of the ophiolite sequence.

The Turkish ophiolite is a harzburgite-type ophiolite (Nicolas 1989) in which chromite forms a large number of relatively larger deposits (average size is 20,000 metric tons) chromitite pods in the upper part of the mantle section. Chromitites are almost always associated with the dunitic metasomatism of the harzburgitic host. The chromitite bodies take a number of different forms and occur as:

• magma-chamber-like, layered, dunite–chromitite bodies in the dunites of the Moho transition zone,

• irregular chromitite pods in a dunitic sheet, varying in length from a few tens of centimeters to > 100 m. These occur throughout the mantle section. Some are aligned concordant with the mantle layering (pods), whereas others are strongly discordant (podiform dykes),

• tabular chromitite bodies up to several meters wide, forming concordant sheets and discordant dykes,

• disseminated chromite–dunite bodies.

3. Chromitite deposits

Most of the chromite deposits are podiform and occur in the mantle sequence of the ophiolite. Only a few of them are found in the transition zone of the ophiolite sequence (Bingöl, 1978; Rahgoshay et al., 198; Anıl et al., 1986; Engin et al., 1986). Podiform chromite deposits are an important economic source for refractory-grade chromite and an interesting rock type in the upper mantle. Podiform chromite mines have produced 57.4 percent of the world's total chromite production (Stowe, 1987). In 2010, about 25 percent of the world's chromite production came from podiform chromite deposits, and this percentage has held for the past 50 years (Papp, 2011). Podiform chromite production has been reported from, in decreasing order of importance: Kazakhstan, Turkey, Philippines, Albania, Yugoslavia, New Caledonia, Cuba, Russia, Iran, Japan, Pakistan, Sudan, Greece, Canada, United States, Cyprus, Norway, Shetland Islands, and Australia (DeYoung and others, 1984; Stowe, 1987; Silk, 1988).

The major podiform chromite deposits are relatively large deposits (average size is 20,000 metric tons) that occur in Turkey, Cuba, Philippines, Iran, and New Caledonia. Turkey has a 6% share in world chromite mining and possesses 25 million tons of reserves. In 2007, Turkey ranked 3rd in chromite exports in the world with a share of 12.8%. The most important chromite reserves are located in six main districts (Fig. 1). These are: 1) Guleman District 2) Sivas-Erzincan-Kop Dağ District 3) Fethiye-Köyceğiz-Denizli District, 4) Mersin-Adana-Kayseri District, 5) Bursa-Kütahya-Eskişehir District, and 6) İskenderun-Gaziantep District. The Guleman district accounts for 45% of total Turkish chromite production (Fig. 2).

Exploration for podiform chromite deposits has been a challenge because of the unpredictable nature of their occurrence. In most locations, the podiform chromite deposits appear to be randomly distributed within the ultramafic rocks, which makes exploration difficult. Although podiform chromite deposits are associated with dunite bodies, not all dunites contain podiform chromite deposits, and dunite bodies themselves appear to be randomly distributed in the peridotite (Wells et al., 1946). The shallow deposits are commonly mined by open pits or quarries and the deeper extensions by underground workings. There are many exploration drilling opened by MTA around these deposits in different districts.

The Turkish chromitites display a great variety of textures: massive, nodular, disseminated and rarely banded. Turkish Chromite ores have been classified into metallurgical, refractory, and chemical ores. Metallurgical ore in which contents of Cr_2O_3 up to 46wt% and Al_2O_3 is low. Refractory ore and chemical ore in which the Cr_2O_3 content can be lower than in metalurgical ore (30-46 wt %). Most chromite ore is smelted in an electric arc furnace to produce ferrochromium for use in the metallurgical industry. Ferrochromium is the most important product in production and exports. The majority of Turkey's chromite production has been utilized by the ferrochromium industry. There are a low-carbon ferrochromium smelter at Antalya and a high-carbon ferrochromium plant at Elazığ.

Turkey's total export of chromite was US$465,3 million with a 3,4% decrease in 2011. Major markets were China (%82), Russia (%5), Sweden (%2) and India (%2). The most important ferrochromium markets for Turkey were the Netherlands, Italy and Belgium.

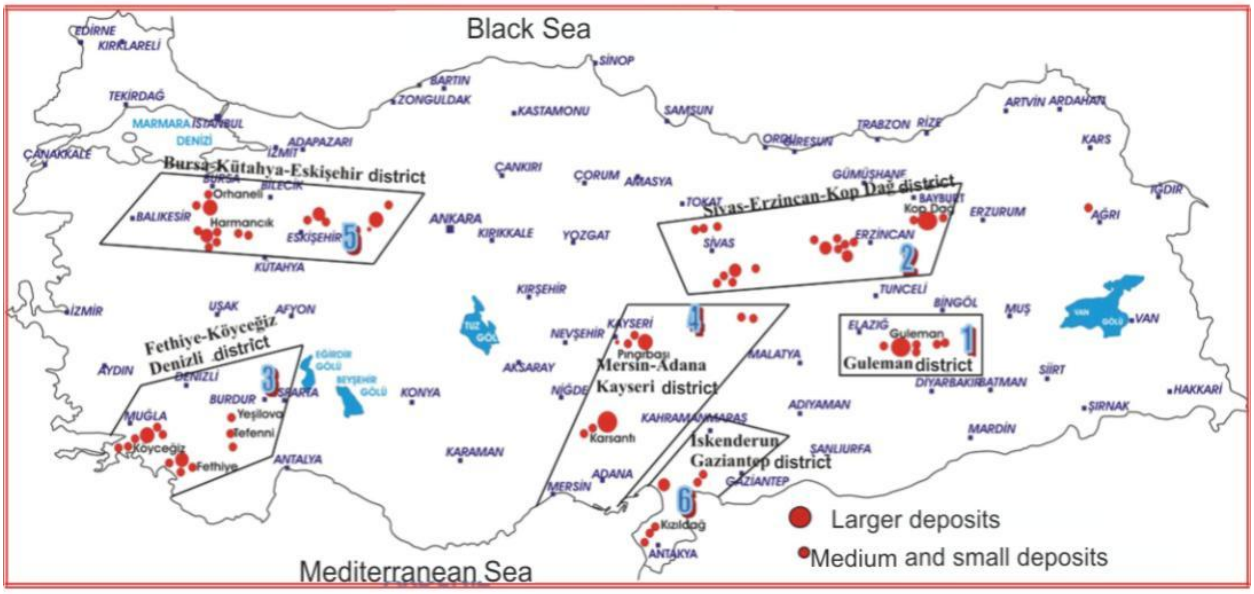

Figure 1. Chromitite deposits in Turkey (MTA, *www.mta.gov.tr*)

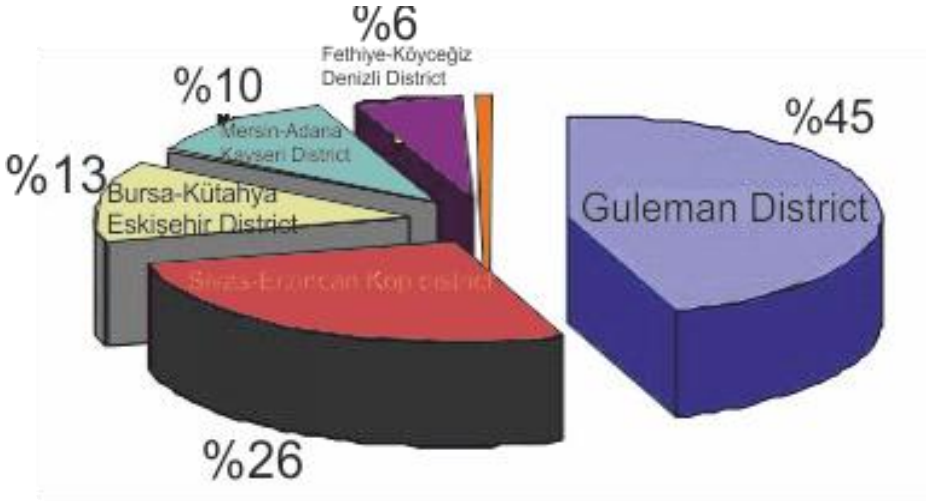

Figure 2. Regional Distribution of Chrome Reserve in six districts of Turkey (*www.turkkrom.com*)

4. Conclusıon

Chromian spinel is a ubiquitous accessory mineral and is a primary chromium reservoir in the mantle peridotites. The major podiform Turkish chromite deposits are relatively larger deposits (average size is 20,000 metric tons) inside the mantle peridotites. The most important chromite reserves are located in six main districts.

Turkish Chromite ores have been classified into metallurgical, refractory, and chemical ores. Turkey ranked 3rd in chromite exports in the world with a share of 12.8%.

5. References

Anıl, M., Billor, Z., Ve Ozus, S., 1986. Le Complexe ophiolitique chromifer, groupe de Gerdibi de Pozantı-Karsantı (Adana-Turquie). 11th annual earth sciences meeting. Reunion annualle des sciences de la terre 11, p.4.

Bingöl, A. F., 1978. Petrologie du massif ophiolitique de Pozantı-Karsantı (Taurus Cilicien-Turquie): Etude de la partie orientale thesis Strassbourg, 227 s.

Boudier, F. and Nicolas, A., 1985. Harzburgite and lherzolite subtypes in ophiolitic and oceanic environments. Earth and Planetary Science Letters, 76, 84-92.

DeYoung, J.H., Jr., Lee, M.P., and Lipin, B.R., 1984, Interna- tional strategic minerals inventory summary report—Chro- mium: U.S. Geological Survey Circular 930-B, 41 p. Engin T.,Özkoçak O.and Artan U., 1986. General geological setting and character of chromite deposits in Turkey. IGCP, Project No.197, 199-228.

Irvine, T.N., 1977. Chromite crystalization in the join Mg_2SiO_4-$CaMgSi_2O_6$-$CaAl_2SiO_2O_8$-$MgCr_2O_4$-SiO_2. Carnegie Inst.Wash. Yearb. 76, 465-472.

Jackson, E.D.,1969. Chemical variation in coexisting chromite and olivine in chromitite zones of the Stillwater Complex. In magmatic ore deposits. Econ.Geol. Monogr. No.4, 41-75.

Nicolas, A., 1989.Structures of ophiolites and Dynamics of oceanic lithosphere, Kluwer Academic Publishers, 367 p.

Papp, J.F., 2011. Chromium: U.S. Geological Survey Mineral Commodity Summaries 2011, p. 42, last accessed Septem- ber 20, 2011, at http://minerals.usgs.gov/minerals/pubs/ commodity/chromium/mcs-2011-chrom.pdf.

Rahgoshay, M., Whitechurch, H., Juteau, T., 1981. Petrology of the chromite bearing rocks of the Pozantı-Karsantı ophiolites (Taurus-Turkey). First meeting of the EUG, Terra –Cognita, p.23.

Robertson, A.H.F.,2002. Overview of the genesis and emplacement of Mesozoic ophiolites in the Eastern Mediterranean Tethyan Region. Lithos, 65, 1-67.

Silk, M.H., 1988, World chromite resources and ferrochromium production: Randburg, South Africa, Council for Mineral Technology, Mintek Special Publication no. 11, 149 p.

Stowe, C.W., 1987b, The mineral chromite, in Stowe, C.W., ed., Evolution of chromium ore fields: New York, Van Nostrand Reinhold Company, p. 1–22.

Thayer, T.P., 1960. Some critical differences between Alpine-Type ans Stratiform peridotite-gabbro complexes

Rom. J. Mineral Deposits, vol. 87 (2014), No. 1, p. 25-30

SLATE FORMATIONS WITH GAS POTENTIAL IN THE EASTERN CARPATHIANS

Nicolae ANASTASIU[1*], Mihai BRÂNZILĂ[2]

[1] University of Bucharest, 1, Nicolae Balcescu Blv., 010041 Bucharest, Romania;
[2] University "Al.I.Cuza" Iasi, Department of Geology, 20A Carol I Blv, RO -700505 Iasi
[*] *nicanastasiu@gmail.com*; Tel.: 0040 21 3107947; Fax.: 0040 21 3107947

Abstract: The GS and slate formations occur extensively along the Eastern Carpathians and are delimited by the Crystalline-Mesozoic zone or, partially, by the southern sector of Neogene vulcanites - to the west, and by the structures of the Moldavian and Moesian Platforms, to the east and south-east. In many cases, there is an overthrust of these formations (overthrust sheet structures).
The facies covered by GSFm are flysch facies with folded formations (folded basin). Their extent, on the west-east, direction is much less (km) compared to the extent on the north-south direction (thousands of km).
In terms of **organic matter content**, the maximum values (8-15%) are in the *Audia Formation* and in *dysodile formation* (including the lower and upper dysodiles). The values of the **Total Organic Carbon** (TOC) obtained by the Rock-Eval analyses go beyond the limit of interest, compared to the classic standards of gas-bearing argillites (gas slate) only in the case of the menilite formations (TOC = 6.64), of the brown marl formations (TOC = 12.69) and of the dysodile formations, for which TOC reaches considerable values = 17.62%). **Vitrinite reflectance** could not be assessed in all cases. The Ro values are compliant with the requested standards (Ro>1.3) only in the case of the Audia Formation, which reaches the required maturity for the *dry gas* window.

Keywords: shale, slate, diagenessis, organic matter, TOC%, vitrinite

Introduction

In the Eastern Carpathians, many fine clastic formations with age from Cretaceous to Neogene have a bitumineous character, and could be defined as slates: Black shale or Organic siliceous Shale, Organic mudstone, Gray Siliceous Shale, Gray mudstone (marls) or Silty shale, claystone. It is posible as at 2000-3000 m dept organic matter contents to become a *thermogas*, and all these petrofacies to become „shale gas".

Regional setting

The tectogenetic unit of the Eastern Carpathians, in fact a *fold belt basin*, extends from the northern boundary of the country to Dâmboviţa Valley and it is enclosed in the East, by Paleozoic to *Tertiary Foreland Basins*: the Moldavian Platform and the Schytian Platform (Săndulescu, 1984, 2011, Mutihac, 2010).
The main tectonics and structural units succeed from west to east, along the Eastern Carpathians and are represented by: Middle Dacides with the Crystalline-Mesozoic Zone, the Outer Dacides and the Modavides forming a Flysch Zone (turbidite facies-deep sea), Molasses Zone (shallow marine, delta facies) and Neogene Volcanics from Oaş –Gutâi and Călimani-Harghita (Fig.1).

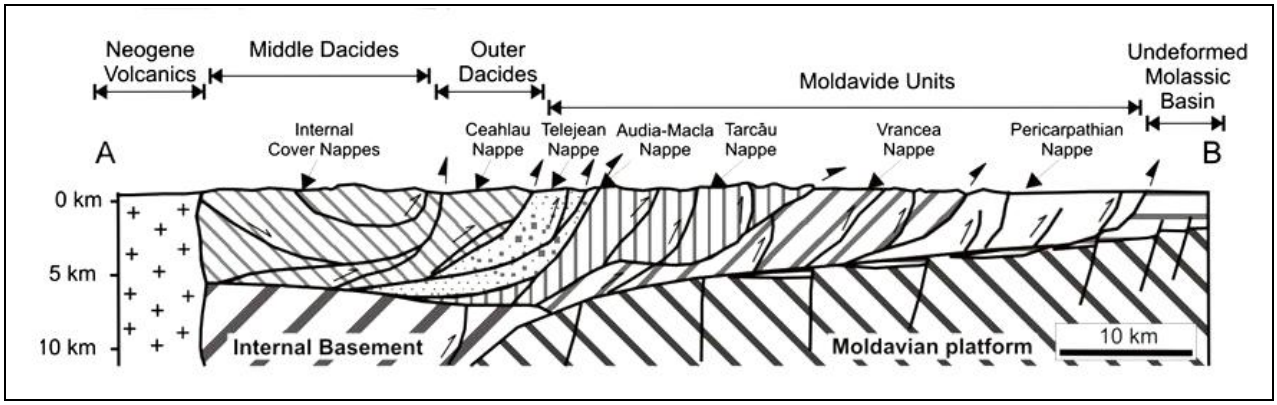

Fig.1. Geological cross-section of the central area of the Eastern Carpathians (according to Amadori et al. 2012).

Formations with shale gas potential have a large extent, along the Eastern Carpathians and are delimited by the Crystalline-Mesozoic Zone or, partially, by the southern sector of the Neogene volcanics – to the west, and the structure of Moldavian and Moesian Platforms, to the east and south-east. In many cases, the relations between these formations are overthrusting relations (structures of overthrust sheets) (Ştefănescu, 1993, Amadori, 2012, Mațenco, 2000).
The **facies** which wrap the shale gas potential formations are flysch and mollasse facies, with folded formations. Their extent, on west-east direction, is much more diminished compared to the north-south extent.
Their age spans from Cretaceous to Late Neogene (Table 1).

Table 1. Thickness of formations with features of source rocks.

EC – Eastern Carpathians	Age	Thickness (m)
Sinaia Formation	K1	100
Audia Formation	K1	600
Cașin Formation	Pg1	600
Bisericani Formation	Pg2	200
Tărcuța Formation	Pg3	70
Lower Menilite Formation	Pg3	30
Brown Bituminous Marl Formation	Pg3	100
Dysodile Formation	Pg3	250
Podu Morii Formation	Pg3	150

Total **thickness** GSFm varies from 60 to 600 m and covers all the series of a formation. Potentially gas-bearing shales included in each formation have much smaller thicknesses and often, lithologically, represent associations of lithological types (shales, argillites (slate), dysodiles, menilites, marls alternating with thin levels of sandstones) (Anastasiu et al., 2011, Popescu, 1995).

Materials and methods

The **sedimentological and oil generating parameters** result from the synthesis of analyses performedon samples from natural outcrops or drill cores (located in Cretaceous and Paleogene formations from the Carpathian Flysch (**FAud** – Audia Formation, **FBM** – Bituminous Marl Formation, **FLD** – Lower Dysodile Formation, **PMF** – Podu Morii Formation).
Our study on the slate Formations comprises a field reconstruction of the stratigraphic record, and sampling for mineralogical, petrographic, and geochemical analyses; mineralogical analyses of black slates, and shales or silty-shales by semi-quantitative X-ray diffraction (XRD) ; a geochemical analysis of the organic-matter content of the black-shale levels (total organic carbon (TOC), Rock-Eval pyrolysis data (RE). For petrofacies we used ternary diagram by AGI DATA – R. Compton, 1956 (Fig.3).

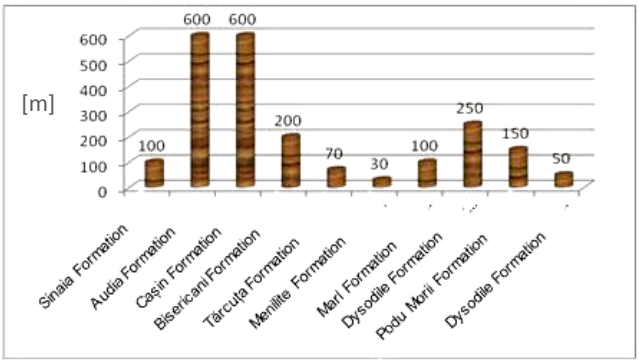

Fig. 2. Thickness of potentially gas bearing shale formations (GSF) in the Eastern Carpathians.

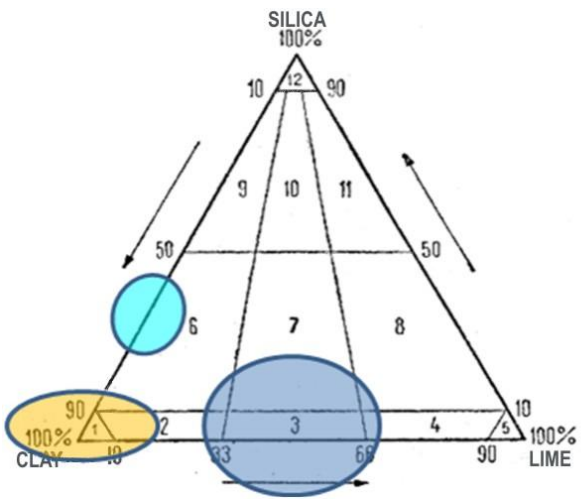

Fig. 3. Slate fields plotted on Silica-Clay-Lime Comton diagram.

Results, Discussion

The quartz-illite ratio in the potentially gas-bearing shale formations may influence the behavior of the gas-bearing formations in the process of hydraulic fracturing, the free quartz stimulating the release of gas during exploitation and the constancy of production. Figure 4 shows the ratio between Quartz/Illite for Cretaceous-Miocene slate formations.

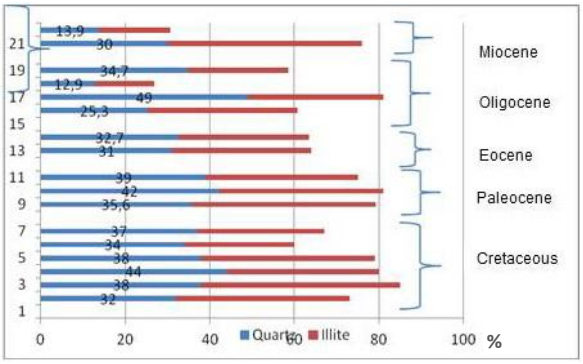

Fig. 4. Quartz-illite ratio in the potentially gas bearing shale formations of ages between Cretaceous and Miocene.

Chemical analyses (oxides) show some differences in between Cretaceous versus Oligocene flysch slate formations (Fig. 5).

The parameters based on which the gas-bearing potential of a shale formation (thermal gas reservoir) are: Organic matter; Vitrinite reflectance, of TOC value respectively (Total Organic Carbon in % weight); S1 and S2 peaks obtained by Rock Eval Pyrolysis (mgHC/g rock); Maturity degree of the analyzed samples.

The average of the values of these parameters, for each potentially gas-bearing formation related to TOC values, kerogen, S1 and S2 standard leads to their categorization according to the maturity level obtained and thus, by their behavior as thermal gas reservoir (See Table 2).

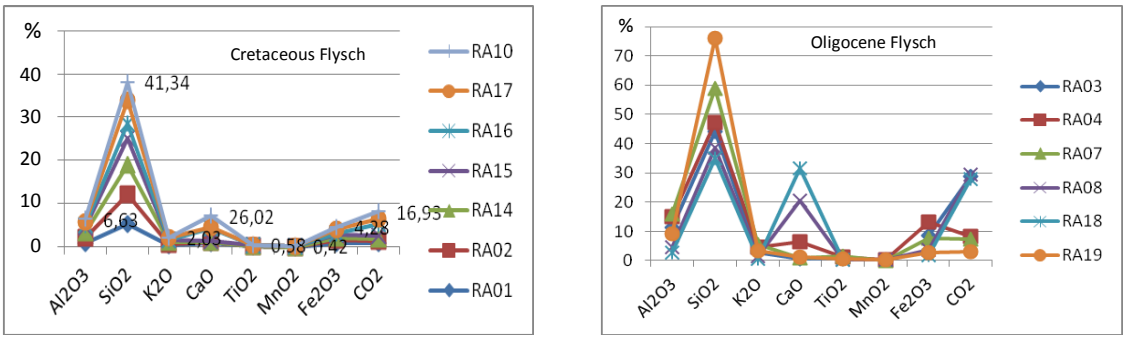

Fig. 5. The SiO_2 content of Cretaceous and Oligocene potentially gas-bearing shale formations indicates the same behaviour.

Shales and slates potential of the Eastern Carpathian Formations

Potentially gas-bearing shales included in each formation have much smaller thicknesses and often, lithologically, they represent an association of **lithological types** (shales, argillites, dysodiles, menilites, and marls, alternating with thin levels of sandstones). Therefore, the dilution degree of shales and argillites may reach 50 % or may exceed this value.

As regards the content of **organic matter**, by their maximum value, Audia Formation and Dysodile Formation (including lower and upper dysodiles) are to be noted. The large difference between minimum and maximum in case of Ausia Formation must be explained by the dilution of some samples and the small thicknesses of lamina, together with the increased frequency of some micro-granule, clastic and silicate-rich layers (Fig.6).

Values of **Total Organic Carbon** (TOC) obtained by Rock-Eval analysis go beyond the limit of interest related to the classic standards of gas shale only in case of Menilite Formation (TOC=6.64), Brown Marl Formation (TOC=12.69) Dysodile Formation (for which TOC reaches considerable values=17.62%). The large differences, within dysodiles, between minimum (0.82) and maximum (17.62) suggest the lack of homogeneity of sequences and the diversity of rhythms which represent the formation in its entirety.

These differences will burden the assessment of the gas-bearing potential and, implicitly, a possible calculation of reserves.

The requirement of **organic substance maturation** and the entry of sediments in the dry-gas window is given by the temperatures, higher than 420-430 ^{o}C. In the Eastern Carpathians, these temperatures were reached by Sinaia, Audia, Tărcuța, Podu Secu, menilite, brown marl and dysodile formation. The temperatures of Sinaia Formation and partially, of Dysodile Formation seem exaggerate (503 ^{o}C). The maturity degree in all these cases varies from submature to mature.

Table 2. Organogenic parameters of Eastern Carpathians related to the international standards (source: Grasu, 1988, 1999, Roban, 2012, Amadori, 2010, Anastasiu, 2011)

	Organic matter – international standard US Dept. of Energy - 2009				**Eastern Carpathians – TOC %, S1 and S2**		
	TOC (% weight)	Kerog	Rock Eval Pyrolysis		GSF of interest		
			Peak-S1 **(mgHC/g-rock)**	Peak-S2 **(mHC/g-rock)**	TOC	S1	S2
The maturity degree increases in ascending order	0-0.5	very poor	0-0.5	0-2.5	Dysodile Form.	Sinaia 1 Form. Sărata Form. Biseric. Form. Podu Morii Form.	Sinaia Form. Sărata Form. Biseric. Form. Dysodile Form. Podu Morii Form.
	0.5-1	poor	0.5-1	2.5-5	Sinaia 1 Form. Sărata Form. Bisericani Form. Brown Marl Form. Dysodile Form.	Audia 1 Form. Podu Secu Form. Brown Marl Form. Dysodile Form.	Audia Form. Sărata Form. Menelite Form.
	1-2	average	1-2	5-10	Audia 1 Form. Sărata Form. Tărcuța Form. Menelite Form. Podu Morii Form.	Tărcuța Form. Dysodile Form.	Tărcuța Form. Brown Marl Form. Dysodile Form.
	2-4	good	2-4	10-20	Podu Secu Form. Brown Marl Form. Dysodile Form.		Podu Secu Form. Brown Marl Form.
	> 4	very good	>4	>20	Menelite Form. Dysodile Form.		Menelite Form. Dysodile Form.

Table 2 – continuation.

A Kerogen Type	HI - standard (mg HC/g TOC)	S2/S3(mgCO2/g-rock	Hl Eastern Carpathians	Notes
I – of lacustrian sapropel - lipids	>600	>15	Podu Secu Form. (643) Dysodile Form.	
II – of marine sapropel - lipids	300-600	10-15	Menilite Form (328-356, 484) Brown Marl Form. (354-625) Dysodile Form. (342-559)	
II/III	200-300	5-10	Bisericani Form. (263-269) Tărcuța Form. (237-308) Brown Marl Form. (249-297)	
III – cellulose lignin - continental	50-200	1-5	Audia 1 Form. (54-58) Sărata Form. (50-196) Podu Secu Form. (129)	
IV	<50	<1	Sinaia 1 Form. (14-31) Podu Morii Form. (82)	

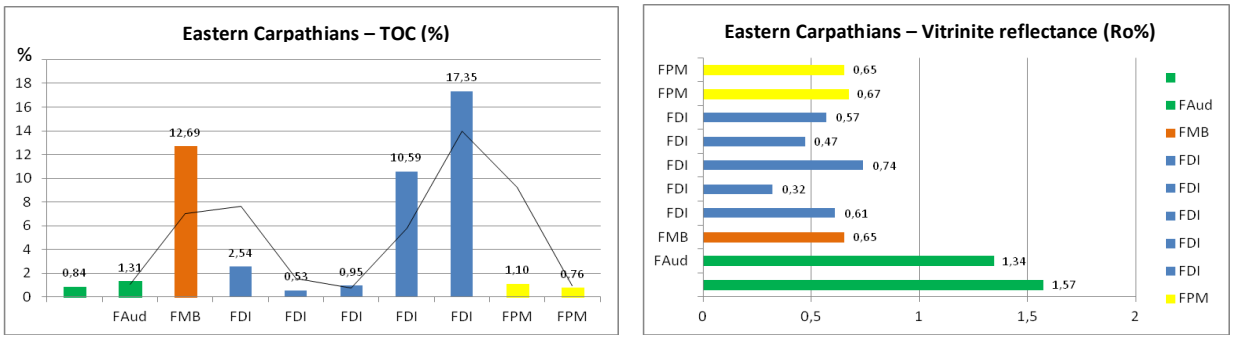

Fig. 6. The average values of the TOC (%) and vitrinite reflectance (Ro%) for several Cretaceous and Paleogene formations from the Carpathian Flysch (**FAud** – Audia Formation, **FBM** – Bituminous Marl Formation, **FLD** – Lower Dysodile Formation, **PMF** – Podu Morii Formation) seem vary variable and show the *gas shale* feature of Audia Formation.

Conclusion, Interpretation

The slate formations could be interpreted as having originated in a deep-water slope-to-basin setting (Fig. 7). Lithofacies suggest that the sea floor was below storm wave base and the oxygen-minimum zone (Melinte, 2005, 2011, Roban, 2012). Oceanic circulation was restricted and the water column stratified, accounting for the dysaerobic to anaerobic conditions of deposition. Probably, LOG record, facies succession (couples, and microsequences) considered , deposition began during a second-order highstand of sea level, and superimposed on this overall fall were numerous third-order fluctuations (parasequences) of relative sea level.

The sediment burial, and diagenesis permitted an evolution of organic matter to dry-gas window because:

- the shale source rock formed from type II kerogen (mainly marine algae) under normal-marine salinity and dysaerobic conditions;
- The total organic carbon (TOC) is reported to average 1.28, and is generally highest in the slate, and black shale beds;
- Vitrinite reflectance (Ro) reflects a greater thermal maturity of the source rock, which in turn influences the expected hydrocarbons generated;
- Kerogen II is sub-mature to mature, and within the oil window.

  In this way, the slate rocks from many formation of the Eastern Carpathians can be considered a good potential mature oil- and gas-prone source rock.

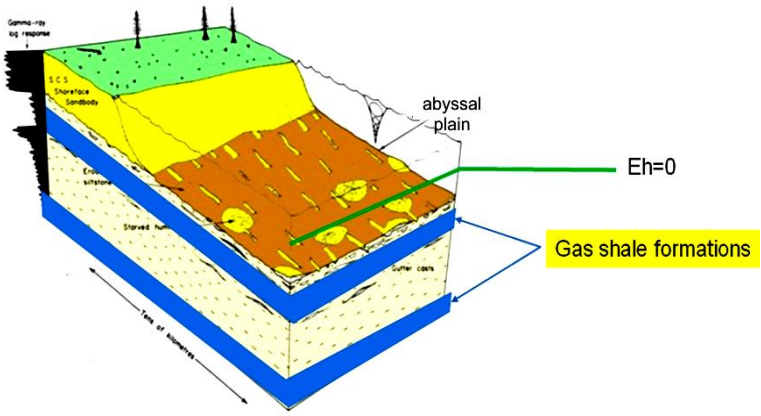

Fig. 7. Depositional model for Black shales from Audia Formation.

References

Amadori M. L., Belayouni H., Guerrera F., Martin Manuel, Martin-Rojas I., Miclăus Crina, Raffaelli G., 2012. New data on the Vrancea Nappe (Moldavidian Basin, Outer Carpathian Domain, Romania): paleogeographic and geodynamic Reconstructions. Int. J. Earth Sci. (Geol. Rundsch.), 101, p. 1599-1623. Springer Verlag.

Anastasiu N., Marius P., Vârban B., 1995. Facies analysis on Oligocene Formations from Outer Flysch Zone (the East Carpathians); a reconsideration. Asoc. Geol. Carp. – Balk., Congr. XV, 4, p. 317 – 323, Athens, Greece.

Anastasiu N., Filipescu S., Brânzilă M., Roban R-D., Seghedi A., 2011. Geological study, regional assessment and possibilities of capitalization of the gas-bearing shales in Romania (an unconventional resource-I). (in Romanian) Report, Archives of DGRM-MECMA, ANRM. 343 p.

Grasu C., Catană C., Grinea D.,1988. The Carpathian flysch. Petrography and economic considerations. (in Romanian). 208 p. Editura Tehnică, Bucharest.

Grasu C., Catană C., Boboş I., Miclăuş Crina, 1999. The molasses of the Eastern Carpathians. Petrography and sedimentology. (in Romanian) 224 p. Editura Tehnică, Bucharest.

Matenco, L., Bertotti, G., 2000. Tertiary tectonic evolution of the external East Carpathians (Romania). Tectonophysics 316, p. 255-286.

Melinte, M.C., 2005. Oligocene palaeoenvironmental changes in the Romanian Carpathians, revealed by calcareous nannofossils. Studia Geologica Polonica 124, p. 341-352.

Melinte-Dobrinescu MC, Roban RD., 2011. Cretaceous anoxic–oxic changes in the Moldavids (Carpathians, Romania). Sediment. Geol. 235, p. 79–90.

Mutihac V., Mutihac G., 2010. The geology of Romania. Editura Did.Pedag., Bucureşti, 690 p.

Popescu B., 1995. Romania's petroleum systems and their remaining potential. Petroleum Geoscience, 1, p. 337-350. London

Roban, R.D., Melinte-Dobrinescu, M. C., 2012. Lower Cretaceous Lithofacies of the black shales rich Audia Formation, Tarcău Nappe, Eastern Carpathians: Genetic Significance and Sedimentary Palaeoenvironment. Cretaceous Research, 38, 52-67.

Săndulescu M.,1984. Geotectonics of Romania. (in Romanian) 335 p. Editura Tehnică, Bucharest.

Săndulescu M., 2011. Structural and paleogeographic correlation of the Moldavides within the East Carpathians. Rev. Roum.Géologie.T.53-54,2010-2011, p. 85-87. Bucharest.

Ştefănescu M., Popescu B., 1993. Romania's Petroleum System. A.A.P.G. Bull., 77, p. 1668, Tulsa, Oklahoma.

A GIS MINERAL POTENTIAL MODELING IN THE SKELLEFTE DISTRICT (SWEDEN)

Sorin TAMAS-BADESCU[1], Gabriela TAMAS-BADESCU[1]

[1]Geoexpert S.R.L., Iuliu Maniu Blv., Bl. L4/31, 330152 Deva, Romania
geoexpert@smart.ro; Tel./Fax: 0040 254 234811

Abstract: This paper presents an attempt of carrying out a GIS mineral potential modeling study with the practical purpose to identify the most prospective areas for exploration, particularly but not exclusive for copper, within the Skellefte District (Sweden). Based on the analysis of the spatial relations between the known deposits and occurrences, we have calculated the "weighting scores" for various available data sets, which were further combined to obtain various "prospectivity scores". The map of the RFIMGOHBTD score, which reflects the prospectivity of the all datasets, can be used with high confidence for targeting further exploration programs, taking into account that 95.5% of the medium to large size deposits are reflected by values of RFIMGOHBTD exceeding the mean, 73% by values exceeding the mean + 1 x the standard deviation and 60% by values exceeding the mean + 2 x the standard deviation. Several highly prospective areas have been selected for further detailed review of the geological setting and existent historical exploration data and results.

Keywords: GIS mineral potential modelling, Skellefte District, Sweden

Introduction

The GIS mineral potential modeling could be a powerful tool for targeting the exploration in areas for which adequate digital datasets are available. Conducting such study involves dedicated software, advanced skills in the GIS techniques and a good training in geostatistics. This paper presents an attempt of conducting a GIS mineral potential modeling study in a friendly way for the exploration geologists, using simple mathematics and the processing tools offered by the ArcGIS for Desktop Basic software. This study had also a practical purpose: to identify the most prospective areas for exploration, particularly but not exclusive for copper, within the Skellefte District (Sweden).

Short review of the geology, metallogeny, mining and exploration activities in the study area

The study area is located in the northern part of Sweden, approximately between $64^0$15'-$65^0$45' North latitude. Almost the entire surface of the study area is covered by the Fennoscandian Shield. The Fennoscandian Shield formed during the Svecokarelian orogeny (c. 1.96 to 1.75Ga) and consits of a complexe sequence of Palaeoproterozoic supracrustal rocks (mostly marine-sedimentary and subaqueous to sub-aerial volcanic rocks) that were intruded by syn- to post-volcanic granitoids (fig. 1). The lithostratigraphy is quite complex and interfingers and upwards and laterally transitions between the various units exist. At least two major phases of deformation and metamorphism have affected the supracrustal and/or intrusive rocks and certain mineralizations, between ca. 1.9–1.8Ga (Kathol and Weihed ed., 2005, Carranza and Sadeghi, 2010).

The Skellefte area is one of the most prolific metallogenic zones in Sweden. According to the Geological Survey of Sweden (Sveriges Geologiska Undersökning – SGU), about 300 ore deposits and occurrences of various metallogenic types and belonging to several metallogenic districts are known within this area (fig.1). Within the *Skellefte Zn-Cu-Pb-Ag, Au District s.s.* (located in the central part of the study area) there are about 150 deposits, spread in an area of 140km/50km. About 30 deposits were mined in the period 1924-2011. The total production of the mines located in this district in the period 1924–2009 was of 105Mt grading in average 2.4g/t Au, 60g/t Ag, 0.94% Cu, 4.6% Zn and 0.5% Pb. Probably the best known deposit is Boliden. In the period 1926-1967, this deposit produced 8.35Mt of ore grading 15.5g/t Au, 50g/t Ag, 1.4% Cu, 0.3% Pb, 0.9% Zn (Hallberg in Eilu, ed., 2012). Currently, 6 mines are active (Kristineberg, Maurliden, Maurliden Östra, Renström, Kankberg, Björkdal) with cumulated reserves and resources totaling 118t Au, 1740t Ag, 757t Te, 195kt Cu, 1202kt Zn and 152kt Pb – acc. to the reserves and resources statements of the companies Boliden AB (*www.boliden.com*) and Björkdalsgruvan AB (*www.bjorkdalsgruvan.se*). One deposit (Vindelgransele) is under development stage. Most of the deposits in the Skellefte District s.s. are considered of VMS type. Replacement processes were involved at least partly in some cases. Some of the Au-rich deposits (i.e. Boliden) are considered by some authors as possibly hybrids between the classic VMS deposits and epithermal deposits. In some deposits, the gold is possibly remobilized due to deformation and metamorphism (Carranza and Sadeghi, 2010). Low-grade porphyry Cu and numerous sub-economical Au-As quartz vein deposits are also known in this district (Hallberg in Eilu ed., 2012). The so-called *Gold Line* is the most recent mining district in Sweden. This

district was detected by a regional till survey in the late 1980s. Since then, 50 deposits and occurrences were found: 14 of gold, 19 of base metals and 17 of W, Sn, Mo. Two mines have been in production: Blaiken Zn-Au (closed down in 2007) and Svartliden Au (still in production, with reserves of 0.649Mt grading 2.89g/t Au – acc. to Dragon Mining Ltd. -*www.dragon-mining.com.au*). A new deposit, Fäboliden, is in the development stage (with resources of 65.5Mt grading 1.06g/t Au, 2.81g/t Ag – acc. to Lappland Goldminers AB (*www.lapplandgoldminers.com*). Most of the gold deposits in this district are considered to be orogenic gold deposits (Perdahl in Eilu, ed., 2012). The *Lappvattnet metallogenic district* includes at least 30 nickel deposits. The historical resource estimates for 9 deposits are of 6.37 Mt grading 0.60% Ni, 0.16% Cu and 0.02% Co. Only test mining was carried out in one of the deposits (Lappvattnet). The Ni-Cu mineralization occurs as disseminated veinlets and massive ore hosted in metamorphosed Palaeoproterozoic mafic to ultramafic intrusive rocks (Hallberg in Eilu, ed., 2012). Many other small deposits and occurrences (Mo-W-Sn, Pb-Zn-Ag; Cu-Ni, As-Cu-Au, Cu, Au) are also known outside of above mentioned well defined metallogenic zones.

Currently, various companies are carrying out intense mining and exploration within the study area. According to the Mining Inspectorate of Sweden (Bergstaten), 69 mining licenses, 235 exploration licenses and 18 applications for exploration license were registered in January 2014. They cover about 3175km^2 (about 7% of the total surface of the study area) and include about 50% of all deposits and occurrences that are known in this area.

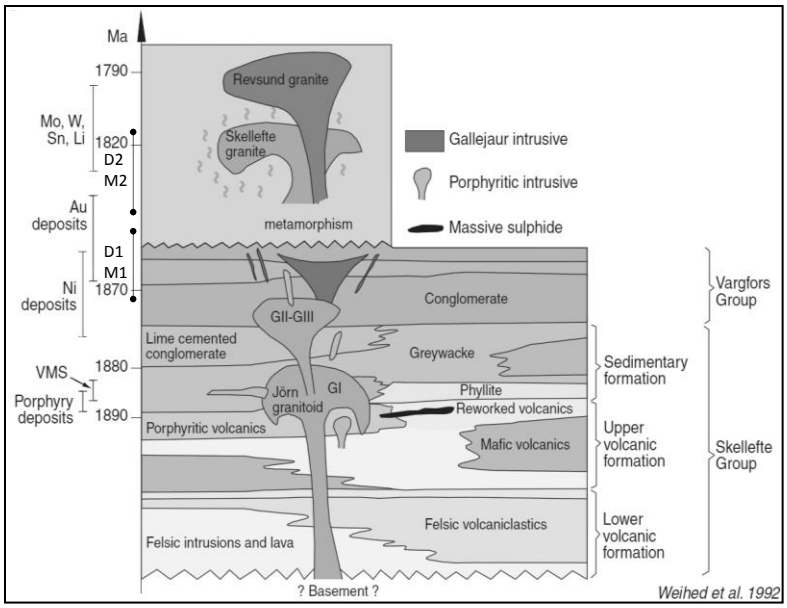

Fig. 1. Simplified litostratigraphy of the Skellefte region (Weihed et al., 1992 in Kathol and Weihed ed., 2005). D1, D2 - deformational phases; M1, M2 - metamorphic phases.

GIS mineral potential modeling - a tool for exploration targeting

A quite complex GIS predictive mapping and quantitative estimation of undiscovered VMS deposits study was carried out by Carranza and Sadeghi (2010) for the Skellefte District s.s. Apart of outlining the prospective zones for VMS deposits, Carranza and Sadeghi (2010) made estimates on the number of undiscovered deposits (48) and metal endowments (709Kt Cu and 3190Kt Zn). Most of the prospective ground within the study area is now explored by various companies.

The theory of the GIS mineral potential modeling (or GIS predictive modeling, GIS targeting etc.) could be considered quite "opaque" for most of the exploration geologists. In simple terms, the GIS mineral potential modeling implies to express numerically (to score) the spatial relation between the geologic, geophysical and geochemical datasets representative for the deposits of a certain type from a zone, and to combine those scores for delineating and ranking the prospective areas for exploration. Two basic techniques are used for such studies: "data-driven" (i.e. weights of evidence analysis) and "expert-driven" (i.e. fuzzy logic). The "data-driven" techniques imply to use a representative dataset of "training" mineral occurrences from the area in order to score the various input datasets. The "expert-driven" technique implies to weight each dataset using a function which expresses the degree of importance of the various datasets as predictors for the deposit type taken under consideration.

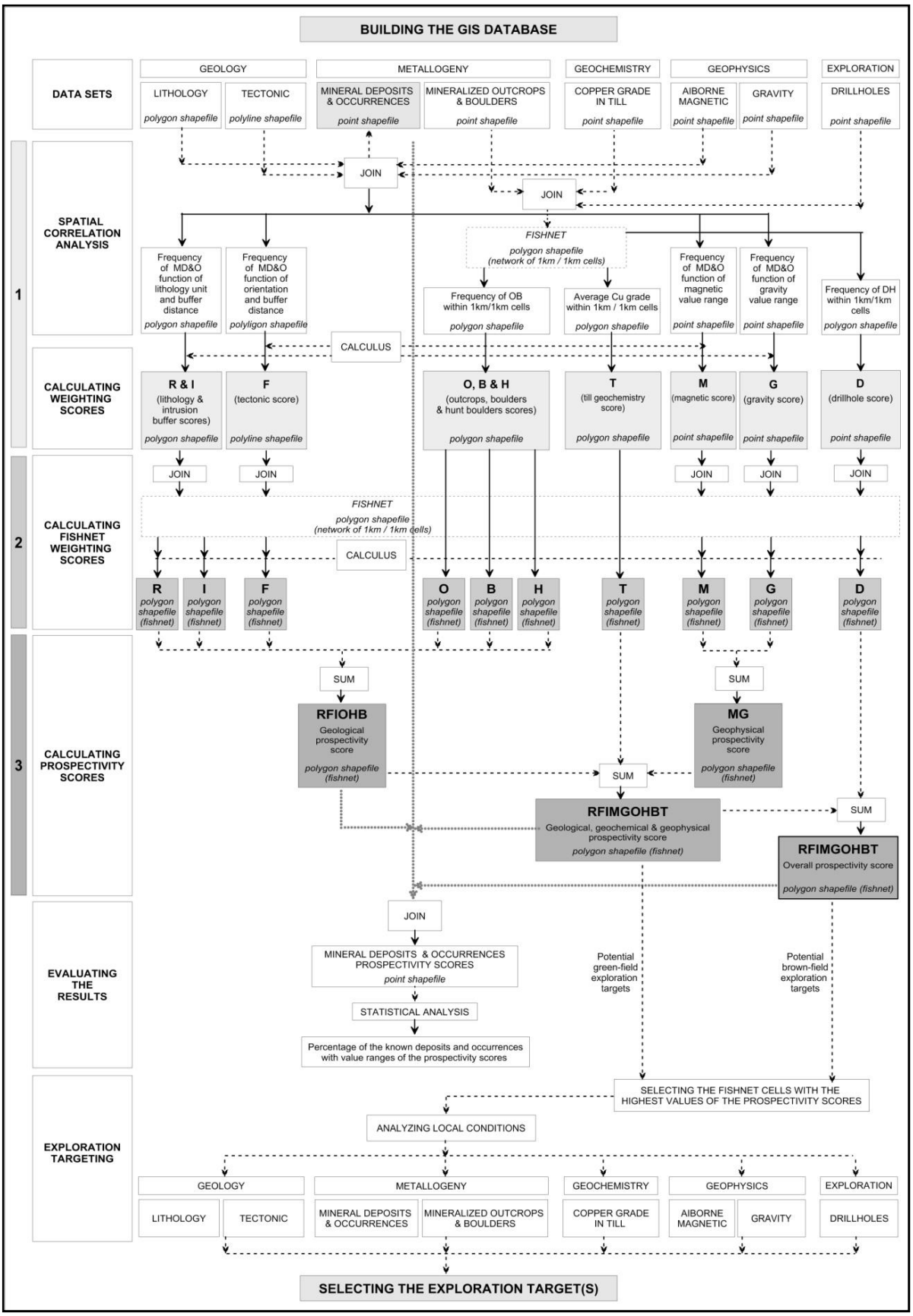

Fig. 2. The GIS mineral potential modeling workflow.

Such GIS mineral potential modeling study could not be handled by any exploration geologist, mostly because it requires dedicated software (i.e. Spatial Analyst extension for ArcGIS), which are expensive and generally is not purchased by the exploration companies. This paper presents an attempt of carrying

out such study in a more friendly way for the exploration geologists, using the processing tools offered by the ArcGIS for Desktop Basic software (without the Spatial Analyst extension). This study had also a practical purpose: to identify, using the GIS techniques, the most prospective areas for exploration within the Skellefte region (Sweden), particularly but not exclusive for copper, in areas with no active mining or exploration licenses.

In contrast with the dedicated studies that generally focus on a certain genetic type of deposit existent (or likely to exist) within an area, this study takes into consideration all the deposits and occurrences recorded by the Geological Survey of Sweden (SGU) containing Cu, from practical considerations:

- The SGU data does not include information about the genetic type of deposits or occurrences from the database. For completing this kind of information, a quite important volume of work for literature review is needed;
- The geology of the area is quite complex (including multiple magmatic phases with different characteristics and several phases of deformation and metamorphism) and in many cases the deposits could not be classified with certitude as belonging to a certain genetic type;
- From the exploration point of view, it is less important if a deposit belongs to a genetic type or another as long as this contains the desired commodity, obviously in a quantity that might make the deposit economic;
- There are not "infallible rules" related to the geological characteristics and/or geophysical expression of a certain type of deposits;
- Indifferently of the genetic type, some general factors control the presence of a deposit, respectively the existence of suitable host rock lithology, adequate tectonics structures controlling the mineralized fluid migration and eventually mineral deposition and the heating source for generating the convective movements of fluids.

Spatial data sets

The datasets of the "ArcGIS exploration package for the Skellefte District", prepared by the SGU, were used in this study. This data package includes the geological map scale 1:250,000 (lithology polygons shapefile and tectonics polyline shapefile), mineral deposits and occurrences (points shapefile), magnetic data (points shapefile), gravity data (points shapefile), copper contents in till samples (points shapefile), mineralized outcrops and boulders (points shapefile) and drillhole collars (points shapefile).

GIS mineral potential modeling technique

This study could be considered as "data driven" type and basically comprises three steps (fig. 2):

1. Analyzing the spatial correlation between the known deposits and occurrences and other data sets and calculating the "weighting scores";
2. Converting the data sets with "weighting scores" in networks of 1km/1km cells;
3. Calculating the "prospectivity scores" considering various data sets.

1. Analyzing the spatial correlation between the known deposits and occurrences and other data sets implied firstly to join the deposits and occurrences point layer with the layers of other datasets. By joining, for each point (deposit/occurrence) we have got the attributes of the polygon that it falls in or the attributes of the nearest point/polyline/polygon that is closed to it (and the distance to this).

Joining the deposits and occurrences point layer with the lithology polygons layers was straightforward. Other datasets, particularly the point datasets (i.e. magnetic, gravity and copper in till) required some pre-processing before joining because of the relatively low density of data. The "pre-processing" implied the gridding of magnetic, gravity and geochemical point data and extracting the point data from grids at higher density than the original data. For carrying out the above mentioned operations, we have used the Surfer software. Further on, the point data was converted into polygon data by creating a network of 1km/1km cells (using the Fishnet tool from the Data Management Toolbox, Feature Class tools subset) and joining this polygon layer with the point layers (using the option for averaging the values of the points that fall in a cell). The "pre-processing" of the tectonics polyline data implied separating the faults with various orientations and creating buffers polygons at various distances (using the Buffer tool from the Analysis Toolbox). Buffers polygons at various distances were also created for various intrusive units. Querying the attributes of the deposits and occurrences point layer joined to the layers of other datasets, it was counted the number of the deposits and occurrences that spatially correlate (fall in) with a certain lithology unit, buffer distance to faults with various orientation, buffer distance to intrusive units, and ranges of magnetic and gravity values.

The analysis of the join results gives an image on the prospectivity of the main controlling factors of mineralizations. The results indicate that about 29% of the known deposits and occurrences spatially correlate with the felsic metavolcanic rocks of the so-called Skellefte Group and about 23% of them with the metagreywacke (turbiditic), meta-argillite rocks of the so-caled Bothnian Supergroup. The percentages of the deposits and occurrences that spatially correlate with other lithological units separated by the SGU vary between 0-7%. This suggests that the main host lithologies are those that were mentioned before. About 16% of the known deposits and occurrences are placed with a 100m buffer distance to faults, about 60% in a buffer distance of 1000m and about 95% in a buffer distance of 4000m. This suggests that the faults played an important role, at least in the migration of fluids. Regarding the orientation of faults, the most favorable orientation is WNW-ESE and the less favorable orientation is NNW-SSE. About 71.5% of the known deposits and occurrences place within a buffer distance to the exposed intrusions of 4km and about 34% of them are placed within a buffer distance of 1km. The most prospective heating source seems to be the granitoide - syenitoide intrusions of the Sorsele, Adak and Ale units. Those results suggest that the buffer distance to intrusions must be considered as a moderate indicator of prospectivity. It should be taken into account that, apart of the exposed intrusives, the heating source could be also represented by some buried intrusions. The analysis indicates that the known deposits and occurrences are associated with a large range of magnetic field values but the most prospective range of values is -71nT to -28nT. About 30% of the deposits and occurrences place in this range of values. Similarly, the analysis indicates that the known deposits and occurrences are associated with a large range of the Bouguer gravity values but the most prospective range of values is -39mGal to -32mGal. About 38% of the deposits and occurrences place in this range of values. Taking into account these results, it could be considered that the magnetic and gravity values should be considered as a low to moderate factor of prospectivity.

Based on the standard deviations of frequencies of spatially associated deposits, we have calculated the "evidence scores" for various lithological units (R), various buffer distances to faults with various orientations (F), various buffer distances to intrusive units (I) and various ranges of magnetic (M) and gravity value (G). For calculating these scores, we divided the frequency to the standard deviation using the Calculate Field tool from the Data Management Toolbox.

2. For carrying out the second step, it was created a network of 1km/1km cells (using the Fishnet tool from the Data Management Toolbox, Feature Class tools subset). This layer was further joined with the layers containing the so-called "weighting scores". In this way, to each cell it was assigned the value of the "weighting score" of the polygon that it falls in, from the joined dataset layer. The fishnet was also joined with the point layers of the mineralized boulders and outcrops and drillhole collars. The weighting scores for these have been calculated in a similar manner, taking into account the standard deviation of the frequency of observations.

3. The final step implied calculation of the "prospectivity scores" as sums of the "weighting scores" of various datasets. The "prospectivity scores" were plotted as classified classes using the standard deviation algorithm.

GIS mineral potential modeling results

The map of the RFI score (calculated as sum of the weighting scores of lithology, faults and intrusive datasets) reflects the prospectivity of the geological factors that control the mineralizations. 80.5% of the known deposits and occurrences are reflected by values of RFI exceeding the mean, 45% of them by values exceeding the mean + 1 x standard deviation and 15% by values exceeding the mean + 2 x standard deviation. The map of the MG score (calculated as a sum of the weighting scores of magnetic and gravity datasets) reflects the prospectivity of the geophysical reflection of the mineralizations. 64.5% of the known deposits and occurrences are reflected by values of MG exceeding the mean, 29% by values exceeding the mean + 1 x standard deviation and 14% by values exceeding the mean + 2 x standard deviation. The map of the RFIMG score (calculated as a sum of the RFI and MG scores) reflects the prospectivity of the geological controlling factors and geophysical reflection of mineralizations. 77.5% of the known deposits and occurrences are reflected by values of RFIMG exceeding the mean, 42% by values exceeding the mean + 1 x standard deviation and 15% by values exceeding the mean + 2 x standard deviation. The map of the RFIMGOHBT score (calculated as a sum of the RFIMG prospectivity score and the weighting scores of mineralized outcrops and boulders datasets) reflects the prospectivity of the geological and geophysical datasets. 87% of the known deposits and occurrences are reflected by values of RFIMGOHBT exceeding the mean, 55% by values exceeding the mean + 1 x standard deviation

and 31% by values exceeding the mean + 2 x standard deviation. The map of the RFIMGOHBTD score (calculated as a sum of the RFIMGOHBT prospectivity score and the weighting scores of drillholes dataset) reflects the prospectivity of the all datasets. 91% of the known deposits and occurrences are reflected by values of the RFIMGOHBTD score exceeding the mean, 61% by values exceeding the mean + 1 x standard deviation and 42% by values exceeding the mean + 2 x standard deviation. 95.5% of the medium to large size deposits are reflected by values of RFIMGOHBTD exceeding the mean, 73% by values exceeding the mean + 1 x standard deviation and 60% by values exceeding the mean + 2 x standard deviation (fig. 3).

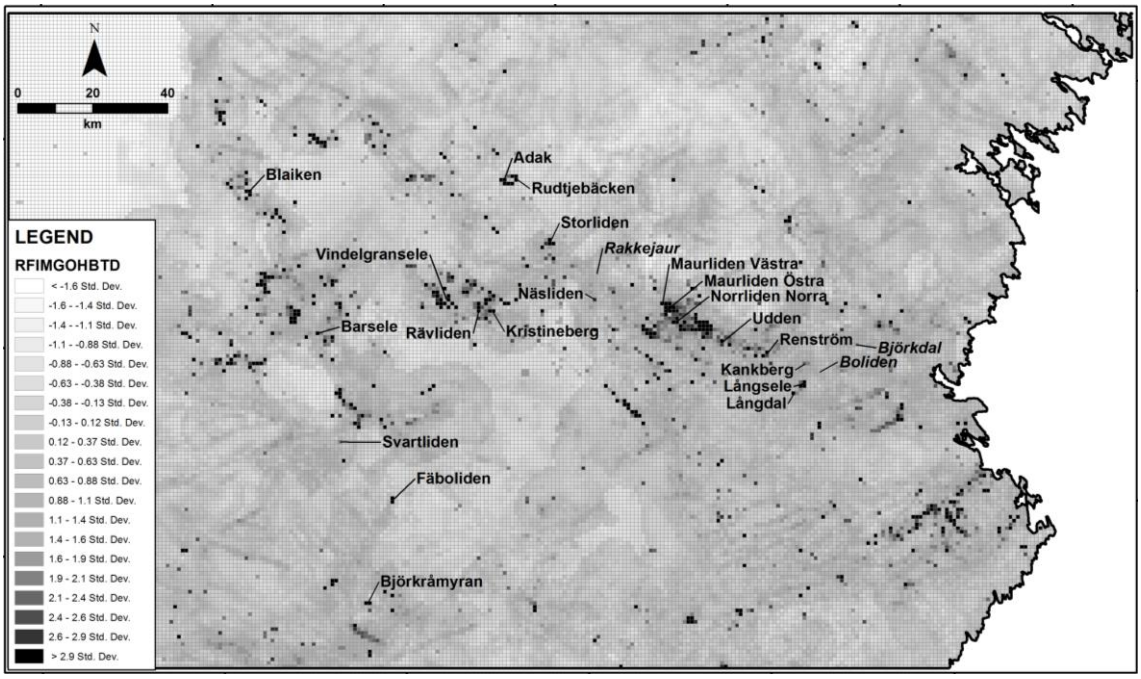

Fig. 3. The prospectivity map of the Skellefte region. The prospectivity increases from white to black. The values in the legend are multiples of the standard deviation in respect with the mean of the RFIMGOHBTD scores (see the text). The labels indicate the main deposits in this region.

Conclusion

Taking into account the last observation, the authors of this study consider that the map of the RFIMGOHBTD score can be used with high confidence for targeting further exploration programs. Several highly prospective zones (with the RFIMGOHBTD score exceeding the mean + 2 x standard deviation) have been selected for further detailed review of the geological setting and historical exploration data and results).

Acknowledgments

The authors thank to the management of Eurasian Minerals Inc. for the permission to make public this study that originally was carried out for this company. Special thanks to Mr. Eric Jensen, General Manager of Exploration, who encouraged us to carry out such study. Eurasian Minerals Inc. (TSX-V: EMX; NYSE: EMXX) is a Canadian registered company that carries out exploration in Sweden, Turkey, United States, Australia, New Zeeland and Haiti. This company currently holds 28 exploration licenses in Sweden.

Selected references

Bonham-Carter, G.F., 1997. Geographic Information Systems for Geoscientists (2nd edition). Computer Methods in the Geosciences series, Vol. 13, Pergamon Ed., 398 p.

Carranza, E.J.M., Sadeghi, M., 2010. Predictive mapping of prospectivity and quantitative estimation of undiscovered VMS deposits in Skellefte district (Sweden). Ore Geology Reviews 38 (2010), 219–241.

Eilu, P. (ed.), 2012. Mineral deposits and metallogeny of Fennoscandia. Geological Survey of Finland, Special Paper 53, 401 p.

Kathol, P., Weihed, P. (ed), 2005. Description of regional geological and geophysical maps of the Skellefte District and surrounding areas. Sveriges Geologiska Undersökning Ba 57.

COST BENEFIT ANALYSIS IN VERMINCE LIMESTONE DEPOSIT REPUBLIC OF KOSOVO

Sylejman HYSENI[1]*, Bedri. DURMISHAJ[1], Ahmet BYTYQI[2]

[1]Public University of Mitrovica, Faculty of Geosciences, Mitrovice 54000, Kosovo
[2] Departments of Engineering, DPQ-KEK, Kastriot, Prishtine 10000, Kosovo
*Tel +377(0) 44136020; E-mail: *sylejman.hyseni@uni-pr.edu*

Abstract: In this paper a functional model is presented as an important tool for the economic evaluation study of the deposits of carbonate rocks. One such model is applied to limestone mineral deposit "Vermnice" exploited by the company "Bajraktari". So for a fair assessment of investment in technology to acquire a cubic meter of useful minerals should refer to Benefit/Cost Analyses (B/C) for these mineral resources in Kosovo.

Keywords: limestone, cost benefit, deposit, reserves, Vermnice, Kosovo

Introduction

Kosovo is rich in deposits of carbonate rocks (Fig.1), which include limestone, dolomite and marbles. There are 402 deposits of carbonate rocks in Kosovo, having a total of geological reserves of 25,134.7 Mill.m^3. These resources, together with deposits of silicate rocks represent a good basis for economic development of Kosovo (Barth, et. al., 2006). Therefore for these geological resources it is necessary a planning and evaluation exploitation of these row minerals. Therefore, for evaluation of capital investment in this segment of economy it should be taken into the current level of scientific achievement and technological possibilities of production, the possibility of a applying method called Cost Benefit Analyses (B/C). Cost benefit analysis during the implementation of projects using limestone provides a more appropriate basis for assessing the perspective of deposit exploitation through implicit forecast costs and potential effects arising during conduct of mining activities (Hyseni. et. al., 2013).

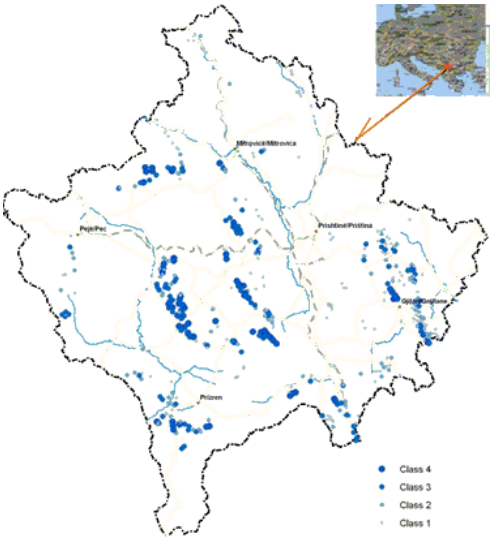

Figure 1. Spatial Distribution of Mine ability of Carbonate Hard Rocks. Scale 1:1,000,000 (modified after Beak, 2006)

Assessing the cost of opening and use of the limestone deposit

Given the analysis of economic evaluation process we use surface deposits of useful minerals besides technical and technological indicators should be analyzed the level of investment and production costs as the main factors to evaluate the costs of the extraction and processing as well as sale price than 1m^3 of limestone rock. In determining the cost of extraction and processing of 1m^3 limestone usually one have to take into account all the necessary actions that enable exploitation and processing and therefore also in this context the building structure of the sale price that 1m^3 should be based on the costs that are made during production (exploitation). Income from carbonate rocks fractions benefit can be filed on the basis of the relation (1) who expresses the amount of product between annual production and selling price per unit product:

$$\mathbf{R = S\,(Qy * Ps)} \quad [€] \qquad (1)$$

Where : R= revenue from the sale of production
Qy = annual production
Ps= product selling price per unit

Selling price of a unit of limestone fractions (Ps) said the amount of the cost of expenses (Cp) and profit planning (P).

$$\mathbf{Ps = Cp + P} \qquad (2)$$

Where : Cp = cost price
P = planned profit

The cost of gaining 1 [m^3] fractions of carbonate rocks is determined by the amount of direct (Dc) and indirect (Ic) expenses

$$\mathbf{Ps = Dc + Ic} \qquad (3)$$

Where : Dc = direct costs (these are the costs of labour, materials and equipment costs)
Ic = indirect costs

For operating costs (Oc): submit costs for engaging the workforce in the manufacturing process (Mp)

$$\mathbf{Oc = Mp} \qquad [€/m^3] \qquad (4)$$

Material costs (Mc): represent the costs necessary for the implementation of certain technological process operations: drilling-blasting, loading, separation, etc. To carry out these operations in the process of using beneficial minerals needed: fuel, explosive etc. **(**Mc_{fe}**)**

$$\mathbf{Mc = \Sigma\ (Mc_{fe})} \qquad [€/m^3] \qquad (5)$$

To carry out every technological process during the development of mining activity in the utilization of useful minerals, different materials are needed, such as: fuels, explosives, oils etc. It is therefore of course that with this case for determining the necessary quality of materials used normative consumer's productive work.

Operating costs of equipment (O_{ce}): represent the commitment costs of the equipment necessary for carrying out the process (O_{ce}):

$$\mathbf{O_{ce} = \Sigma\ O_{ccp}} \qquad [€/m^3] \qquad (6)$$

Indirect costs (Ic) - represent expenses that are not made directly from the working process: deposit geological research, drafting technical documentation technology, infrastructure construction, various compensations properties that will be included in mining activity and royalties (Hyseni, et. al., 2012). Drafting of technical documentation: has the value of **32 000 €.**

Compensation: Any company that uses any useful mineral reserves is regulated by legal acts to compensate the damage caused to the environment and the community in the form of royalty, for the waters, environment and depreciation of plant.

Royalties: The holder of the license for the use of mineral raw material is obliged to pay 2% of the value of revenues from the sale of limestone products.

The Water: The holder of the license is obliged to pay 0.5% of the value of revenues from the sale of limestone products.

Forests: The holder of the license is obliged to pay 1% of the value of revenues from the sale of limestone products when using field previously forested.

Environment: The holder of the license is obliged to pay 1.5% for emission of gas and dust from the value of revenue from the sale of limestone products.

Depreciation of equipment: Mining Equipment of the investor has the value of 630000 € where the depreciation is estimated of 12% / year.

Cost of **loading** the **fragmentation**, **crumbling and transport** of 1m^3 carbonate rock is 2.435€/m^3.

According to the data is presented a summary of the cost of 1h job of mining equipments, which are engaged for loading, transport and crumbling, and drilling costs-blast of 1.43 €/m^3 (Bytyçi, 2010 and Hyseni, 2013) while detailed estimates of expenditure for earning 1 m^3 limestone fractions are presented in the Table.1

Determining the cost of using 1m^3 carbonate rocks based on annual costs by the use of 100,000 m^3, so in this case the cost is around 7.75 €/ m^3. To estimate the economic cost of production received 1 m^3 of fractions 0/90 mm, for which the annual costs are calculated according to the formula (1) and expression (2) which can be formed where the sales price fractions produced by the company, "Bajraktari" if arrange advance rate margin (profit) that usually ranges between (20-30 %) of the value of cost where to take our case 26%, then it could have P = 2.1€/m^3. Ps = 7.75+2.1 Ps = **9.85** €/m^3

Given this calculated sales price of fractions 0/90 mm, and annual production of 100,000 m^3,the revenues are: P= 100 000 x 9.85 **P= 985000** [€/y]

After determining the revenue from the sale of carbonate rocks products, this should be compared with the costs that are created in order to have an overview about how much usually gross profit represents profit excluding VAT (value added tax). So the company, "Bajraktari", has in its production plan these fractions of the carbonate rocks.

Annual degree production costs **are 374840 €,** in addition to the cost of production one have also to add the cost of marketing, sales, financial management and control and other administrative costs, such costs typically range between 5-6.5 % in our case will be 18,742**€.**

Therefore, gross profit could be: $Pg = P - (Ps + P*0.05)$ (7)

$Pg =$ **935740 €**

While net profit is determined after deduction of 16% VAT $P_n = P_g - 0.16\ P_g$ (8)

$P_n = 7\ 860\ 21$ **€**

Sale price of 1 m^3 limestone rock is for Crushed rock fractions 0/90 mm of 15.0 €/m^3, Rock without separation - 5.98 €/m^3, Buffer (0-60) mm Class II 6.55 m^3.

Table - 1 The costs of production of 1 m^3 carbonate rock with separation

Type of costs	Unit measuring	100000	Unit	Unit	Annual costs	Total
			[€/m^3]	[%]	[€/year]	[€/ 24 year]
Personal income	**Salaries**		**0.42**	**0.06**	**42000**	**1008000**
Anual production 100,000 m^3/y						
Tailing	€/m^3	Random 10% Qy	1.23	0.18	10000	240000
Drilling-blasting	€/m^3	100000 m^3/vit	1.43	0.20	143000	3432000
Secondary Crumbling	€/m^3	Assumption 6% for Qy	1.46	0.21	4380	140160
Uploading	€/m^3	100000 m^3/y	0.358	0.05	35800	859200
Crumbling and separation	€/m^3	And other activities	1.321	0.19	132100	3170400
Transportation	€/m^3	100000 m^3/y	0.756	0.11	7560	181440
Countable value of spending			6.55	0.94	332840	
			6.975	**1.00**	**374840**	**7841760**
Annuities						
Royalties	2% carrying value of expenditure		0.02	0.003	7497	179928
Forestry	1% annual income value		0.01	0.0014	3748	89952
Waters	0.5% annual income value		0.005	0.0007	4925	118200
Environment	1.5% annual income value		0.015	0.0021	14775	354600
			0.05	0.0072	30945	**742680**
			7.025	**1.0072**	**405785**	**8584440**

Cost benefit analysis of opening and exploitation deposit

Methods used for the evaluation of Cost-benefit analysis of almost all projects in mining activity and other works are: Method return deadline invested assets, net present value (NPV) and the internal rate of return (IRR). Today for such assessments there are software packages such as the Xeras, Runge mining co, Enginea etc. To have such a rating and target towards the use of limestone from deposit, Vermnice "Bajraktari" Company highest on paper is set out in detail the cost benefit analysis of 1 m^3 is of such rocks. Therefore, direct investment, according to data from the deposit are approximately I_d^1 = 42,000 €. Opening deposit is associated with a preliminary administration-bureaucratic phase during which a variety of procedures must be performed ranging from research license, wide legal property procedures drafting of technical documentation so the investments made for this phase amounted to I_d^2 = 32,000 €.

Total investment in this field can be determined by: $It = (I_d^1 + I_d^2)$ (9)

It = 74000 €

So the decision on such investments in this deposit will be based on the calculation of the Net Present Value (NPV), which could be based on the service of this project as well as production costs. Benefits from investment in the future in this deposit will be compared with the generated cost of the project:

$$\mathbf{NPV} = \left[\frac{P_n}{(1+r)^n} - It \right] \qquad (10)$$

NPV = 169350 €

Where: Pn = Income

It = Total investment

R = the interest rate (discount rate) proposed by FTSE Euro top 300 is 5%

n = Exploitation time deposit (n = 1, 2, 24) in years

As NPV value > 0, the project may qualify as both profitable and acceptable. From the above analysis, we believe that the same important role plays the interest rate,"- r" in the profitability of the investment project.

Internal rate of return (Pohl, 2011) for the project of opening and using "Vermnice" limestone rock deposit can be assigned according to the expression:

$$\textbf{IRR} = \left[\frac{P_n}{(1+j)^n}\right] - It = 0 \qquad (11)$$

Or in the form of explicit:

$$\left[\frac{P_n}{(1+j)^n}\right] = It \qquad (12)$$

Where : n = time use of deposit (n = 1 year)
J = Marginal efficiency of investment

IRR calculation for a period of one year deals n = 1, then the expression (12) becomes;

$$j = \frac{P_n - I_t}{It} \qquad (13)$$

j= **9. 62**

$$IRR = \left[\frac{P_n}{(1+j)^n}\right] - It \qquad (14)$$

IRR = 13.27%

Efficiency limit value is higher than the interest rate (discount rate) (j> r).

The B/C ratio of a cash flow is the ratio of the present worth of benefits to the present worth of costs. This is defined as**:**

$$B/\ C = 1.94 \qquad (15)$$

If the B/C ratio is greater than one, then the investment is acceptable. If the ratio is less than one, the investment is not acceptable (Baritu & Omitaum 2007). Calculation of B/C is 1.94 for the exploitation project of ”Vermnice” limestone deposits of “Bajraktari Company, so it may qualify as profitable because revenues are greater than the value of the expenditure.

Conclusion

This form of exploitation project evaluation through the limestone surface Cost Benefit analysis is an argument to justify the capital investment in this branch of the economy. The bases for this assessment are superficial exploitation costs, while respecting the environment. In this case is necessary to use norms that arise from the current legal acts in compliance with the directives of the European Community (EU) and the current broad experiences of many companies involved in this activity in relation to costs that are needed to perform the whole technological process in the production of $1m^3$ fractions of carbonate rocks. Economic assessments according to the calculated data show that the deposit has perspective and the positive business.

Acknowledgements: We are grateful to Professor Ilir Alliu from the Faculty of Geology and Mining Tirana, who provided valuable suggestions, and improvements to the English text.

References

Barth, A., 2006, The Kosovo Quarry Plan Final Report (ICMM), Prishtine.

Baritu, B. A., and Omitaum, O. 2007, Computational Economic Analysis for Engineering and Industry. Francis Group, LLC-USA.

Bytyçi, A., 2010, The main project of exploitation of carbonate rocks from the deposit "Astrazub" Prishtine.

Pohl. L. W., 2011, Economic Geology, Principles and Practice, Stuttgart, Germany.

Hyseni. S., and Bytyçi. A., 2012, Economic evaluation of the deposit in the limestone quarries "BAIC - Kosmaç" MA Gllogovac, Mitrovica.

Hyseni. S, Durmishaj. B., Bytyci. A, Alliu.I, Berisha.A, etc 2013, Cost Benefit Analysis in Kosmaç limestone deposit Republic of Kosovo, International Journal of Basic and Applied Science (Vol. 01) (03): pp 664–672, Turkey.*www.insikapub.cm*/

CONSIDERATIONS ABOUT ECONOMIC OUTLOOK OF JIU VALLEY HARD COAL DEPOSITS, ROMANIA

Grigore BUIA[1], Csaba LORINȚ[1*], Monica RĂDULESCU[2]

[1]University of Petrosani, Mining Faculty, Management, Environmental Engineering and Geology Department, Universitatii street, No. 20, 332006, Petrosani, Romania
[2]Conestoga-Rovers and Associates, 1880 Assumption Street, Unit 200, Windsor, ON N8Y 1C4, USA
[*] *csabigeo@yahoo.com*, Tel.: 0040 72 355 717, Fax.: 0040 254 542 580

Abstract:
Within the current context of Romanian energy resources, the hard coal contributes about 5 to 7 percent to the electricity generation sector, as thermal coal. In the light of coal's significance for the Romanian economy, the paper analyses the opportunities of coal valorization, framed by the wider perspective of mineral production technologies, energy factors and geological reserves.

Keywords: Jiu Valley, hard coal deposit, geological reserves, energy balance

Introduction

The main aim of this paper is to bring to the attention of interested parties, such as experts from mineral production and energy generation sectors, the current state of hard coal reserves in the Jiu valley; valorization opportunities, dictated essentially by the heating value and geological reserves, are also discussed.

Regional setting

The beginnings of mining activities in the Jiu Valley date back in the 1840's, when brothers Hoffman and Karol Mardepash initiated the open pit mining of coal reserves at Vulcan, Petrosani and Petrila mines. In 1854, the founders of mining activities in Jiu Valley formed "Societatea de Mine din Transilvania-Vest" (Association of Mines from Western Transilvania).

At the end of the XIXth century, the mining activities in the Jiu Valley were organized into mining perimeters, with a total surface of 8,991.5 ha. The division by perimeters was as follows: Salgotorjan Society, with 5,572.9 ha, Uricani - Valea Jiului Society, with 2,713.1 ha, and Valea Jiului de Sus Society, with 705.5 ha.

Following World War II, a significant and profound restructuring of the coal organizational system was initiated; on September 14, 1956, according to the Order of Ministry of Finances, "Combinatul Carbonifer Valea Jiului" (Coal Entreprise Jiu Valley) was created. "Combinatul Carbonifer Valea Jiului" functioned as a standalone authority until the first of April 1969, when it has been converted into "Centrala Cărbunelui Petroşani" (Central of Coal Petrosani). "Centrala Cărbunelui Petroşani" functioned until August 1977, when it became "Combinatul Minier Valea Jiului" (Mining Entreprise Jiu Valley). In 1991, "Regia Autonoma a Huilei (RAH) România" (the Autonomous Romanian Society of Hard Coal) was created, leading to significant restructuring of the mining activities; the restructuring measures culminated with the closing (decommissioning) of the following mining perimeters: Lonea Pilier (1994), Câmpu lui Neag and Petrila Sud (1999), Dâlja (2003), Valea de Brazi (2004), Aninoasa (2006).

The series of emblematic coal history moments in the Jiu Valley are linked to the transformation of RAH into "Compania Naţională a Huilei S.A. – Petroşani" (CNH SA) (National Company of Hard Coal- SA Petrosani). On first of November 2012, several mining perimeters dissociated from CNH SA and unified into "Societatea Naţională de Închideri Mine Valea Jiului" (the National Society of Mining Decommissioning Jiu Valley). Starting December 18, 2012, the mining perimeters Lonea, Livezeni, Vulcani, Lupeni, "Prepararea Cărbunelui Valea Jiului" (Mining Processing Jiu Valley), "Staţia de Salvare Minieră şi Aparat Administrativ" (Mining Rescue Station and Administration quarters), former subsidiaries of the "CNH SA- Petrosani", constituted by union "Societatea Naţională a Huilei SA" (the National Society of Hard Coal SA).

Currently, the mining activities in the Jiu Valley are carried out under the coordination of "Societatea Naţionala de Închideri Mine Valea Jiului" (the National Society of Mining Decomissioning Jiu Valley), within the perimeters of the mining sectors Petrila, Paroşeni and Uricani and also under the coordination of the entity known as "Complexul Energetic Hunedoara S.A" (Energy Complex Hunedoara). "Complexul Energetic Hunedoara S.A" was created by the unification of several

commercial entities, namely “Electrocentrala Deva S.A.”, “Electrocentrala Paroşeni S.A.” and “Societatea Naţională a Huilei S.A.”; its main role consists of electricity generation using hard coal sourced from the mining perimeters Lonea, Livezeni, Vulcan and Lupeni, Figure 1. (CEH Portal, 2014)

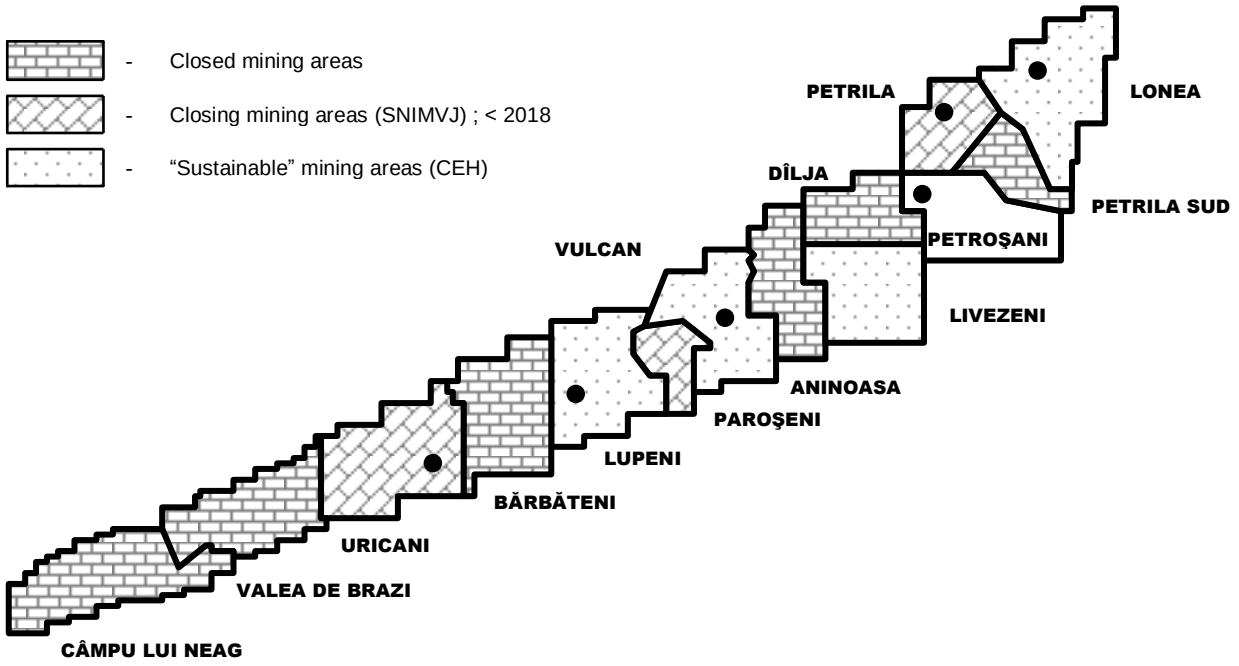

Figure 1. Spatial distribution and status of mining perimeters in the Jiu Valley

Geology of the study area

The Jiu Valley (Valea Jiului) / Petroşani basin (Figure 2) is an asymmetrical synclinal structure formed during the Alpine orogeny, and sliced by transverse faults (Figure 2). The Jiu Valley basin, with a SW–NE orientation, is 48-km long and 10-km wide on the eastern side and 2-km wide on the western side; the coal mines are distributed along the center of the valley, following the western and eastern tributaries of the Jiu River (Figure 2).

The Jiu Valley basin (Figure 2) is underlain by a crystalline basement, filled with molasse sedimentary deposits. On the basin rims, rocks of Danubian and Getic ages crop out; these rocks are represented by Neoproterozoic, Paleozoic, and Mesozoic sedimentary, volcanic and magmatic formations, presenting different degrees of metamorphism (Burchfiel, 1976; Pop, 1993; Preda, 1994; Petrescu et al., 1987; Iancu et al., 2005). The Getic crystalline rocks crop out in the north-eastern side of the basin and partially on the southern rim, consisting of gneisses, mica-schists, quartzites, and amphibolites. The overlying sedimentary deposits are of Jurassic, Cretaceous, Paleogene, and Neogene age, mostly covered by Quaternary formations. The oldest sedimentary rocks in the basin are Cretaceous, consisting mostly of flysch deposits, located on the northern and southern rims. The Cretaceous deposits are represented by conglomerates, green-grey sandstones, red marls, and minor limestones. From an economic perspective, the Oligocene deposits are the most important, as these formations contain all the coal layers, of Rupelian and Chattian ages. The Rupelian overlying the metamorphic sediments of the bedrock and the Cretaceous deposits crops out as discontinuous layers on both rims of the basin. The Rupelian deposits, 200 m to 600 m thick, consist of sandstones and green and red conglomerates with ferruginous and limestone clasts. Dîlja–Uricani Formation, of Chattian-age, also known as the „productive horizon”, contains coal seams and crops out on the southern rim of the basin, as well as in the northeastern, central, and western rims (Figure 2). The thickness of these paralic deposits ranges from 270-m to west to 350-m to east (Baron, 1998). Twenty-two layers of coal have been identified in the Chattian-age rocks, numbered as beds 0 to 21, from the bottom to the top. Beds 3, 4, 5, 7, 8/9, 12, 13, 14, 15, and 17/18 are economically feasible for extraction, bed 3 being the most productive. The thickness of these beds varies from several meters up to several tens of meters (bed 3); the estimated percentage of the Jiu Valley reserves are as follows: bed 3-48 percent, bed 5-16 percent; bed 13-10 percent; beds 4, 6, 7, 8, 9, 12, 15, 17, and 18 are thin, discontinuous and each contributes about 1-3 percent; beds 1, 2, 10, 11, 14, 16, 19, and 20 are very thin, representing a small fraction of the reserves (Pop, 1993; Preda, 1994;

Petrescu et al., 1987; Fodor et al., 2000; Fodor and Plesa, 2006; Belkin et al., 2010; Buia and Lorinţ, 2010). The Miocene deposits are between 300 m and 550 m thick, formed of grey sandstones, marls, clays, sands, and coarse conglomerate. The Quaternary consists of alluvial and pro-luvial deposits.

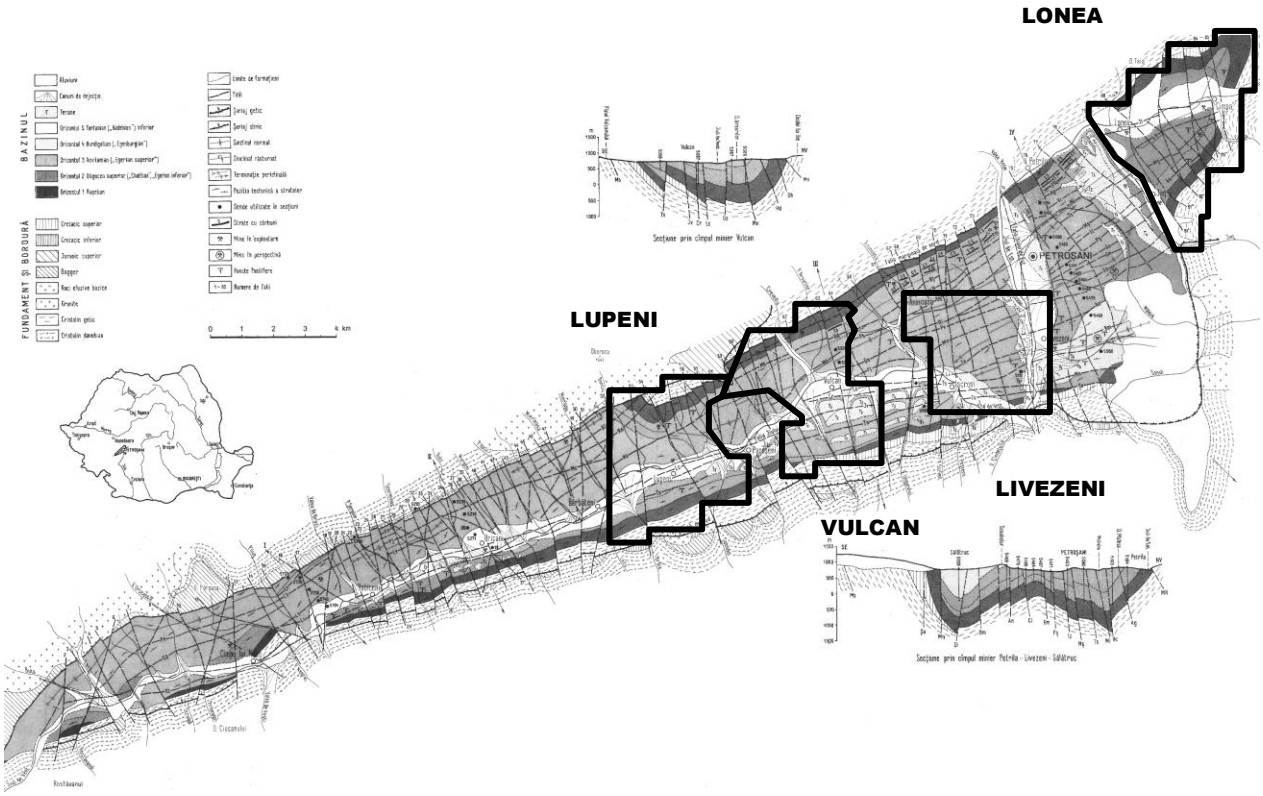

Figure 2. Geo-tectonic map of Jiu Valley / Petroşani basin study area showing the regional geology, the major synclinal axis, tectonic units and few sections in major point of interest.
Modified from Pop E.I. (1988)

Technical properties and statistics of hard coal reserves in the Jiu Valley

This section describes the main characteristics of the hard coal in the Jiu Valley. From a valorization potential perspective, the classification falls into three categories, depending on the current state of the mining perimeters, as follows; Closed (decommissioned) mining Perimeters (Table 1), Closing mining perimeters (Tables 2 and 4) and Sustainable mining perimeters (Tables 3 and 4).

Table 1. Statistics of the reserves pertaining to the closed mining perimeters (thousands of tonnes at the closing date)

Group/Category	Lonea Pilier	Petrila Sud	Dâlja	Aninoasa	Valea de Brazi	Câmpul lui Neag
Ab	0	269	746	90	710	54
Bb	0	769	0	72	393	0
C1b	52,660	48,484	56,710	0	59,128	716
C2b	0	10,332	2,657	0	9,766	0
Total recoverable, (proven) geological reserves	**52,660**	**59,854**	**60,113**	**162**	**69,997**	**770**
Aaf.b	0	98	5	461	232	0
Baf.b	0	0	0	632	209	0
C1af.b	41,693	17,783	14,869	75,109	12,270	199
C2af.b	0	9,328	9,380	23,485	5,644	779
Total probable geological reserves	**41,693**	**27,209**	**24,254**	**99,678**	**18,355**	**978**
Total geological reserves/perimeter	**94,353**	**87,063**	**84,367**	**99,849**	**88,352**	**1,748**
Total geological reserves Closed perimeters	**455,732**					
Heating value/perimeter Q (kal/kg)	**5,788**	**5,566**	**5,434**	**5,539**	**5,343**	**4,776**
Average heat content Q (kal/kg)	**5,535**					

Table 2. Reserves Statistics - Closing mining perimeters (thousands of tonnes)

Group/Category	Petrila		Paroşeni		Uricani		TOTAL	
	Quantity	Aanh (%)	Quantity	Aanh (%)	Quantity	Aanh (%)	Quantity	Aanh (%)
Ab	337	22.05	538	19.74	48	24.43	**923**	**20.83**
Bb	810	22.73	0	0.00	406	30.25	**1,216**	**25.24**
Ab+Bb	1,147	22.53	538	19.74	454	29.63	**2,139**	**23.34**
C1b	16,109	19.42	20,683	21.77	38,980	24.76	**75,772**	**22.81**
A+B+C1	**17,256**	**19.63**	**21,221**	**21.72**	**39,434**	**24.82**	**77,911**	**22.82**
C2b	1,481	32.56	1,213	24.88	8,411	23.37	**11,105**	**24.76**
Total recoverable (proven) geological reserves	**18,737**	**20.65**	**22,434**	**21.89**	**47,845**	**24.56**	**89,016**	**23.06**
Aaf.b	343	22.72	315	23.60	354	26.46	**1,012**	**24.30**
Baf.b	81	29.00	83	20.66	595	30.92	**759**	**29.59**
C1af.b	55,761	18.64	13,216	21.95	50,589	21.47	**119,566**	**20.20**
C2af.b	13,535	18.18	5,425	23.14	11,386	21.74	**30,346**	**20.40**
Total probable geological reserves	**69,720**	**18.58**	**19,039**	**22.31**	**62,924**	**21.64**	**151,683**	**20.32**
Total geological reserves Closing perimeters	**88,457**	**19.02**	**41,473**	**22.08**	**110,769**	**22.90**	**240,699**	**21.33**

Table 3. Reserves statistics – Sustainable mining perimeters (thousands of tonnes)

Group/ Category	Lonea		Livezeni		Vulcan		Lupeni		TOTAL	
	Quant.	Aanh (%)	Quant.	Aanh (%)	Quant.	Aanh (%)	Quant.	Aanh (%)	Quant.	Aanh (%)
Ab	785	19.23	113	22.47	251	24.75	1,117	27.82	**2,266**	**24.24**
Bb	362	18.25	1,246	29.78	308	27.26	1180	26.87	**3,096**	**27.07**
Ab+Bb	1,147	18.92	1,359	29.17	559	26.13	2,297	27.33	**5,362**	**25.87**
C1b	21,501	18.79	70,176	23.74	22,997	21.36	29,379	24.48	**144,053**	**22.77**
A+B+C1	**22,648**	**18.80**	**71,535**	**23.84**	**23,556**	**21.47**	**31,676**	**24.69**	**149,415**	**22.88**
C2b	0	0.00	4949	20.18	13	26.47	0	0.00	**4962**	**20.20**
Total recoverable (proven) geological reserves	**22,648**	**18.80**	**76,484**	**23.61**	**23,569**	**21.48**	**31,676**	**24.69**	**154,377**	**22.80**
Aaf.b	59	15.00	1,390	27.08	288	29.61	471	30.41	**2,208**	**27.80**
Baf.b	317	13.81	1,710	29.72	288	17.73	756	26.27	**3,071**	**26.10**
C1af.b	39,769	17.16	53,225	20.81	24,389	21.42	34,304	22.05	**151,687**	**20.23**
C2af.b	4,280	19.12	36,875	22.74	8605	20.66	16	27.40	**49,776**	**22.07**
Total probable geological reserves	**44,425**	**17.32**	**93,200**	**21.83**	**33,570**	**21.26**	**35,547**	**22.25**	**206,742**	**20.84**
Total geological reserves Sustainable perimeters	**67,073**	**17.82**	**169,684**	**22.63**	**57,139**	**21.35**	**67,223**	**23.40**	**361,119**	**21.68**

Based on the data presented in Tables 1, 2 and 3, the reserves of hard coal are as follows: **455.732** millions of tonnes in the closed mining perimeters Lonea Pilier, Petrila Sud, Dâlja, Aninoasa, Valea de Brazi, Câmpul lui Neag, **240.699** millions of tonnes in the closing mining perimeters Petrila, Paroşeni, Uricani and **361.119** millions of tonnes in the sustainable mining perimeters Livezeni, Vulcan, Lupeni –leading to a total of **1,057.550** million tonnes.

Of the total reserves, only the recoverable (proven) reserves are available for valorization, as follows: **243.556** million tonnes in the closed mining perimeters, **89.016** million tonnes in the closing mining perimeters and **154.377** million tonnes in the Sustainable perimeters, totalling to **486.949** million tonnes. To note that within the closed mining perimeters, the recoverable (proven) reserves belong over 90 percent to category C1 of reserves.

As it can be observed from table 4, the reserves from the active mining perimeters, including the closing and sustainable perimeters, amount to **94.189** million tonnes which are currently available.

Table 4. Statistics of proven and probable reserves in the active mining perimeters (thousands of tonnes)

Mining Perimeter	Coal Bed	Characteristics of the coal bed	Proven			Probable			Total		
			Quantity	Aanh (%)	Q (kal/kg)	Quantity	Aanh (%)	Q (kal/kg)	Quantity	Aanh (%)	Q (kal/kg)
Lonea	3	block II - III level 200, block VII, level 380	1,389	40.40	3,861	12,042	41.90	3,739	13,431	41.74	3,752
	5	block II - III level100	127	27.80	4,881	344	32.60	4,492	471	31.31	4,597
	Total		**1,516**	**39.34**	**3,946**	**12,386**	**41.64**	**3,760**	**13,902**	**41.39**	**3,781**
Petrila	3	block II level -300, eastern side block II -200 - 250	1,352	40.25	3,922	7,194	45.10	3,537	8,546	44.33	3,598
	Total		**1,352**	**40.25**	**3,922**	**7,194**	**45.10**	**3,537**	**8,546**	**44.33**	**3,598**
Livezeni	3	block VI, VIA, III, VII and VIII to level 150	1,563	47.21	3,332	12,085	50.30	3,088	13,648	49.95	3,116
	5	block VII				3,159	39.07	3,974	3,159	39.07	3,974
	13	block X-VIII Iscroni, between level 50 and 200	197	40.16	3,888	1,121	23.24	5,223	1,318	25.77	5,023
	Total		**1,760**	**46.42**	**3,394**	**16,365**	**46.28**	**3,405**	**18,125**	**46.29**	**3,404**
Vulcan	3	block VI, VII, VIII and IX to level 260	656	44.7	3,837	5,412	36.31	4,532	6,068	37.22	4,457
	5	block VII to level 250, block VIII-IX	55	49.52	3,437	1,247	45.78	3,747	1,302	45.94	3,734
	Total		**711**	**45.07**	**3,806**	**6,659**	**38.1**	**4,385**	**7,370**	**38.76**	**4,329**
Paroşeni	3	block 0 - VI between 350 and 200			7,545	11,032	47.68	3,590	11,032	47.68	3,590
	5	block 0, I and II between level 200 and 400	763	42.95	3,982	1,356	39.94	4,232	2,119	41.02	4,142
	Total		**763**	**42.95**	**3,982**	**12,388**	**46.83**	**3,660**	**13,151**	**46.61**	**3,679**
Lupeni	3	block II to 200, block II N, IV,V and VI	2,881	44.12	3,957	13,032	45.10	3,876	15,913	44.92	3,890
	5	block VI level 300-350				744	49.32	3,524	744	49.32	3,524
	Total		**2,881**	**44.12**	**3,957**	**13,776**	**45.33**	**3,857**	**16,657**	**45.12**	**3,874**
Uricani	3	block IIIN, IV, V and VI between level 350 and 250	545	46.61	3,778	13,454	46.92	3,753	13,999	46.91	3,754
	5	block IIIN, IV, V and VI between level 400 and 250	57	38.02	4,483	2,382	33.45	4,859	2,439	33.56	4,850
	Total		**602**	**45.80**	3845	**15,836**	**44.89**	**3,919**	**16,438**	**44.93**	**3,916**
TOTAL	**3**		**8,386**	**43.66**	**3,798**	**74,251**	**45.50**	**3,676**	**82,637**	**45.31**	**3,688**
	5		**1,002**	**41.11**	**4,095**	**9,232**	**39.24**	**4,193**	**10,234**	**39.42**	**4,183**
	13		**197**	**40.16**	**3,888**	**1,121**	**23.24**	**5,223**	**1,318**	**25.77**	**5,023**
	Total		**9,585**	**43.32**	**3,831**	**84,604**	**44.52**	**3,753**	**94,189**	**44.40**	**3,761**

- closing mining perimeters

Conclusion

Based on the current organizational structure of the coal system, the 2013 coal production from the active mining perimeters, respectively closing perimeters Petrila, Paroşeni and Uricani and sustainable perimeters Lonea, Livezeni, Vulcan and Lupeni amounted to 1.5 million tonnes (0.4 million tonnes, respectively 1.1 million tonnes), with a heating value of 3,600 kal/kg; this resulted in 2,700 GWh/year, for combustion factors representative of the current technology of 3.6 Gkal/t hard coal of Jiu Valley and 2 Gkal/Mw), representing about 5-7 percent of the electric energy produced in Romania, this being 54,358 GWh/year.

Given the energy balance, 94 million tonnes of hard coal from the currently proven reserves in the active mining perimeters can sustain the coal consumption for the next 60 years.

The recoverable reserves from the closed and closing mining perimeter can also be valorized through alternative methods, such as internal combustion.

References

Baron M., 1998. Coal and society in Jiu Valley. The period between the two World Wars. (Cărbune şi societate în Valea Jiului. Perioada interbelică.) (in Romanian). Ed. Universitas, Petroşani, p. 109–130.

Belkin H. E., Tewalt S. J., Hower J. C., Stucker J.D., O'Keefe J. M.K., Tatu C. A., Buia Gr., 2010. Petrography and geochemistry of Oligocene bituminous coal from the Jiu Valley, Petroşani basin (Southern Carpathian Mountains), Romania. International Journal of Coal Geology 82, p. 68–80.

Buia Gr. and Lorinţ C., 2010. Hard Coal Deposits in Romania. (Depozite de huilă din România) (in Romanian). Revista Minelor, vol. 16, No. 3, p. 9-14.

Burchfiel B.C., 1976. Geology of Romania. Geological Society of America Special Paper 158, p. 82.

Fodor D., Baican G., Pasarin C., Bonci G., 2000. Coal mining in Romania at the beginning of the 21st Century. In: Ghose A.K., Dhar B.B. (Eds.). Mining: Challenges of the 21st Century. A.P.H. Publishing Corp, New Dehli, p. 117–135.

Fodor D. and Plesa V., 2006. Present situation of underground coal mining in Valea Jiului-Romania. Journal of Mines, Metals & Fuels 54, p. 266–273.

Iancu V., Berza T., Seghedi A., Maruntiu M., 2005. Palaeozoic rock assemblages incorporated in the south Carpathian Alpine thrust belt (Romania and Serbia): a review. Geologica Belgica 8, p. 48–68.

Petrescu I., Nicorici E., Biţoianu C., Ţicleanu N., Trodos C., Ionescu M., Mărgarit Gh., Nicorici M., Duşa A., Pătruţoiu I., Munteanu A., Buda, 1987. Geology of coal deposits. Vol. II – Deposits from Romania. (Geologia zăcămintelor de cărbuni. Vol. II – Zăcăminte din România). (in Romanian) Ed. Tehnică, Bucureşti.

Pop E.I., 1993. Geological Monography of Petroşani Basin. (Monografia geologică a Bazinului Petroşani.) (in Romanian) Ed. Academiei Române, Bucureşti.

Preda I., Bădăluţă A., Turculeţ I., Barus T., Androhovici A., 1994. Geology of coal deposits. Vol. II. (Geologia zăcămintelor de cărbuni. Vol. II). (in Romanian) Ed. Universităţii din Bucureşti.

*

CEH Portal, 2014. Mining in Jiu Valley. Historical milestones. (Mineritul în Valea Jiului - Repere Istorice. Date de referinţă pentru mineritul din Valea Jiului.) (in Romanian) *http://www.sdm-cenhd.ro/istoric.aspx*

Transelectrica Portal. *https://www.transelectrica.ro/web/tel/productie*

Rom. J. Mineral Deposits, vol. 87 (2014), No. 1, p. 47-52

GEOLOGICAL AND STRUCTURAL CONSTRAINTS ON THE LOCALIZATION OF NEOGENE PORPHYRY– EPITHERMAL RELATED Cu-Au (Mo), AND EPIGENETIC HYDROTHERMAL DEPOSITS/PROSPECTS FROM SOUTH APUSENI MTS., ROMANIA

Ion BERBELEAC[1]*, Sorin Silviu UDUBAȘA[2], Elena-Luisa IATAN[1], Mădălina VIȘAN[1]

[1]Institute of Geodynamics "Sabba S. Ștefănescu" of Romanian Academy, 19-21, Jean-Louis Calderon Str., 020032, Bucharest, Romania
[2]Faculty of Geology and Geophysics, University of Bucharest, 1, Nicolae Bălcescu Blv., 010041, Bucharest, Romania
*ionberbeleac@gmail.ro, Tel.: (+4021)317.21.26, Fax.: (+4021)317.21.20

Abstract: In the South Apuseni Mountains 20 porphyry epithermal Cu-Au (Mo) and related epigenetic hydrothermal deposits/prospects are known, their localization being influenced especially by the preexisting geologic elements such as: 1) the nature and geometry of rocks existing before of major extensional event and 2) the Karpatian-Badenian (17-15 Ma) volcano-tectonic basins of Zarand, Hălmagiu-Brad-Săcărâmb and Zlatna-Stănija existing before the main extensional events. The extensional events were associated with coupling steeply fault systems and deeply detached, transverse steep faults and faults intersection, strong uplift and exhumation of Mesozoic nappes with competent units of flat-laying stratigraphic packages. As the result of these events the region has been divided into tectonic basins and blocks in which the deposits/prospects appear within the basins or/and at the margin of basins.

Key words: South Apuseni Mountains, volcano-tectonic basins, extension, porphyry epithermal Cu-Au (Mo) and epigenetic hydrothermal deposits/prospects

1. Introduction

The porphyry epithermal Cu-Au (Mo) and related epigenetic hydrothermal deposits/prospects from South Apuseni Mountains (SAM) occurred during Neogene magmatic-metallogenetic events overprinting earlier extensional tectonic settings. Structural localization of ore deposits arises several basic assumptions(Gow and Walshe, 2005), including: 1) the basement architecture concerning the rocks before the major extensional events; 2) the nature and geometry of basement rocks that host the ore deposits and 3) the structural architecture concerning the faults developed during the extensional events. This paper reviews, at regional-scale, the relationships and the role of preexisting extensional crustal architecture in the localization of Neogene porphyry epithermal Cu-Au (Mo), and epigenetic hydrothermal deposits/prospects from SAM.

2. Regional Tectonic and Geologic Setting

The SAM consist of Drocea Mountains (DM), Metaliferi Mountains (MM) and Trascău Mountains (TM). They are separated from the South Carpathians by the WNW-ESE South Transylvanian Fault (Savu, 1996) (Fig. 1) and from the North Apuseni Mountains (NAM) by a "late" NE-SW Variscan shear belt (320-300 Ma) named Highiș-Biharia shear zone (Dallmeyer et al., 1999, in Seghedi, 2004) and composed of mylonitic granites and low-grade metamorphic schists. The SAM belong to the European Tethyan Chains and lie in the eastward prolongation of Eastern Alps and probably from here they continue south-eastwards in the Balkanides, Serbo-Macedonian Massive and the Vardar Zone (Săndulescu, 2013).

The present-day SAM is a region of Cenozoic heterogeneous distributed deformations, subjects of debate. We subdivided the SAM region into tectonic blocks based on fault orientations, and the position of Hălmagiu-Brad-Săcărâmb, Zlatna-Stănija and Bucium-Roșia Montană tectonic basins (Fig.1).

The Middle Jurassic oceanic crust (tholeiitic ophiolites) and Late Jurassic island arc calc-alkaline volcanics, and Late Jurassic-Late Cretaceous sedimentary formations, represent Transylvanides (Săndulescu, 1984) – a Middle and Late Cretaceous nappe systems. The evolution of SAM continues with Late Cretaceous-Paleogene "banatitic" magmatism (65-80 Ma; Berza et al., 1998; Ciobanu et al., 2004), focused along two alignments: 1) one, major, N-S strike, situated between Luncșoara and Ilia, represented by intrusions and volcano-sedimentary formations (Ștefan, 1986; Ștefan et al., 1992) and 2) another one, minor, WNW-ENE, in the central part of MM (Porcurea-Voia-Almășel; Berbeleac, 1975) and Trascău Mountains (Ștefan et al., 1992). The both alignments cut the ophiolites. The sedimentation continues with Late Cretaceous-Paleogene Fața Băii Formation (Roșu et al., 2001), continental sedimentary and volcano-sedimentary deposits. The Tertiary geotectonic evolution of the SAM area is pointed out by a restless tectonic regime associated to main deformations occuring within Tisza block (Csontos, 1995, in Seghedi, 2004) and Transylvanide unit (Săndulescu, 1984). A successive compression-extension events occurred along the contact between South Carpathians and SAM, reflected in South Transylvanian Fault system (Săndulescu, 1984) and Hălmagiu-Brad-Săcărâmb volcano-tectonic basin. As a consequence of these

events, the basement of crystalline schists and/or ophiolites and their Mesozoic and Lower-Middle Miocene cover deposits underwent a great varieties of deformations (rifting, faulting and graben-like small pull-apart basins) all or partially caused by the Miocene (14 - 12 Ma) rapid Tisza block clockwise rotation (~ 60°; Panaiotu et al., 1998, in Seghedi, 2004). This setting was favorable for development of the Miocene (14-7.4 Ma) - Pliocene (1.6 Ma) (Roșu et al., 2001; Seghedi, 2004) dominant andesitic, calc-alkaline, partial adakitic-like volcanism and Miocene related mineralizations. The authors agree with the following general assumptions, with respect to the Neogene magma compositions and related ore fluids in SAM: 1) the Tertiary Cu and/or Au porphyry deposits are formed from dominantly magmatic fluids (Gustafson and Hunt, 1975, in Gow and Walshe, 2005) ± basinal or wall rock derived fluids components (Bowman et al., 1987, in Gow and Walshe, 2005); 2) the deposits have formed close to a hot intrusive system probably with the aid of advective hydrothermal system (Dille and Einaudi, 1992, in Gow and Walshe, 2005) and 3) the deposits have formed at collisional margins (Sillitoe, 1972, in Gow and Walshe, 2005).

3. The Alpine major extensional events

The SAM, in their geodynamic Alpine evolution, had four major extensional regimes more or less accompanied by magmatism and metallogenetic events, such as: 1) the Middle-Late Jurassic ophiolites and island arc calc-alkaline volcanites with base metals ± gold mineralizations, Vorța type; 2) the Upper Cretaceous - Paleogene calc-alkaline magmatites ("banatites") with Au-Ag and Au-Ag-Pb-Zn-Cu mineralizations, Băița-Crăciunești type; and 3) the Karpathian - Early Badenian (17-15 Ma) episode considered as the opening moment of the Hălmagiu-Brad-Săcărâmb volcano-tectonic basin, along NW-SE fault and possibly along WNW also, Zarand basin (Drew and Berger, 2001); similar ages seems to be recorded also for the other basins; a pre-existing anisotropy inherited from the Jurassic geological elements being favorably; and 4) the Badenian-Pannonian (13.5-9.3 Ma) productive and dominant calc-alkaline magmatism and related porphyry epithermal Cu-Au(Mo) and/or Au-Cu(Mo) as well as a great variety of epigenetic hydrothermal mineralizations. The volcanic activity had two peaks at 14.6-10.77 Ma and 9.3-7.4 Ma (Roșu et al., 2001).

4. Basement

The major preexisting geological architectures with implications in the formation and localization of Neogene porphyry epithermal Cu-Au(Mo) and related epigenetic hydrothermal deposits can be influenced by (Gow and Walsh, 2005): 1) the nature and the geometry of pre-extension event rocks, and 2) the crustal faults, the thrust and nappe structures.

The basement of SAM belongs to: 1) the pre-Alpine Paleozoic metamorphic schists of Păiușeni series in Răstoci-Miezeș area (ZM) (Berbeleac et al., 1984), Precambrian high-grade schists of Baia de Arieș series (MM) (Ciobanu et al., 2004) and Padeș Paleozoic schists at Bocșa-Săcărâmb deposits (Udubașa et al., 1976); and 2) the Alpine basement composed of Middle Jurassic ophiolites, especialy basalts (e.g. Musariu, Băița Crăciunești deposits), Late Jurassic island arc calc-alkaline volcanics, dominantly andesites, Late Jurassic - Early Cretaceous limestones (Voia) and Cretaceous sedimentary rocks (Muncăceasca Vest, Runculețe, Valea Tisei, Bucium-Tarnița, Roșia Poieni) superposed as Transylvanide nappes (Săndulescu, 1984, 2013) – complex nappe structure.

5. Stratigraphic blocks

In SAM the rock package that hosts porphyry related deposits/prospects predominates in the interior and at the margin of the blocks, in the both cases this mean the Zarand, Hălmagiu-Brad-Săcărâmb, Zlatna-Stănija and Bucium-Roșia Montană volcano-tectonic basins. From west toward east, the basin areas formally can be roughly divided in the following tectonic blocks (Fig. 1): 1) central-western part of MM, dominant ophiolitic and island arc calc-alkaline volcanics and Jurassic granitoides, partially interrupted by the Hălmagiu-Brad-Săcărâmb volcano-tectonic basin filled by Fața Băii Fm., lesser Neogene volcanic rocks; 2) eastwards, the ophiolites of the first block continue in Ribița, Curechi-Stănija and Balșa-Techereu-Almașul Mare mini-blocks; at east of these, the blocks (3) Bucium and (4) Feneș-Trascău can be separated, where Early and Late Cretaceous flysch formations and Neogene dacite and andesite rocks prevail; in comparison to blocks 1 and 2, there are no ophiolites within the block 3.

There are sedimentary rocks (e.g. shales and marls) within SAM that played the role of barriers in the fluids way and imprinting heterogeneous features to the stratigraphic sequence. As examples of barrier rocks we mention the Cretaceous shales from Neagra gold deposit (MM) in which the vein mineralization disappears quickly (Ghițulescu and Socolescu, 1941), or the Badenian marls from Fața Băii-Larga gold pyrite lenses where the marls acted like a screen for ore solutions (Ciobanu et al., 2004). A similar role

had the black shales from Bucium Rodu gold deposit. Contrary, the andesites, conglomerates and sandstones are mechanically competent and very good receivers for mineralizations.

6. Fault, thrust and nappe architecture

The development of large mineralizing systems from Neogene volcanic structures of SAM that host porphyry epithermal Cu-Au (Mo) and other epigenetic hydrothermal deposits/prospects is strongly influenced by both mechanical and chemical processes. According to Gow and Walshe (2005) the mechanical properties of the basement in continental arcs affect the intensity, geometry and distribution of faults development and the magnitude of displacements. Due to these favorable properties, it was possible that the Sarmatian-Panonnian multi-stadial andesitic-porphyry diorite subvolcanic intrusions (Musariu, Valea Morii Nouă, Muncăceasca Vest, Roșia Poieni and others) to be hosts of porphyry Cu-Au(Mo) and epigenetic hydrothermal systems; in addition to contrasting rock types, the chemical properties of basement rocks, fluids and thermal events are associated. The mosaic block style is generally characteristic for Sarmatian - Pannonian NW-SE volcano-tectonic basins. This style is associated with syn-rift structures, coupling steeply fault systems and deeply detached, transverse steep faults and fault intersections, strong uplifts or down-lift and exhumations of Mesozoic nappes with competent units of flat-laying stratigraphic packages (e.g. Voia, Fig 2). These aspects are known within the Drocea-Techereu ophiolitic nappe and other nappe blocks. One of the most important crustal faults, formally named Mureș-Brad-Beiuș transcrustal fault, possibly limits the east side of Hălmagiu-Brad-Săcărâmb volcano-tectonic basin. This fault seems to have right-lateral displacement and between Brad-Săcărâmb alignment it concentrates important volcanic structures and deposits/prospects (e.g. Săcărâmb, Hondol, Măgura, Troița-Voia and Musariu-Valea Morii, Fig. 1). Another important trans-crustal fault situated in the southern part of the Metaliferi Mountains is the South Transilvania Fault that delimitates the SAM from the South Carpathians.

Strike-slip and normal faults are related to Neogene reactivation. They form a parallel group with E-W strikes as in Brad and Băița areas (Fig.1). The parallel system of the faults with NW-SE strikes, borders the Curechi-Stănija, Balșa-Techereu, Bucium and Trascău blocks.

The distribution of ore deposits seems to be especially controlled by a parallel set of Miocene faults with E-W and NW-SE strikes. The intensity of other kind of deformations, especially E-W faults, increases in the north and south parts of SAM. This is probably due to the pressing of Supragetic block in the south and the resistance of the North Apuseni Mountains in the northern part.

For the deep structure and the stratigraphic architecture (Fig. 2) we used the general geological cross-sections, scale 1:5.000.000 and 1: 2.000.000, edited by Geological Institute of Romania (M. Ștefănescu).

SAM area is built up of pre-Alpine Neogene rock packages that host porphyry Cu-Au(Mo) and gold epithermal deposits/prospects; these packages consist of mixed, dominantly volcanic and sedimentary sequences, followed by ophiolites ± island arc volcanics; in a single place, at Baia de Arieș, the crystalline schists are hosts of gold and polymetallic deposits. In general, at regional scale the mechanical properties and geometry of the basement host rocks, apparently are similar, but in detail they differ from one to another deposit/prospect, or setting. For instance, the strength contrast becomes more evidently in variable deformation styles and strong strain partitioning in the stratigraphy with respect to: the geometry of blocks and rocks, the degree of coherence, the intensity of thermic and hydrothermal processes, the petrographic composition and the degree of faulting. The Fața Băii Paleogene and Badenian-Sarmatian volcano-sedimentary formation, Jurassic ophiolites and island arc volcanics, as well as Neogene andesitic and dacitic packages have a heterogeneous distribution of rock strength and permeability through the stratigraphic sections. In each deposit or mineralization there exist strength contrast which is not similar with another deposit/prospect even if it is situated in the same tectonic setting (e.g. Musariu-Valea Morii Nouă, Cireșata, Muncăceasca Vest-Trâmpoiele).

The mechanical proprieties of the basement affect the intensity and faults localization as well as the magnitude of displacement. The SAM represents Middle and Upper Cretaceous nappe systems well documented by a great volume of exploration and mapping data. These nappe systems consist and include (Fig. 2) Supra-getic nappe with Paleozoic crystalline schists which crops within the SAM, in Rapolt area (Berbeleac, 1967). Mapping by many authors (Ianovici et al., 1976; Ghițulescu and Socolescu, 1941) has shown that these systems have been partially reactivated (nappes, faults) in Tertiary. The E-W, NE-SW and NW-SE faults alignments are characteristic for Alpine basement in SAM.

The nappe systems have been cross cut by Mesozoic and Tertiary faults, many of them being, in fact, reactivated in Tertiary. They have been generated by the deformations of European Continental Margin, the Oceanic Tethyan Domain and the Preapulian microcontinent (Săndulescu, 2013). The nappes are

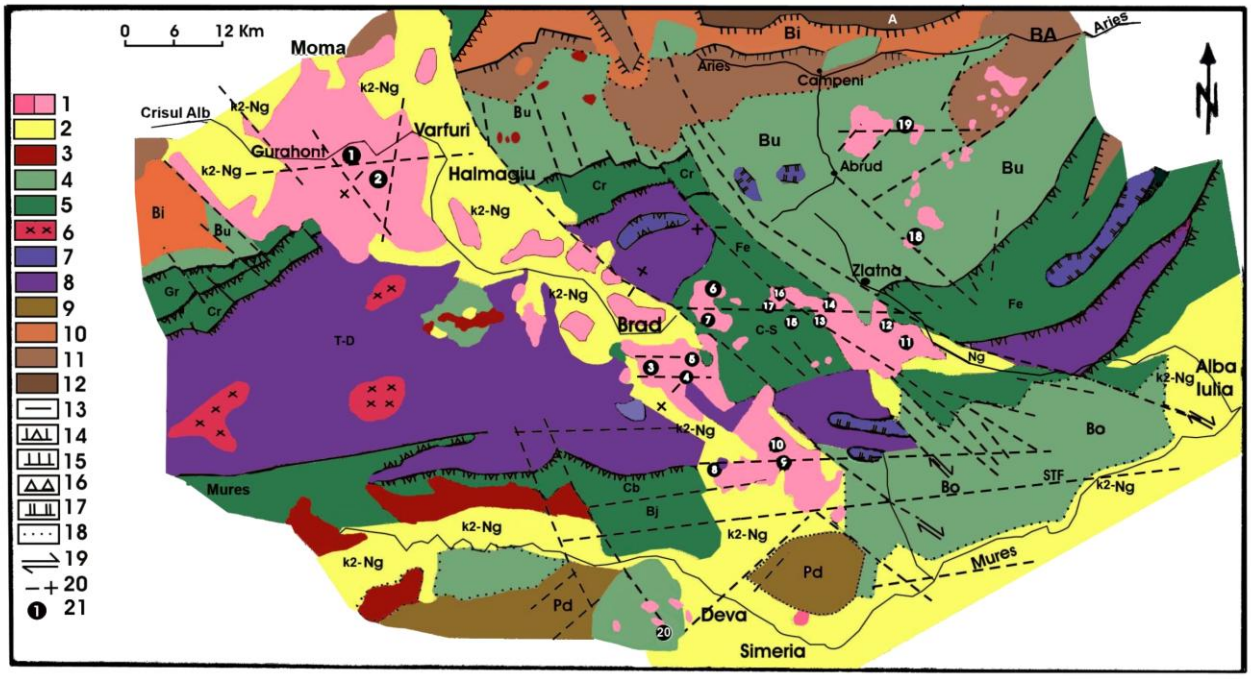

Fig. 1: Sketch map of the SAM with location of porphyry epithermal Cu-Au(Mo) and epigenetic hydrothermal deposits/prospects (simplified after the Geological Map of Romania edited by the Geological Institute of Romania, scale 1:50.000, Abrud, Zlatna, Geoagiu, Deva, Brad sheets; modified by Berbeleac et al, 2005). 1. Tertiary volcanic rocks: a. Neogene and b. undifferentiated volcanics (Uroi trahyandesite rocks); 2. K_2-Ng: Fața Băii Fm. – Upper Cretaceous - Neogene sedimentary deposits; 3. K_2-Pg: Banatitic rocks, undifferentiated; 4. Late Cretaceous Fm. (dominantly Bucium Unit); 5. Early Crataceous Fm. (dominantly Feneș nappe); 6. Jurassic granitoides; 7. Ardeu nappe and others; 8. Jurassic ophiolite (Drocea-Techereu nappe); 9. Padeș crystalline shists (Pz); 10. Biharia nappe system - shear zone; 11. Baia de Arieș series (Pcb); 12. Finiș-Gârda Nappe; 13. Geological boundary; 14. K_2-Pg nappes; 15. Pre-Gossau nappes; 16. Variscan nappes; 17. Mesocretaceous nappes; 18. Unconformity; 19. Thrust faults; 20. Normal fault and block movement; 21. Ore deposits/prospects.
A – Finiș-Gârda nappe, Bo – Bozeș nappe, Bu - Bucium nappe, Bi - Biharia nappe, BA- Baia de Arieș nappe, Bj - Bejani nappe, Cb – Căbești nappe, T-D - Techereu-Drocea, Cr – Criș, Gr – Groși, C-S - Curechi-Stănija, STF - South Transylvanian Fault.
Ore deposits/prospects: 1. Tălagiu North, 2. Tălagiu Central-South, 3. Musariu, 4. Valea Morii Nouă, 5. Cireșata, 6. Remetea, 7. Colnic, 8. Bolcana, 9. Voia, 10. Voia North, 11. Fața Băii-Larga, 12. Trâmpoiele, 13. Muncăceasca Vest, 14. Popa-Stănija, 15. Măgura Poieni, 16. Valea Tisei, 17. Runculeț, 18. Bucium Tarnița, 19. Roșia Poieni, 20. Deva.

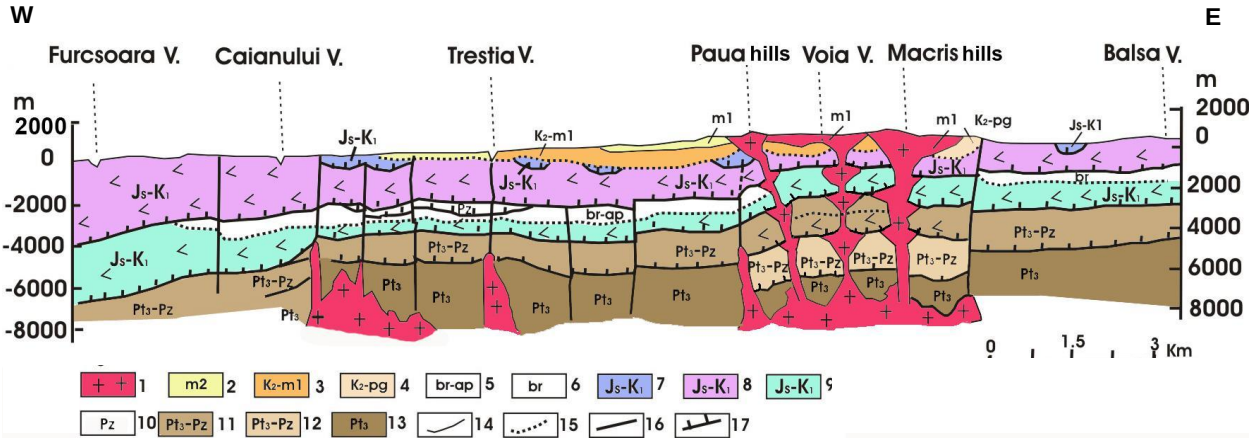

Fig. 2. Schematic tectonic section across South Apuseni Mountains (conceived by I. Berbeleac on the basis of IGR Geological cross-section Secueni-Malu Mare, Sc. 1:200.000): 1. Tertiary volcanics; 2. Late Miocene sedimentary deposits (m2); 3. Fața Băii sedimentary and volcano-sedimentary continental deposits (K_2-m1) ± Bd-Sm volcano-sedimentary deposits; 4. Fața Băii (K_2-Pg); 5. Barremian-Aptian sediments (Br-Ap); 6. Barremian sediments (Br); 7. Ardeu Nappe: Late Jurassic-Early Crecaceous limestones; 8. Middle Jurassic ophiolites - late Jurassic calc-alkaline island arc volcanic rocks; 9. Late Jurassic-Early Cretaceous sediments ± ophiolites-nappe; 10. Paleozoic shists (Highiș-Poiana nappe); 11. Muncel-Baia de Arieș nappe; 12. Curechi-Stănija Unit; 13. Biharia Unit; 14. Boundary; 15. Unconformity; 16. Fault; 17. Nappe.

composed of Cretaceous deformed units and, partly, obducted Triassic and Jurassic oceanic crust (tholeiitic ophiolites) and Upper Triassic, Jurassic and Lower Cretaceous formations. The nappe system crops out in South Apuseni - the Transylvanides. The Jurassic ophiolites cover large areas from the Main Suture Zone and Transylvanian nappes especially within Drocea-Techereu nappe. Mesozoic and Tertiary elements of previous extensional architecture can be considered: 1) the E-W alignments and faults of Jurassic ophiolites and island arc calc-alkaline volcanics; 2) the N-S and NE-SW Late Cretaceous - Paleogene banatitic alignments and faults and 3) the NW-SE Tertiary volcanic alignments, faults, inter-mountain basins (17-15 Ma), rifting, normal, strike-slip, transverse, duplex faults and crustal faults (Drew and Berger, 2001).

7. Localization of Deposits/Prospects

The Neogene deposits/prospects overprinted earlier extensional different tectonic settings, such as: 1) the interior of Hălmagiu-Brad-Săcărâmb volcano-tectonic (rifting) basin, cross cut by Mesozoic E-W reactivated parallel crustal faults and intersected by Tertiary tectono-volcanic and metallogenic alignments (e.g. Musariu, Valea Morii Nouă, Cireșata, Bolcana, Voia; Fig.1, no. 3-5, 8-10); 2) the interior of Zarand volcano-tectonic basin at the intersection of WNW crustal fault with other NW-SE and N-S strike-slip faults (Fig. 1, no.1-2); 3) the interior of Zlatna-Stănija volcano-tectonic basin (e.g. Trâmpoiele, Muncăceasca Vest, Măgura Poieni, Popa-Stănija, Valea Tisei and Runculețe; Fig. 1, no. 11-17); and 4) the interior of Bucium-Roșia Montană volcano-tectonic basin (Fig.1, no. 18-20).

It is to mention that the porphyry Cu-Au mineralizations are situated in areas with ophyolitic basement while the porphyry Cu-Mo are located in areas with crystalline basement (Boștinescu, 1985).

8. Conclusions

In the South Apuseni Mountains four major Alpine extensional events took place, related to: 1) Late Jurassic calc-alkaline volcanites with polymetallic ± Au mineralisations of Vorța Type; 2) Late Cretaceous-Paleogene ("Banatitic") magmatism and metallogenesis with Au ± polymetallic mineralizations of Băița Crăciunești type; 3) approx. 17-15 Ma rifting and opening of volcano-tectonic basins; and 4) Badenian-Pannonian volcanic and metallogenetic activity with porphyry-epithermal Cu-Au (Mo) and epigenetic-hydrothermal deposits/prospects.

In present, 20 porphyry-epithermal Cu-Au (Mo) and epigenetic-hydrothermal deposits/prospects are known in SAM from which just 2 are situated in Tălagiu area (Zarand Mts.), the rest being in the Metaliferi Mountains. Here is also formaly included the deposit situated in Deva (Poiana Ruscă Mountains).

The location of the mentioned mineralizations was controlled by: 1) the volcano-tectonic basins in deeply detached extensional faults with localized rapid magma intrusion, fracturing and fluids-fluid or fluid-wall-rock interaction, and 2) by Mesozoic deformations (faults, tectonic thrusts, nappes), Neogene and post-Paleozoic deformations and superimposed by Neogene deformations (a great variety of normal and reversed faults) etc., associated with subvolcanic structures and shallow magmatic chambers.

Acknowlegements

Authors thanks to the Director of the Institute of Geodynamics "Sabba S. Ștefănescu" of the Romanian Academy, Dr. Crișan Demetrescu, for the access to the data and the permission to publish this paper.

References

Berbeleac, I., 1967. Petrographycal and metallogenetical aspects of Rapolt Cristaline Island (Metaliferi Mountains) (in Romanian). D.S. Șed. IGG, Vol LIV/4, p. 5-21, Bucharest, Romania.

Berbeleac, I., 1975. The Petrography and Metallogenetic study of Vălișoara (Porcurea) region, Metaliferi Mountains (in Romanian). An. Inst. Geol. Geofiz., XLIV, p. 1-189, Bucharest, Romania.

Berbeleac, I., David, M., Zămârcă, A, 1984. Petrological and petrochemical data on Tertiary volcanics in eastern part of Zarand Mountains. D.S. Inst. Geol. Geofiz., 68. p. 27-46, Bucharest, Romania.

Berbeleac, I., Sandi, H., Mitrofan, H., Nutu. M-L., 2005. Structural localization of Neogene hydrothermal mineralization from South Apuseni Mountains.(in Romanian). Geological Report, Ach. Institute of Godynamics, Romanian Academy, Bucharest.

Berbeleac, I., Rădulescu, V., Iatan E.L., Vișan, M., 2012. Relationships between crustal faults, shallow magmatic chamber and Neogene porphyry Cu-Au systems at Voia, Metaliferi Mts., Romania. Rom. J. of Min. Dep., Vol. 85, no. 1, p. 38-42.

Berza, T., Constantinescu, E., Vlad, S.N., 1998. Upper Cretaceous magmatic series and associated mineralisation in the Carpathian-Balkan Orogen. Resource Geology, Tokyo, 48/4, p. 281-306.

Bostinescu S., 1984. Porphyry copper systems in the South Apuseni Mountains – Romania, Ann. Inst. Geol. Rom. LXIV, p. 163–175.

Ciobanu, C.,L., Găbudeanu, B., Cook N., J., 2004. Neogene ore deposits and metallogeny of the Golden Quatrilateral, South Apuseni Mts., Romania., In Cook N.J. and Ciobanu C.L. (Eds.) Au-Ag telluride deposits of the Golden Quatrilateral, Apuseni Mountains, Romania. Guidebook of the International Field Workshop of IGCP project 486, Alba Iulia, Romania, 31 August- 7 September 2004, IAGOD Guidebook Series, II, p. 23-88., Alba Iulia, Romania.

Dimitrescu R., 1988. Apuseni Mountains. In: Zoubek V. (ed.) Precambrian in younger fold belt, Wiley, Chichester, p. 665-673.

Drew, L.J. and Berger, B.R., 2001. Model of the porphyry copper/polymetallic vein kin-deposit system; Application in the Metaliferi Mountains, Romania. In Piestrzyński A. (ed.) Mineral deposits at the beginning of the 21st century. Exton, Penn., A.A. Balkema Press, p. 519–522.

Ghiţulescu, T. P. and Socolescu, M., 1941. Étude géologique et minière des Monts Metallifères. An Inst. Geol., 21, p. 181-464, Bucharest, Romania.

Gow, P.A. and Walshe J.L., 2005. The role of preexisting geologic architecture in the formation of giant porphyry-related Cu±Au deposits: Examples from New Guinea and Chile. Economic Geology, v. 100, p. 819-833.

Ianovici, V., Borcoş, M., Bleahu, M., Patrulius, D., Lupu M., Dimitrescu, R., Savu H., 1976. Geology of Apuseni Mountains (In Romanian). Ed. Acad. Rep. Soc. Romania, 631 p., Bucharest, Romania.

Roşu, E., Szakacs, A., Downes, H., Seghedi, I., Pecskay, Z. and Panaiotu C., 2001. The origin of Neogene calc-alkaline and alkaline magmas in the Apuseni Mountains, Romania: the adakite connection. Rom. J. Min. Dep., 79, Suppl. 2, Special Issue of the Second ABCD-GEODE Workshop, Vaţa Băi 2001, Abstracts Volume, p. 3-23.

Săndulescu, M., 1984. Romanian Geotectonics (In Romanian): Bucharest, Ed. Tehnică, 366p.

Săndulescu, M., 2013. Geological structure of Romania (in Romanian). Rom. J. Earth Sciences, vol. 87 (2013), Special issue 1, p. 51-70, Geological Institute of Romania, Bucharest.

Savu, H. 1996. A comparative study of the ophiolites obducted from two different segments of the Mureş Ocean "Normal" Median Ridge (Romania). Rom. J. Petrology, 77, p.49-60, Bucharest, Romania.

Seghedi, I., 2004. Geological Evolution of the Apuseni Mountains with Emphasis on the Neogene Magmatism – a Review. In: Cook N.J. and Ciobanu C. L. (Eds.) Au-Ag –telluride Deposits of the Golden Quadrilateral, Apuseni Mts., Romania. Guidebook of the International Field Workshop project 486, Alba Iulia, Romania, 31 August - 7 September 2004. IAGOD Guidebook Series II, p. 5-22, Alba Iulia, Romania.

Ştefan, A., 1986. Eocretaceous granitoides from the South Apuseni Mts. D.S. Inst. Geol. Geofiz., 70-71/1, p. 229-241, Bucharest, Romania.

Ştefan, A., Roşu, E., Andăr, A., Robu, L., Robu, N., Bratosin, I., Grabari, G., Stoian, M., Vâjdea, E., Colios, E., 1992. Petrological and geochemical features of Banatitic Magmatites in northern Apuseni Mountains. Rom. J. Petrology, 75, p. 97-115, Bucharest, Romania.

Udubaşa, Gh., Istrate, G., Dafin, E., Braun, A. 1976. Polymetallic mineralizations from Bocşa (North of Săcărâmb), Metaliferi Mts. (in Romanian). D.S. ale Şed. IGG, 62, p. 97-124, Bucharest, Romania.

MINERALOGY OF THE GRADISTEA DE MUNTE RARE ELEMENT MINERALS OCCURRENCE, SEBES MTS., SOUTH CARPATHIANS, ROMANIA. PART I: OXIDES AND CARBONATES

Paulina HÎRTOPANU[1*], Robert J. FAIRHURST[2]

[1]University of Bucharest, 1, Nicolae Balcescu Blv., 010041 Bucharest, RO;
[2]Technical Laboratory at Lhoist North America, Inc., 3700 Hulen Street, Forth Worth, Texas 76107, US;
* *paulinahirtopanu@hotmail.com*

Abstract. The rare element minerals Gradistea de Munte (GM) occurrence is situated in the Precambrian migmatitic gneisses of Sebes-Lotru Series, in Sebes Mts, South Carpathians, being localized in the upper course of the Orastie River. The host of mineralization contains magnetite and the zircon/cyrtolite as constituent minerals, and their rare element minerals are occurring as accessory ones and even more. The mineralogy of GM rare element minerals is very complex. Its rare Nb, Ta, REE(Y), Zr, Sn, Th and U minerals belong to the following four classes: oxides, carbonates, phosphates and silicates. The oxides class is represented by 9 supergroup/groups: pyrochlore super group (with 2 groups, proper pyrochlore and betafite) and fergusonite, columbite, euxenite, Nb-rutile, cassiterite, baddeleyite, uraninite+thorianite+cerianite groups. The secondary REE(Y) carbonates, although less widespread, are diversified, being represented by bastnasite-(Ce), bastnasite-(Y), thorbastnasite, parisite-(Ce), synchysite-(Y) and synchysite-(Ce).

Key words: pyrochlore, betafite, columbite, fergusonite, euxenite, samarskite, Nb-rutile, cassiterite, baddeleyite, uraninite-thorianite groups; REE(Y)Th-carbonates.

Introduction

The previous studies of this rock/ore mentioned the presence of the following minerals: fergusonite, columbite, loparite, thorite, cassiterite, monazite, orthite, pyrochlore, xenotime, torneboehmite, lessingite, uranothorite (Popescu et al., 2003). Also, the authors presented the distribution maps of Nb, Zr, Y, Th, U rare elements of ore in GM area. They considered the presence of the two mineralizations: of rare metal Zr, Nb, Th, U, Rb, Sn represented by zircon, pyrochlore, fergusonite, thorite, cassiterite and of rare earth elements Y, Ce, La, represented by orthite and monazite. In our study, major minerals found in about 100 polished thin sections of samples from GM rare element minerals occurrence, were studied by optical, scanning electron microscopy (SEM), and electron microprobe. The samples were collected from the main tabular body of "microcline radioactive gneiss". First, a minute optical study on the Nb,Ta,Ti, REE(Y), Zr, Sn, Th, U minerals was carried out, then they were analyzed by microprobe and SEM, which provided us the compositional information. Also, many backscattered electron images (BSEi) were carried out, these being invaluable aids in establishing textural relationships, fine scale mineral intergrowths and subtle compositional zoning. The electron microprobe data were collected on a JEOL8200 instrument located at Camborne School of Mines, University of Exeter, Cornwall, UK. Images and chemical analyses were collected using an accelerating voltage of 15KeV and 30nA beam current. X-ray spectra were collected using EDS and WDS detectors calibrated with natural and synthetic standards. Generally, some minerals were analyzed semiquantitatively for main oxide components, after which, in the future, more accurate analyses of these rare element minerals will follow.

Geological setting

The Gradistea de Munte (GM) rare element minerals occurrence is situated on the north slope of the Sebes Mts, South Carpathians, in the upper course of the Orastie River ($45^0$27'-$45^0$49' latitude North and $23^0$09'-$29^0$31' longitude East). From a geologically and structurally viewpoint, the GM area belongs to the Getic Cry- stalline, being localized in the Upper Proterozoic Sebes-Lotru Series.The Sebes-Lotru Series, metamorphosed in amphibolite facies, is represented by micaschists with cyanite and garnets, quartz-feldspat gneisses, amphibolites and amphibolite schists. The migmatitic gneisses, the host of mineralization, contain: microcline, albite, quartz, biotite/phlogopite, muscovite, zircon/cyrtolite and magnetite. The rare element minerals occur as accessory and even more, as little veins and nests, of a few cm, in the host rock. The GM rare elements mineralization comprised 4 bodies of microcline gneisses, among them the body I (one) is the best. It has dimensions of about 8Km in length, 20-80m width, with slope of 70-80^0 toward N, being oriented E-W.

Mineralogy

The mineralogy of GM rare element minerals is very complex. Its rare Nb,Ta,Ti, LREE(Y), Zr, Sn,Th and U minerals belong to the following four classes: oxides, carbonates, phosphates and silicates.

In this paper we describe rare element Nb,Ta,REE,Y,Zr,Th,U-oxides and REE(Y)Th-carbonates. The REE-Th phosphates and Nb-LREE-Y-Th-U-Zr -silicates are described in Part II (this volume).

I. Oxides class.

The GM oxides rare element minerals belong to pyrochlore supergroup (with 2 groups: pyrochlore and betafite) and to fregusonite-(Y), columbite, Nb rutile, baddeleyite, cassiterite and uraninite-thorianite groups. The pyrochlore supergroup minerals crystallize in cubic system, and have the general formula: $\boldsymbol{A}_{2-m}\boldsymbol{B}_2\boldsymbol{X}_{6-w}\boldsymbol{Y}_{1-n}$ (Atencio et al., 2010). The ***A*** site may host Na,Ca,Sr,Pb,Sn,Sb,U,Th, ***B*** may contain Nb,Ta,Ti,Sb,W,Zr, ***X*** is O with subordinate OH and F, ***Y*** is an anion, OH^-, F, H_2O, O. The symbols *m, w* and *n* represent parameters that indicate incomplete occupancy of the ***A***, ***X*** and ***Y*** sites, respectively.

A. Pyrochlore group, with Ca, Pb, Y, U^{4+}, H_2O, □, in ***A*** site; OH, F, O, H_2O and □ in ***Y*** site; high field-strength cation (Nb, Ta, Ti, Sb, W) in ***B*** site; ***X*** typically is O, but can include subordinate OH and F (Atencio et al.,2010), have the following terms in GM: **a. Hydroxycalciopyrochlore** $(Ca,Na,U,□)_2(Nb,Ti)_2O_6(OH)$, (old name "proper pyrochlore"), has Ca dominant with some U, Th, Y in ***A*** site. It is omnipresent as grains of a few mm, even one cm. In transmitted light it is light yellow, orange, amber yellow (Figs. 1.A, 2.B). Its representative variable chemical composition, with the main constituent oxides is (%wt): Nb_2O_5=44.17-60.24, Ta_2O_5=16.58-26.44, UO_2=0-27.19, ThO_2=0-5.84, CaO=2.19-4.63. Some hydroxylcalicopyrochlore grains contain ZrO_2 (≈2% wt) in *B* site. The "old uranpyroclore"**,** was discredited, and now it belongs to oxycalciopyrochlore (Atencio et al, 2010). Some grains of **"uran-pyrochlore"** have (%wt): UO_2≈20-25, Ln_2O_3≈4, CaO+ BaO ≈10, Y_2O_3≈1.5-6, and ThO_2≈2 in *A* site . Its Nb_2O_5 content varies between 40-50 and Ta_2O_5 between 10-15, U is not the dominant cation of the dominance valence at *A* site, but Ca is, reason for which we named this pyrochlore hydroxyl-calciopyrochlore. No Na content has been determined in this pyrochlore; **b**. **Oxycalciopyrochlore** $(Ca_2Nb_2O_6O)$ has the main component oxides (%wt): CaO=10.96, TiO_2= 6.75, Nb_2O_5=64.25, Ta_2O_5 = 5,Y_2O_3=9.2; **c. Oxyyttropyrochlore-(Y),**$(Y,□)_2Nb_2O_6O$, old name **yttropyrochlore-(Y),** is the most widespread pyrochlore in GM occurrence. It is yellow brown, chocolate or yellow under the microscope (Fig. 2.A). It contains beside Y dominant (≈15-25% Y_2O_3) in *A* site and some Ce, La, Nd, Dy, Gd, Yb (≈10% wt). The Nb_2O_5 content varies between 40-50 and Ta_2O_5 between 1-2%wt. The oxyyttropyrochlore-(Y) has some UO_2 and ThO_2 contents, metamictisation being very common. Also, it has very little SiO_2 content, common in metamictic and late stage hydrated pyrochlore, and also, very little Zr. The OH and H_2O contents were not determined yet.

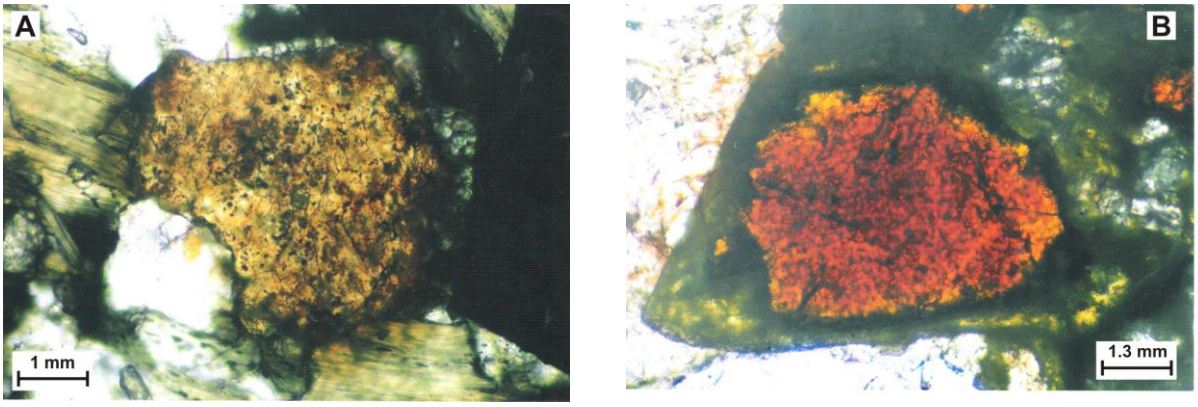

Fig 1. A Oxycalciopyrochlore (yellow), zircon (small grey grains around), sample G11-2/3; B. yttrobetafite-(Y) (big red grain), Ta-rich yttrobetafite-(Y) (yellow, around), zircon (light grey), transmitted light, NII, sample G11-4/18.

B. Betafite group. In accordance with the new nomenclature (Atencio et al., 2010) the betafites have Ti the dominant M^{4+} cation, and the new members of the betafite group were named in accordance with the dominant-valence group at the *Y* site and the dominant element in *A* site. In GM occurrence the old **"yttrobetafite-(Y)"** is present as big octahedral or elongated grains of a few mm, sometimes up to one cm. It has a red, yellow brown colour under microscope (Fig.1.B). Its representative chemical composition is (%wt): Y_2O_3=16.84, Nb_2O_5 =24,77, Ta_2O_5=1.39, ThO_2 =2.44, Nd_2O_3=0.17, UO_2=11.06, Gd_2O_3=0.44,CaO=0.5, Dy_2O_3=1.78, Yb_2O_3=1.73, TiO_2=24.5TheH_2O/OH were not determined. Generally, the main constituents of yttrobetafite-(Y) chemical composition are variable (%wt): TiO_2 = 26.94-36.08, Y_2O_3=14.65-28.84, Nb_2O_5=21.99-32.97, Ta_2O_5= 3.58-18.52, ThO_2=0-6.05, UO_2=0-13.27, CaO=0-2.41. The Y has the highest content in *A* site, reason for which we kept the old mineral name. Some yttrobetafite-(Y) grains have a zoned composition, being a very Ta rich composition towards, the

rims, Ta_2O_5=31.2%, Y_2O_3=28.8%, TiO_2=36.0%, and they do not contain Nb_2O_5. In the middle of the grain the composition is rich in Nb_2O_5, so the composition changed from yttrobetafite-(Y) inside to Ta-yttrobetafite-(Y) outside (sample G11-4/2) (Fig 1.B). The CaO content is too low to consider these minerals as oxycalciobetafite or hydroxylcalicobetafite, according to Atencio et al. (2010).

C. Columbite group. The orthorhombic minerals of this group have a general formula AM_2O_6, where *A*=Fe,Mn,Mg and *M*=Nb,Ta (Černý & Ercit, 1989). Minor quantities of Fe^{3+},Ti,Sn,W are commonly present. The GM columbites have three varieties: **a. Ferrocolumbite,** $FeNb_2O_6$, has variable chemical composition: Nb_2O_5=58.3-72.8, Ta_2O_5=4.2-13.2, FeO=16.13-23.73, TiO_2=2.43-1.79, ThO_2=0-4.23, UO_2 =0-3.35(%wt); **b.Yttrocolumbite-(Y),** $(Y,U,Th,Fe)(Nb,Ta)O_4$**,** has Nb_2O_5=49.78-58.90, Ta_2O_5=5.48-10.39, Y_2O_3=15.16-15.23, FeO=8.56-10.98, TiO_2= 2.25-5.74, ThO_2=3.57-3.59, UO_2=0-3.41, CaO=3.34-3.55 (%wt) (samples G11-2/5, GM40/2); **c. Mangancolumbite**, $MnNb_2O_6$, determined by EDS spectrum.

D. **Fergusonite group**. The general formula of fergusonite is ABO_4, where position *A* is occupied by Y and REE, and position *B* is occupied by Nb and Ta. Fergusonites have predominantly tetragonal habit with a scheelite type structure (Černý and Ercit, 1989; Ercit, 2005). The metamictization of fergusonite group in GM is very common because of the U and Th subordinated, but omnipresent contents. In transmitted light it has a brown color, and seems to be relics in yellow oxycalciopyrochlore (Fig. 2.B). Ferusonite group has two varieties: **a. Fergusonite-(Y)** is Nb rich, with variable representative

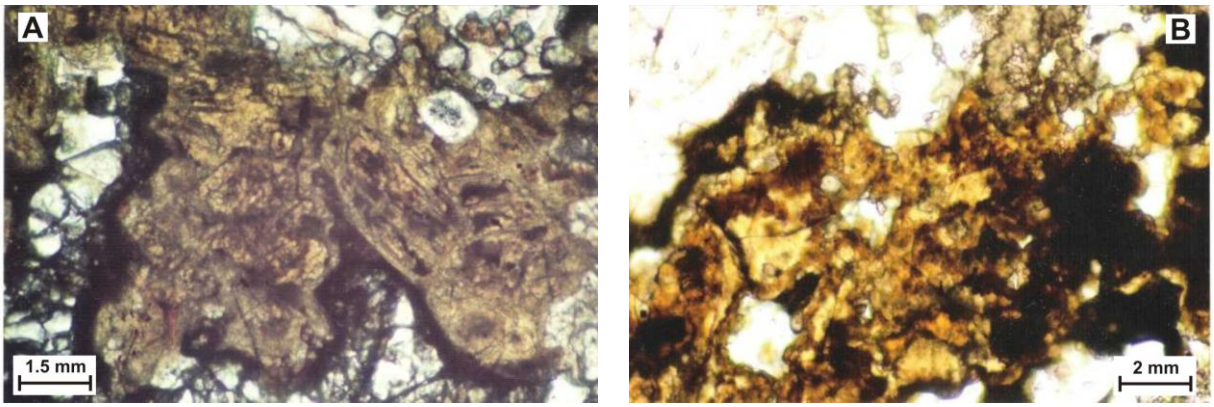

Fig. 2. A. Yttrobetafite-(Y) (brown), relics in oxyyttropyrochlore-(Y) (yellow), apatite around them (white), sample GM19B/6; B. Fergusonite-(Y) (brown) hydroxycalciopyrochlore (yellow), transmitted light, NII, sample G11-5/2.

chemical composition (%wt): Nb_2O_5=57.42-60.89, Y_2O_3=33.19-33.64, Ce_2O_3=0-15, ThO_2=1.91-3, UO_2= 3.03-3.47, CaO=0.47-0.52, TiO_2=0-0.86 (samples GM40, G15a, G1-11, GM31). The fergusonite-(Y) in the sample G11-5/2b has chemical composition (%wt): Y_2O_3=30.34, Nb_2O_5=58.43, Ce_2O_3=3, CaO=1.17, Eu_2O_3=0.28, Yb_2O_3=1.79, ThO_2=1.93, UO_2=2.95 (%wt); **b. Formanite-(Y),** $TaYO_4$, Ta rich fergusonite, was determined by EDS-spectrum in sample GM16A/1, showing only Ta and Y.

E. Euxenite group. It has general formula AM_2O_6 and an ordered columbite type structure (Černý & Ercit, 1989). **Euxenite-(Y),** $(Y,Ca,Ce,U,Th)(Nb,Ta,Ti)_2O_6$, determined in GM has brown to yellow brown colour in transmitted light and has the following variable representative chemical composition: TiO_2=20-31, Y_2O_3=9-15, Nb_2O_5≈40, Ta_2O_5=5-7, ThO_2=0-8, UO_2=7-8, CaO≈2.5 (%wt) (samples G11-4A, GM15-2, GM19B, G11-4). The euxenite-(Y) is frequently replaced secondary by yttropyrochlore-(Y).

F. Samarskite group, orthorhombic, with general formula AMO_4 and three varietes. In contrast to euxenite it has characteristic Fe-content; **a**. **Samarskite-(Y),** $(Y,Fe,U,Ca)(Nb,Ta)O_4$, has representative chemical composition (%wt): Y_2O_3 = 4.07, FeO=11.54, CaO=2.38, ThO_2=10.31, TiO_2=3.62, Ce_2O_3=4.20 Nb_2O_5=49.72, Ta_2O_5=14.13 (sample GMC /4); **b. Ishikawaite,** $(U,Fe,Y,Ca)(Nb,Ta)O_4$, has representative chemical composition: FeO=13.3, ThO_2=8.27, UO_2=19.13, Nb_2O_5=41.22, Ta_2O_5=13.32, TiO_2=4.74 (%wt) (sample G15-1b/3); **c. Plumboniobite**, a samarskite variety with PbO has as main component oxides (%wt): CaO=1.37, TiO_2=2.03, FeO=10.46, Nb_2O_5=46.49, Ta_2O_5= 18.54, PbO=14.38, UO_2= 6.69, (sample GM16A/5); **d. Khlopinite,** a Ti enriched samarskite variety has: CaO=4.77, TiO_2=13.27, FeO=7.8, Y_2O_3 =9.72, UO_2=10.35, Nb_2O_5=43.71, Ta_2O_3=10.34 (%wt) (sample G19B/5).

G. Niobian rutile group. Nb-rutile $(Nb,Ti)O_2$, tetragonal**,** occurs as the main constituent mineral of GM associations. The black grains of niobian rutile of a few mm occur in the host rocks associated with magnetite, ilmenite and Mn-ilmenite. The high Nb-containing variety of rutile is similar with that of old "ilmenorutile" $(Nb,Fe,Ti)O_2$, which was discredited by IMA. Its Nb_2O_5 content has generally variations between 25-35%wt and sometimes just more over the TiO_2 content. The Nb-rutile has variable

representative chemical composition (%wt): TiO_2=37.63-52.5, FeO=7.24-12.76, Nb_2O_5=21.79-36, Ta_2O_5 =7.71-13.31, Y_2O_3=0-2.18, ThO_2=2.65-4.77, UO_2=0-1.85, CaO=0.45-2.56. The Nb-rutile in sample G11-4/7 has representative chemical composition (%wt): TiO_2=46.98, FeO=12.76, Nb_2O_5=23.49, Ta_2O_5= 12.9, ThO_2=2.57, CaO=0.45, Y_2O_3=0.8. It has an important strüverite $(Ti,Ta,Fe)O_2$ solid solution.

H. Cassiterite group. Cassiterite, SnO_2**,** usually occurs in little veins**.** Its big grains can have one cm in size. In transmitted light it is twinned and has high refringence and birefringence. Some grains are compositionally zoned, with more Th content in the centre and less on the rims of the grains.

I. Baddeleyite group. Baddeleyite, the monoclinic form of ZrO_2, is the stable phase in equilibrium with most natural hydrothermal solutions (in absence of silica, which would stabilize zircon). The baddeleyite forms short transparent prisms of mm size with nearly perfect cleavage. It appears to be one of the oldest mineral, being enclosed in phlogopite, zircon and Y-silicates. Its presence indicates that the first vein mineralization solutions were subsaturated in silica. The chemistry of baddeleyite shows only ZrO_2, with very little ThO_2, UO_2, Y_2O_3. Its BSE image one can see in Fig. 1.B, part II of the paper (this volume).

J. Uraninite-thorianite group: **a. Uraninite,** UO_2, and **b. thorianite,** ThO_2 in GM, usually form solid solutions with the composition: UO_2= 49.1, ThO_2=49.9 (%wt). Separate, uraninite has composition: $UO_2 \approx 96.6$ with little ThO_2 ,Y_2O_3, PbO, FeO, and thorianite ThO_2=96.3, PbO=3.27, FeO=0.23, SiO_2=0.16, and little Pb, Ce, La contents (%wt). The uraninite occurs enclosed in cyrtolite (Fig.3.A) and thorianite in monazite-(Ce) (Fig. 3.B); **c**. **Cerianite**, $(Ce,Th)O_2$, was determinated only by microprobe, as very small inclusions in monazite-(Ce), being produced through the oxidation and leashing of Ce^{4+} from it, caused by hydrothermal fluids. It has low Y, Th, U and REE concentrations, being below microprobe sensitivity.

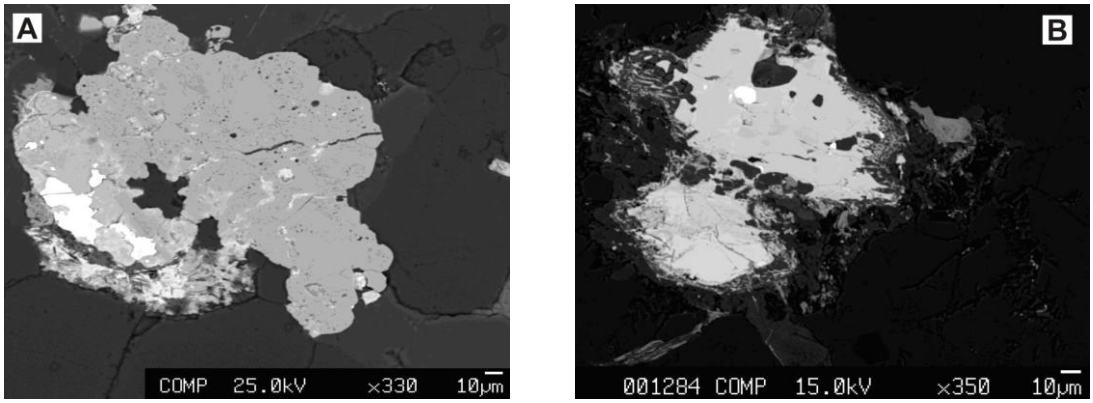

Fig. 3. A. BSE image of uraninite (white) in zircon (grey), below left pyrochlore (dark white) in Y-carbonate (grey, fibrous), sample Gmc/5; B. BSE image of thorianite (white, round) in monazite-(Ce) (grey), apatite around it (dark grey), sample GM31/7.

II. REE(Y) Carbonates class.

The Y/LREE-carbonates are more rare comparatively with the silicates, phosphates and oxides of the same elements. Considering the relations between REE(Y)-carbonates and others REE(Y) minerals existing here, they are secondary, appearing as a product of the decomposition of monazite-(Ce) and xenotime-(Y); **a**.**Bastnasite-(Ce),**$CeLa)CO_3F$, hexagonal, granular, yellow to reddish brown. The representative chemical composition shows some variations (%wt): La_2O_3=12-14.5, Ce_2O_3=41.68-45.8, Nd_2O_3=7.48-10.59, Gd_2O_3= 0.41-2.91, Y_2O_3=0-0.74, F=7.27-8.72; **b**. **Bastnasite-(Y),**$(Y,Ce)(CO_3)F$, has the main constituent oxides:Y_2O_3= 33.6, La_2O_3=6.5, Ce_2O_3=27.7, Nd_2O_3=20.1, ThO_2=5.57, F=5.5 (%wt); **c.Thorbastnasite,** $Th(CaCe)(CO_3)_2F_2$. $3H_2O$, hexagonal, has a representative chemical composition (%wt): Ce_2O_3=24.27, Nd_2O_3=9.22, ThO_2=18.52, Y_2O_3=7.19, Nb_2O_5=5.35, CaO=11.39, FeO=8.52, SiO_2= 1.99; **d. Parisite-(Ce),** $Ca(CeLa)_2(CO_3)_3F_2$, monoclinic, pseudohexagonal. It is colourless to yellow in transmitted light with weak pleochroism from pale yellow to golden yellow. Chemistry of parisite-(Ce) (wt%): Y_2O_3=5.06, La_2O_3=12.16, Ce_2O_3=30.82, Nd_2O_3=8.98, Dy_2O_3=0.47, Gd_2O_3=2.74, Yb_2O_3=0.04, ThO_2=3, UO_2=2, CaO=6.14, F=5.6; **e. Synchysite-(Y),** $Ca(YCe)(CO_3)_2$, monoclinic, pseudohexagonal. It occurs as very fine grained aggregates. In transmitted light it is red brown, pale yellow, pale pink, colourless. The representative analysis of synchysite-(Y) shows the main constituent oxides (%wt): Y_2O_3=8.08, La_2O_3=2.34, Ce_2O_3=7.59, Nd_2O_3=3.5, Gd_2O_3=1.39, Dy_2O_3=0.51, Yb_2O_3=0.08 ThO_2=1.11, UO_2= 0.75, CaO=19.80, F=4.12; **f. Synchysite-(Ce),** $Ca(CeLa)(CO_3)_2F$**,** orthorhombic. It is pale brown, pale grayish brown, pale violet to colorless in transmitted light and it is rich in Y.

Conclusions, **Acknowledgements** and **References** are presented in Part II of the paper, this volume.

Rom. J. Mineral Deposits, vol. 87 (2014), No. 1, p. 57-60

MINERALOGY OF THE GRADISTEA DE MUNTE RARE ELEMENT MINERALS OCCURRENCE, SEBES MTS., SOUTH CARPATHIANS. PART II: PHOSPHATES AND SILICATES

Paulina HÎRTOPANU[1*], Robert J. FAIRHURST[2]

[1]University of Bucharest, 1, Nicolae Balcescu Blv., 010041 Bucharest, RO;
[2]Technical Laboratory at Lhoist North America, Inc., 3700 Hulen Street, Forth Worth, Texas 76107, US;
* *paulinahirtopanu@hotmail.com*

Abstract. The rare element minerals Gradistea de Munte (GM) occurrence is situated in the Precambrian migmatic gneisses of Sebes-Lotru Series, in Sebes Mts, South Carpathians. The host of mineralization, contains magnetite and zircon/ cyrtolite as constituent minerals, the rare element minerals occurring as accessory ones and even more. The mineralogy of GM rare element minerals is very complex. Its rare Nb,Ta, REE(Y), Zr, Sn, Th and U minerals belong to following four classes: oxides, carbonates, phosphates and silicates. Amongst rare phosphates, are present the Th-phosphate (brabantite), LREE-phosphates represented by monazite-(Ce), Y-phosphates represented by xenotime-(Y) and cheralite-(Ce), a solid solution cheralite-huttonite. In the GM occurrence the most widespread rare element minerals are silicates, represented by Nb, LREE, Y, Th, Zr and U, and among them the Y-silicates and Th-silicates are the predominant. The Nb-silicates is present with 5 varieties, the LREE-silicates are represented by allanite-(Ce), yttrian allanite-(Ce) and cerite-(Ce). The Y-silicates are predominant, being represented by very diverse terms: yttrialite-(Y), thalenite-(Y), rowlandite-(Y) and tombarthite-(Y). The ThNbZr(REE)Y-silicates have two important minerals, thorite and thorogummite, and 6 varieties.

Key words: LREE(Y)Th-phosphates, Th-phosphates-silicates, NbThZrREE(Y)-silicates, Y-silicates, Zr-silicates.

Introduction (previous studies, analytical methods, geological setting) and **Mineralogy** (oxides and carbonates rare element minerals classes) were discussed in Part I (this volume).

III. Phosphates class.

a. Monazite-(Ce), (Ce,La,Nd,Th)PO_4**,** monoclinic **(**Fig.3B), has the following representative composition (%wt): Y_2O_3=1.8, La_2O_3=10.42, Ce_2O_3=24.63, Nd_2O_3=5.77, Gd_2O_3=1.95, Dy_2O_3=0.3, ThO_2=18.5, UO_2= 12.4, F=0.54, CaO=0.94, P_2O_5=22.7. Also, it contains small quantities of B_2O_3, ZrO, Nb_2O_5, Al_2O_3; **b. Xenotime-(Y),** YPO_4, tetragonal, the less widespread phosphates than monazite in GM occurrence. It has

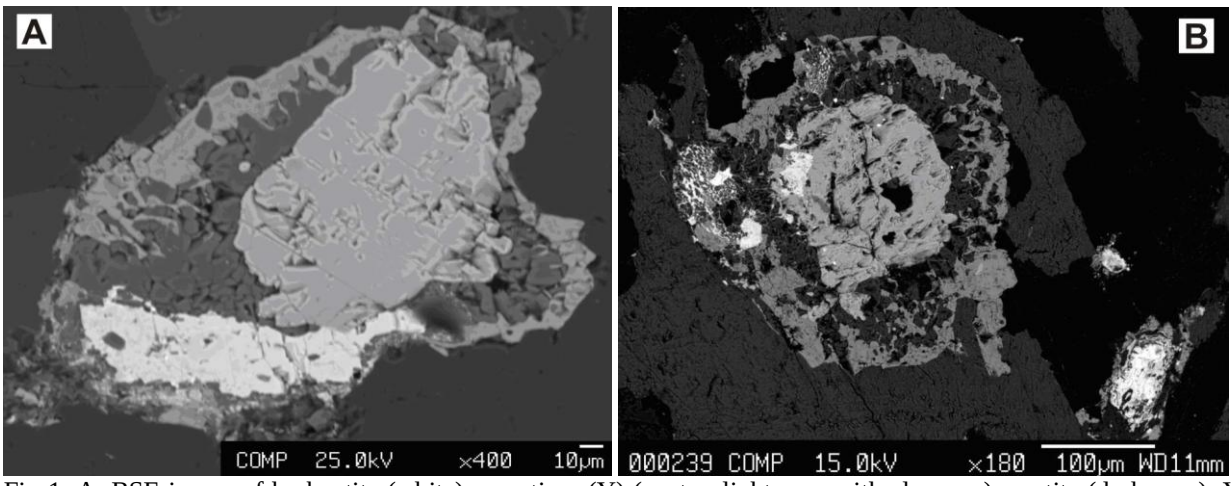

Fig 1. A. BSE image of brabantite (white), xenotime-(Y) (centre, light grey with cleavage), apatite (dark grey), Y-silicate (grey, on the edges), sample GM31/2; B. BSE image of baddeleyte (centre, grey light) with small monazite-(Ce) (white), inside it, apatite (dark gray) and yttrialite-(Y) with Th (grey, outside), thorite (white, right corner, bottom), sample, G15-4/7.

isometric or short prismatic crystals with perfect cleavage (Fig. 1.A). Its refringence and birefringence are relatively high, but less than that of monazite-(Ce). It has a yellowish color (Fig 3.A) with a weak pleochroism. The representative chemical composition of xenotime-(Y) is (%wt): Y_2O_3=48.97, P_2O_5= 31.3, Dy_2O_3=3.9,Yb_2O_3 =2.63, CaO=0.1, Nd_2O_3=0.1, Gd_2O_3=0.55, SiO_2=0.11, ThO_2=0.27. The xenotime-(Y) substitutes monazite-(Ce), being formed later. Its chemical composition in sample GMM/6 is: P_2O_5 =41.8, Y_2O_3=58.2, NiO=0.16, CaO=1.86, UO_2=1.06 (%wt); **c. Churchite-(Y),** $YPO_4.2H_2O$, monoclinic, occurs as crusts on xenotime-(Y). It is colorless in transmitted light. Its main component oxides are (%wt): Y_2O_3=41.0, Yb_2O_3=2, P_2O_5=27.1, ThO=0.21, Nd_2O_3=0.12, Gd_2O_3=0.96, Dy_2O_3=4.36, CaO=0.96.

Also, it has some Al_2O_3, MgO, FeO, MnO and UO_2 contents. Its H_2O content was not determined (sample G15-4/46); **d. Cheralite-(Ce),** (ThCaCe)(PO_4,SiO_4), monoclinic, is isostructural with monazite-(Ce). There is a systematic substitutions of Ca and Ce ions by Th and U. The huttonite, $ThSiO_4$, forms the end member silicate in the ternary system, $ThSiO_4$-(REE)PO_4-(CaTh)$(PO4)_2$. The cheralite-(Ce) was determined with X-ray and microprobe analyses. Sample G15-4/62 has the following representative chemical composition: SiO_2=5.43, P_2O_5=22.1, ThO_2=23.68, CaO=1.29, UO_2=15.82, Y_2O_3=1.95, Ce_2O_5 =15.22, La_2O_3=4.99, Nd_2O_3=4.25, Gd_2O_3=1.22, Dy_2O_3=0.32, F=0.77, Al_2O_3=0.40 (%wt). Because of the Th and U contents, the grains of cheralite-(Ce) are metamictic. The unmetamictised areas of the cheralite-(Ce) grains have high birefringence like that of monazite; **e. Brabantite,** CaTh$(PO4)_2$, monoclinic, associated frequently with xenotime-(Y) and apatite, one can see in BSE image in Fig.1A. Its chemical composition is (%wt): SiO_2=14.77, P_2O_5=7.82, ThO_2=41.34, CaO=10.21, UO_2=10.01, Y_2O_3=4.61, LREE=2.32, F=0.92, Al_2O_3=0.73, MgO=0.19, Nb_2O_5=5.89. It has some huttonite component.

IV. Silicates class

In the GM occurrence the most widespread rare element minerals are silicates, represented by Nb, LREE, Y, Th, Zr and U, and among them the Y-silicates and Th-silicates are predominant. Their chemical composition include the main constituent oxides. The OH group and H_2O were not determined yet.

A. **Nb-silicates**, have 5 varieties: **a**. **Nb-silicate** (%wt): SiO_2=18.3, Nb_2O_5=61.53, Y_2O_3=4.63, CaO=7.75, Ce_2O_3=1.61, ThO_2=7.89, TiO_2=2.80 (sample G1-11); **b**. **Nb, Zr silicate**: EDS spectrum, sample G15-5/6; **c**. **Nb, Th, U, Zr silicate** (%wt): SiO_2=14.30, Nb_2O_5=30.43, ThO_2=19.35, UO_2=12.12, ZrO_2=7.41, Y_2O_3 =3.69, CaO=4.15 (sample G15-5/63); **d**. **Nb, U silicate**: SiO_2=11.80, Nb_2O_5=39.20, UO_2=10.42, Y_2O_3=3, CaO=3, (sample G15BA/1); **e**. **Nb, Th silicate:** SiO_2=15.39, Nb_2O_5=41.89, ThO_2=37.16, CaO=2.98, TiO_2 =1.2, FeO=0.47, MgO=0.52 (%wt), sample G11-3/43. **B**. **LREE-silicates**: **a**. **Allanite-(Ce),** monoclinic, Ca(CeLa)$(AlFe)_3(SiO_4)_3$(OH) in sample G15/5 has the composition: SiO_2=35.1, CaO=9.86, Al_2O_3=17.2, FeO=18.50, La_2O_3=4.60, Ce_2O_3=14.68 (%wt); **b**. **Yttrian allanite-(Ce)** has in sample GMM/5 (%wt): SiO_2=9.52, Al_2O_3=4.43, CaO=5.45, FeO=5.84, Y_2O_3=9.29, Ce_2O_3=33.05, La_2O_3=14.72, Nd_2O_3=9.12, ThO_2=8.54; **c**. **Cerite-(Ce),** $(Ce,Ca)_9(Mg,Fe)Si_7(O,OH,F)_{28}$, rhombohedral, is brown in transmitted light and partially metamictized. It has following main constituent oxides (%wt): SiO_2=15.24, CaO=19.46, Fe_2O_3=25.98, Ce_2O_3=23.63, La_2O_3=8.2, Nd_2O_3=5.7, ThO_2=1.75 (sample G11-5/5). Its composition varies widely. **C**. **Y-silicates** are the most frequent amongst all the rare silicates in GM occurrence, with the following minerals: **a**. **Yttrialite-(Y),** $(Y,Th)_2Si_2O_7$, monoclinic, has olive colour in ansmitted light, becoming yellow-orange with alteration (Fig. 4.A). Its composition is (%wt): Y_2O_3=51.18, SiO_2=29.75, ThO_2=7.61, REE=4.18, CaO=4.39, FeO=3.05; **b**.**Thalenite-(Y),** $Y_3Si_3O_{10}$(F,OH), monoclinic, colourless in thin sections. It has a representative composition (%wt): SiO_2=18.78, Y_2O_3=77.95, CaO=3.26 (sample G15-3/6); c. **Rowlandite-(Y),** $(Y,Fe^{2+},Ce)_3Si_4O14(F,OH)$(?), green grayish in thin section (Fig.4.B), contains (%wt): SiO_2=31,03, CaO=3.86, FeO=28.10, Y_2O_3=34.63, Al_2O_3=2.3 (sample GM16A/8).

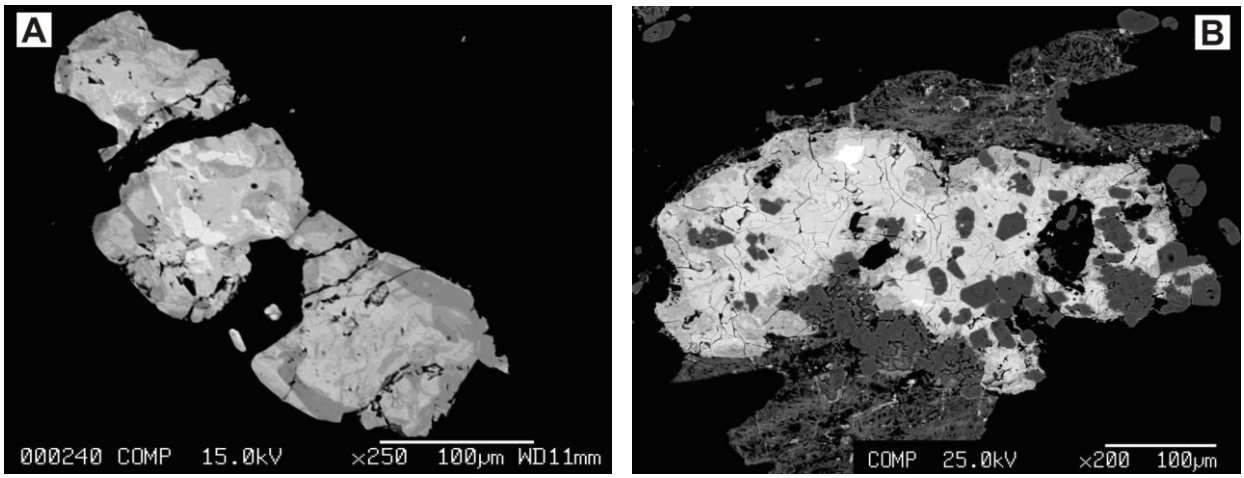

Fig. 2.A. BSE image of Y-silicates with variable composition: yttrialite (white), rowlandite-(Y) (light grey), thombartite-(Y) (grey), sample G15B/7; B. BSE image of thorite (white), thorogummite (white grey), zircon (small crystals inside and outside, dark grey), Y-carbonate (around, fibrous, grey white), sample Gm40/5.

d. Tombarthite-(Y), $Y_4(SiH_4)O_{12-x}(OH)_{4+2x}$, has a lower refringence and birefringence than thalenite. Its chemical representative composition (sample GM40/2) (%wt) is: SiO_2=22.26, Y_2O_3=35.52, CaO=5.69, FeO=0.16, La_2O_3=4.71, Ce_2O_3=16.44, Nd_2O_3=12, ThO_2=3.19. The Yttrium silicates with oscillatory composition one can see in BSE image in Fig. 2.A, where the yttrialte-(Y) is substituted by rowlandite-

(Y), and the last one is substituted by thombartite-(Y). The chemical composition of mineralizing solutions goes from rich in Y and poor in Si, to rich in Si and OH/H_2O, and poor in Y.

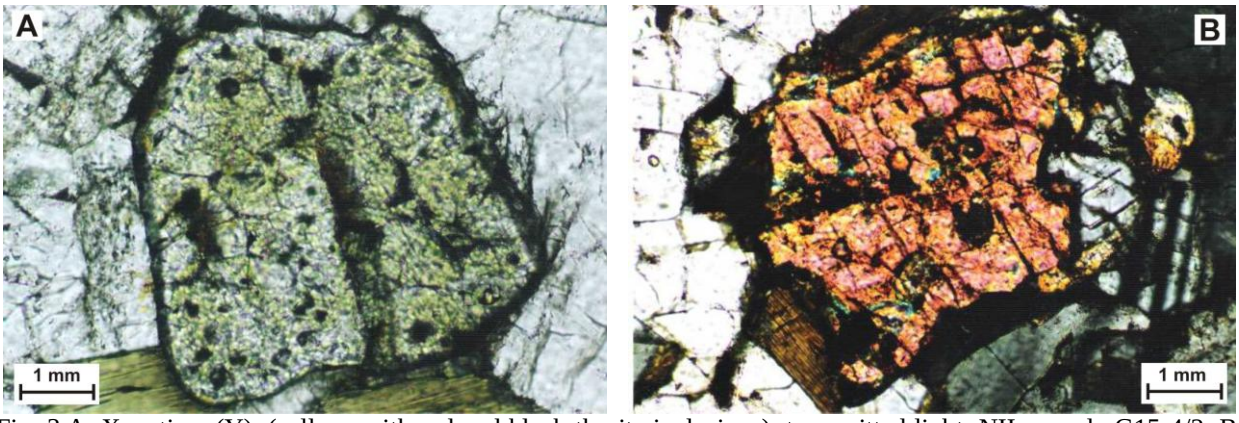

Fig. 3.A. Xenotime-(Y), (yellow, with red and black thorite inclusions), transmitted light, NII, sample G15-4/2; B. Monazite-(Ce), (high birefringence and refringence), transmitted light, NII, sample G15B.

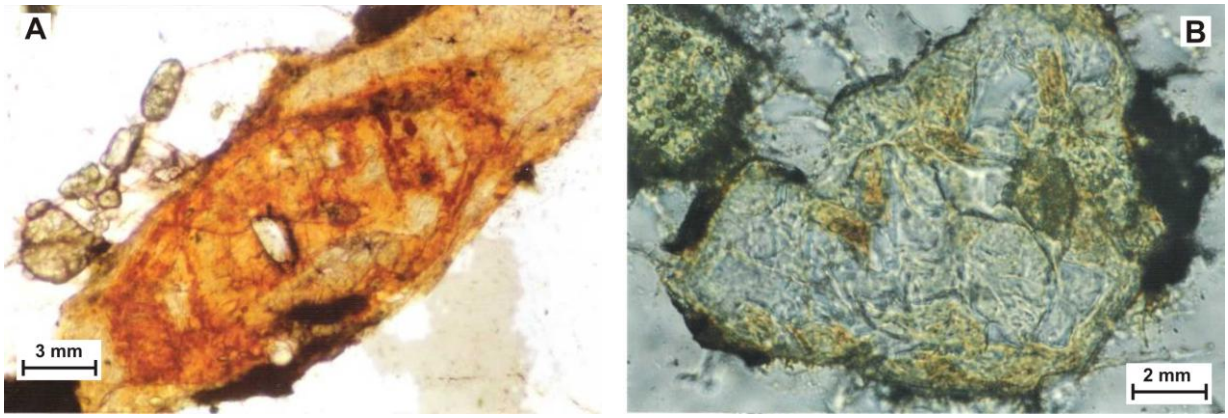

Fig. 4. A.Yttrialite-(Y) (big zoned grain with orange alterations), zircon (white small), NII, transmitted light, sample GM16A; B. Rowlandite-(Y) (green, grayish white), transmitted light, NII, sample G15B/13.

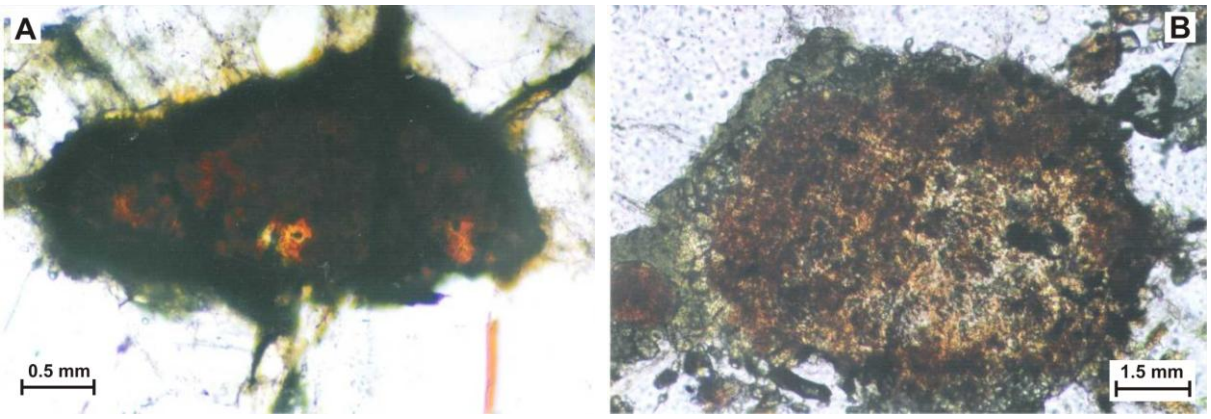

Fig. 5. A.Thorite (red, black), transmitted light, NII,sample G15-5; B. Thorogummite (yellow brown) with apatite (grey) and chlorite (green) around it, transmitted light, NII, sample G11-2/2 (right).

D.**Thorium silicates: a**.**Thorite**, $ThSiO_4$, tetragonal, is isostructural with zircon, with which it forms a complete series and has a monoclinic dimorph, huttonite. It is red black in thin section (Fig 5.A). The main oxides of thorite are: SiO_2=15.77, ThO_2=83.55, PbO=0.68 (sample G15a/2); SiO_2=17.75, ThO_2 = 79.65, CaO=0.96, FeO=1.6 (wt%) (sample G11/2/1/4); **b**.**Thorite with Zr and Ce**, (sample GM40/7) contains: SiO_2=12, ThO_2=41.51, Ce_2O_3 =27.56, ZrO_2=12.26, CaO=2.76 (wt%); **c**.**Thorite with U, Zr, Y** and **Nb,** contains: (sample G15B/3): SiO_2=20.39, ThO_2=28.98, UO_2=19.20, ZrO_2=13.87, Y_2O_3=9, Nb_2O_5 =6.13 (wt%); **d**. **Thorite with Y and Ce,** contains: SiO_2=16.78, ThO_2=51, Y_2O_3=17.4, Ce_2O_3= 7.57, CaO =4.34, FeO=2.94 (sample GMC/3); **e**.**Thorite with Nb** has (%wt): SiO_2 =20.1, FeO=3.1, Nb_2O_5=33.59, ThO_2=43.21 (sample G1-11/1); **f**. **Thorogummite,** $(ThU)(SiO_4)(OH)_4$, a product of hydrothermal alteration of thorite, is yellow dark brown in transmitted light (Fig. 5.B), having the refringence and

birefringence lower than that of thorite. Its main component oxides are (%wt): SiO_2=15.38, ThO_2=47.39, UO_2=31.5, Y_2O_3=8.71, Nb_2O_5=4.23, ZrO_2=0.33 (sample G11-2/14), having less Th than thorite. Also, it could have some content of Ce_2O_3 and PbO. The water content was not determined yet.

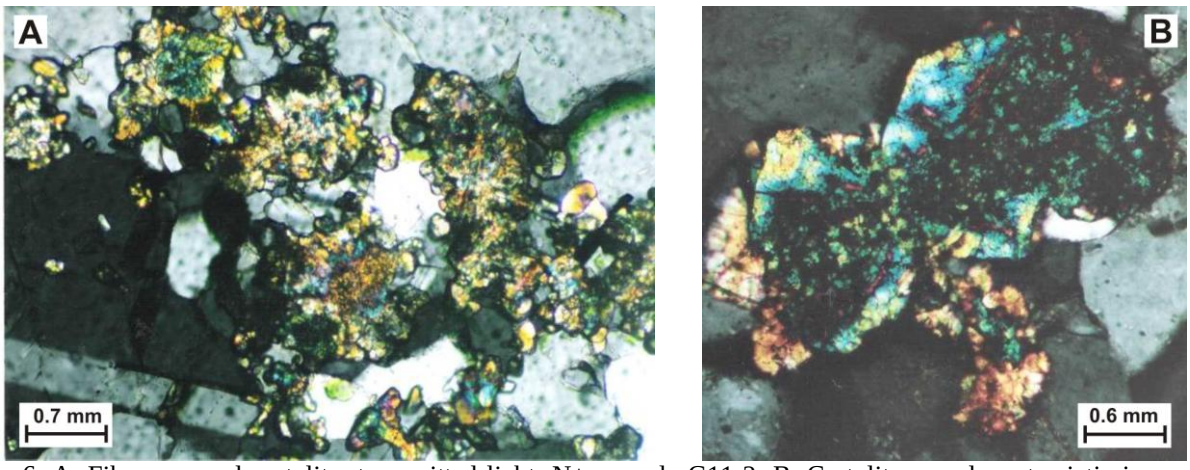

Fig. 6. A. Fibrous zoned cyrtolite, transmitted light, N+, sample G11-2; B. Cyrtolite zoned metamictic in centre (isotropic, with Hf ≈6%), and unmetamictic outside (anisotropic and less Hf), transmitted light, NII, sample GM31.

E. Zirconium silicates: **a. Zircon, $ZrSiO_4$,** and its hydrated variety, **b. Cyrtolite,** $ZrSiO_4(OH)_4$, have some Hf, (Fig 6.B), Th and U owing to replacement of Zr. Also, some Y content owing to solid solution with xenotime-(Y). The concentrations of Th (≈5%wt), U (≈2-5%wt) and Hf (≈ 6%wt in cyrtolite in Fig.6 B) are variable, even among grains from the same thin section.Cyrtolite has fibrous, zoned structure (Fig. 6.A, 6.B) and it is radioactive.

Conclusions

About 50 rare element minerals are described in GM, many of them first occurrences in Romania: 21 oxides (3 pyrochlores, 2 betafites, 3 columbites, 2 fergusonites, 4 samarskites, and also euxenite-(Y), Nb rutile, cassiterite, baddeleyite, uraninite, thorianite and cerianite), 6 REE-(Y) carbonates, 5 REE-(Y) and Th phosphates, and 17 Nb, LREE, Y, Th and Zr silicates and their varieties. The oxide minerals, with the greatest variety, are the only important sources of Nb and Ta. The niobo silicates with significant Nb contents (≈40%wt Nb_2O_5) represent potential ore minerals for the future. All terms of LREE(Y) carbonates seem to be formed as secondary. The silicates, specially of Y and Th, change their composition in the same crystal, and pass from one variety to another. Early phosphates, such as monazite and xenotime, are replaced by later bastnasite and churchite, respectively, whereas silicate minerals evolve to silicate-carbonate and carbonate. Generally, the content of Nb+Ta in all rare minerals is higher than that of YREE, and the Y content is much higher than Ce. Also, the Th content is much higher than U. The zirconium has the highest content. Their post-magmatic genetical process is characterized by multiphases of metasomatism and recrystallization. Many of the GM rare element minerals must be reanalyzed, for all the elements of the series, with accuracy. For the time being, the great variety of these minerals and their varieties are most likely to be of mineralogical interest only.

Acknowledgements. We are grateful to Prof. Nicolae Ludusan for providing samples and to Prof. Jens Andersen for his help with the analytical work at Camborne School of Mine, Exeter University, UK.

References

Atenció D., Andrade B., Christy A., Giere R., Kartashov P. (2010). The pyrochlore supergroup of minerals: nomenclature, Canad.Miner. Vol. 48, pp. 673-698.

Černý P. and Ercit T.S. (1989): Mineralogy of Niobum and Tantalum: Crystal Chemical Relationships, Pagarenetic Aspects and Their Economic Implications, In: P. Möler, P. Černý, F. Saupé (ed.): Lanthanides, Tantalum and Niobium, p. 27-79.

Hirtopanu P., Andersen, J.C., Fairhurst, R.J., Ludusan, Jakab G. (2012). Nb, Ta, Ti, REE(Y), Zr, Sn, Th, U oxides in Gradistea de Munte rare element minerals occurrence, South Carpathians, Sebes Mts, Romania, Acta Mineralogica Petrographica, Abstract series, Vol. 7, Miskolc, pag.54.

Popescu G., N.Ludusan, M.E. Cioaca (2003). The study of rare earth and rare metal mineralizations in Gradistea de Munte, Sebes Mts, “Petrology global context”, Bucharest University, p.43.

Rom. J. Mineral Deposits, vol. 87 (2014), No. 12, p. 61-64

FLORISTIC COMPOSITION ON THE ABANDONED COPPER HEAPS IN CENTRAL SLOVAKIA

Ingrid TURISOVÁ[1*], Tomáš ŠTRBA[1], Peter ANDRÁŠ[1], Štefan ASCHENBRENNER[1]

[1]Faculty of Natural Sciences, Matej Bel University Banska Bystrica, Tajovského 40, 974 01 Banská Bystrica, Slovakia.
* *ingrid.turisova@umb.sk*; Tel.: 00421 48 446 5801; Fax: 00421 48 446 7000.

Abstract: The paper presents the results of floristic research on the three copper mine heaps: Maximilián, Piesky and Richtárová situated in Špania Dolina – Staré Hory mining area in Starohorské vrchy Mts (Central Slovakia). Research was performed during the growing seasons 2011 and 2013. We have determined 238 species of vascular plants but only 37 of them were identified at all the three heaps. The dominant herbs are *Acetosella vulgaris*, *Agrostis capillaris*, *A. stolonifera*, *Arabidopsis arenosa*, *Arrhenatherum elatius* and *Silene dioica*, while the dominant tree species are *Abies alba*, *Betula pendula*, *Picea abies*, *Pinus sylvestris* and *Salix caprea*. 12 species are classified as metallophytes, 6 of them have occurrence at all localities and therefore they are suitable for potential phytoremediation activities. Specific floristic compositions with 11 taxa were found on the two places for feeding of wildlife animal species on the dump-field Piesky.

Keywords: copper heaps, flora, metallophytes, the Starohorské vrchy Mts., Slovakia

Introduction

Mine waste heap is the habitat with the specific environmental conditions differs from the surrounding environment. It contains elevated or extreme heavy metal concentrations in comparison with natural content in soil unaffected by human activities. Those habitats are colonized by plant taxas, which can adapt to these conditions by special mechanisms. As the heaps are from different time periods, therefore they have developed vegetation in different successional phases. Low vegetation cover of mine dump-fields is typical because a species composition is limited by ability of plant adaptation (Banásová, 1976, Reeves and Baker, 2000).

The abandoned mining area Špania Dolina – Staré Hory in Central Slovakia was one of the most important Middle Age European regions where the copper was exploited. The pH and Eh (pH 5.57 – 7.19; Eh -58 – 45) affect the concentration and mobility of heavy metals (mainly Cu, Zn, Co, As etc.) in soil and both in surface water (pH 6.49 – 7.66; Eh -2 – -65) and groundwater (pH 7.91 – 8.80; Eh -79 – -89) . The aim of floristic research was to identify the autochtonous metallophytes, which could be suitable for potential phytoremediation.

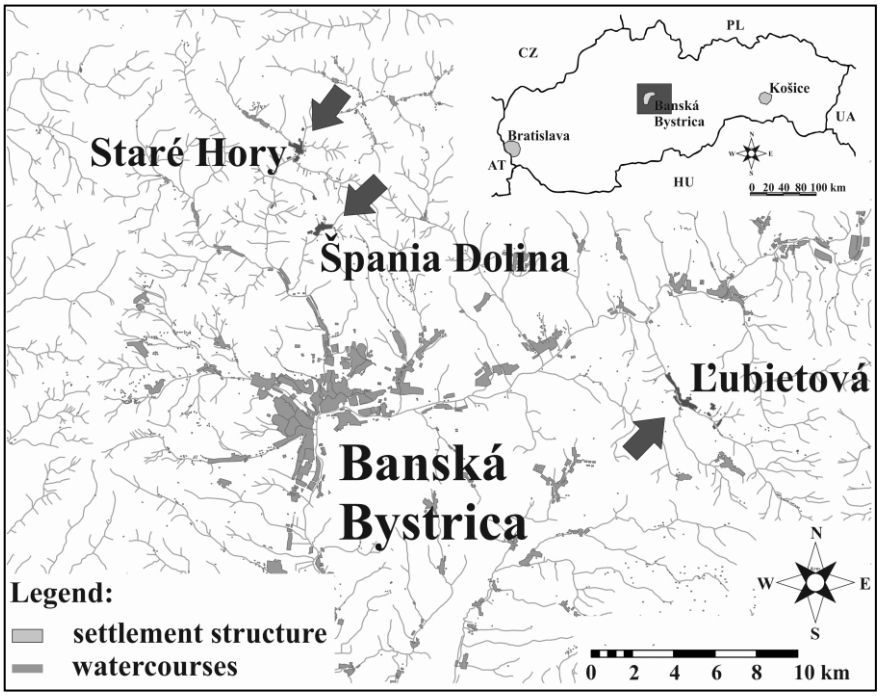

Fig. 1. The studied area in the surrounding Špania Dolina and Staré Hory (central Slovakia)

Materials and methods

Field research was realized in the growing seasons 2011 and 2013 on heaps Maximilián (marked as 1 in list of vascular plants) and Piesky (no. 2) in Špania Dolina cadastre and Richtárová (no. 3) in Staré Hory cadastre by transect method (Fig. 1). These transects were realized in such a way to respect all types of habitats in different successional phases. The nomenclature of the plant taxas was elaborated according to Marhold and Hindák (1998). Metallophytes (cf. Zarzycki et al., 2002) in list of vascular plants are highlighted in bold. The taxa with occurrence at all three localities are underlined.

Characteristics of the localities

1. Heap Maximilián in Špania Dolina, Starohorské vrchy Mts., Central Slovakia, 772 m a. s. l., N 48.483099°, E 19.080280°. This is the largest heap in the mining region, which is situated nearby the Špania Dolina village. The whole heap is skeletal and sandy.
2. Heap Piesky near Špania Dolina village, Starohorské vrchy Mts., 780 m a. s. l., N 48.490493°, E 19.074037°. On the straight habitats are growing coniferous trees (*Picea abies* and *Pinus sylvestris*) and pioneer species (especially *Betula pendula*).
3. Heap Richtárová near Staré Hory village, Starohorské vrchy Mts., 653 m a. s. l., N 48.493141°, E 19.075282°. It is one of the oldest mining localities in the Starohorské vrchy Mts. and the first one where the mining activity has been finished. This fact is also corresponding to the most developed vegetation cover. Also this heap is very skeletal. The lower part of heap is covered by moss and lichens, with dominated by *Cladonia arbuscula* subsp. *mitis*. These are skeletal soils with a shortage of essential nutrients and water.

Results

On the all dump-fields 238 taxa of vascular plants (Maximilián 83 taxa, Piesky 155 taxa and Richtárová 145 taxa) were determined, 37 of them occurr at all three localities and 12 taxa were defined as metallophytes. Six metallophytes (*Agrostis stolonifera, Arabidopsis arenosa, Arrhenatherum elatius, Festuca rubra, Fragaria vesca, Rubus idaeus*) are growing on studied heaps and they can be used for potential phytoremediation. The characteristic dominants are *Agrostis capillaris, A. stolonifera, Arabidopsis arenosa, Silene dioica, Acetosella vulgaris, Arrhenatherum elatius, Festuca rubra* and *F. pratensis*. Specific floristic composition is on places for feeding of wildlife animal species on dump Piesky with *Datura stramonium, Echinochloa crus-galii, Hibiscus trionum, Zea mays* etc. (marked with symbol *). The list of vascular plants is following:

A**bies alba* 1,2,3 – *Abuthilon theophrasti** 2 – *Acer platanoides* 3 – *A. pseudoplatanus* 1,2,3 – *Acetosa pratensis* 2,3 – *Acetosella vulgaris* 1,2,3 – *Achillea millefolium* 1,2,3 – *Acinos alpinus* 3 – *Acinos arvensis* 1 – *Aegopodium podagraria* 3 – *Agrostis capillaris* 1,2,3 – ***A. stolonifera 1,2,3 – *Ajuga reptans* 3 – *Alchemilla* sp. 2,3 – *Allium scorodoprasum* 1 – *Alnus incana* 2,3 – *Amaranthus retroflexus** 2 – *Angelica sylvestris* 3 – *Anthoxanthum odoratum* 1,3 – *Anthriscus sylvestris* 1,3 – ***Arabidopsis arenosa*** 1,2,3 – *Arenaria serpyllifolia* 1,3 – *Armoracia rusticana* 3 – ***Arrhenatherum elatius*** 1,2,3 – *Artemisia vulgaris* 1,2,3 – *Aruncus vulgaris* 2,3 – *Asplenium septentrionale* 1,3 – *Astragalus glycyphyllos* 2,3 – *Athyrium filix-femina* 2 – *Avenella flexuosa* 1,2,3 – *Avenula pubescens* 1,3

***B**etula pendula* 1,2,3 – *Brachypodium pinnatum* 3

Calamagrostis epigejos 2 – *Calystegia sepium* 2, 3 – *Campanula patula* 1,3 – *C. trachelium* 3 – *Cannabis sativa** 2 (two individuals) – *Carduus acanthoides* 2 – *C. personata* 2 – ***Carex hirta*** 2,3 – *C. michelii* 3 – *C. muricata* 1,2 – *C. ovalis* 1,3 – *C. sylvatica* 2 – *C. vesicaria* 2 – *Carpinus betulus* 3 – *Cerastium holosteoides* 1,2,3 – *Chaerophyllum aromaticum* 2,3 – *Chamerion angustifolium* 3 – *Chelidonium majus* 1,3 – *Chenopodium abum** 2 – *Chenopodium* sp.* 2 – ***Cichorium intybus*** 2 – *Cirsium arvense* 2 – *C. eriophorum* 3 – *Consolida regalis* 1 – *Corylus avellana* 1,2,3 – *Crepis biennis* 2,3 – *Crocus discolor* 3 – *Cruciata glabra* 1,3 – *Cystopterix fragilis* 1,3

***D**actylis glomerata* 1,2,3 – *Datura stramonium** 2 – *Daucus carota* 2,3 – *Deschampsia cespitosa* 2 – *Dianthus carthusianorum* 1,3 – *Dryopteris filix-mas* 1,2,3

***E**chinochloa crus-galii** 2 – *Echium vulgare* 1,2,3 – *Elytrigia repens* subsp. *repens* 1,2 – *Epilobium collinum* 2 – *E. lamyi* 2 – *E. montanum* 1,2,3 – *Epipactis* sp. 2 – *Equisetum arvense* 2,3 – *E. sylvaticum* 3 – *Erigeron annuus* subsp. *annuus* 2 – *Eupatorium cannabinum* 2 – *Euphrasia rostkoviana* 2,3

F**agus sylvatica* 1,2,3 – *Fallopia dumetorum* 2 – *Festuca ovina* 1 – ***F. pratensis 2,3 – ***F. rubra*** 1,2,3 – ***Fragaria vesca*** 1,2,3 – *Fraxinus excelsior* 1,2,3

***G**aleopsis pubescens* 1,2 – *Galeopsis* sp. 3 – *Galium aparine* 2 – *G. mollugo* 1,2,3 – *G. verum* 2 – *Geranium phaeum* 3 – *G. pratense* 2,3 – *G. pyrenaicum* 3 – *G. robertianum* 1,3 – *G. rotundifolium* 1 – *Glechoma hederacea* 3

***H**eracleum sphondylium* 2,3 – *Hibiscus trionum** 2 – *Hieracium lachenalii* 2 – *H. murorum* 1,3 – *Humulus lupulus* 2 – *Hylotelephium maximum* 1,2,3 – *Hypericum perforatum* 1,2,3

***I**nula hirta* 2 – *Iva xanthiifolia* 2

***J**uncus articulatus* 2 – *J. effusus* 2 – *J. inflexus* 2

***K**nautia arvensis* agg. 3

L**amium maculatum* 1,3 – *Lapsana communis* 1,3 – *Lathyrus pratensis* 2,3 – *L. tuberosus* 2 – *L. vernus* 3 – ***Leontodon hispidus 3 – *Leucanthemum vulgare* 3 – *Linaria vulgaris* 2 – ***Lotus corniculatus*** 2,3 – *Lupinus polyphyllus* 3 – *Luzula luzuloides* 1,3 – *L. sylvatica* 3 – *Lychnis flos-cuculi* 3 – *Lysimachia nummularia* 3 – *L. vulgaris* 2

***M**aianthemum bifolium* 1,2 – *Medicago falcata* 3 – *M. lupulina* 2,3 – *M. sativa* 2 – *Melampyrum pratense* 1,3 – *M. sylvaticum* 1,2,3 – *Melilotus albus* 2,3 – *Mentha arvensis* 2 – *M. longifolia* 2 – *Myosotis sylvatica* 3

***O**dontites vulgaris* 2 – *Omalotheca sylvatica* 2 – *Ononis spinosa* 2 – *Origanum vulgare* 2

***P**arthenocissus quinquefolia* 3 – *Pastinaca sativa* 2,3 – *Petasites albus* 3 – *Phleum pratense* 2 – *Phyteuma spicatum* 2,3 – *Picea abies* 1,2,3 – *Picris hieracioides* 2 – *Pimpinella major* 2 – *P. saxifraga* 3 – *Pinus sylvestris* 1,2,3 – *Plantago lanceolata* 3 – *P. major* 2 – *Platanthera bifolia* 2 – *Poa nemoralis* 3 – *P. pratensis* 1,2 – *Polygonum aviculare* 2,3 – *Polypodium vulgare* 2,3 – *Populus tremula* 1,2,3 – *Potentilla collina* 1 – *P. heptaphylla* 2,3 – *Prenanthes purpurea* 1 – *Primula veris* 1,3 – *P. vulgaris* 2 – *Prunella vulgaris* 3 – *Prunus domestica* 3 – *Pseudotsuga menziesii* 1

***Q**uercus petraea* 1

R**anunculus acris* 2,3 – *R. bulbosus* 1 – *R. repens* 1,2,3 – *Ribes uva-crispa* 3 – *Robinia pseudoacacia* 3 – *Rorippa palustris* 2 – *Rosa canina* agg. 1,2,3 – *Rubus fruticosus* agg. 1,2,3 – ***R. idaeus 1,2,3 – *Rumex obtusifolius* 2

***S**alix caprea* 1,2,3 – *S. purpurea* 2,3 – *Salvia glutinosa* 2 – *S. pratensis* 3 – *S. verticillata* 1,3 – *Sambucus nigra* 2 – *Sanguisorba minor* 3 – *Scrophularia nodosa* 3 – *S. scopolii* 2 – *Securigera varia* 2,3 – *Sedum acre* 1 – *S. sexangulare* 1 – *Sempervivum* sp. 1 – *Senecio germanicus* 3 – *S. ovatus* 2 – *Silene dioica* 1,2,3 – *S. latifolia* subsp. *alba* 1 – *S. nemoralis* 3 – *S. vulgaris* 1,3 – *Solanum nigrum** 2 – *Solidago canadensis* 2 – *Sorbus aucuparia* 1,2 – *Stachys sylvatica* 2 – *Stellaria nemorum* 2,3 – *Stenactis annua* 2,3 – *Steris viscaria* 3 – *Swida sanguinea* 3 – *Symphytum officinale* 2

***T**anacetum vulgare* 2,3 – *Taraxacum* sect. *Ruderalia* 1,2,3 – *Thesium linophyllon* 2 – *Thlaspi arvense* 2 – *Thymus pulegioides* 3 – *Tilia platyphyllos* 1,2,3 – *Tithymalus cyparissias* 2 – *Torilis japonica* 2 – *Tragopogon orientalis* 3 – *Trifolium alpestre* 2 – *T. aureum* 2,3 – *T. flexuosum* 2 – *T. montanum* 3 – *T. pratense* 2,3 – *T. repens* 1,2,3 – *Tripleurospermum perforatum* 1,2 – *Tussilago farfara* 2,3

***U**rtica dioica* 2,3

***V**accinium myrtillus* 1,2,3 – *Valeriana officinalis* 2 – *Verbascum chaixii* subsp. *austriacum* 3 – *V. densiflorum* 1,2 – *V. nigrum* 2,3 – *Veronica chamaedrys* 1,2,3 – *V. officinalis* 2,3 – *Vicia cassubica* 2 – *V. cracca* 1,2,3 – *V. tenuifolia* 3 – *Viola tricolor* 1,2,3 – *Viscum album* subsp. *abietis* 2

***Z**ea mays** 2

Asplenium septentrionale is one from vascular plants species that occurs in the initial phases of succession on the heaps. It was determined at the Maximilián heap. Two neophyte taxa (*Parthenocissus quinquefolia*, *Lupinus polyphyllus*) were found on the heap Richtárová, which are rare grown in nearby.

Discussion and conclusions

Some next mentioned metallophytes in another European studies are e.g. as follows: *Anagalis arvensis*, *Echium vulgare*, *Plantago lanceolata*, *Poa annua*, *Rubus caesius* from copper heap in Gyöngyösoroszi (Hungary) (Tamás and Kovács, 2005), *Juncus effusus*, *J. conglomeratus*, *Scripus holoschoenus* from the Portuguese Sao Domingos (Frietas et al., 2004), *Silene vulgaris*, *Saxifraga stellaris*, *Pohlia drummondi*, *Mielichhoferia* spp. from Salzburg~~h~~ in Austria (Adlassing et al., 2012). The complex study of metallophyte vegetation in Central Europe was published by Baumbach (2012) where as the most important species are mentioned *Armeria martima*, *Minuaria verna*, *Silene vulgaris*, *Viola calaminaria*, *Thlaspi caerulescens* and genus *Cardaminopsis* (= *Arabidopsis*). Some of them were identified also at our studied area.

In present time the applicability of the selected species is studied. The detail study of the native metallophytes will enable successful remediation of contaminated areas.

Acknowledgements
The work was financially supported by grant scheme APVV-0663–10, VEGA 2/0099/13.

References

Adlassing, W., Wernitznig, S., Lichtscheidl, I.K., 2012. Historic Copper Spoil Heaps in Salzburg/Austria: Geology, Mining History, Aspect of Soil, Chemistry and Vegetation. Soil Biology, 31, 201-231.

Banásová, V., 1976. Vegetation of copper and antimony mine heaps (in Slovak). Biologické Práce, 22, 1-109.

Baumbach, H., 2012. Metallophytes and Metallicolous Vegetation: Evolucionary Aspects, Taxonomic Changes and Conservational Status in Central Europe, In: Tiefenbacher, J. (Ed.), Perspectives on Natural Conservation – Patterns, Pressures and Prospects. InTech, Rijeka, p. 93-117.

Freitas, H., Prasad, M.N.V., Pratas, J., 2004. Plant community tolerant to trace elements growing on the degraded soil of Sao Domingos mine in the south east of Portugal: environmental implications. Environment International, 30, 65-72.

Hobbs, R.J. and Streit, B., 1986. Heavy Metal Concentrations in Plants Growing on a Copper Mine Spoil in the Grand Canyon, Arizona. American Midland Naturalist, 115, 277-281.

Marhold, K. and Hindák, F., 1998. Checklist of non-vascular and vascular plants in Slovakia (in Slovak). Veda, Bratislava, 687 p.

Reeves, R.D. and Baker, A.J.M., 2000. Metal-accumulating plants. In: Raskin, I. and Ensley, B.D. (eds.), Phytoremediation of toxic metals: using plants to clean-up the environment. John Wiley and Sons, New York, p. 193-230.

Tamás, J. and Kovács, E., 2005. Vegetation Pattern and Heavy Metal Accumulation at a Mine Tailing at Gyöngyösoroszi, Hungary. Journal of Biosciences, 60, 362-367.

Zarzycki, K., Trzinska-Tacik, H., Rózański, W., Szelag, Z., Wolek, J., Korzeniak, U., 2002. Ecological indicator values of vascular plants of Poland. W. Szafer Institute of Botany, Polish Academy of Sciences, Krakow, 153 p.

HEAVY METAL CONTAMINATION IN WATER AT LIBIOLA ABANDONED COPPER MINE, ITALY

Giuseppe BUCCHERI[1], Peter ANDRÁŠ[2*], Maria Luisa ASTOLFI[3], Silvia CANEPARI[3], Mara CIUCCI[1], Alessandra MARINO[1]

[1]INAIL, ex ISPESL, via Alessandria 220, 00198 Rome, Italy
[2] Faculty of Sciences, Matej Bel University, Tajovského 40, 974 01 Banská Bystrica, Slovakia
[3] Sapienza University of Rome, Department of Chemistry, Piazzale Aldo Moro 5, 00185 Rome, Italy
* *peter.andras@umb.sk*

Abstract: This paper reports about heavy metal contamination concerning water at *Libiola* (Italy) abandoned copper mine. By studying past literature and by inspecting *Libiola* mining area, we could elaborate an investigation plan in order to characterize the environmental matrices there. The knowledge of the pollution situation can give us useful indications about the influence of mining activities on the surrounding environment. Starting from considering valley of *Gromolo* Stream as the largest area to be investigated, we inspected the zones included in the mentioned valley which, according to our preliminary study, could be mostly affected by mining activity, and we also collected some water samples in order to check contamination by heavy metals. *Libiola* mining site was chosen for our study among other Italian abandoned copper mines because of its geological, environmental and mining features; of its representativeness among other mines; because of available data and contamination aspects.

Key words: Contamination, dump-field, heavy metals, water.

Introduction

In Italy, mines and quarries represent an important sector of National economy and, even when they are ruled, serious environmental problems derive from extraction activities. Besides temporary impacts (noise, powder, pollution, etc.), they also cause deep and definitive changes to landscape, irreparable loss to soils, possible pollution to groundwater and some problems about use destination of abandoned areas.

Mining activity in Italy had an increasing trend till the mid of the 20th century. Nowadays, it is residual and it mainly concerns extraction of marls for concrete, ceramic and industrial minerals. Progressive decrease in extraction activities, particularly the ones concerning metals (whose refuses present high pollution), has surely relieved territories of mining impact. Nevertheless, structural and healthy problems remain because many abandoned mines also have their tailings and their washers, which have not been restored, yet.

In spite of its diffusion all in the National territory, mining activity must be differentiated both for concentration and for type of extracted minerals. About copper, Italy is not particularly rich, and its small or medium mines are enough widespread through the National territory, usually as thin veins whose extracted minerals did not contain a big amount of copper.

Our preliminary environmental study about abandoned copper mines located in the Italian territory has been focused on the following aspects:

a) Information on location of mining sites site and on history of mining activities
b) Information and data on natural features of mines
c) Data concerning past samplings

Among the Cu ores located in Italy, *Libiola* has got a special historic importance. Mineralization there is mainly associated to pillow basalts and basaltic breccias and, subordinately, to serpentinitic rocks from ophiolites of Internal Ligurian Units belonging to the *Supergruppo della Val di Vara* Unit (Bertolani, 1952; Ferrario and Garuti, 1980).

The primary mineralogic association is pyrite and chalcopyrite, with subordinate sphalerite, pyrrhotite, marcasite, hematite, mackinawite, magnetite, cubanite, and gold. Scarce gangue minerals include quartz and carbonates (Bertolani, 1952; Ferrario and Garuti, 1980).

Known since Copper Age, its maximum exploitation level occurred at the end of the 19th century (under the English Society "Libiola Copper Mining Company"), giving yearly almost ten thousands tons of cupriferous pyrite and chalcopyrite. The end of activity, in 1962, surely left many questions about the probable pollution of soil and groundwater and about the instability of excavations, galleries and dumps. *Libiola* mining area is currently abandoned at all, galleries are totally inaccessible due to collapses and floods as well as gas exhalations; many degraded infra-structures and mining buildings are moreover

present. Sterile materials and rests from selection and enrichment processes were deposited into five main disposals and, subordinately, into several minor disposals, near the galleries' mouths and enrichment plants.
The waste-rock dump is extremely heterogeneous from mineralogical and geochemical viewpoints. The significant lateral variations as well as vertical heterogeneity are common, and expected features of all mine dumps constructed over long periods of time (Marescotti et al., 2009).
Libiola mine dumps were formed within a period of over 50 years, during which different techniques of exploitation were used and several lithotypes and economic minerals were extracted, both underground and by open-air excavations. Waste materials that were piled up during exploitation include both host rocks and non-economic mineralization derived from hand picking, milling and other treatments (Marescotti et al., 2009).
The area of the dump along the pathway which is imposed on the contact between serpentinites and basalts (where we could observe some disseminated mineralization on serpentinites), and which borders the main open excavation, was also used in the past as a municipal disposal.

Materials and methods

In order to investigate our selected site in a correct way, we firstly confined our investigation area starting from identification of potential danger centers within the territory (tunnels, excavations, dumps, banks and basins containing rests from mineral processing, etc.), by using thematic old documents, and by inspecting the mining area of interest.
Primary pollution centers are generally classified according to their origin into pollution centers connected to extraction activities (i.e. mining excavations, discharges for tracing deposit or for mining research), pollution centers connected to mineral processing (i.e. basins for mine steriles[1], banks of fine rests, steriles from gravimetry), pollution centers connected to presence of different waste from extraction one (i.e. reagents used at plants, oils, coverings or detritus with concrete-asbestos).
Primary contamination sources at *Libiola* mining area are represented by dumps, excavations and galleries, which can undergo erosion, powders emission and solid transport to soils and stream sediments as well as infiltration, percolation and leaching, causing hydro-geological instability; secondary contamination sources are here represented by hydro-geological instability and by soil / sediments, which can move pollution to groundwater (by solid transport or in solution) and to wind/atmosphere (by emission of powder).
After identifying the possible polluting sources, our second step is identification of the potential migration pathways of contaminants from sources to targets, according to features of the sources themselves and according to geologic, hydro-geologic and geo-morphologic features of the site.
Considering that contamination is mainly diffused into a mining area by surface water eroding banks of extraction and treatment rests and transporting potentially polluted materials to valleys, it was basic for us to identify the hydrographic basin involving all contamination sources, primary and secondary. Identifying the surface subtended by the interested hydrographic basin allowed us to describe perimeter of the largest area to be considered for our study. *Libiola* ex mining area is included in the hydrographic basin of *Gromol*o Stream. Such a basin starts its path about 10 km from the coast and debouches in *Mar Ligure*, just north of *Baia delle Favole* (northern seaside of *Sestri Levante*). The basin covers an area of about 21 km^2, and the total length of the main river is about 9 km.
Such a hydrographic network is asymmetric with respect to the river course. Distribution of rivers inside the network is rather homogeneous. Among the most important tributaries on the left bank, *Rio Boeno* and *Rio Cattan* are the most important ones from our viewpoint because they represent confluence points of mining waters, continuously coming from the northern and from the southern slopes of mining area respectively. Mining area is in fact confined by *Gromolo* Stream itself at the western side; by *Rio Boeno* at the northern side; and by *Rio Cattan* at the southern side. Presence of the abandoned mine at *Libiola*, on the slopes of *M. Rocchetto*, along the ridge from *M. Bianco* to *M. Tregin*, is relevant both for geologic and for morphologic aspects and for the high altitude near the coast (Tomaselli A., 2011).Hydrologic regime of the whole area in which *Libiola* abandoned mine is included, is very affected by mining activities; in fact, one can notice acid water constantly flowing out of the several galleries (in particular in correspondence with downward galleries *Ida* and *Castagna*) and discharged into *Gromolo* Stream, thus determining a strong impact on this aqueous environment and on vegetal and animal species living there. This feature is due to presence of an extended network of interconnected

[1]Solid material or mud, which remain after mineral treatment for separation (i.e. crashing, milling, sieving, floating and other physical-chemical techniques) in order to obtain precious minerals from precious rock.

galleries and wells, which facilitates drainage of raining water. At higher quotes, extended open excavations (showing a sinklike morphology) are moreover present: they increase drainage of water and represent important artificial basins for water collection.
Starting from past investigations and by inspecting the area itself, a Conceptual Model (MCP) could be elaborated in order to organize successive investigations in a correct way. MCP allows to identify contamination sources, potential targets, active connections and eventual connections to be defined by further investigations. MCP should be supported by a graphic scheme (flow chart, Fig. 1) which can allow a quick and easy interpretation of pollutants' transfer from sources to targets.

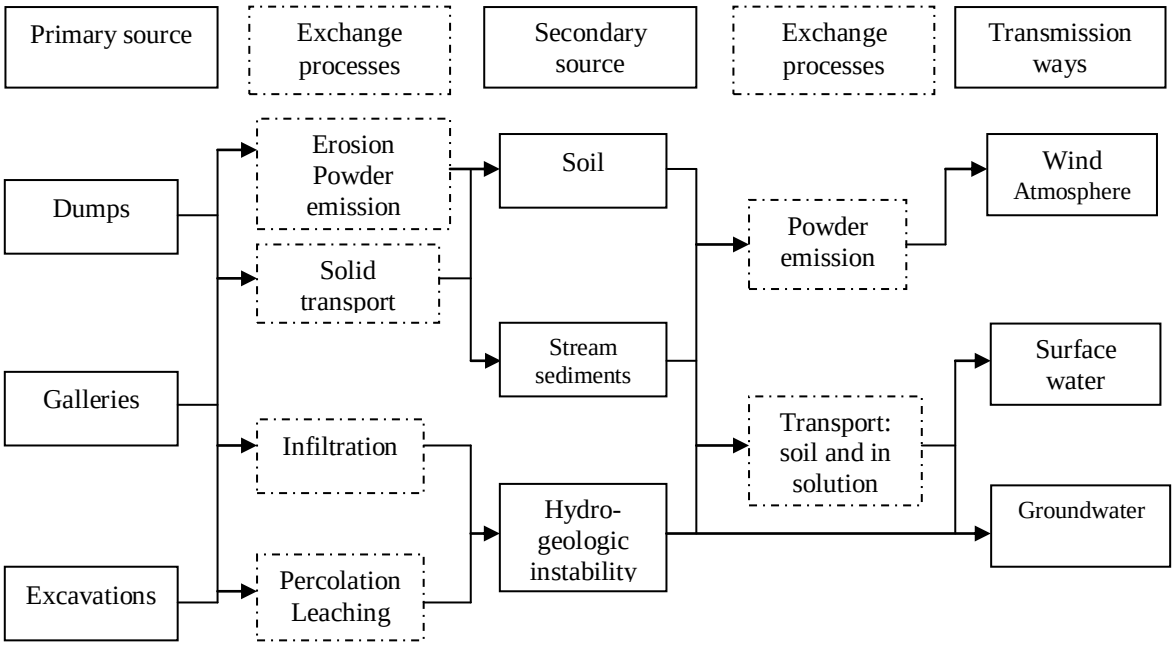

Fig. 1. Flow chart showing Conceptual Model (MCP). Source: Boi et al. (2009).

An important part of our environmental characterization consisted in locating sampling points. Location of sampling points was ended to obtain a correct definition of features of danger centers and of quality status of environmental matrices within the investigation area.
Location of sampling points (Fig. 2) was "reasoned": as a matter of fact, the choice of sampling points was based on knowledge of the site (morphology, type of materials, active erosion, results of past investigations, etc.), which allowed to identify the most vulnerable areas and the most probable contamination sources.
Sampling operations were documented by pictures showing collecting points of each sample and the area in its context. Each sample was identified with univocal initials and with geographic coordinates.Considering the largest area to be investigated as discussed above, we inspected *Libiola* mining area during winter 2013-2014, and we collected six water sample from the most interesting locations according to our preliminary study. We measured on field both temperature and pH of the collected water sample.
The six water samples are as follows:

- W1 was collected from the mouth of *Castagna* Gallery (72 m a.s.l.), whose highly acid water directly flows into *Gromolo* Stream. That gallery is located near the old mining buildings where minerals were worked (coordinates 44.303215, 9.436215).
- W2 was collected from water flowing out of *Margherita* Gallery (coordinates 44.300015, 9.44505), 206 m a.s.l., about 15 meters under the gallery itself. Basic water from *Margherita* gallery flows downstream to *Rio Cattan* which, after a short pathway, flows into *Gromolo* Stream about 200 meters after confluence of water coming from *Castagna* Gallery.
- W3 was collected from the mouth of *Santa Barbara* Gallery, 243 m a.s.l. (coordinates 44.300633, 9.446107).
- W4 was collected some meters downstream of *Speranza* Gallery's mouth, 291 m a.s.l. (coordinates 44.304188, 9.448467), along the creek flowing out of the gallery itself. This gallery

is located under an open excavation which was used as a disposal in the past. Such water also shows weird whitish foam.

- W5 was collected from the creek river which drains the discharge (coordinates 44.305424, 9.448500), near the old buildings and *Weirs* Gallery (238m a.s.l.).
- W6 was collected from *Ida* Gallery at 106 m a.s.l. (coordinates 44.308768, 9.442325), whose mouth is located along the orographic left of *Rio Boeno*, some upstream than introduction of *Rio Boeno* itself into *Gromolo* Stream. Its high acid solutions, together with the important discharge in front of the gallery, make this site the most important one within the area as far as the environmental impact is concerned.

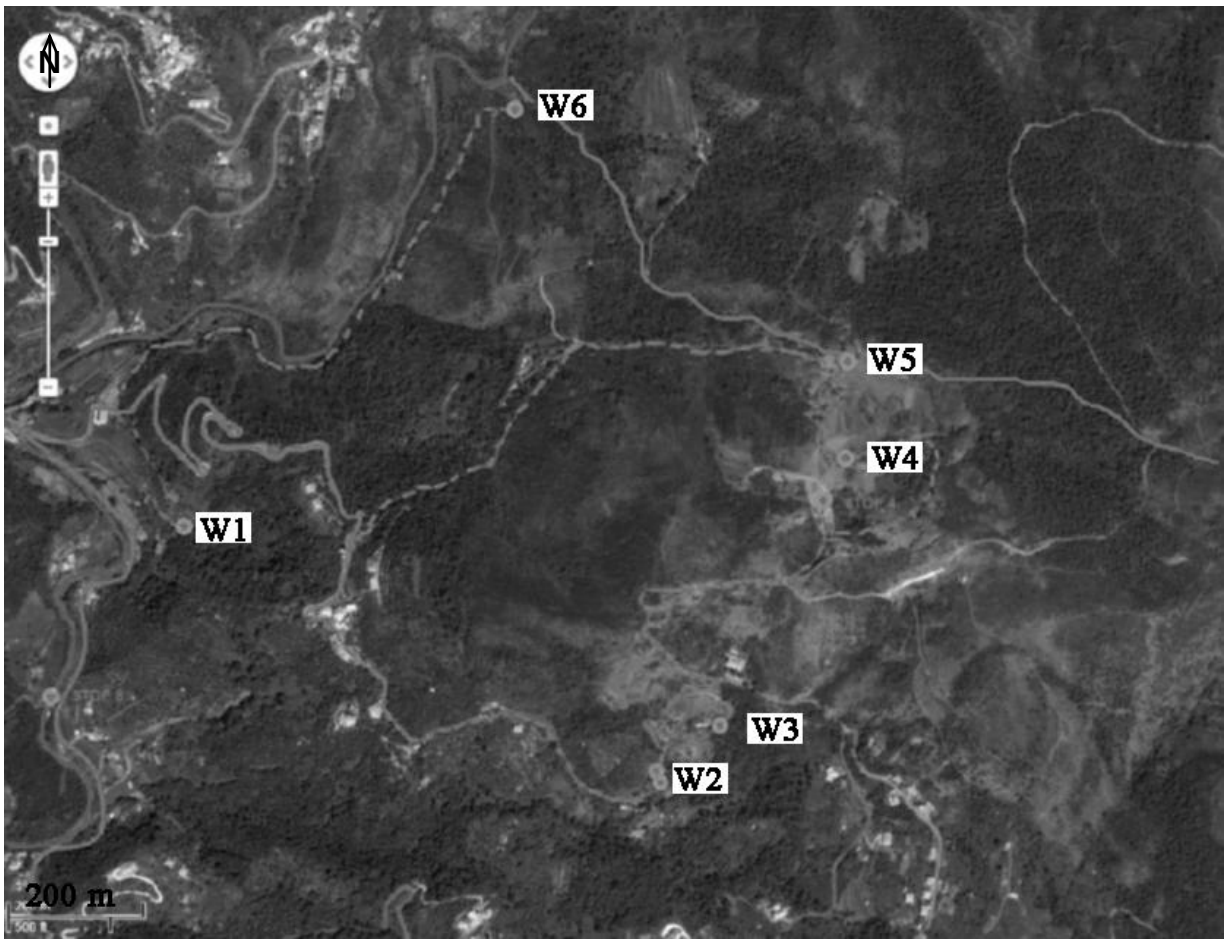

Fig. 2. Location of sampling points at *Libiola* mining area

Experimental

Concentrations of 14 elements (As, Bi, Cd, Co, Cr, Cu, Fe, Mn, Ni, Pb, Sb, Se, Sn and Tl) were determined in sample using a simultaneous ICP–OES (Varian ICP/VISTA MPX) equipped with a cyclonic spray chambers. Standard solutions for calibration were matrix—matched by preparation in HNO_3 1% (w/w). In order to control nebulizer efficiency, an internal standard (yttrium 100 µg/L – wavelength 371.030 nm) was used. About ICP-OES instrumental parameters, we list them as it follows: incident plasma power (RF) (kW) 1.00; plasma gas flow (L min^{-1}) 15.0; auxiliary gas flow (L min^{-1}) 1.50; nebulizer pressure (kPa) 200; replicate read time (s) 45; instrument stabilization delay (s) 40; sample uptake delay (s) 40; sample uptake delay (s) 40; pump rate (20); rinse time (s) 20; replicates (2).

The ICP-OES operating parameters were properly optimized to meet the appropriate detection limits (LOD).

Results and discussion

The analysis of the heavy metal content at the dump-field area of *Libiola* is presented in table 1. As it is a Cu-deposit, it is not surprising that highest are (with the exception of Fe: 9.27 – 19.07 %) the Cu contents. They vary from 945 in the sample SL-1 to >10 000 $mg.kg^{-1}$ in the sample SL-4, obtained from the brook

bank at the little waterfall below the dump-field. Also the highest Ni content (1104 mg·kg^{-1}) was found in the C horizon of the same soil sample SL-4. Also high Zn (227 – 951 mg·kg^{-1}) and (variable) Cr (33 – 539 mg·kg^{-1}) contents were described. Interesting is also the relatively high V content (98 – 279 mg·kg^{-1}). The As, Sb, U, Th and Ag contents are very low.

If we compare the heavy metal contents with the Italian National Law 152/06, we can see that at *Libiola* the heavy metal contents in soils and dump material are higher, even the ones mentioned in the (less strict) limits of National Law 152/06 for industrial/commercial site (Cu – 0.300 mg·kg^{-1}; Fe – 0.300 mg·kg^{-1}). They exceed the law limits in case of Cu, Ni (±Co, Cd, V, Cr). If we compare our data with th stricter limits of the mentioned law (residential / for public green sites) also Zn and Sn (in several samples also Pb) exceed the allowed limits for soils.

Table 1. ICP-MS analyses of soils and dump material.

Sample	Fe	Mn	Cu	Pb	Zn	As	Sb	Mo	Ni	Co	Th	U	Cd
	%		mg·kg^{-1}										
SL-1	15.89	0.10	945	74	410	10	3.9	7.7	80	33	0.2	1.0	1.0
SL-3	14.21	0.06	2991	16	227	6	0.5	10.6	509	61	0.1	1.8	9.4
SL-4	11.88	0.34	>10 000	48	605	7	1.6	5.8	1022	461	0.4	1.6	2.2
SL-5	15.08	0.46	>10 000	69	690	14	3.0	11.5	907	539	0.9	3.7	2.7
SL-6	9.27	0.14	7345	30	435	11	1.8	4.8	1104	195	0.4	1.5	1.3
SL-7	10.81	0.10	5638	33	434	8	4.7	5.5	713	108	0.3	1.1	3.6
SL-8	19.07	0.07	3238	113	264	14	7.6	14.6	667	81	0.5	1.6	0.5
SL-9	9.86	0.12	1627	17	951	6	1.4	4.6	883	132	3.8	1.2	1.1

Table 2 reports temperature in °C and pH values concerning water samples collected at *Libiola* mining area, measured on field.

Table 2. Temperature and pH values measured on field at *Libiola* mining area.

Values	W1	W2	W3	W4	W5	W6
T °C	12.6	14.9	14.4	14.8	12.3	13
pH	3.06	5.52	4.94	5.25	6.24	3.06

Table 3. Concentration values concerning water samples collected at *Libiola* mining site, compared with Italian law limits provided by the Italian Law 152/06 for groundwater.

Element	Unit	W1	W2	W3	W4	W5	W6	Law Limits
As	µg/L	< 15	< 15	< 15	< 15	< 15	< 15	10
Bi	µg/L	2.4	8.1	14	12	<0.1	3.5	-
Cd	µg/L	55	20	15	9.2	1.0	50	5
Co	mg/L	1.1	0.21	0.32	0.16	0.01	0.91	0.05
Cr	µg/L	708	< 5	< 5	14	10	354	50
Cu	mg/L	93	8.0	9.4	11	0.51	54	1.0
Fe	mg/L	366	0.04	0.06	8.4	0.07	284	0.20
Mn	mg/L	4.6.	1.3	1.7	1.1	0.05	3.9	0.05
Ni	mg/L	3.2	0.77	0.46	0.31	0.096	1.8	0.02
Pb	µg/L	< 10	< 10	< 10	< 10	< 10	< 10	10
Sb	µg/L	< 10	< 10	< 10	< 10	< 10	< 10	5
Se	µg/L	< 20	< 20	< 20	< 20	< 20	< 20	10
Sn	µg/L	1.9	1.5	1.5	3.3	2.3	5.1	-
Tl	µg/L	-	-	-	3.7	1.0	-	2

Table 3 reports results from *Libiola* mining area from ICP-OES analysis in comparison with limit values for groundwater provided by the Italian Law 152/06. In spite of the mere scientific end of our study, nevertheless we found useful to report National law limits for a comparison.
By Tables 2 and 3, we can observe that:

- pH values (3.06-6.24) are included in a smaller range than it could be expected from past studies (Dinelli et al., 2007; Marini et al., 2003), and it could be explained by seasonal variations.
- W1 and W6 are the samples showing the lowest pH, thus they also show the highest exceeds in Cd, Co, Cr, Cu, Fe, Mn, Ni. *Castagna* and *Ida* galleries are in fact the lowest tunnels of the columnar structure showed by both yards extracting the mineralized mass, thus they collect the highest deal of percolate and show the highest interaction between percolate and mineral phases.
- No sample shows higher content in As, Pb, Sb and Se than instrumental LOD.
- W5 is the sample showing the lowest pollution. In spite of it, its content in Ni exceeds law limits.
- All samples exceed law limit as far as Ni is concerned. The high content in Ni could also indicate presence of Ni sulphides in the main mineralization; moreover, small amounts of Ni are often present in some of the most common Cu-Fe sulphides.
- W4 is the only sample showing high content in Tl.

Conclusions

The presence of heavy metals at abandoned copper mines is given by ore composition assemblage and can become a very important source of contamination for the surrounding environment. Our main concern was to investigate water contamination at *Libiola* (Italy) abandoned copper mine. Water analysis showed different rates of pollution according to location of collected water. Main contamination with heavy metals in analyzed water is represented by presence of Cd, Co, Cr, Cu, Fe, Mn and Ni because of presence of tailings containing high levels of ore minerals (Tab. 1). In the case of Ni, all collected samples exceed law limits. Water collected from *Castagna* and *Ida* galleries shows the lowest pH and the highest pollution because these tunnels are the lowest ones for altitude, thus we can expect the highest interaction between percolate and mineral phases. The values of pH measured on field are lower than the values showed in the past literature and it can be motivated by the influence of rainy season. It could be interesting to repeat sampling activity periodically for a better characterization of this mining site, starting from the discussed investigation plan and even by improving it. The results from this study can represent a starting point for a more constant monitoring activity within this mining area. It could be also suitable to extend monitoring activity to soils and plants.

Acknowledgement: This work was also supported by grant N° APVV-0663-10. The authors thank Dr. Geol. Emery Vajda from Sestri Levante (Italy), who kindly offered his technical and scientific collaboration..

References

Bertolani M.,1952. I giacimenti cupriferi nelle ofioliti di Sestri Levante (Liguria). Per. Min. 21, 149–170

Boi B., Delrio G., De Martini A., Demuru S., Dessì R., Murgia A., Persod P., Pilurzu S., Serra S., Urpi I., Zillo E., 2009. Linee guida per la caratterizzazione e la bonifica delle aree minerarie dismesse, Regione Autonoma della Sardegna

Dinelli E., Perkins W.T., Pearce N.J.C., Hartley S., 2007. Treatment of acidic mine drainage at Libiola mine, Liguria, Italy. IMWA Symposium 2007: Water in Mining Environments, R. Cidu & F. Frau (Eds), Cagliari, Italy

Ferrario A. and Garuti G.,1980. Copper deposits in the basal breccias and volcano-sedimentary sequences of the Eastern Ligurian Ophiolites (Italy). Mineralium Deposita15, 291–303

Marescotti P., Azzali E., Servida D., Carbone C., Grieco G., De Capitani L., Lucchetti G., 2009. Mineralogical and geochemical spatial analyses of a waste-rock dump at the Libiola Fe–Cu sulphide mine (Eastern Liguria, Italy). Environ Earth Sci DOI 10.1007/s12665-009-0335-7

Marini L., Saldi G., Cipolli F., Ottonello G., Vetuschi Zuccolini M., 2003. Geochemistry of water discharges from the Libiola mine, Italy. Geochemical Journal. 37, 199-216.

Tomaselli A., 2011. Provincia di Genova - Ambito Regionale di Bacino 17 - Piano di Bacino Stralcio sul rischio idrogeologico (ai sensi dell'art. 1, comma1, del D.L. 180/1998 convertito in L. 267/1998) - Torrente Gromolo - Relazione Generale

Rom. J. Mineral Deposits, vol. 87 (2014), No. 1, p. 71-74

DETAILED MINERALOGY OF BLASTFURNACE SLAG SAMPLES FROM GALAȚI METALURGICAL PLANT, ROMANIA

Paulina HÎRTOPANU*, Sorin Silviu UDUBAŞA

University of Bucharest, Faculty of Geology and Geophysics, 1, N. Bălcescu Blv., 010041 Bucharest, Romania
* *paulinahirtopanu@hotmail.com*

Abstract
In the southeastern part of Romania, near Galaţi, there is the largest slag waste dump in the country as a result of the metalurgicsl plant (now ArcelorMittal Galaţi) activity during the last decades. In order to asses the eventually re-use of the waste dump material, a detailed mineralogical study was carried out. Some 100 slag samples have been investigated and revealed a quite uniform composition. Their mineralgy is quite complex, from the point of view of mineral classes and comprises native elements, oxides, sulfides, phosphates and silicates. The main component is melilite, twinned and zoned, having with fine inclusions of native iron and oldhamite. Fayalite is rather frequent and zoned. Wüstite inclusions occur within the anorthite glass. Skeletal grains of merwinite have been observed, as well as perowskite associated with melilite. Hercynite and whitlockite occur as accessory components. The potential use of the slag material coud be as construction material but also as a potential source of some rare elements.

Keywords: slag, melilite, fayalite, calcium disilicate, native iron, wüstite, magnetite, troilite, oldhamite.

1. INTRODUCTION

The Galaţi blastfurnace, the largest in Romania, was built in the 1960s. The plant, now ArcelorMittal Galaţi, a subsidiary of ArcelorMittal Steel Holdings AG, is located in southeastern part of Romania, at the Danube port of Galaţi, 80 km from the Black Sea. The steelmaking process starts with the processing of iron ore which is brought, from worldwide, as far as West Africa, North Canada, Brazil, Kazakhstan, etc. The samples studied here were collected from the furnace slag waste dumps.
A mineralogical investigation was carried out in order to reveal the mineral composition of the slag as a basis for eventual reprocessing. The mineralogy of Galaţi slag (GS) shows that it is predominantly silicate (melilite, wollastinite, dicalcium silicate, monticellite, anorthite and fayalite). In order of predominance, after the silicate class, follow the oxide class (wüstite, magnetite, hercynite, spinel, spinel-hercynite mixture) sulfides (oldhamite, troilite, pyrrhotite, Ni-sulfides) and native elements (native Fe). Rarely, some phosphates occur (whitlockite) as accessory minerals. This estimation is based upon careful microscopic investigation (in transmitted and reflected light) of over 100 slag samples covering almost the whole surface of the slag heaps.

2. MINERALOGY

2.1 Native elements

Native iron, Fe, cubic. It occurs typically in small blebs (Fig. 1). In polished sections it has a white colour, high reflectivity, and is isotropic. In the GS the native iron is associated with wüstite, troilite, magnetite and fayalite. The native iron is a very good indicator for highly reduced environments.

2.2. Oxides

Wüstite, FeO, cubic. In the GS wüstite occurs as massive or individual anhedral grains between other slag minerals like fayalite, or magnetite. In reflected light it has a light grey colour, with a faint greenish tint (Fig. 1). The wüstite from GS is formed at high temperatures and in a highly reducing environment, usually on fayalite.

Magnetite, $Fe^{2+}Fe^{3+}O_4$, cubic. It occurs rarely, as relic grains usually transformed in wüstite. In reflected light it is light gray with a brownish tint and has troilite inclusions (Fig. 1b).

Hercynite, $FeAl_2O_4$, cubic. In transmitted light hercynite from GS has a red colour and is isotropic. It occurs in a very small quantity, being associated with fayalite (Fig. 2a).

Spinel, $MgAl_2O_4$, no colour, isotrop. Spinel rarely occurs but in big grains.

Spinel-hercynite solid solution intermediate members, $(Fe,Mg)Al_2SiO_4$, yellow colour, isotrop. All spinel terms occur in the Al rich areas, with some variations of Mg and Fe.

2.3. Sulphides

Oldhamite, (CaMg)S, cubic. It occurs as dendritic inclusions in melilite (Fig. 2b). In some melilite crystals there occur dendritic inclusions of oldhamite. Sometimes the oldhamite inclusions are very concentrated almost throughout the crystal giving it an opaque appearence. In some melilite samples, larger inclusions of oldhamite and stellate clusters (ca 0,4mm) occur. Oldhamite appears also as euhedral individual crystals.

Troilite, FeS, hexagonal. It is a rare sulphide mineral, being the end member of the pyrrhotite group. The pyrrhotite has the formula $Fe_{(1-x)}S$, with iron deficient. Troilite is enclosed in magnetite as small grains (Fig. 3a). In wüstite the troilite occurs as very fine filliform veins. In reflected light it has a light yellow colour and is anisotropic.

Pentlandite (?), $(Ni,Fe)_9S_8$, cubic**,** optically determined. It occurs rarely, as large grains. In reflected light it has a white colour, no cleavages, and it is isotropic. It is associated with magnetite (Fig. 3b). It will be correctly determined in our future researches by microprobe analyses.

2.4. Silicates.

The mineralogical constituents of GS silicates are in predominance order the following: melilite group, fayalite, dicalcium silicate and anorthite.

Melilite is the major crystalline phase in all samples and occurs as euhedral, prismatic forms with crystals sometimes twinned. It is a solid solution of akermanite ($2CaO{\cdot}MgO{\cdot}SiO_2$) and gehlenite ($2CaO{\cdot}Al_2O_3{\cdot}SiO_2$). The melilite occurs in clusters and as isolated crystals in concentric and sector type zones (Hîrtopanu et al, 2004). The microscopic features of melilite are very similar to those presented by Scott et al. (1986). The iron, oldhamite and troilite inclusions in melilite are common.

Fayalite, Fe_2SiO_4, orthorhombic. Fayalite is very rare in nature but is common in metallurgy, especially in iron slags. In the GS it presents a granular prismatic habit with moderate and imperfect cleavages. In transmitted light, the fayalite has a pale yellow to amber colour, with very faint pleochroism (Fig. 2a). Optically it is biaxial (-). It has inclusions of native iron and troilite, and is frequently substituted by wüstite (Fig. 4a).

Anorthite, $CaO{\cdot}Al_2O_3{\cdot}2SiO_2$, triclinic, occurs in the domain of low lime and high alumina contents, where the mineral may be formed. It is grey black, glassy and isotropic.

Dicalcium silicate, $2CaO{\cdot}SiO_2$, orthorhombic, may be formed in slag having a high lime content. It occurs as striated grains. The dicalcium silicate occurs in at least three different forms (Lee, 1974). The α-form occurs at temperatures above 1.420°C, when the slag is in a liquid state. When the temperature falls to about 675°C, the dicalcium silicate occurs in the β-form. So, the dominant form in the GS is β-form. When the dicalcium silicate changes from the β to the γ form, which it can be done at atmospheric temperatures, it increases in volume by about 10 % (Lee, 1974), and if the silicate is in sufficient quantity, the expansion will cause disintegration of the slag matrix, which has happened to the GS. Also, the oxidation of the reduced iron oxides from GS leads to expansion, which may cause disintegration of the GS.

2.5. Phosphates

Whitlockite, $Ca_{18}(Fe,Mg)_2(H_2,Ca)(PO_4)_{14}$, rhomboedral, anhydrous apatite, occurs rarely in GS, as accessory, in large grains (Hîrtopanu et al, 2004). The withlockite, identical with the beta polymorph of $Ca_3(PO_4)_2$, first known from slag systems, was later found in nature. In transmitted light the whitlockite occurs as rhombohedral, colorless grains and has no cleavages. It is optically (-).

3. DISCUSIONS

There is no silica present in the GS. It is probably all bound up in the melilite, fayalite, dicalcium silicate and anorthite. The anorthite is present as glass in which the iron reduced oxide, wüstite, and the silicates were dissolved. The small quantity of Al_2O_3 remaining after the forming of anorthite contributed to form the hercynite. The mineralogical composition of the GS in terms of hercynite, fayalite and wüstite assists in determining its melting temperature. If the mineralogical composition is inserted in the phase diagram in Fig. 5 for anorthite, silica and wüstite (Lee, 1974), the theoretical melting temperature can be read off. This can be seen to be about 1.100-1.200°C, which approximates the working temperature of the furnace.

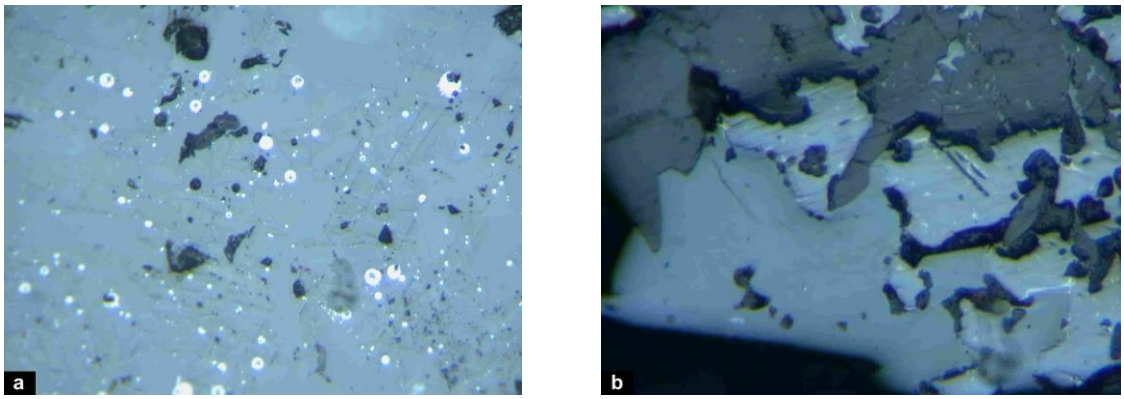

Figure 1. (a) Native iron (white, blebs) in wüstite (grey white); (b) wüstite (grey), magnetite with troilite inclusions (whitish grey) and fayalite (dark grey) with wüstite inclusions. Reflected light, x160, NII.

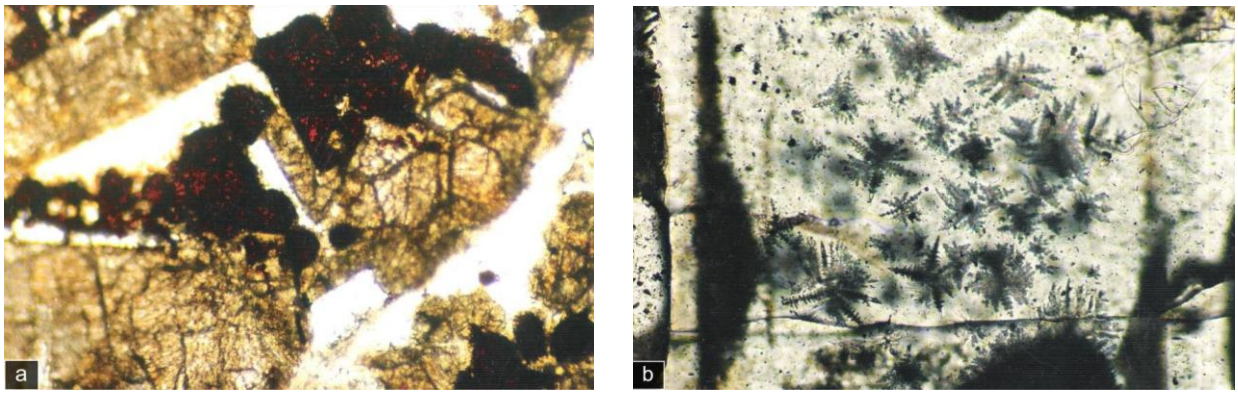

Figure 2. (a) Hercynite (red-brown), fayalite (yellow-brownish), x25, NII; (b) stellate oldhamite crystals and its dendritic growth within a melilite crystal (white grey). Transmtited light, x25, NII.

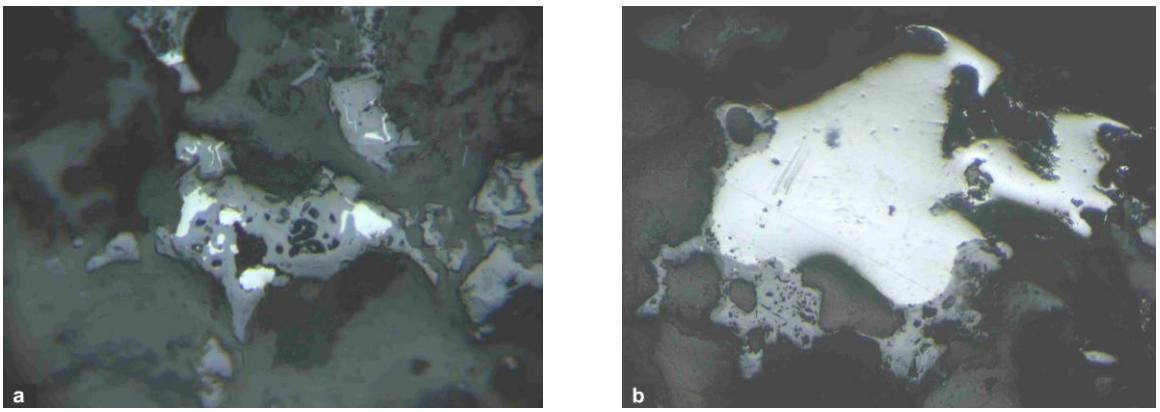

Figure 3. (a) Magnetite (grey) with troilite inclusions (white, anisotropic), x210, NII; (b) Ni-sulphides (pentlandite ?) (white, isotropic) and magnetite (grey, porous), x160, NII.

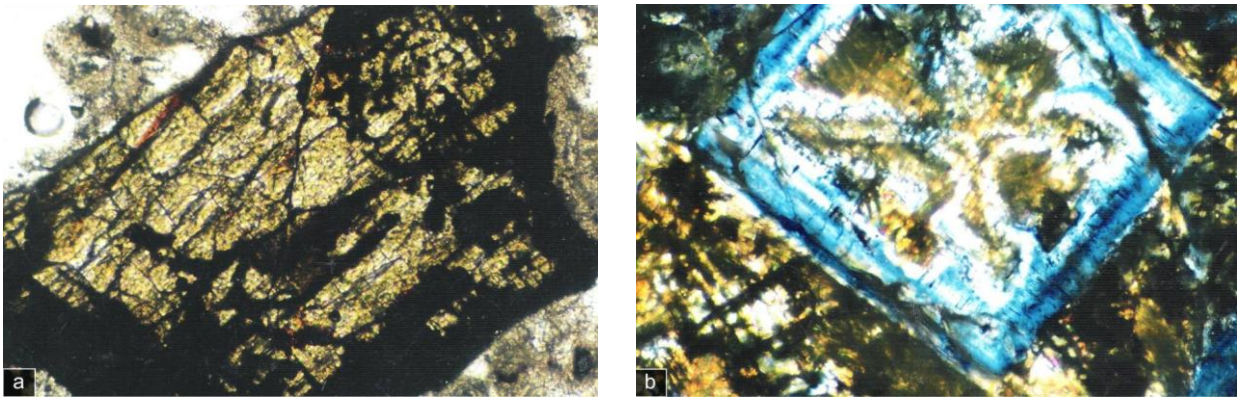

Figure 4. (a) Fayalite (brown-yellow) and wüstite (black), x20, NII; (b) zoned melilite crystal (bluish), x40, N+.

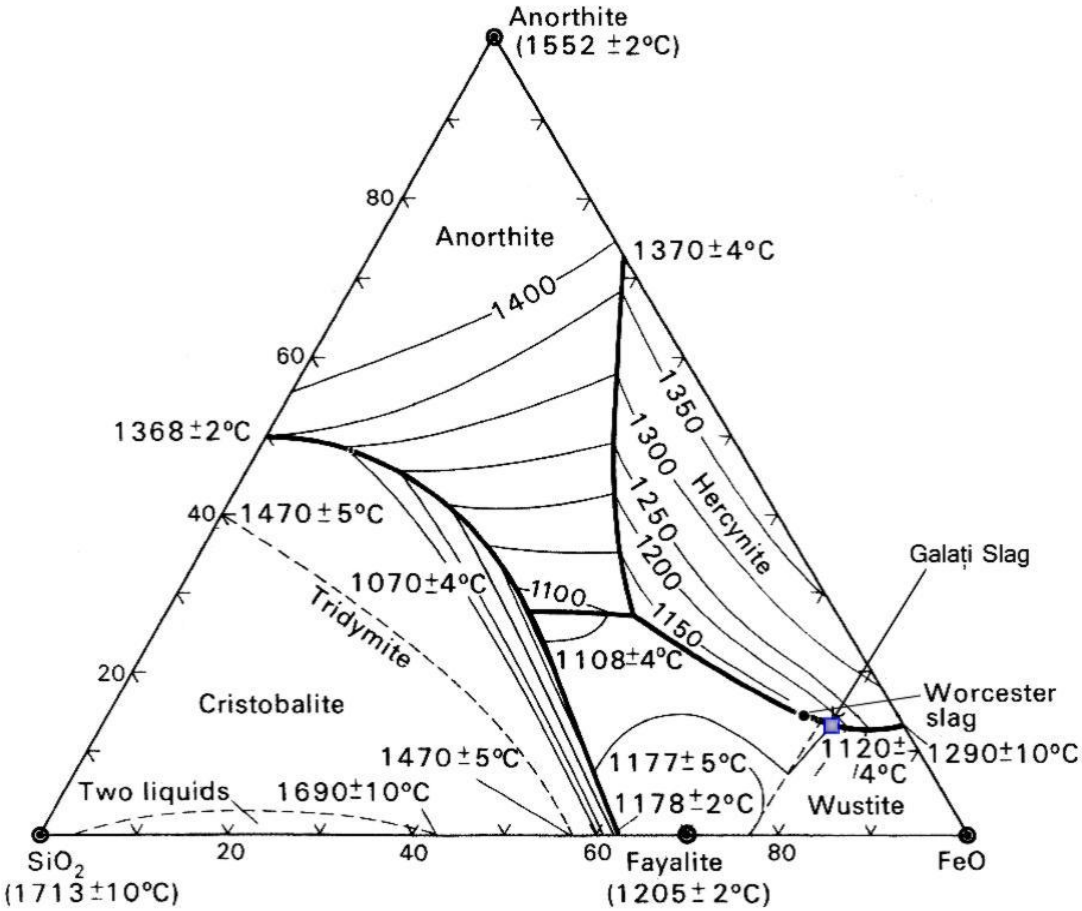

Figure 5. The system anorthite-wüstite-silica phase diagram; GS are situated within FeO right corner in the wüstite-fayalite-hercynite area (Lee, 1974).

4. CONCLUSIONS

In spite of common appearance (black to greyish colors) the microscopic analysis of GS revealed its diverse mineral composition. The determined minerals belong to 5 mineralogical classes: native elements, oxides, sulphides, silicates and phosphates. Most minerals are very rare, occurring in meteorites or on Mars and the Moon (troilite, oldhamite, native Fe). The most dominant mineral phases are those occuring at high temperature, resembling either the sideronitic textures or rapid quenching of high temperature assemblage (skeletal crystals, stellate crystals, e.g. oldhamite in melilite) etc. The mineralogy of GS could be more various and a complex study is in progress. Such a study is necessary to assess the potential for the re-use of GS as construction material. The GS could also be a source of some rare elements.

REFERENCES

Hîrtopanu P., Udubașa G., Hârtopanu I., 2004. Mineralogy of Galați blastfurnace slags. Rom. J. Mineral Deposits, 81, p. 104-107.

Lee A.R., 1974. Blastfurnace and steel slag, Production properties and uses. John Wiley and Sons, New York, 130p.

Scott P.W., Critchley S.R., Wilkinson F.C.F., 1986. The Chemistry and Mineralogy of Some Granulated and Pelletized Blastfurnace Slags. Mineral. Magazine, 50 141-147.

RESEARCH ON METHODS OF TREATING MINE WATER GENERATED FROM EXPLOITATION OF ROSIA POIENI, ROMANIA

Teodor VELEA, Andreea MITU, Andreea GRĂDINARU*, Georgiana MOISE, Luminita MARA, Cornel FRAȚILĂ, Mihai GHIȚĂ, Valentin DRĂGUȚ

National R&D Institute for Non-ferrous and Rare Metals, 102 Blvd, 077145, Pantelimon, Ilfov, Romania
*e-mail: *andreea.gradinaru@yahoo.com*

Abstract The purpose of this research is to investigate the possibility to characterize in terms of geochemistry of the mine water resulted from exploitation and concentration of porphyry copper deposits in Rosia Poieni in order to assess the water treatment techniques, as cost-effective and reduced impact on the environment. Mine water samples have been taken from several points of the mining area; chemical analyses showed a good correlation between their composition in terms of content of Cu, Fe, pH, conductivity and content of precipitated hydroxides of iron. Preliminary research of mine water treatment studies revealed three main action applicable on the adsorbent materials: nano-sized iron oxides, polymers, biochar, which will be studied in detail in the future.

Keywords: acid rock drainage (ARD), mine water treatment, adsorbents, spectroscopy analyses, porphyry copper.

1. Introduction

Exploration and exploitation of natural deposits of copper are essential for our society as long as metallic copper market demand is high. The interest is even higher as copper price quoted on international markets has increased significantly in recent decades, from about USD 1000/ton in the 80s, with fluctuations between USD 2000-3000/ton in the period 1998-2004, up to USD 8000/ton currently (Bostan, 2013).

Copper sulfide minerals provide 90% of global copper production. Characterized by low concentrations of copper, they require processing by preparation and concentration by flotation activities in order to be economically exploited (Almasan, 1984).

In our country, the most important copper deposits are in the Baia Mare region (Nistru, Baia Sprie, Herja, Cavnic) consisting of polymetallic sulphide mineralizations (Almasan, 1984; Kouzmanov et. al., 2005a; Lang, 1979), Balan (with chalcopyrite and pyrite in crystalline schists), Baia de Arama, Moldova Noua (Almasan, 1984), in the Apuseni Mountains from Deva, Rosia Poieni, Valea Morii, Rovina Tarnita-Deva, in porphyry type deposits as part of famous South Apuseni Mountains Neogen ore district, known as “Gold Quadrangle”, associated with volcanic activity and hydrothermal mineralizations containing chalcopyrite, bornite, covellite (Udubasa et.al., 2001; Kouzmanov et. al., 2005b; Neubauer et. al., 2005, Kouzmanov et. al., 2005a, Ivascanu et. al., 2003) with an industrial exploitable ore reserves estimated at about 16 million tons, containing approximately 0.28% Cu and 2.8% S (Almasan, 1984).

An important problem in the exploitation and processing of copper ore with a potential negative impact on the environment are acid mine drainage waters resulting from copper ore solubilization phenomenon mainly controlled by sulfides from mining quarry and mineral deposit, used as oxidation and leaching agents: water, air and soluble salts of Fe (III) , (Bird, 1987; Bird et. al., 2008; Bird et. al., 2009; Bird et. al., 2010; Byrne et. al., 2012; Byrne et. al., 2013; Chanpiwat and Sthiannokao, 2014; Mayes et. al., 2013). The main copper solvent is an acidic solution of ferric sulfate formed by oxidation of pyrite (eq. 1, 2), this phenomenon being favored by natural bacteriological solubilization in the presence of two types of bacteria: thiobacillus-ferooxidans and thiobacillus-thiooxidans. The first type of those uses energy from the oxidation of divalent iron to trivalent iron , and the second type has the role to oxidize the sulfur (from sulfides) in sulfate, in the presence of O_2 and CO_2 at temperatures between 35-40°C, the reaction of hydrolysis and solubilization of iron sulfides acid (eq. 3-6), (Jiang et. al., 2007) :

$$2FeS_2 + 2H_2O + O_2 \rightarrow 2FeSO_4 + 2H_2SO_4 \,, \quad (1)$$

$$4FeSO_4 + 2H_2SO_4 + O_2 \rightarrow 2Fe_2(SO_4)_3 + H_2O \,, \quad (2)$$

$$Fe_2(SO_4)_3 + 6H_2O \leftrightarrow 2Fe(OH)_3 + 2H_2O \,, \quad (3)$$

$$Cu_2S + 2Fe_2(SO_4)_3 \rightarrow 2CuSO_4 + 4FeSO_4 + S \,, \quad (4)$$

$$CuFe_2S_2 + 2Fe_2(SO_4)_3 + 2H_2O + 3O_2 \rightarrow CuSO_4 + 5FeSO_4 + 2H_2SO_4 \,, \quad (5)$$

$$2S + 3O_2 + 2H_2O \xrightarrow{bact.} 2H_2SO_4 \,, \quad (6)$$

The problem of sulfides oxidation and associated phenomenon of acid mine drainage waters, solutions and precipitation processes of metals and minerals have been extensively examined in recent decades. Essential aspect is related to the understanding and control the formation of mine waters, stability sulphide potential coverage of Fe (III) hydroxide, the development of effective methods of prevention and various treatment techniques of contaminated waters.

In general, the physicochemical treatments of wastewaters offer various advantages such as rapid process, easy of operation and control, flexibility to temperature changes. There are many methods currently used to remove and recover metals from environment and many proposals make reference to the physicochemical methods for their removal from wastewater.

These include chemical oxidation and reduction, membrane separation, liquid extraction, carbon adsorption, ion exchange treatment, electrolytic treatment, electro-precipitation, coagulation, flotation, evaporation, sulphides and hydroxides precipitation, crystallization, ultrafiltration, electro-dialysis, etc.

In this paper there are presented the results of the analyses on a sample of copper concentrate and several samples of mine water through physico-chemical and structural methods (ICP-OES, FAAS, XRD and optical microscopy) with the aim to characterize them in order to assess treatment methods applied and for selecting effective adsorbent materials.

2. Materials and methods

2.1. Sampling

Mine water samples have been taken from different points of the mining area, by sampling equal volumes of 500ml/sample and have been studied by spectroscopy ICP-OES, AAS spectroscopy. After analyzing the composition, they were mixed to obtain a medium sample with homogeneous composition and a significant volume (50 liters), for treatment.

2.2. Spectroscopic analysis

Spectroscopic analyses have been performed using ICP-OES and FAAS methods, in the laboratories of the National Institute of Research and Development for Non-ferrous and Rare Metals.

2.3. X-Ray Powder Diffraction analysis

X-Ray Powder Diffraction has been carried out on a Bragg-Brentano Bruker D8 Advance diffractometer, using the Bruker DIFFRACplus BASIC software (20060 and the ICCD database PDF-2 release 2006. X-ray diffraction data have been carried out in the 2θ range from 4 to 74 degrees, 0.02 degrees step size and 3 sec time per step with CuKα radiation at 40kV and 40mA. CuKβ radiation was removed by SOL-X detector.

2.4. Microscopic analyses

Microscopic analyses have been performed using an AXIO IMAGER. A1m microscope with polarized light.

3. Experimental

Laboratory equipment for mine water treatment studied is composed of a mechanical stirring system rotating type GFL 3025 - used for the extraction of copper on nanomagnetite and ion exchange with incorporated magnetite.

4. Results and discussion

4.1. Treatment technique selection and the adsorbent material

In order to remove toxic metals from aqueous solutions a number of conventional techniques there are currently applied such as: ion exchange, reverse osmosis, complexation and precipitation, and others, but the adsorption is the most effective and most commonly used for removal of heavy metal wastewater.

The study is the scientific basis for obtaining further innovative adsorbent materials with improved performance in the retention of heavy metals from solutions that will generate alternatives compared to traditional technologies that currently exist in the purification of water containing heavy metals. These new materials alone or in combination can be effective adsorbents in processes of purification of aqueous solutions containing heavy metals.

That is why we propose further research and experimentation to study this new class of materials representing by nano-magnetite, bio-charcoal and reticulated polymers, in processes for purifying aqueous solutions containing metallic ions provided from mining industry.

4.2. The results of physico-chemical and structural characterization

Table 1 shows the types of minerals resulting from copper concentrate processing by concentration (flotation) of porphyry-copper type ore from Rosia Poieni exploited in open pit, their distribution in concentrated mass, performed by XRD analysis and evidenced by optical microscopy (Fig.1. and Fig.2.). The XRD spectra revealed 8 minerals. The first type XRD spectrum is characteristic to chalcopyrite ($CuFeS_2$) showing typical peak for copper sulfide mineral. The second type XRD peak was found to correspond to pyrite (FeS_2). In small quantities the following minerals have been identified: biotite, bornite, ramsbeckite.

Table 1. The results of the beam analysis for the copper concentrate

Compound Name	Formula	S-Q (%ms.)
Chalcopyrite	$CuFeS_2$	~ 65
Pyrite	FeS_2	~ 16
Biotite	$KFeMg_2(AlSi_3O_{10})(OH)_2$	~ 4
Bornite	Cu_5FeS_4	~ 1
Ramsbeckite	$Cu_{15}(OH)_{22}(SO_4)_4(H_2O)_6$	~ 1

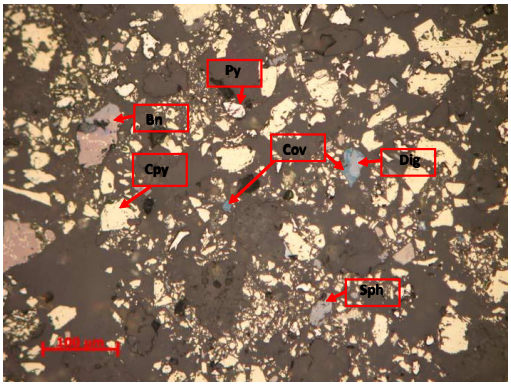

Fig. 1. Microphotograph of the copper concentrate in reflected light.
Chalcopyrite (Cpy), pyrite (Py), sphalerite (Sph), bornite (Bn), covellite (Cov), digenite (Dig)
Scale bar = 100 µm

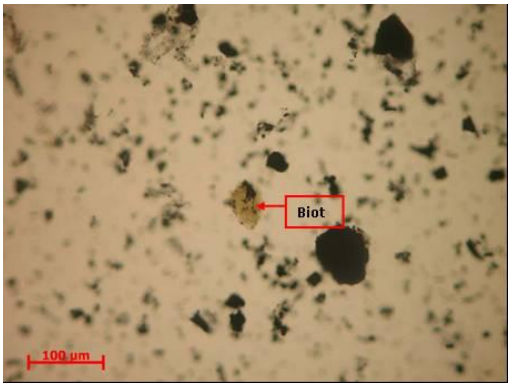

Fig. 2. Microphotograph of the copper concentrate in transmitted light.
Biotite (Biot)
Scale bar = 100 µm

Composition of mine water collected is mainly controlled by sulphides. It was observed a good correlation between the composition of samples taken from different points regarding the contents of Cu, Fe, pH and the iron hydroxide precipitates with relatively high concentrations of SO_4^{2-}, and high levels of some metals. An average composition of mine waters is shown in Table 2.

Table 2. Chemical composition of mine waters from Rosia Poieni

Elem.	Cu	Fe^{3+}	Zn	Pb	Mn	Mg	Cd
g/L	0.51	2.68	0.003	0.007	0.063	1.00	0.001
Elem.	**Al**	**As**	**Ca**	**Fe^{2+}**	**Cl^-**	**SO_4^{2-}**	**pH**
g/L	2.64	<0.0005	0.14	0.29	0.032	26.33	2.44

4.3. The test results of the preliminary treatment in the presence of the adsorbent based on magnetite

Following the performed experimental data there were obtained appreciable results regarding the nano-magnetite used for the mine wastewater treatment, rich in copper, iron and aluminum.

In the interpretation of data it has been observed that this nano-adsorbent was effective in adsorption of iron and then for copper. The optimum adsorption time was 60 minutes.

5. Conclusions

Mine water samples collected from different points of porphyry-copper ore deposit from Rosia Poieni have been analyzed by ICP-OES and FAAS spectroscopy. These techniques allow rapid and easy identification of the amount of metals present in mine water samples.

Levels of concentrations of metals and their type allowed an evaluation of potentially effective treatment techniques for remediation (cleaning), as well as the selection of the adsorbents types and preliminary tests to treat with magnetite-based adsorbent.

The results revealed that using magnetite as adsorbent is effective and can be applied with good efficiency, the degree of reduction in copper content for tested samples showed a decrease from 0.51 g /L to 0.32 g/L, with an efficiency of 40%, and a good separation of the precipitated iron hydroxides.

Acknowledgments The authors gratefully acknowledge ANCS and MEC for financial support by the research grant PN0924.01.11/2014.

References

Almasan B., 1984. Exploatarea zacamintelor miniere din Romania. Vol. 2. Editura Tehnica, p. 310-396.

Bird S.C., 1987. The effect of hydrological factors on trace metal contamination in the river Tawe, South Wales, Environmental Pollution, 45(2), 87-124, doi:10.1016/0269-7491(87)90051-0.

Bird G., Brewer P.A., Macklin M.G., Balteanu D., Serban M., Driga B., Zaharia S., 2008. River system recovery following the Novat-Rosu tailings dam failure, Maramures County, Romania, Applied Geochemistry, 23, 3498-3518.

Bird G., Macklin M.G., Brewer P.A., Zaharia S., Balteanu D., Driga B., Serban M., 2009. Heavy metals in potable groundwater of mining-affected catchments, northwestern Romania. Environmental Geochemistry and Health, 31(6, 741-58.

Bird G., Brewer P.A., Macklin M.G., 2010. Managing the Danube drainage basin: implications of contaminant metal dispersal for the implementation of the EU Water Framework Directive. International Journal of River Basin Management, 8, 63-78, doi:10.1080/15715121003715115.

Bostan I., 2013. Economic opportunities for the eploitation of copper ore in the Romanian Carpathians. Metalurgia, 52 (2), 282-284.

Byrne P. Reid I., Wood P.J., 2013. Stormflow hydrochemistry of a river draining an abandoned metal mine: the Afon Twymyn, central Wales. Environmental Monitoring and Assesment, 185(3), 2817-2832.

Byrne, P, Wood, PJ, Reid, I., 2012. The impairment of river systems by metal mine contamination: A review including remediation options. Critical Reviews in Environmental Science and Technology, 42(19), 2017-2077.

Chanpiwat P., Sthiannokao S., 2014. Status of metal levels and their potential sources of contamination in Southeast Asian rivers. Environmental Sci.Pollut. Res.,21(1),220-233, doi 10.1007/sl1356-013-1858-8.

Jiang L., Zhon H., Tong X., 2007. Acidiothiobacillus ferrooxidans. Chinese Science Bulletin, 52(19), 2702-20714, doi 10.1007/sl1434-007-0352-4.

Kouzmanov K., Bailly L., Tamas C., Ivascanu P., 2005a. Epithermal Pb-Zn-Cu(-Au) deposits in the Baia Mare district, Eastern Carpathians, Romania. Ore Geology Reviews, vol. 27, no.1-4, 48-49.

Kouzmanov K., Ivascanu P., O'Connor G., Rosu E., 2005b. Porphyry Cu-Au and epithermal Au-Ag deposits in the southern Apuseni Mountains, Romania. In: Geodinamics and Ore Deposit Evolution in Europe, 2005, D. Blundell, N. Arndt, P.R. Cobbold, C. Heinrich (Eds.), p. 46-47. ISBN-13: 978-0-444-52233-7; ISBN-10:0-411-52233-6.

Ivascanu P.M., Pettke Th., Kouzmanov K., Heinrich C.A., Pintea I., Rosu E., Udubasa Gh., 2003, The magmatic to hydrothermal transition: Miocene Deva porphyry copper-gold deposit, South Apuseni Mts, Romania. Proceedings of the 7th SGA Biennial Meeting, Greece, August 2003, p. 24-28.

Lang B., 1979. The base metals-gold hydrothermal ore deposits of Baia Mare, Romania. Economic Geology, 74 (6): 1336-1351, doi:10.20113/gsecongeo.74.6.1336.

Neubauer F., Lips A., Kouzmanov K., Lexa J., Ivascanu P., 2005. Subduction, slab detachment and mineralization: The Neogen in the Apuseni Mountains and Carpathians. Ore Geology Reviews, 27, p. 13-44.

Mayes W.M., Potter H.A.B., Jarvis A.P., 2013. Riverine Flux of Metals from Historically Mined Orefields in England and Wales, Water Air and Soil Pollution, 224, p. 1425.

Udubasa Gh., Rosu E., Seghedi I., Ivascanu P.M., 2001. The “Golden Quadrangle” of the Metaliferi Mts, Romania: What does this really mean? Rom. J. Mineral Dep., 79/1, p. 23-32.

MAGMATIC AND HYDROTHERMAL FEATURES OF THE FLUID AND MELT INCLUSIONS FROM THE QUARTZ XENOLITHS, FRAGMENTS AND PHENOCRYSTS FROM SĂPÂNŢA VALLEY (IGNIŞ MOUNTAINS, ROMANIA)

Ioan PINTEA

Geological Institute of Romania; ipinteaflincs@yahoo.com

Abstract. Quartz fragments and former magmatic phenocrysts were entrapped in basaltic andesite magma during their ascent at an estimated temperature of ≥1050° and calculated pressure between 25-51 MPa (1000-2044m) based upon microthermometry of the vapor-rich (H_2O+CO_2) inclusions and reequilibrated below 573°C and 15-30 MPa (612-1232m). The "in situ" sublimated halite, melted between 636-681°C indicating salinity of 79-86 wt % NaCl eq. The majority of the fluid and melt inclusions studied were firstly trapped during the magmatic-hydrothermal events which predated basaltic andesite magma emplacement.

Keywords fluid and melt inclusions, quartz xenoliths, phenocrysts, basaltic andesite, magmatic condensates, vapor, caldera, Săpânţa Valley

Introduction

The main goal of this work is to present the typology and microthermometry of the fluid and melt inclusion trapped in quartz xenoliths, fragments and phenocrysts sampled from the Săpânţa Valley area. The paper emphasized that the melt and fluid phases are magmatic-to-hydrothermal in origin and were exolved from different magma batches. Preliminary features of fluid and melt inclusions trapped in quartz xenoliths were already described by Pintea, 1998 (unpubl.).

Geological setting

Săpânţa caldera is situated in the Oaş-Gutâi volcanic region in the northeast of the Gutâi Mountains from Eastern Carpathians (e.g. Giuşcă et al., 1973; Kovacs, 2002; and references therein). Volcanic activity started with an explosive-effusive activity followed by a complex of two intrusive stages (Edelstein et al., 1992). Pyroxene andesite ± quartz, quartz andesite to porphyry quartz diorite, clinopyroxene bearing andesite and dacite are the main magmatic petrotypes. These were described as lava flows and shallow intrusive bodies. Hydrothermal alterations and Pb-Zn-(Cu) mineralization associated with the buried intrusions were also mentioned.

Quartz samples description

Q_1- quartz xenoliths. They were sampled from a small basaltic andesite quarry situated on the Săpânţa Valley ("Faţa Stancii"), as quartz aggregates (up to 10 cm in length) composed mostly by quartz grains of 1mm up to 15mm, in diameter. The quartz grains are transparent and shown color from white to yellowish, gray or reddish. The contact with the host rock is marked by a thin rim of amorphous silica or by a carbonate cemented micro-breccias with small andesite fragments and partially melted and agglutinated quartz grains. The carbonates cement shown colloform microtexture and contain small druses with calcite or aragonite (?) crystals. The quartz xenoliths shown specific laminar microtexture which suggest the plastic deformation and partial recrystallization of the polygonal quartz grains during basaltic-andesite lava ascent and flowing. Microfissures (< 1mm wide) of amorphous silica cut the xenoliths in two or three directions. Frequently tabular feldspar microphenocrysts were recrystallyzed in the silicate glass matrix, suggesting partial remelting of enclosed quartz during thermo-metamorphism. Micro-veinlets and intergranular voids filled with a black metallic condensate were often observed.

Q_2- fragments and phenocrysts. This sample is composed by transparent quartz fragments, slightly violaceous, having up to 10 mm in diameter, probably of hydrothermal origin, and magmatic bypiramidal quartz phenocrysts of 1-2 mm. Both quartz varieties were sampled from surface outcrops (soil) locally named "Cărbunarişte" from Săpânţa valley-Runc zone (Ghiurca, 1986 pers. com). We presumed in this study, based upon fluid and melt inclusion characteristics, that this kind of quartz were also entrapped as xenoliths in the basaltic andesite at different depth within the Săpânţa caldera.

Fluid and melt inclusion typology.

Two main types of inclusions were microscopically documented in both Q_1 and Q_2 samples (Fig. 1): silicate melt and aqueous vapor-rich inclusions.

Silicate melt inclusions are biphasic (silicate glass + vapor, three-phasic (silicate glass + solid (s)+ vapor), and complex ones with two different color silicate glass and vapor ± solid (s). They are primary, secondary and pseudosecondary inclusions, based upon their occurrence mode in the host quartz samples.

Vapor-rich inclusions contain a dominant mixture of aqueous vapor + CO_2 gas, and solid silicate phase(s). Frequently one ore more solid salt microcrystal(s) occurred. Opaque solid phase is rarely present. Vapor-rich inclusions seem to be enriched in silica, i.e. H_4SiO_4 and $H_6Si_2O_7$ complexes which are stable at high P-T conditions (Zotov and Keppler, 2002), and from which precipitated mainly quartz and feldspar as daughter phases (e.g. Fig. 1- h). Their presence suggest an exceptional chemical composition of the magmatic fluids (supercritical ?), and when they were re-heated up, experimentally to around 1000°C, the globular silicate phase(?) was formed by decreasing temperature in the stage, under the microscope (Fig.1- l). Vapor-rich inclusions are mainly primary in quartz phenocrysts and secondary in fragments and xenoliths.

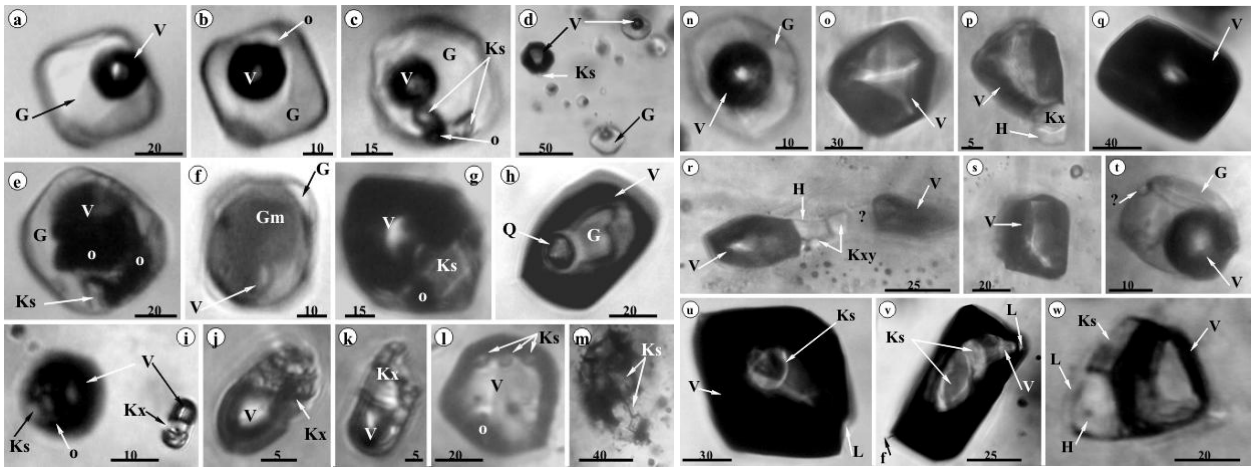

Fig.1. Some typical fluid and melt inclusion types in both quartz fragment, phenocrysts and xenoliths from Săpânţa Valley. Notations: G-glass, V-vapor, Ks- silicate, Kx- salt (s), Gm-immiscible silicate melt (now glass), o- opaque, H- halite, Q- presumably β-quartz Scale bar in µm.

Results

High temperature microthermometry was done for silicate melt inclusion in an original device calibrated with potassium dichromate (398°C), halite (801°C), silver (962°C) and gold (1064°C) with reading accuracy of ± (1.5%+3°C). Low temperature measurement of aqueous (±CO_2 gas) inclusions were done in a USGS-stage with precision of ±1-2°C. Loner18 (Bakker, 2003) and SoWat (Driesner and Heinrich, 2007) software were used for calculations.

Biphasic silicate melt inclusion heated up to 1050-1120°C (n=50) failed to homogenizing at 1 bar pressure by the direct heating method, under the microscope. They showed only a slight bubble volume reduction at the highest temperature, suggesting final homogenization temperature above 1150°C. The minimum homogenization temperature was estimated around 1050°-1100°C based upon their microthermometric-trend behavior and others external petrological evidences such as the presence of feldspar + glass assemblage in the marginal crust or micro-veinlets in the quartz xenoliths, the same silicate melt assemblages in similar β-quartz phenocrysts (Pintea, 1999) or independent mineral geothermometry (Kovacs, 2002).

Reequlibrated vapor-rich inclusions contain one or more salt microcrystals, sublimated "in situ" which melted at two distinct temperature intervals, firstly between 396-486°C (n=7) and the second melting point ranged between 636-681°C (n=14). The second phase was taken as halite and their melting point gave a salinity of 79-86 wt% NaCl eq (Fig. 2). Halite and other salts were sublimated "in situ" during the reequilibration process which happened at the β/α quartz transition at ≤573°C and ≤ 300 bars. The CO_2 phase was revealed as a thin liquid rim around the bubble in the vapor-rich inclusions, freezes during microthermometry down to -100 ^{o}C. The solid CO_2 melted around -56.6^{o}C, suggested the presence of pure CO_2 phase. The CO_2 homogenization temperature in the vapor phase ranged between -1.5^o and + 15.8^{o}C (n=9). Clathrate formed sporadically and melted at +9.1^{o}C. The aqueous liquid rim observed sometimes in the vapor rich inclusions gave a salinity of about 14 wt % NaCl eq., based upon ice melting temperature. Secondary biphasic inclusions (L + V) are very scarce and shown salinity less than 2 wt% NaCl and Th= +131.9^{o}C. Based upon microthermometry of the CO_2 gas phase from vapor-rich inclusions

it was estimated that the quartz phenocrysts and fragments were entrapped in the mafic andesite lava at ≥1050° and 25-51 MPa (1000-2044m), and then reequilibrated at ≤573°C and 15-30 MPa (612-1232m), assuming a lithostatic load of 1 km at 25 MP (e.g. Muntean and Einaudi, 2000.

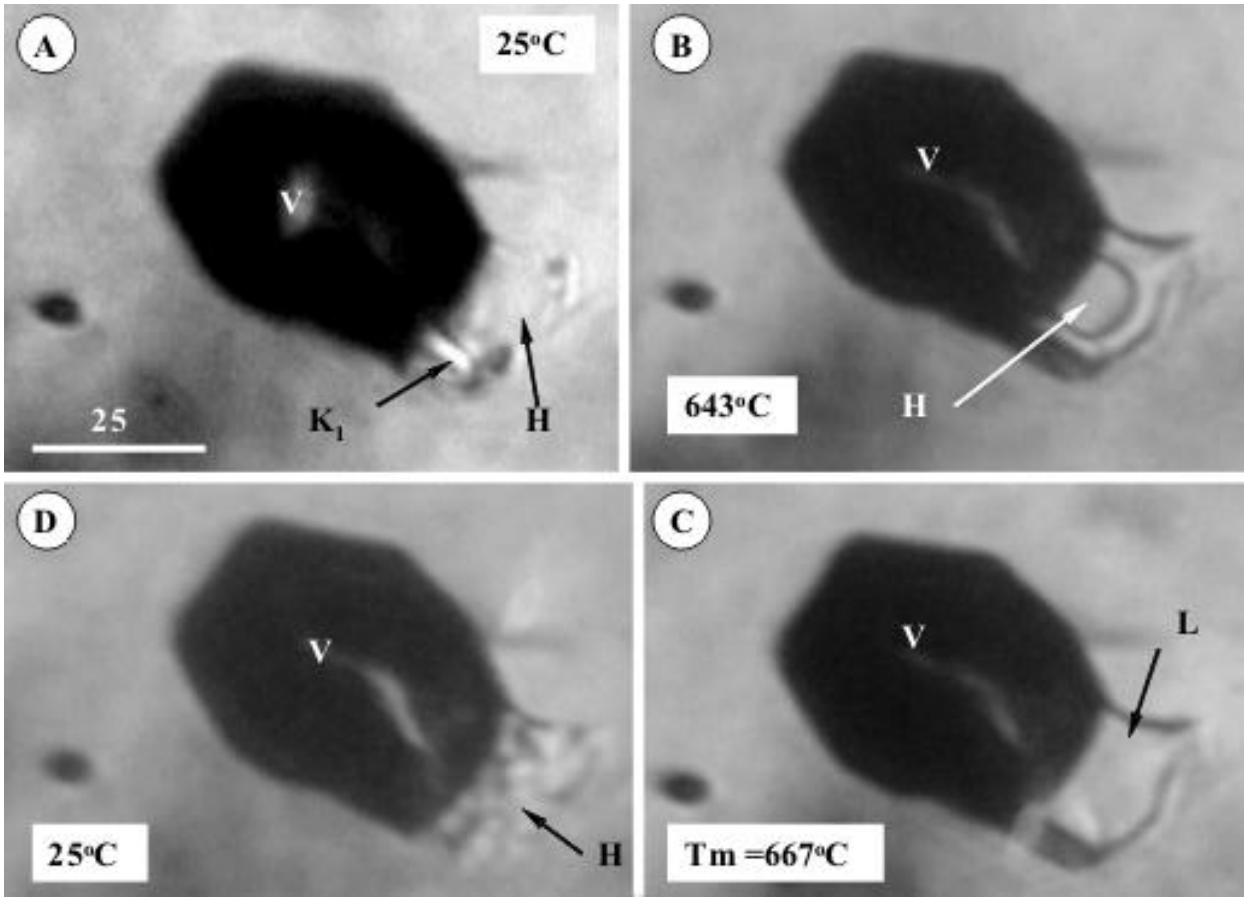

Fig. 2. Microthermometric sequences in reequilibrated vapor - rich inclusions showing the melting behavior of condensed halite, during heating under microscope. Tm- halite melting temperature, V- vapor, L- liquid, H-halite, K_1- another salt grain. Scale bar in µm.

Discussion

Data presented in this study could be discussed in the context of relationships between the caldera collapse and resurgence with the associated magmatic-to-hydrothermal activity (e.g. Popescu et al., 2012).

Firstly, magmatic processes as mixing/mingling between mafic volatile-rich melt and a more viscous felsic melt are suggested by the presence of multiphasic silicate melt inclusion types and vapor-rich inclusions trapped in the quartz phenocrysts from diorite, andesite and dacite. Exceptionally composition of the vapor- rich inclusions containing high temperature silicate complexes and the presence of pure CO_2 in the aqueous fluids indicated additionally fluid-melt immiscibility at trapping condition. This could be the main cause of the homogenization failure of the silicate melt inclusions during direct microthermometry.

Secondly, the hydrothermal processes described by Edelstein et al. (1992) were probably associated to the fluid phases trapped as secondary trails in the presumed hydrothermal quartz fragments described in this study. They activated before the mafic magma emplacement, probably as intense "silica-rich magmatic degassing" related to the hidden shallow intrusions. These generated a convective hydrothermal system in the epiclastic suite, above the shallow magma chamber and around intrusions.

Thirdly, the quartz xenoliths in the mafic andesite suggest that they were collected during lava ascending through the epiclastic suite within the caldera, after collapse and resurgence. The very high salinity of the vapor-rich fluid inclusion is related to halite sublimation during the reequlibration of the microcavities below 573°C and less than 500 bars, and is not the original salinity of the magmatic (supercritical ?) fluid, which occasionally showed salinity only up to 14 wt% NaCl eq. This kind of microthermometric behavior was described for example by Koděra et al. (2012) at Banska Štiavnica

(Western Carpathians) and also by Muntean and Einaudi (2000) in the Maricunga belt (Andes) for fluid phases related to a new type of porphyry-Au deposit. There are not such evidences yet in the Igniş Mountains, although buried hydrothermal activity could be emphasized because the area belongs to an important metallogenetic district (Borcos et al., 1998; Pintea, 2012).

Conclusions

- Quartz fragments and magmatic quartz phenocrysts were entrapped as xenoliths at high temperature and low pressure from the epiclastic suite within Sapânţa caldera;
- Quartz phenocrysts contain silicate melt inclusions associated with vapor-rich inclusion assemblages suggesting magmatic processes as melt mixing/mingling and fluid-melt immiscibility. The quartz fragments contain secondary vapor- rich inclusions trapped as trails, representative for an intense hydrothermal stage;
- Fluid and melt inclusions from quartz xenoliths were reequilibrated during entrapment and transport by the hosting mafic lava;
- The fluid and melt inclusions indicated a magmatic-hydrothermal activity related to multiple intrusive-effusive stages during caldera collapse and resurgence.

References

Bakker R.J., 2003. Package FLUIDS1.Computer programs for analysis of fluid inclusion data and for modeling bulk fluid properties. Chem. Geol. 194, 3-23.

Borcoş M., Vlad S., Udubaşa G. Gabudeanu B. 1998. Qualitative and quantitative metallogenetic analysis of the ore genetic units in Romania. Rom. J. of Mineral Dep., 78, spec iss., 158p.

Driesner T., Heinrich C.A., 2007. The system H_2O–NaCl. Part I: Correlation formulae for phase relations in temperature–pressure–composition space from 0 to 1000 °C, 0 to 5000 bar, and 0 to 1 X_{NaCl} Geochim.Cosmochim.Acta. 71, 20, 4880-4901.

Edelstein O., Istvan D., Kovacs M., Bernad A., Stan D., Istvan E., Gabor M., Balint B., Haranth G., Vărşecu I., 1992. Données préliminaries concernant la constitution géologique de la zone de Săpânţa-Valea Barazilor (Monts de Igniş). Rom. J. Petrology, 75, 131-143.

Giuşcă D., Borcoş M., Lang B., Stan N., 1973. Neogene volcanism and metallogenesis in the Gutăi Mountains.Guide to Excursion 1 AB, Symp. “Volcanism and Metallogenesis”, Bucharest.

Kovacs M.,2002. Petrogenesis of the subduction magmatic rocks from central-southeast zone of Gutâ Mountains. Dacia Edit., 201 p (in romanian).

Koděra P., Bakos F., Lexa J., Heinrich C.A., Wälle M., Fallik A.E., 2012. Au-porphyry systems in Western Carpathians-mineralisation, alteration patterns and outstanding fluid properties. Eur. Mineral Conference vol 1, EMC2012-667.

Muntean J.L., Einaudi M.T. 2000. Porphyry gold deposits of the Refugio district, Maricunga belt, northern Chile. Econ. Geol., 95, 1445-1472.

Pintea I. 1999. New microthermometric data on fluid inclusions from Rosia Montana quartz crystals. Mineralogy in the System of Earth Sciences. Abstr. Vol. suppl. An: XLVIII/1999, p.74-75.

Pintea. I. 2012. Fluid and melt inclusions: a precious tool in selective exploration strategy. Rom. J. of Mineral Dep., 85, 1, 85-89.

Popescu G., Neacsu A. 2012. Modeling of epithermal gold and porphyry copper deposits from Metaliferi Mountains (Romania). Rom.J. of Mineral Dep., 85, 1, 7-13.

Zotov N., Keppler H., 2002. Silica speciation in aqueous fluids at high pressures and high temperatures. Chem.Geol., 184, 71-82.

NEW HIGH-PRECISION LEAD ISOTOPE ANALYSES OF GALENA FROM ROMANIAN ORE DISTRICTS AND A REVIEW

Igor V. CHERNYSHEV[1], Vladimir A. KOVALENKER[1], Andrei CHUGAEV[1], Gheorghe DAMIAN[2, 3], Floarea DAMIAN[3], Luisa Elena IATAN[4], Ioan SEGHEDI[4*]

[1]Institute of Geology of Ore Deposits, Petrography, Mineralogy and Geochemistry Russian Academy of Sciences, Staromonetny per. 35, 119 017 Moscow, Russian Federation, *kva@igem.ru*
[2]Tech. University of Cluj Napoca, North University Center of Baia Mare, Romania
[3]"Alexandru Ioan Cuza" University of Iaşi, Department of Geology, 20A Carol I Boulevard, 700505 Iaşi, Romania
[4]Institute of Geodynamics, Romanian Academy, 19-21. Jean-Luis Calderon, str., 020032 Bucharest, Romania, [*]*seghedi@geodin.ro.*

Abstract

We report new 15 lead isotope analyses performed on galena from different ore deposits in western Romania, by using a high-precision version of MC-ICP-MS method. The data were compared with already published data in the literature and split in 4 distinct groups in $^{206}Pb/^{204}Pb$ vs. $^{208}Pb/^{204}Pb$ and $^{207}Pb/^{204}Pb$ diagrams. Lead isotopes of the Neogene group, the most representative, show distinctive behavior for each area, as related both to the magma source and the local crustal influence during magma passing to the surface. The data are in agreement with the recent geodynamic models that suggest that magmatism and associated ore deposits were the result of extensional processes that accompanied the convergence processes of ALCAPA and Tisza-Dacia with European Platform.

Keywords: Lead isotopes, galena, Apuseni Mts., Oaş-Gutâi Mts.

Introduction

15 new lead isotope analyses were performed on galena from ore deposits of different ages in Poiana Ruscă (Paleozoic), Apuseni Mountains (Paleozoic, Mesozoic and Neogene), and Oaş-Gutâi Mountains (Neogene) (see Table 1). The data were compared with already published ones (Cook and Chiaradia, 1997; Marcoux et al., 2002; Baron et al., 2011) and also with 25 unpublished analyses on galena from East Slovakia (Neogene) and with some additional isotope analyses performed on igneous rocks (Mason et al., 1996).

Methods

We applied a high-precision version of Multicollector-Inductively Coupled Plasma Mass Spectrometry (MC-ICP-MS) method based on isotope analysis of Pb from Tl-doped solutions and the normalization of all current Pb isotope data relative to the standard $^{205}Tl/^{203}Tl$ ratio. A total error of lead isotope ratios measurements estimation, which was based on the long-term reproducibility of the duplicate analyses of standard SRM 981 and the galena samples, is evaluated as ±0.02% (±2SD) (Chernyshev et al., 2007).

Results

The new results are very similar with the previous published data. Isotopic lead in ore (galena) group in four fields in $^{206}Pb/^{204}Pb$ vs. $^{208}Pb/^{204}Pb$ and $^{207}Pb/^{204}Pb$, while those from igneous rocks are scattered (see Figure 1):

(I) Least radiogenic values correspond to VMS (volcanogenic massive sulfide) deposits of Mesozoic age at Vorţa and Dealul Mare (south Apuseni ophiolite area) and from a galena-rich vein in Highiş granite, Permian in age. Our new data confirm the previous ones.

(II) The second group, belonging to Apuseni epithermal, base-metal or porphyry type and VMS in Poiana Ruscă show some variation along $^{207}Pb/^{204}Pb$ and $^{208}Pb/^{206}Pb$ ratios. There is a minor similarity of ore lead data with the igneous rocks from Apuseni of similar age (Marcoux et al., 2002). Again, our new data confirms the previous.

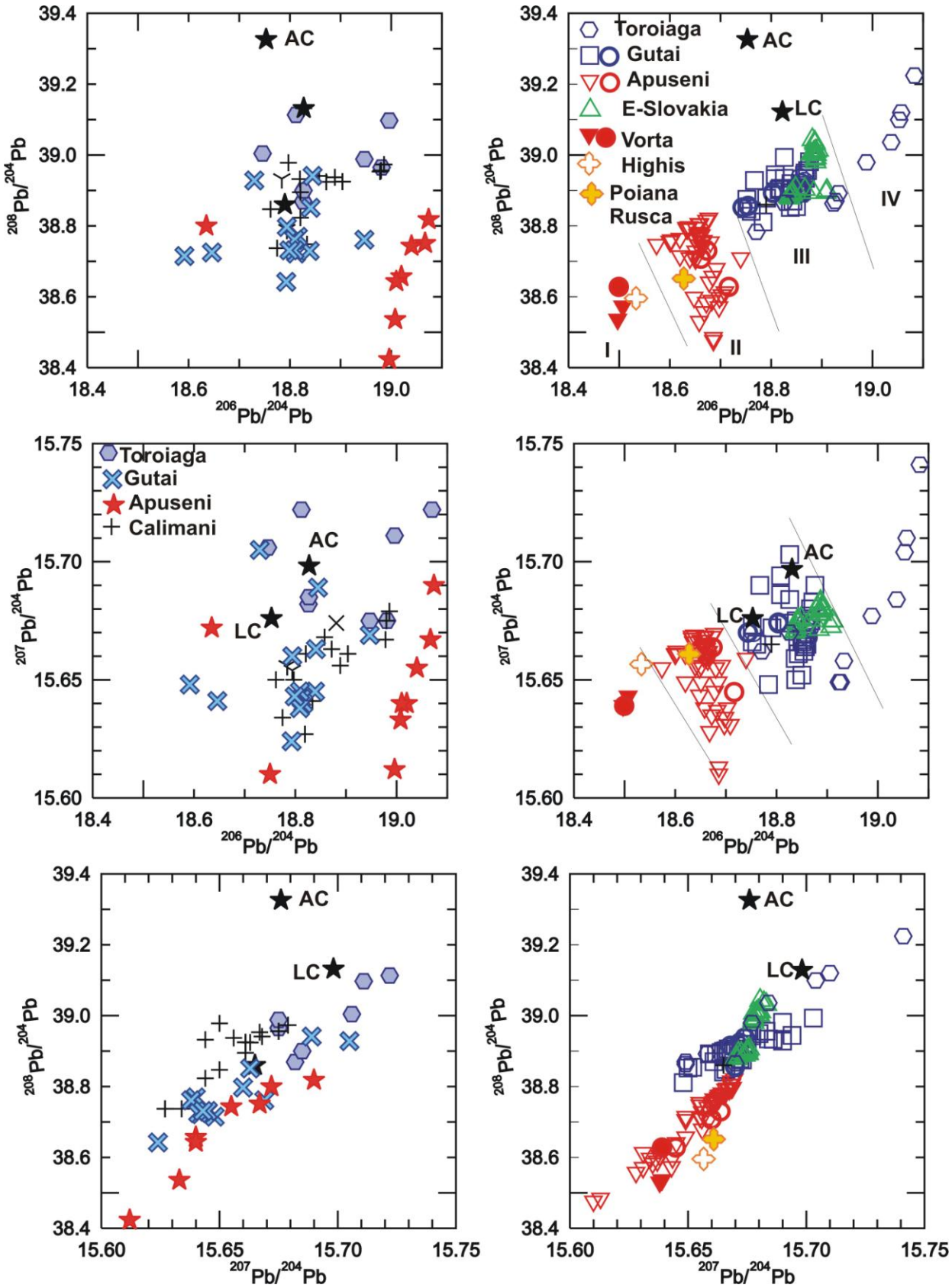

Fig. 1. Pb/Pb diagrams of Romanian ore deposits, mainly galena (right diagrams) and fresh igneous rocks (left diagrams) (Mason et al., 1998; Cook and Chiaradia, 1997; Marcoux et al., 2002, Boron et al., 2011, new data, as thicker circles in diagrams). Abbreviations: AC- average crust (Rudnick and Fountain, 1995); LC-average local crust (Mason et al., 1998).

(III) The third group corresponds to Neogene epithermal deposits from Baia Mare ore district and Oaş, to the East Slovakia and a few to Ţibles area. This group is closer to the average and local crust values (Rudnick and Fountain, 1995; Mason et al., 1998). The igneous rocks from Baia Mare, although scattered, plot similar with the ore data. This suggests that magma generation processes played the major role in ore deposits production (Marcoux et al., 2002). The new data confirms the previous.

(IV) The fourth group corresponds to the majority of epithermal vein-deposits in Ţibles area and is the most radiogenic. Only a few igneous rocks are similar with the ore data. A stronger crustal influence is suggested (Cook and Chiaradia, 1997).

Table 1. Pb isotope analyses of galena from Romanian ore deposits.

Nr.	Sample	Characteristics	$^{206}Pb/^{204}Pb$	$^{207}Pb/^{204}Pb$	$^{208}Pb/^{204}Pb$
Apuseni areas					
Neogene Coranda ore district					
1	1/2012	Polymetalic vein	18.6617	15.6599	38.7073
2	3/2012	Polymetalic vein	18.6738	15.6637	38.7298
Neogene Măgura ore district					
3	11/2012	Pb-Zn impregnation	18.7165	15.6448	38.6276
Mesozoic Vorţa ore district					
4	12/2012	VMS galena	18.4994	15.6390	38.5618
Oaş-Gutâi Neogene areas					
Baia Sprie ore district					
5	28/2012	Polymetalic vein	18.8631	15.6679	38.9147
6	30/2012	Polymetalic vein	18.8656	15.6718	38.9261
Cavnic ore district					
7	33/2012	Polymetalic vein	18.8582	15.6710	38.9212
Herja ore district					
8	37/2012	Polymetalic vein #90	18.8029	15.6736	38.8957
9	39/2012	Polymetalic vein #50	18.8037	15.6742	38.8927
Turţ ore district					
10	40/2012	Polymetalic vein	18.8571	15.6740	38.9376
11	41/2012	Polymetalic vein	18.8600	15.6724	38.9221
Ilba ore district					
12	43/2012	Quartz-pyrite galena vein	18.7437	15.6700	38.8520
13	44/2012	Quartz-chacopyrite galena vein	18.7544	15.6699	38.8563
Other sites					
14	45/2012	Highiş Mts., Permian granitoids, quartz-galena vein	18.6279	15.6609	38.6512
15	46/2012	Poiana Ruscă Mts. Muncel, VMS-Paleozoic	18.5334	15.6566	38.5956

Discussion and conclusions

The data proves the importance of both magmatic source and crustal basement that strongly influenced the assimilation processes in the genesis of Neogene magmas and associated ore deposits, the largest ones in Romania (e.g., Marcoux et al., 2002). The 3 groups (II, III and IV) corresponding to Neogene ore

districts are in agreement with the recent geodynamic models, which suggest that magmatism and associated ore deposits were the result of extensional processes in response to an interplay of compression and extension within two composite microplates: ALCAPA and Tisza–Dacia (e.g. Seghedi and Downes, 2011).

For the Apuseni (II), magma generation was closely related to extensional processes crossing the limit between Mesozoic ophiolites (I) and Tisza block, without significant assimilation; for Oaş-Gutâi and East Slovakia (III) magma generation was associated to counterclockwise rotation and core-complex extension of the Transcarpathian block, belonging to NE ALCAPA; for Ţibles area (IV) that belongs to Dacia block important transtensional movements took place during the collision processes with East European platform that favored variable, but mostly significant assimilation processes during magma generation.

Acknowledgements

The studies were carried out in the framework of an inter-Academic Joint Project between IGEM RAS and the Institute of Geodynamics of the Romanian Academy and were financially supported by the Russian Foundation for Basic Research, project nos. 13-05-00622a.

References

Baron S., Tămaş C., G., Cauuet S., Munoz M., 2011. Journal of Archaeological Science, 38, 5, 1090-1100., DOI: 10.1016/j.jas.2010.12.004

Chernyshev I.V., Chugaev A.V., Shatagin K.N., 2007. High-precision Pb isotope analysis by multicollector-ICP-mass-spectrometry using $^{205}Tl/^{203}Tl$ normalization: optimization and calibration of the method for the studies of Pb isotope variations. Geochem. Int., 45, 11, 1065-1076.

Cook, N.J., Chiaradia, M., 1997. Sources of base metal mineralization in the Baia Borşa orefield, NW Romania: constraints from lead isotopes. In: Papunen, H. (Ed.), Mineral Deposits. Balkema, Rotterdam, 813-816.

Marcoux, E., Grancea, L., Lupulescu, M., Milési, J.P., 2002. Lead isotope signatures of epithermal and porphyry-type ore deposits from the Romanian Carpathian Mountains. Mineralium Deposita 37, 173-184.

Mason P., Downes H., Thirlwall M.F., Seghedi I., Szakács A., Lowry D., Mattey D., 1996. Crustal assimilation as a major petrogenetic process in the East Carpathian Neogene and Quaternary continental margin arc, Romania. Journal of Petrology 37, 4, 927-959.

Rudnick, R.L., Fountain, D.M., 1995. Nature and composition of the continental crust – a lower crustal perspective. Review of Geophysics 33, 267-309.

Seghedi, I., Downes, H., 2011. Geochemistry and tectonic development of Cenozoic magmatism in the Carpathian-Pannonian region. Gondwana Research 20, 655-672.

SPHALERITE ASSEMBLAGES AND COMPOSITION IN THE BAIA MARE REGION, EASTERN CARPATHIANS, ROMANIA (PRELIMINARY DATA)

Olga Yu. PLOTINSKAYA[1]*, Gheorghe DAMIAN[2], Floarea DAMIAN[2]

[1] IGEM RAS, 35, Staromonetny per., 119017 Moscow, Russia;
[2] Technical University Cluj-Napoca, North University Center Baia Mare, 62, Victor Babes Str., 433003 Baia Mare, Romania;
* *plotin@igem.ru*; Tel.: 007 499 230 82 44.

Abstract: The paper describes sphalerite composition (Fe, Mn, and Cd contents) from five epithermal base-metal deposits of the Baia Mare district: Nistru, Herja, Baia Sprie, Cavnic, and Cisma. Sphalerite is usually featured by X_{FeS} decrease with lowering temperature and sulfur fugacity.

Keywords: Baia Mare; epithermal; Nistru; Herja; Baia Sprie; Cavnic; Cisma, Fe, Mn, and Cd contents in sphalerite

Introduction

Geology and mineralogy of epithermal base-metal deposits of the Baia Mare district (fig.1) have been described in detail by a large number of papers, e.g. Lang, 1979, Neubauer et al., 2005 and references therein. In particular, chemical composition of sphalerite from certain deposits was discussed, e.g. from Cavnic (Pomârleanu et al., 1968), Herja (Cook and Damian, 1997), Baia Sprie (Buzatu et al., 2013), Cisma (Plotinskaya et al., 2012) etc. The present paper is aimed at comparing sphalerite from five deposits of the Baia Mare district: Nistru, Herja, Baia Sprie, Cavnic and Cisma, as well as to trace the evolution of the main substitutional metals (Fe, Cd, Mn, etc.) in sphalerite and to discuss major PTx controls of the main trends revealed.

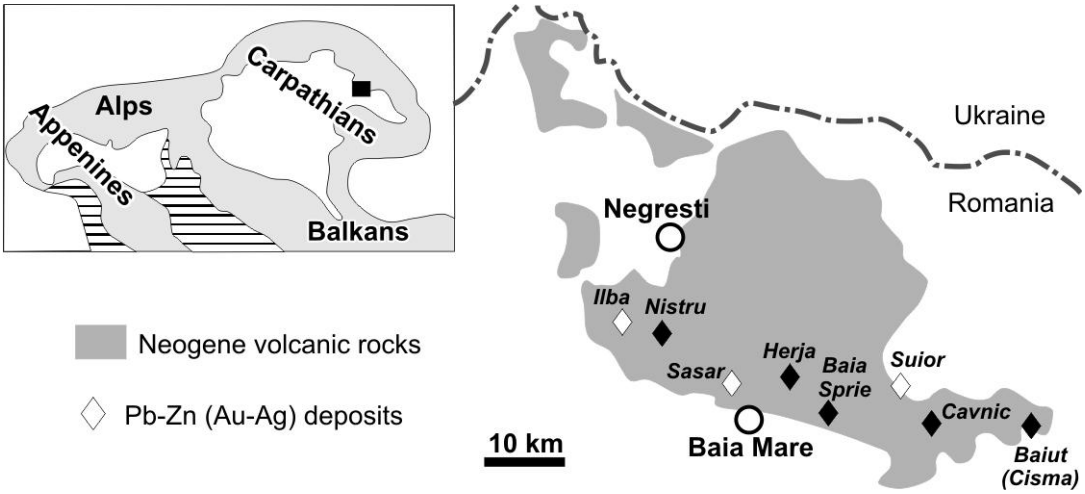

Fig. 1. Schematic map of the Baia Mare region showing locations of major ore deposits. Black lozenges indicate deposits under study.

Analytical methods

The chemical composition of sphalerite was studied with a Cameca-SX-100 electron microprobe with four WDX detectors, at TU Clausthal, Germany (A.R. Cabral, analyst) and with a Jeol JXA-8200 with five WDX detectors, at IGEM, Moscow, Russia (I.G. Griboedova, analyst). The following conditions were used on both equipments: accelerating voltage 20 keV, sample current 20 nA, beam diameter 1 μm; analytical lines: Kα for S, Cu, Fe, Zn, and Mn, Lα for Cd and Sn, Mα for Hg; standards: ZnS for S and Zn, HgS for Hg, CuFeS2 for Fe and Cu (Cameca), CdS (Cameca) and CdSe (Jeol) for Cd, pure metals for Mn, Sn, and Cu (Jeol). For the Cameca SX-100 peak time was 10 s for S and Zn, 20 s for Cu, 60 s for Mn and 100 s for Cd; detection limits (wt.%) were: 0.08 for S, 0.09 for Cu, 0.07 for Cd, 0.15 for Zn, 0.03 for Fe and 0.02 for Mn. For the Jeol JXA-8200 peak time was 10 s for S and Zn, 20 s for Cu, Fe, Hg, Mn, and Sn, and 30 s for Cd; detection limits (wt.%) were: 0.01 for S, Fe, Mn, and Sn, 0.02 for Cu and Hg, 0.03 for Cd, and Zn.

Results

The Nistru ore field located in the western end of the Baia Mare ore district consists of the Northwest and Northeast-Southeast ore fields. The latter establishes a remarkable horizontal mineral zoning around the stock of quartz-monzodiorites: (1) Cu-Bi-Au mineralization is confined to the central part within the stock, (2) Pb-Zn mineralization occurs in the periphery, and (3) Au-Ag veins are confined to the margins of the ore field (Damian, 2003). Three ore stages were distinguished at Nistru: (1) Pyrite-copper ± Au and Bi, T>325°C, (2) Base-metal, T 325 to 210°C, and (3) Gold stage 160 to 250°C (Borcoş et al., 1974).
We studied sphalerite from (1) and (2) zones (fig.2). In the zone 1 (central part) sphalerite associates with pyrrhotite, chalcopyrite, and pyrite. It contains small amounts of Cd (0.3 to 0.6 wt.%) and Mn (0.1 to 0.3 wt.%), Fe contents varies from 10.0 to 12.4 wt.% (16.9 to 21.0 mol.% FeS) in the assemblage with pyrrhotite and from 2.1 to 10.3 wt.% (3.6 to 17.8 mol.% FeS) in the assemblage with pyrite. In the zone 2 sphalerite associates with pyrite, chalcopyrite, galena, fahlores, Ag sulfosalts etc. Earlier generation of sphalerites contains 2.1 to 4.8 wt.% of Fe, 0.5 to 1 wt.% of Cd and 0.1 to 0.3 wt.% of Mn. Sphalerite of late generation associating with Mn carbonates has elevated Mn content (up to 1.1 wt.%), low Cd (0.2 to 0.5 wt.%) and variable Fe (1.5 to 9.2 wt.%, i.e. 2.7 to 16 mol.% FeS).

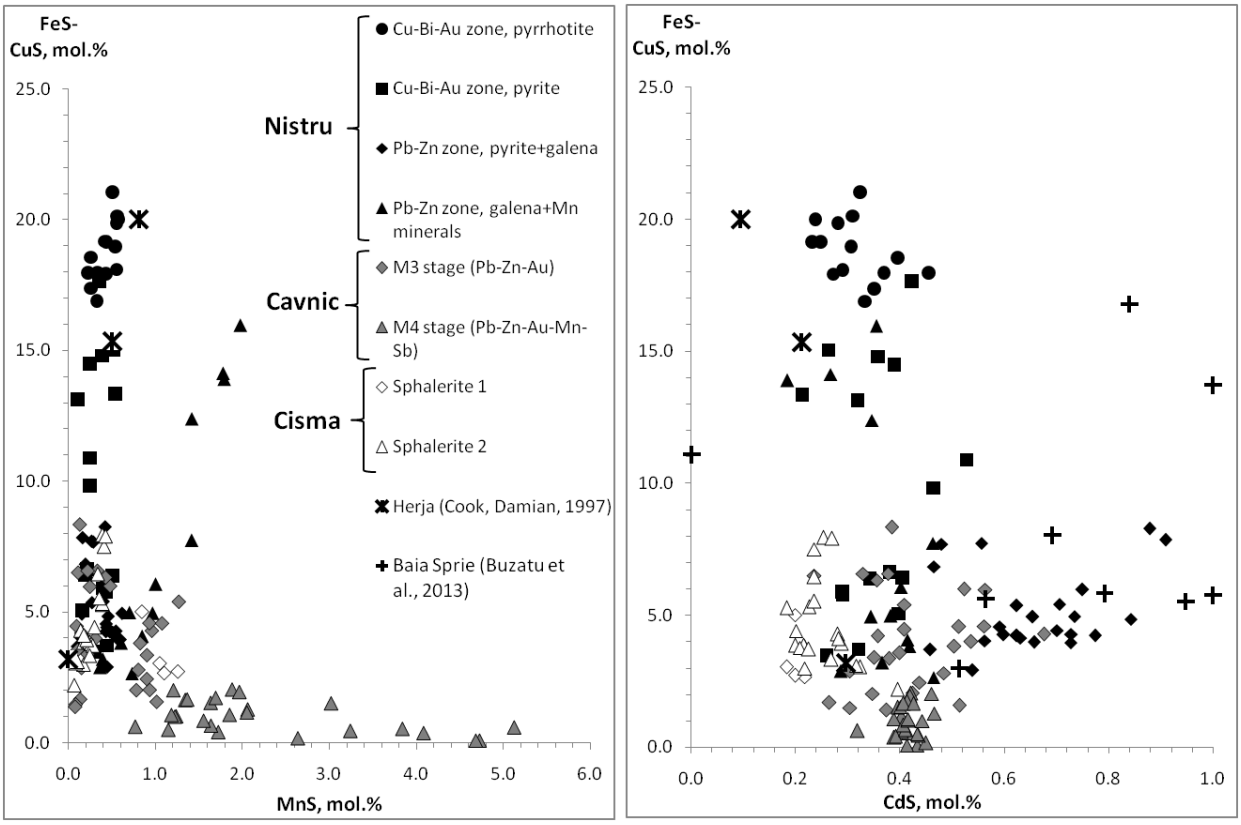

Fig. 2. CdS vs. FeS and MnS vs. FeS diagrams for sphalerite from the deposits of the Baia Mare region

The Cavnic deposit located in the eastern part of the Baia Mare district consists of two zones: Cavnic-Bolduţ in the North-West and Cavnic Roata in the South-East. Mariaş (1996) proposed five mineralization stages for the Cavnic deposit: M0 (pre-ore) − regional propylitic alteration, M1 (Fe-W) − quartz, pyrite, magnetite, scheelite etc., M2 (Cu) − chalcopyrite, pyrite, and covellite, M3 (Pb-Zn-Au) − **sphalerite**, galena, native gold, quartz, adularia, and M4 (Pb-Zn-Au-Mn-Sb) − rhodonite, rhodochrosite, adularia, galena, **sphalerite**, tetrahedrite, stibnite, native gold, etc. Grancea et al. (2002) estimated temperatures, M3 stage 225 to 240°C, and M4 stage from 214 to 290°C for quartz and carbonate. This is in a good agreement with the data of Pomârleanu et al. (1968) who reported temperature 243-306°C for sphalerite and with T 257-291°C in M4 stage quartz reported by Plotinskaya et al. (2009).
The present study focused on M3 and M4 sphalerite from the Cavnic-Bolduţ zone (fig.2). **M3 stage sphalerite** has variable Fe contents (0.8 to 4.8 wt.%, i.e. 1.4 to 8.3 mol.% FeS), and moderate quantities of Cd and Mn (0.3 to 0.8 and up to 0.5 wt.% respectively). **Sphalerite of the M4 stage** on the contrary is low in Fe (0.1 to 1.6 wt.%) and Cd (0.4 to 0.5 wt%) and is significantly enriched in Mn (up to 2.9 wt.%).

The Cisma deposit (Băiuț district), occupies the easternmost part of the Gutâi Mountains**.** It consists of two main veins: Cisma and Bandurița. Two mineralization stages were identified: early hematite-pyrite-chalcopyrite-quartz and base-metal ones (Damian and Damian, 2004). Fluid inclusion data (Plotinskaya et al., 2012) point to depositional temperatures of 270 to 316°C in the Bandurița vein and 143 to 344°C in the Cisma vein.

The base-metal mineralization in the investigated samples is represented by pyrite, chalcopyrite, galena, abundant low-Fe sphalerite, and minor tennantite. Sphalerite is represented by two generations (fig.2). Sphalerite-1 has Fe contents 1.3 to 4.6 wt.% (2.3 to 7.9 mol.% FeS) and Mn (0.5 to 0.7 wt.%) and relatively constant Cd contents (approx. 0.2 wt.%). Sphalerite-2 overgrows sphalerite-1 has similar Fe content (1.9 to 4.5 wt%), is low in Mn (to 0.2 wt.%) and Cd (0.2 to 0.5).

Discussion

Among all chemical impurities in sphalerite only Fe content is a well studied indicator of physical-chemical conditions (Vaughan and Craig, 1997, etc). In epithermal (i.e. shallow) environment FeS content in sphalerite (X_{FeS}) can be discussed in fS_2 – T space (fig.3). Sphalerite from Nistru deposit has the widest X_{FeS} range. Sphalerite deposition started within pyrrhotite stability space and stopped within pyrite-chalcopyrite stability space. However high X_{FeS} content and temperature decrease from >300 to 200°C, suggesting formation conditions near the pyrite/pyrrhotite buffer. Similar trend is observed at Cisma deposit but lower X_{FeS} contents point to higher sulphur fugacity (fig.3). Sphalerite from Cavnic deposit has the lowest X_{FeS} which can be a result of a small fS_2 increase.

Published data on sphalerite from **Herja** (Cook and Damian, 1997) and **Baia Sprie** (Buzatu et al., 2013) deposits (located in the central segment of the Gutâi Mountains) are scarce (fig. 2). However, sphalerite composition from both deposits is close to that found at Nistru; Herja sphalerite deposit is similar to sphalerite in the Cu-Bi-Au zone and sphalerite from Baia Sprie is similar to sphalerite from the Pb-Zn zone of Nistru deposit. This suggests that the fS_2 – T evolution at Herja and Baia Sprie deposits was similar to that recorded for Nistru.

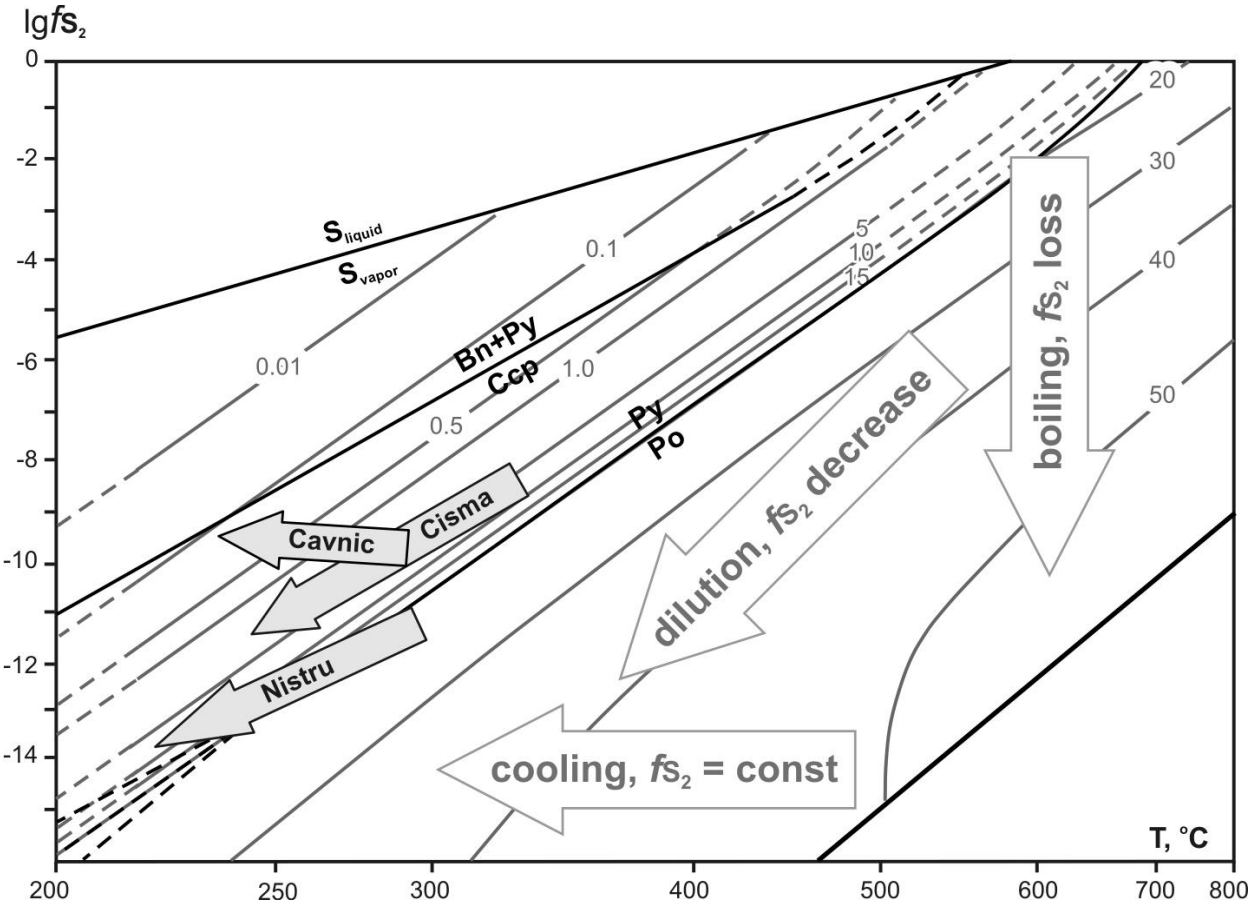

Fig. 3. *f*S2-T diagram of the Fe-Cu-S system. X_{FeS} isopleths for pyrite-chalcopyrite stability field are derived from Czamanske (1974) and for pyrrhotite stability field from Scott and Barnes (1971).

Thus, sphalerite from Nistru deposit shows the widest compositional range among the deposits under study, while the narrowest X_{FeS} range was noted at the Cisma deposit. Sphalerite is usually featured by X_{FeS} decrease from early to late generations, accompanied by lowering temperature and slight decrease of sulfur fugacity.

Acknowledgements. We thank A.R. Cabral (TU Clausthal, Germany) and I. Griboedova (IGEM, Moscow) for E-probe analysis. This study was supported by RFBR No 13-05-00622a and 14-05-00725a.

References

Borcoş, M., Gheorghiţă, I., Lang, B., 1974. Neogene hydrothermal ore deposits in the volcanic Gutîi Mountains. I. Ilba-Baita metallogenetic district. Revue Roumaine de Geologie, Geophysique et Geographie, Ser. Geol., 18, 19-37.

Buzatu, A., Buzgar, N., Damian, G., Vasilache, V., Apopei, A.I, 2013. The determination of the Fe content in natural sphalerites by meansof Raman spectroscopy. Vibrational Spectroscopy, 68, 220–224.

Cook, N.J. and Damian, G.S., 1997. New data on "plumosite" and other sulfosalts minerals from the Herja hydrothermal vein deposit, Baia Mare district, Romania. Geologica Carpathica, 48, 387–399.

Czamanske, G.K., 1974. The FeS content of sphalerite along the chalcopyrite-pyrite-bornite sulfur fugacity buffer. Economic Geology, 69, 1328−1334.

Damian, F., 2003. The Mineralogical Characteristics and the Zoning of the Hydrothermal Types Alteration from Nistru Ore Deposit, Baia Mare Metallogenetic District. Studia Universitatis, Babeş Bolyai, Geologia, XLVIII, 1, 101-112.

Damian, F., Damian, Gh. 2004. Mineral parageneses of the hydrothermal ore deposits from Baia Mare area Romania, Seria D. Exploatari miniere, preparare metalurgie neferoasa, geologie si ingineria mediului, Vol. XVIII, 155-172.

Grancea, L., Bailly, L., Leroy, J., Banks, D., Marcoux, E., Milési, J.P., Cuney, M., André, A.S., Iştvan, D., Fabre, C., 2002. Fluid evolution in the Baia Mare epithermal gold / polymetallic district, Inner Carpathians, Romania. Mineralium Deposita, 37, 630–647.

Lang, B., 1979. The base metals–gold hydrothermal ore deposits of Baia Mare, Romania. Economic Geology 74, 1336–1351.

Mariaş, Z.F., 1996. Cavnic ore field, geostructural and petrometallogenetic characterisation, Unpubl. PhD Thesis, Babeş – Bolyai Cluj University.

Neubauer, F., Lips, A., Kouzmanov, K., Lexa J., Ivăşcanu, P., 2005. Subduction, slab detachment and mineralization: The Neogene in the Apuseni Mountains and Carpathians. Ore Geology Reviews, 27, 13–44.

Plotinskaya, O.Yu., Damian, F., Prokofiev, V.Yu., Kovalenker, V.A., Damian, G., 2009. Tellurides occurrences in the Baia Mare region, Romania. Carpathian Journal of Earth and Environmental Sciences, 4, 89–100.

Plotinskaya, O.Yu., Prokofiev, V.Yu., Damian, G., Damian, F., Lehmann, B., 2012. The Cisma deposit, Băiuţ district, Eastern Carpathians, Romania: sphalerite composition and formation conditions. Carpathian Journal of Earth and Environmental Sciences, 7, 265−273.

Pomârleanu, V., Movileanu, A., Bonya, L., Mikhalka, Sht., 1968. Sphalerite from the Capnik hydrothermal deposit (Baia Mare). Geokhimiya, (9), 1097−1106 (in Russian, English abs.).

Scott, C.D. and Barnes, H.L., 1971. Sphalerite geothermometry and geobarometry. Economic Geology, 66, 653−669.

Vaughan, D.J. and Craig, J.R., 1997. Sulfide ore mineral stabilities, morphologies, and intergrowth textures. In: Geochemistry of hydrothermal ore deposits, Geochemistry of hydrothermal ore deposits, 2nd ed., Barnes H.L. (Ed.) Wiley, John & Sons, 367–434.

PETROGRAPHY, GEOCHEMISTRY AND GEOCHRONOLOGY OF SELECTED SAMPLES FROM TWO BANATITE INTRUSIONS NEAR GLADNA MONTANĂ, POIANA RUSCĂ MOUNTAINS, ROMANIA

Ioan SEGHEDI[1*], Zoltan PÉCSKAY[2], Paraschiva ONESCU[3]

[4]*Institute of Geodynamics, Romanian Academy, 19-21. Jean-Luis Calderon, str., 020032 Bucharest, Romania, [*]seghedi@geodin.ro.*
[2]*Institute of Nuclear Research of Hungarian Academy of Sciences, Bem tér 18/c, 4026 Debrecen, Hungary*
[3]*S.C.Belevion Impex S.R.L., 3, Dr. Clunet, str., Sector 5, Bucharest, Romania*

Abstract
The Gladna Montană intrusions belong to the late Cretaceous Banatitic province, occurring within Paleozoic metamorphic rocks in east Banat and showing porphyry copper mineralization. The main lithological types studied in two exploration boreholes are monzodiorites and granodiorites and rare lamprophyres. The intrusions looks heterogeneous, suggesting that the emplacement of mafic and felsic magmas were relatively contemporaneous. K-Ar data, using whole rock and secondary K-feldspar, yielded ages of 84-79 Ma for intrusions and 75Ma on a K-feldspar marking the alteration - mineralization event. Petrographic and geochemical studies reveal that the different lithologic types define two different compositions, one varying from basic to acid with a typical calc-alkaline signature and another one alkaline, Si-undersaturated, but showing similar geochemical features as the calc-alkaline varieties.

Keywords: Gladna Montană, banatite, calc-alkaline, lamprophyre, K-Ar geochronology, major and trace elements.

Introduction

A small number of petrographic, geochemical and age analyses were performed on samples from two intrusion bodies close to Gladna Montană, emplaced in the Poiana Ruscă metamorphic rocks belonging to the Supragetic Units (Săndulescu, 1984). The occurrences are part of the ”Banatitic Magmatic and Metallogenic Belt - BMMB” (Berza et al., 1998). The samples were collected from two exploration boreholes performed by S.C. Belevion: GDH-3a, a hole that intercepted a hidden intrusive polyphasic structure in Gladna Montană North (depth interception was at 92m) and DHRZ-1 that intercepted an exposed intrusive structure, south of the same locality along Rosalia valley, showing porphyry copper mineralization.

Methods

Element abundances were determined by ICP–AES (major elements) and ICP–MS (trace elements) in A.C.L.S. Minerals. s.r.l. Laboratory, Romania, following a lithium metaborate–tetraborate fusion and dilute nitric acid digestion of a 0.1-g sample. Loss on ignition (LOI) was determined as the weight difference after ignition at 1,000^{o}C. The results are shown in Table 1. The K/Ar dating method used at ATOMKI Debrecen and results of calibration was described in Balogh (1985). The age of the samples is calculated using the decay constants suggested by Steiger and Jäger (1977). Analytical error is given at 68% confidence level (1σ). The results are shown in Table 2.

Results

1. Lithology

The rocks in Bh. GDH-3a are phaneritic, relatively fresh and have homogeneous appearance; however, at the smaller scale, they show important heterogeneities, due to variable mafic mineral content. The rocks in Bh. DHRZ-1 show textural variability; these are mostly porphyritic, with a dominant quartzo-feldspathic matrix, and to a lesser proportion phaneritic equigranular, however, variably affected by late-stage hydrothermal processes. At 296-297m interval, a lamprophyre that can be observed in Figs. 1a,b,c show crosscutting relationships with host intrusive rocks.

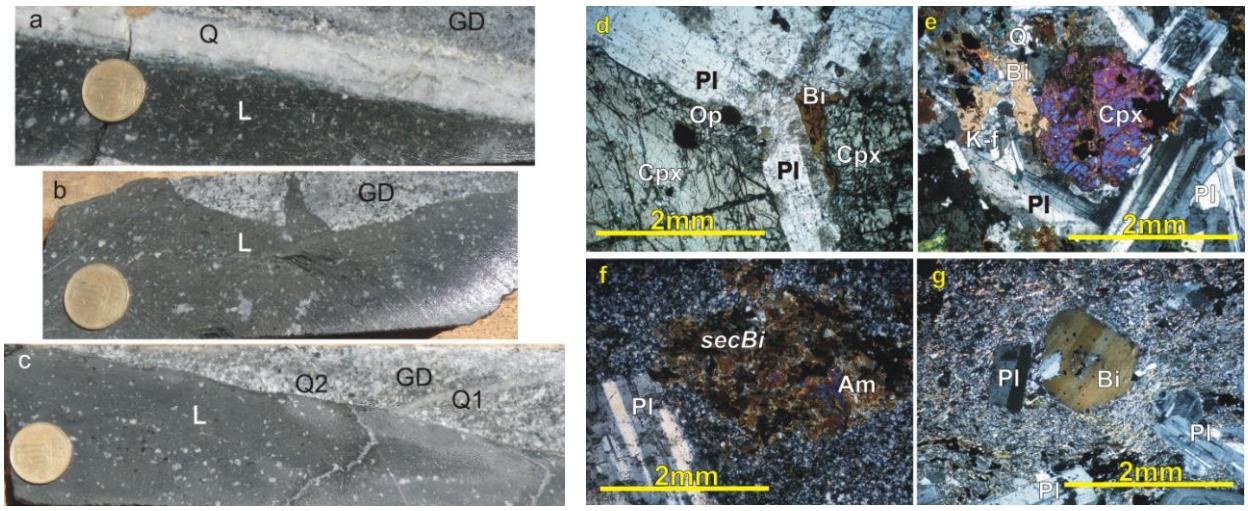

Fig. 1. Photo images showing different relationships between a lamprophyre dyke and granodiorite host at 296-297m in the borehole DHRZ-1: a. Sharp contact marked by a 2.5 cm thick mineralized quartz vein (Q) between lamprophyre dyke (L) and granodiorite(GD); b. Sharp irregular contact between lamprophyre dyke (L) and granodiorite (GD); c. Sharp contact between granodiorite (GD) cut by a quartz vein (Q1) and lamprophyre (L); GD and L are both crossed by a later quartz veinlet (Q2); Petrography: d. Monzogranite-GDH-3a, 142.5 m; e. Monzodiorite-GDH-3a, 180.2 m; f. Porphyritic Granodiorite-DHRZ-1, 50.8 m; g. Lamprophyre- DHRZ-1, 296 m. See explanation in the text. Symbols: Pl-plagioclase; Cpx-clinopyroxene; Am-amphibole; Bi- biotite; K-f – K-feldpar; Q-quartz; Op-opaque minerals.

2. Petrography

The rocks from Bh. GDH-3a show a massive granular texture that ranges from subhedral to anhedral. The dominant mineral is plagioclase, andesine-oligoclase in composition. The mineral sequence displays a gradual increase of felsic minerals (microcline, quartz) and anhedral biotite and a decrease of clinopyroxene and amphibole, shifting the composition from monzodiorites (Fig. 1e) to more felsic monzogranites (Fig. 1d). The initial amphiboles were partially or totally transformed in actinolite, chlorite and opaque minerals. The main components in Bh. DHRZ-1 are plagioclase, amphibole, biotite and small quartz crystals in porphyritic varieties (Fig. 1f). The samples dominantly plot in the granodiorite field. The mafic minerals are variably hydrothermalized, the amphibole being replaced by an irregular patch of biotite (Fig. 1f) and the initial biotite being partly chloritized. The plagioclase is variably replaced by secondary sericite, argillic minerals and carbonates. The rock is crossed in different directions by a sequence of mm-cm thick veinlets filled with sericite, quartz, secondary K-feldpar, carbonates and opaque minerals. The lamprophyres contain plagioclase and rare biotite and amphibole phenocrysts in a fluidal groundmass dominated by biotite, K-feldspar and quartz (Fig. 1g).

3. Geochemistry

A less hydrothermally altered type of rock was analyzed in Bh. DHRZ-1 (sample 1) along with two samples of lamprophyres (samples 2, 3). Two samples were collected from Bh. GDH-3a, an acid one (sample 4) and a more basic one (sample 5) (Table 1). In the multi-element diagrams, normalized to the composition of primitive mantle, the analyzed samples exhibit moderate LILE/HFSE ratios and well defined Nb and Ta depressions for both main intrusions and lamprophyres; the latter, however, are more enriched in most elements (Fig. 2-left). The chondrite normalized REE patterns, shown in Figure 2-right, are characterized by a moderate enrichment in LREE for both calc-alkaline intrusive rocks and lamprophyres. Most samples show a slight negative Eu anomaly. The data suggests that both intrusions are derived from typical calc-alkaline magmas and they show similar pattern distribution with the lamprophyres, which are however alkaline and Si-undersaturated.

Table 1. Major and trace element data for selected samples: 1. DHRZ-1-50.8 m; 2. DHRZ-1-296 m; 3. DHRZ-1-297 m; 4. GDH3A-142.5 m; 5. GDH3A-m180.2 m.

Sample	1	2	3	4	5		Sample	1	2	3	4	5
Rock	Granodio	Lampropl	Lamproph	Monzogr	Monzodio		Rock	Granodio	Lamprophyr	Lamprophyr	Monzogran	Monzodi
SiO_2	62,3	52,4	52,7	64	53,8							
TiO_2	0,64	0,99	0,97	0,64	0,84							
Al_2O_3	16,25	16,4	16,8	14,7	15,6							
Fe_2O_3	4,32	7,98	7,68	3,71	6,43							
MnO	0,04	0,15	0,12	0,03	0,06							
MgO	2,53	4,56	4,69	2,71	6,36							
CaO	3,02	6,79	7,18	2,88	3,39							
Na_2O	3,17	3,44	3,62	2,62	2,38							
K_2O	1,88	3,38	3,28	4,34	2,71							
P_2O_5	0,22	0,69	0,77	0,2	0,25							
LOI	3,83	1,43	1,21	2,4	5,54							
Total	98,3	98,38	99,21	98,34	97,5							
Rb	68,7	132,5	121	122	150,5		Y	20,9	32,3	30,3	18,6	18,4
Sr	414	738	819	473	386		La	32,1	51,2	51,4	17,3	20
Ba	382	572	594	472	241		Ce	64,1	113	112,5	39	41,6
V	172	265	258	170	247		Pr	7,22	13,55	13,45	4,84	5,12
Cr	22	36	40	25	164		Nd	26	51,6	51,3	19,2	19,6
Co	14	33,1	31,9	12,4	18,3		Sm	5,06	10,1	10,05	4,16	4,24
Ni	16	30	30	22	67		Eu	1,47	2,34	2,45	0,99	1,36
Cu	1340	220	219	2280	2470		Gd	4,52	8,91	8,7	3,88	4,1
Zn	48	100	94	36	49		Tb	0,68	1,21	1,17	0,6	0,64
Zr	150	300	270	150	130		Dy	3,72	6,1	5,87	3,23	3,35
Hf	4	7,2	6,4	4	3,4		Ho	0,75	1,2	1,11	0,67	0,67
Nb	8,5	9,7	9,2	8,3	6,6		Er	2,13	3,11	2,95	1,93	1,84
Ta	0,8	0,7	0,7	0,8	0,8		Tm	0,32	0,45	0,43	0,3	0,28
U	4,14	6,18	6	3,06	2,42		Yb	2,03	2,79	2,5	1,84	1,74
Th	12,65	26,4	24,2	12,7	8,08		Lu	0,31	0,42	0,38	0,28	0,26
Pb	19	25	23	16	9							

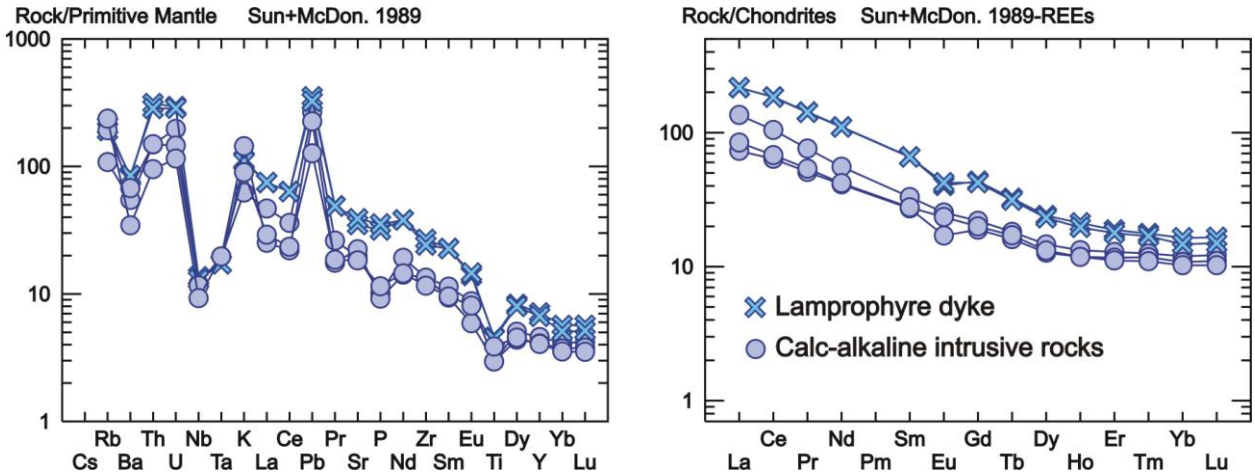

Fig 2. Spider diagrams (rock/primitive mantle and chondrite after Sun and McDonough, 1989) for analyzed calc-alkaline intrusive rocks and alkaline lamprophyre dykes.

4. Geochronology

The emplacement of the banatitic intrusions was dated at about 79.42±2.52 - 84.72±2.66 Ma (K-Ar whole-rock) for Gladna Montană north intrusion and 82.20±2.54 - 84.16±2.58 Ma (K-Ar whole-rock) for Rosalia (Table 2). The lamprophyre was dated at 82.64±2.56 Ma, suggesting to be among the youngest intrusion events. A K-feldspar belonging to the K alteration stage of Rosalia intrusion was dated at 75.70±2.38 Ma. Given the late mineral phases that may have strongly disturbed the K system during late magmatic and/or late stage hydrothermal processes, whole rock ages might not give the most accurate approximation, as they do not record the time of original crystallization. Nevertheless, the 75.70 Ma age given by secondary K-feldspar is more reliable and it represents one of the latest stages in the evolution of the magmatic body. Considering the large time interval between the K-feldspar age and the whole-rock ages, it is possible that the crystallization of the two large intrusions might have happened closer to 79 than 84 Ma.

Table 2. K-Ar data of selected rocks from boreholes in Gladna Montană-Poiana Ruscă banatitic intrusions

Lab. No.	Locality	Rock type	K (%)	$^{40}Ar_{rad}$ (ccSTP/g)	$^{40}Ar_{rad}$ (%)	K/Ar age (Ma)
8281.	Bh. DHRZ-1 50.8 m	whole rock granodiorite	1.498	4.7283 x10^{-6}	72.5	79.42±2.52
8282.	Bh. DHRZ-1 280.2 m	whole rock granodiorite	2.726	9.1912 x10^{-6}	74.9	84.72±2.66
8258.	Bh. DHRZ-1 282.1 m	K-feldspar	4.694	1.4107 x10^{-5}	74.7	75.70±2.38
8283.	Bh. DHRZ-1 296 m	whole rock lamprophyre	2.376	7.8104 x10^{-6}	80.9	82.64±2.56
8284.	Bh. GDH-3A 142.5 m	whole rock monzogranite	3.808	1.2449 x10^{-5}	81.0	82.20±2.54
8285.	Bh. GDH-3A 180.2 m	whole rock monzodiorite	1.500	5.0235 x10^{-6}	84.5	84.16±2.58

Discussion and conclusions

The textural and mineralogical heterogeneities at macroscopic scale are interpreted to define diffusive contact relationships, excepting the lamprophyre that shows clear crosscutting relationships. The presence of the lamprophyre may count as carrier for mineralization processes (e.g. Rock and Groves, 1988). Major and trace element geochemistry reveal that all the intrusive rocks are genetically related; even the lamprophyres that show alkaline affinities and are Si-undersaturated, display higher LILE and REE content, similar in trend with the other intrusions. The main intrusive bodies display distinctive calc-alkaline affinities. The unusual geochemical behavior of lamprophyres can be explained by a difference in melt generation processes of the source, where a lower degree of partial melting of similar composition as for the calc-alkaline intrusive rocks is expected. The crystallization ages of the main intrusions were probably around 79 Ma. Yet, in order to define and propose a viable genetic model, it is fundamental to enlarge the fieldwork, petrographic, geochemical and isotopic database at local and regional scale.

Acknowledgements

The studies were carried out in the framework of an inter-Academic Joint Project between ATOMKI Debrecen and the Institute of Geodynamics of the Romanian Academy. The authors express their gratitude to S.C. Belevion Impex s.r.l. that offered selected samples for study from exploration boreholes and supported the costs of thin sections and geochemical analyses.

References

Balogh K., 1985. K-Ar dating of Neogene volcanic activity in Hungary. Experimental technique, experiences and methods of chronological studies. *ATOMKI Reports* D/1, 277-288.

Berza, T., Constantinescu, E., Vlad, Ş.N., 1998. Upper Cretaceous magmatic series and associated mineralization in the Carpathian–Balkan Orogen. *Resource Geology* 48, 291-306.

Rock N.M.S., Groves D. I., 1988. Do lamprophyres carry gold as well as diamonds? *Nature* 332, 253-255.

Săndulescu, M., 1984. Geotectonics of Romania. Bucharest: *Editura Tehnică*, 336 p. (in Romanian).

Steiger R.H., Jäger E., 1977. Subcommisssion on Geochronology: convention on the use of decay constants in geo- and cosmochronology. *Earth Planet. Sci. Lett*. 12, 359-362.

Sun, S., McDonough, W.F., 1989. Chemical and isotopic systematics of oceanic basalts: implications for mantle compositions and processes. *Geological Society Special Publication* 42, 313-345.

Rom. J. Mineral Deposits, vol. 87 (2014), No. 1, p. 95-98

MINERALOGY OF PRECIOUS METALS ORE FROM LES FOUILLOUX GAUL MINE, LIMOUSIN (FRANCE) FROM METALS TRACEABILITY PERSPECTIVE

Călin G. TĂMAŞ[1]*, Béatrice CAUUET[2], Jean MILOT[2]

[1] University Babeş-Bolyai, 1, M. Kogălniceanu Str., 400084 Cluj-Napoca, Romania; * *calin.tamas@ubbcluj.ro*
[2] University Toulouse le Mirail, TRACES-CNRS, 5, A. Machado Str., 31058 Toulouse Cedex 09, France.

Abstract: Optical microscopy, SEM and EPMA investigations carried out on Au-Ag ore from Les Fouilloux Gaul mine, French Central Massif revealed the mineralogy of the ore really mined by the ancient miners. Stibnite is the most frequent ore mineral, being the main host of native gold. The native gold is Ag poor, with Ag content ranging from 13 to less than 20 wt%. The mineralogical association is completed by chalcopyrite, galena, tetrahedrite, berthierite, and jamesonite together with pyrite and arsenopyrite.

Keywords: Limousin, Gaul mine, metal provenance, mineralogy, native gold, berthierite, jamesonite

Introduction

Iberian Peninsula, French Central Massif and the Carpathians chain represented important precious metals sources during pre-Roman and Roman times in Europe from 5th c. BC to 3rd c. AD. Archaeological and historical evidences (Hirt, 2010) indicate that the former Roman provinces Hispania and Dacia were the most important sources of gold for the Roman Empire, with a mining activity flourishing after the Roman conquest of these two provinces. On the contrary, the mining activity in French Central Massif (Limousin region) ended soon after the Roman conquest of Gaul (Cauuet, 1999). Nevertheless, the pre-Roman Gaul mining in this area was very intense with Au-metal production exceeding 70 tones between 5th and 1st c. BC (Cauuet, 2004), making thus Limousin metallogenetic region (French Central Massif) a major Au source during this period of time in Europe.

The present study dealt with mineralogical characterization of precious metals ore from one of the most important Celtic mine in French Central Massif, namely Les Fouilloux (Cauuet, 1995, 1999 and 2004). This deposit is located in the Saint-Yrieix-La-Perche gold district (Bouchot et al., 1997a and b) and was mined between 5th and 1st c. BC as proved by mining archaeological research (Cauuet, 2004). After about two millennia of inactivity the mining restarted in Les Fouilloux ore deposit at the end of 20th c., precisely in 1988, and continued in 1991-1993. During the recent mining activity the deposit was mined in open pit operation by COGEMA, with a total production of 84600 tons of raw ore with an average grade of 7.8 g/t Au, producing more than 650 kg of gold (Bouchot et al., 1997b).

The reopening of the modern mining exploitation of Les Fouilloux deposit by COGEMA was preceded by mining archaeological research of the mining sites (Cauuet, 1988, 1995 and 1999) allowing the dating of the mining activity and the opening of the Gaul archaeological structures related to domestic and mining activities (surface and underground). In spite of the intense mining and the significant Au production during pre-Roman times in Limousin, the occurrence of gold objects in the region is scarce, being largely dominated by silver objects (Gomez de Soto, 1999). This archaeologically proven reality suggests that the majority of the produced gold was traded while the silver by-product was used by the local Gaul populations known as Lemovices (Cauuet, 2004). The mineralogical study of the ores really mined by the pre-roman miners in Les Fouilloux ore deposit is part of a broad mineralogical and geochemical (trace elements and Pb isotopes) study of the ores aiming the traceability of Au and Ag produced in Limousin Au-Ag province during Celtic times. The ore mined in Fouilloux deposit by Gaul miners consists of a quartz vein with a N60 strike and a dip of about 60° to the NW. Prior to modern mining in open pit, Les Fouilloux site occurred as an alignment of five trenches on 250 m length, 50 m width and a depth of 8-9 m. With the progress of late 20th c. mining it appears that the Celtic mine consists of only one excavation of 260 m length and a total depth (surface and underground) of 30 m (Cauuet, 1988 and 1999).The ancient exploitation started at surface with several benches going down to a depth of 20 m and then it developed in underground on another 10 m depth. The underground stope follows the dip of the ore body and has 2 to 2.5 m width. Ore pillars have been preserved by the Gaul miners for safety reasons. The pillars are high grade and represent a certified archaeological ore occurrence which we use now for metal tracing.

Regional setting

Saint-Yrieix-La-Perche (SYLP) gold district was generated during Variscan metallogenetic event, about 300 Ma ago. The ore district is mainly hosted by Lower gneiss unit of Limousin (Fig. 1), composed

of sillimanite-garnet paragneiss with amphibolites sequences, and orthogneiss. The genesis of the ore deposits was structurally controlled by the so-called Bourneix structure (Bouchot et al., 1997a) generally striking NE-SW. The ore deposits from SYLP gold district are represented by quartz vein structures and lenses up to 10 m width and several tens to hundreds of meters on strike. The ore bodies formed on shear zones situated in the apex of an underlying hidden silicic body (Bouchot et al., 1997b). The ores have an abundant quartz gangue hosting sulfides (stibnite, arsenopyrite, pyrite, chalcopyrite, sphalerite etc.), sulphosalts (tetrahedrite, boulangerite, semseyite, pyrargyrite, etc.) and native gold.

Materials and methods

Our approach on metal provenance study is based on accurate identification of ores really mined by the ancient miners followed by their mineralogical and geochemical (trace elements and Pb isotopes) characterization in order to obtain the mineralogical and geochemical signatures of the ancient ores and metals (Baron et al., 2013; Cauuet et al., 2013). The origin and the significance of the studied samples from Les Fouilloux were validated from archaeological and geological perspective in the field. The samples have been picked up from a safety pillar originally situated in the underground part of a proven Celtic stope. Due to the recent mining operation of COGEMA, this pillar is now outcropping in the south-western part of the modern open pit together with 2200 years old wooden propping which is still in place.

The ore and rock samples were studied by optical polarizing microscope (transmitted and reflected light), electronic microscope (SEM), and electron probe microanalyses (EPMA). The mineralogical study is based on optical microscopy observations on 23 polished sections and 11 thin sections, 5 chemical analyses on oxides (SiO_2, Al_2O_3, Fe_2O_3, CaO, MgO, Na_2O, K_2O, Cr_2O_3, TiO_2, MnO, P_2O_5), as well as on major and minor elements (C, S, Ba, Ce, Cr, Cs, Dy, Er, Eu, Ga, Gd, Hf, Ho, La, Lu, Nb, Nd, Pr, Rb, Sm, Sn, Sr, Ta, Tb, Th, Tl, Tm, U, V, W, Y, Yb, Zr, As, Bi, Hg, Sb, Se, Te, Ag, Cd, Co, Cu, Mo, Ni, Pb, Sc, Zn, Au, Pt), SEM investigations on 5 selected polished sections, and several tens of microprobe analyses made on 4 selected polished sections.

SEM investigations were made on a JSM-6360 electron microscope using a voltage of 20 kV which allowed us to identify all the chemical elements from known and unknown minerals observed on optical microscope. These data were used for further investigations carried out using a CAMECA SX50 electron microprobe with an acceleration voltage of 25 kV, a beam current of 20 nA, a surface of the analysed area of 3 x 3 micrometers, and a counting time of 10 s for peaks and 5 s for background. Two different programs were used for sulfides and precious metals alloys respectively. For standards we used chalcopyrite for S, Fe, and Cu; sphalerite for Zn; galena for Pb; and pure metals for As, Sb, Bi, Ag and Au. We used K alfa lines for S, Fe, Cu, Zn, L alfa lines for As, Sb, Ag, Au, L beta lines for As, and M alfa lines for Bi and Pb. The calculated reflection limits for the sulphides program were 550 ppm for S, 700 ppm for Fe, 700 ppm for Cu, 800 ppm for Zn, 4000 ppm for As, 1500 ppm for Ag, 1000 ppm for Sb, 2700 ppm for Pb and 3000 ppm for Bi. The calculated reflection limits for the Au-Ag alloys program were 600 ppm for Fe, 700 ppm for Cu, 1700 ppm for As, 1300 ppm for Sb, 4500 ppm for Bi, 3800 ppm for Pb, 2300 ppm for Ag, and 3000 ppm for Au.

Results

The chemical analyses of five ore samples confirm the high grade of the ore mined by the Celtic miners (Table 1). These analyses also confirm the As-Sb rich character of the ore and Bi traces as well.

Table 1 - Ore grades (in ppm) of the ore from Celtic mine of Les Fouilloux deposit, France

Sample	Ag	Cd	Cu	Pb	Zn	Au	Sb	As	Bi
4300	6	<0.5	18	233	7	30.6	>250	>250	0.51
4301	11.5	<0.5	21	156	6	56.4	>250	>250	0.33
4302	9.3	<0.5	34	148	6	80.6	>250	>250	0.19
4303	28.3	6.3	66	2890	44	39.9	>250	>250	5.21
4306	9.4	<0.5	53	401	18	94.0	>250	79	10.2

The ore body from Les Fouilloux consists of a major quartz vein structure hosted by mylonitised gneiss/micaschists showing a minor chloritisation. The quartz gangue of the vein suffered a minor brecciation followed by ore metals deposition. The preliminary optical microscopy revealed that stibnite is the most frequent ore mineral (Fig. 2a,d,e,g,h), associated with pyrite (Fig. 2a), arsenopyrite (Fig. 2b,c,i), tetrahedrite (Fig. 2c,f), and electrum (Fig. 2g,h,i).

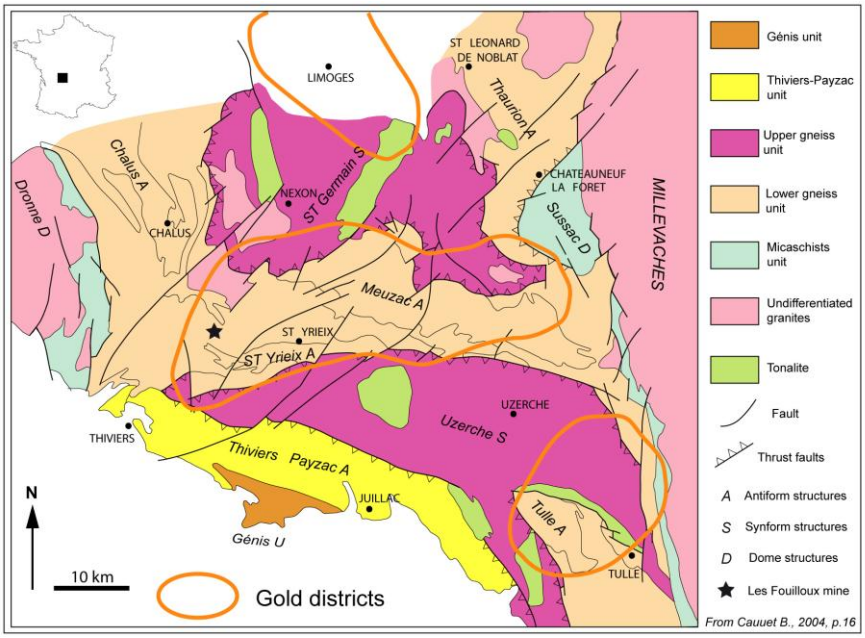

Fig. 1. Simplified geology of Limousin metallogenetic region and location of Les Fouilloux deposit (after Cauuet, 2004, with changes).

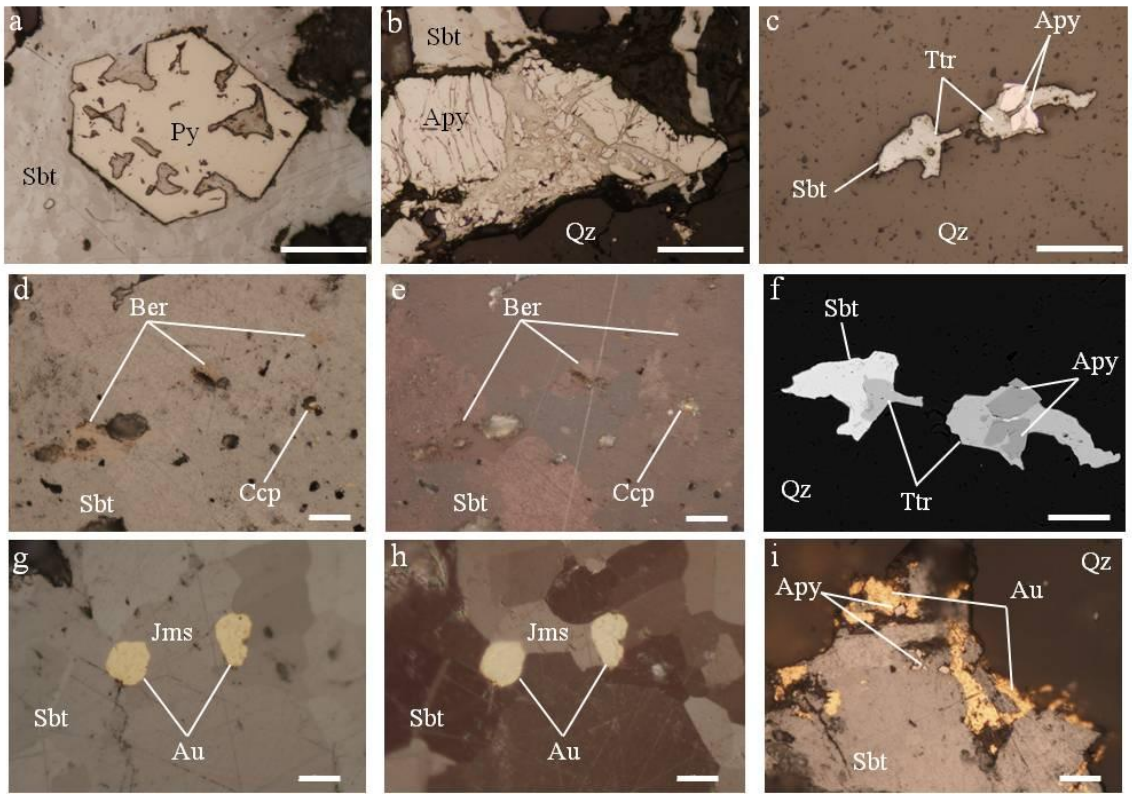

Fig. 2. Microphotographs (plane polarized light if not mentioned) images (**a,b,c,d,e,g,h,i**) and SEM image (**f**). a) idiomorphic pyrite crystal partially corroded by stibnite; b) brecciated arsenopyrite cemented by stibnite; c) arsenopyrite-stibnite-tetrahedrite association filling voids within quartz; d) berthierite blebs hosted by stibnite; e) crossed polars view of the previous image; note the strong anisotropy of stibnite; f) detail of image 2c; g) two native gold grains hosted by stibnite and in mutual contact with an elongated grain of jamesonite; h) crossed polars view of the previous image showing the strong anisotropy of stibnite and the shape of jamesonite grain covering the native gold grains; i) native gold grain filling voids along the contact stibnite-quartz. The scale bar (in micrometers) is 100 for **a,b,c**; 50 for **f**; 20 for **d,e,i** and 10 for **g,h**. Abbreviations: Apy = arsenopyrite; Ber = berthierite; Ccp = chalcopyrite; Au= native gold; Jms – jamesonite; Py = pyrite; Sbt = stibnite; Ttr = tetrahedrite; Qz = quartz.

The stibnite occurs as veinlets within quartz gangue, as cement for brecciated quartz, pyrite and arsenopyrite (Fig. 2b) grains as well as massive zones hosted by quartz. The stibnite crosscuts and covers pyrite and arsenopyrite. Rare chalcopyrite (Fig. 2d,e), galena, sphalerite and tetrahedrite (Fig. 2c,f) blebs

have been observed on optical microscope and have been confirmed by SEM and EPMA data. The occurrence of berthierite (Fig. 2d,e) and jamesonite (Fig. 2g,h) within stibnite was equally confirmed by the means of EPMA data (Table 2). Native gold was observed only hosted by stibnite and quartz (Fig. 2g,h,i), and EPMA data revealed its small Ag content, ranging from 13 to below 20 wt% (Table 3).

The calculated formula of berthierite based on 12 analyses on different mineral grains is $Fe\ Sb_{2.19}\ S_{4.17}$ (idealized formula $Fe\ Sb_2\ S_4$) and the calculated formula of jamesonite based on 8 analyses within one mineral grain normalized to 25 atoms is $Pb_{3.79}\ Fe_{0.85}\ Sb_{6.38}\ S_{13.98}$ (idealized formula $Pb_4\ Fe\ Sb_6\ S_{14}$). The calculated formulas for native gold grains are $Au_{2.268}$ Ag (sample 4303D) and $Au_{3.576}$ Ag (sample 4453C) corresponding to a gold fineness of 805 and 867 respectively.

Table 2. Analytical data (wt %) for berthierite (*ber*) and jamesonite (*jms*), Les Fouilloux, France; n - number of EPMA point analyses.

Sample	S	Fe	Cu	Zn	As	Ag	Sb	Pb	Bi	Total
4306C; n=12 (*ber*)	29.063	12.126	0.012	0.007	0.102	0.019	57.965	0.108	0.004	99.449
4303D; n=8 (*jms*)	21.660	2.279	0.047	0.005	0.099	0.046	37.565	37.895	0.041	99.637

Table 3. Analytical data (wt %) for native gold, Les Fouilloux, France; n - number of EPMA point analyses.

Sample	Fe	Cu	As	Ag	Sb	Au	Pb	Bi	Total
4303D; n=8	0.019	0.009	0.033	19.485	0.298	80.690	0.061	0.015	100.61
4453C; n=5	0.024	0.004	0.047	13.242	0.370	86.316	0.009	0.000	100.012

Conclusions

By means of archaeological and geological common approaches were obtained ore samples which are identical with the ore mined by the Celtic/Gaul miners from Les Fouilloux. These samples represent validated material for further metal tracing research. The mineralogical investigations revealed the mineralogy of the Celtic ore, consisting of stibnite, pyrite, arsenopyrite, tetrahedrite, galena, chalcopyrite, berthierite, jamesonite, native gold and quartz gangue. Stibnite is the most frequent ore mineral. Native gold is poor in Ag (13-20 wt %) and is host in stibnite and quartz.

Acknowledgements

Research carried out in the frame of ANR MINEMET project (2012-2015) conducted by Beatrice Cauuet, CNRS. SEM and EPMA investigations were carried out in GET Laboratory, University Paul Sabatier, Toulouse, France.

References

Baron, S., Tămaş, C.G., Le Carlier, C. (2013). How mineralogy and geochemistry can improve the significance of Pb isotopes in metal provenance studies. Archaeometry; doi: 10.1111/arcm.12037.

Bouchot, V., Lescuyer, J.-L., Milési J.-P., Leistel, J.-M., Lagny, P. (1997a). Information files of metropolitan French gold districts (in French). Chronique de la Recherche Minière, 528, 27-62.

Bouchot, V., Milési J.-P., Lescuyer, J.-L., Ledru, P. (1997b). French gold deposits in their geological setting around 300 Ma (in French). Chronique de la Recherche Minière, 528, 13-26.

Cauuet, B. (1988). The antique mine of Fouilloux (Jumilhac, Dordogne): the first results of the archaeological diggings (in French). Aquitania, 6, Bordeaux, 181-190.

Cauuet, B. (1995). New discoveries on the “aurières” from Isle upper valley, Dordogne/Haute-Vienne (in French). Actes du Colloque International AFEAF - Agen 1992, Aquitania, 12, Bordeaux, 111-123.

Cauuet, B. (1999). The exploitation of gold in Gaul during the Iron Age. In: Cauuet, B. (Ed.) Gold during Antiquity from mine to object (in French). Actes du Colloque International de Limoges 1994, Supplément 9 Aquitania, Bordeaux, 31-86.

Cauuet, B. (2004). L’Or des Celtes du Limousin. Edition Culture et Patrimoine en Limousin, Limoges, 123 pp.

Cauuet, B., Tămaş C.G., Baron, S., Milot, J. (2013). Archaeological practices validating mineralogical and geochemical analyses in metal provenance studies. The gold mines from central Gaul (France) case study. Goldschmidt Conference 2013 (accepted).

Gomez de Soto, J. (1999). Dwellings and necropolises of Metal ages in west central region and in Aquitaine: the question of the absent gold (in French). Actes du Colloque International de Limoges 1994, Supplément 9 Aquitania, Bordeaux, 337-346.

Hirt, A.M. (2010). Imperial Mines and Quarries in the Roman World. Organizational aspects 27 BC – AD 235, Oxford, 420 pp.

ADDITIONAL DATA REGARDING THE PETROGRAPHY AND GEOCHEMISTRY OF THE MAGMATIC PHASES AND HYDROTHERMAL VEIN TYPES FROM BOLCANA PORPHYRY Cu-Au MINERALIZATION (APUSENI MTS., ROMANIA)

Réka DÉNES[1]*, István MÁRTON[2], Gabriella B. KISS[1], Paul IVĂȘCANU[3], Zsolt VERESS[3]

[1]Department of Mineralogy, Eötvös Loránd University, H-1117 Budapest, Pázmány Péter sétány 1/C, Hungary;
[2]Department of Geology, University of Babeş-Bolyai, Cluj-Napoca, (current affiliation: Avala Resources doo, Zeleni Bulevar 27/1, 19210, Bor, Serbia);
[3]DevaGold S.A., Str. Principală, 89 C, Certeju de Sus, Romania;
**reka.denes@gmail.com*, Tel.: 0040-746-089144;

Abstract: The studied zone of the Bolcana porphyry Cu-Au mineralization is hosted by successive magmatic phases and breccias, which underwent hydrothermal alteration. There are two early porphyry stocks, the medium grained porphyry and the coarse grained porphyry phases, which were followed by an intermineral stock with quartz and medium grained porphyry texture and a late fine grained porphyry stock. These intrusions are hosted by a magmatic breccia. The porphyry phases underwent several hydrothermal alteration types: potassic alteration overprinted by sericite-chlorite, sericite, propylitic and argillic alterations. Six porphyry veinlet types and a superimposing epithermal type vein were also observed. The preliminary results of the fluid inclusion study suggest a boiling phenomena which occurred at relatively low temperatures (140-280°C) in A2-type veins. As a result of the Raman spectroscopy the oxidizing character and the sulphur-saturation of the mineralizing fluids were also identified. All the observed features suggest that the studied samples represent a shallow zone of a porphyry mineralization.

Keywords: porphyry mineralization, porphyry stocks, hydrothermal alteration, hydrothermal vein type, fluid inclusion.

1. Introduction

The Bolcana porphyry Cu-Au mineralization is located in the southern part of the Apuseni Mountains, where Miocene calc-alkaline intrusive and volcanic units hosts numerous porphyry Cu-Au and epithermal Au-Ag (Pb-Zn) mineralizations *(Neubauer et al., 2005)*. The Bolcana ore deposit is located in the central part of the Bolcana-Troița-Măgura volcanic structure and is hosted by the Neogene Hondol-Făerag andesite and the Bolcana intrusion. The porphyry mineralization is represented by chalcopyrite, pyrite, bornite, magnetite, hematite, molybdenite and subordinate native gold. This mineral assemblage is associated with potassic, sericitic, sericite-chlorite, propylitic and intermediate argillic hydrothermal alterations. The porphyry mineralization is cross cut by the late stage low sulphidation type epithermal veins. The epithermal mineralization is represented by pyrite, sphalerite, galena, chalcopyrite, tetrahedrite, bournonite, marcasite, native gold, arsenopyrite and pyrrhotite (Milu et al., 2003).

The petrographical and mineralogical examination results of the Bolcana ore deposit appear in some earlier regional studies. Milu et al. (2003) published a study about the hydrothermal alteration assemblages at Bolcana ore deposit in 2003. Cardon et al. (2005) published a structural study and a 3D representation of the sector of Troița-Bolcana-Măgura about the link between porphyry copper and the epithermal deposit. Later Cardon et al. (2008) published a study about the Re-Os age datas made on samples from Bolcana. A fluid inclusion study was published for the Bolcana ore deposit by Cioacă (2011).

Drill cores of three exploration drill holes were studied, which are located along a NW-SE section and expose the system to the depth of 250 m from the surface *(fig.1)*. The drill cores represent distinctive parts of the porphyry system, with variable intrusive phases, alteration types, Cu/Au ratio and epithermal overprinting. Our scope was to provide a complementary and detailed documentation of the magmatic phases, their specific mineral assemblages, alteration features and crosscutting relationship of hydrothermal veins as well as to find out the main changes in lithology, which cause variable metal content in different part of the mineralization. To achieve these goals, transmitted and reflected light microscopy, X-ray powder diffraction, fluid inclusion microthermometry and Raman spectroscopy have been used.

The description of the observed magmatic phases are used according to the nomenclature of review paper of Sillitoe (2010). In this aspect the „early, intermineral and late porphyry phases" nomenclature refers to magmatic stocks intruded in specific relationship to the porphyry Cu-Au mineralization.

Porphyry veinlets nomenclature follows Gustafson and Hunt (1975; A, B, and D types) and Arancibia and Clark (1996; M type).

2. Geology of the studied area

The Bolcana mineralization belongs to the Bolcana-Troița-Măgura-Teascu mining district, which is located in the southwestern part of the Brad-Săcărâmb Basin. As the basement of the area are composed of the Middle Jurassic–Lower Cretaceous ophiolitic rocks and Lower Cretaceous Băița rhyolites. These rocks are overlain by Palaeocene and Middle Miocene sedimentary series *(fig.1)*. In the area the oldest Neogene volcanic rocks are represented by the Sarmatian Hondol-Făerag andesites that occur as lava flows, intrusions and pyroclastics, respectively. The Bolcana intrusion as an subvolcanic body intrudes these andesites. Around the subvolcanic body intrusive polymictic breccias are observed (Milu et al., 2003).

3. The time relationship between the magmatic phases and the hydrothermal vein types

Based on the petrographical results the studied zone of the Bolcana prospect is formed by successive porphyry phases of dioritic composition, which are locally associated with fluid driven breccias *(fig. 2)*. The hydrothermal alteration zones developed during the porphyry phases are accompanied by different porphyry Cu-Au stage veinlets and epithermal vein types: M-type (magnetite), A1-type (quartz-magnetite), A2-type (quartz-magnetite-pyrite-chalcopyrite-bornite), A3-type (quartz-pyrite-chalcopyrite), D1-type (chalcopyrite), D2-type (pyrite) and E-type (sphalerite, chalcopyrite, pyrite, calcite) veins. Veinlets nomenclature follows (Gustafson et al., 1975) and (Arancibia et al., 1996). In the case of the A1- and A2-type veinlets, sulphides do not form continuous bands veinfilling and only the A3-type veinlet has sericitice-chlorite selvedge.

Considering the time relationships, there are two early porphyry stocks, the medium grained porphyry (MGPO) and the coarse grained porphyry phases (CGPO), both underwent an earlier, high temperature most likely potassic alteration, overprinted by sericite(-chlorite) alteration *(fig. 3a,b.)*.

The quartz bearing medium grained porphyry (QMGPO) occurs as an intermineral stock, which was affected by a moderate sericite alteration *(fig. 3c.)*. The porphyry type veinlets in the intermineral stock are cut by polymetallic ore mineral (mostly sphalerite, but chalcopyrite, pyrite and calcite also occur) filled E-type veins *(fig. 3e.)*. Locally the QMGPO underwent an intermediate argillic alteration and is cross cut by stockwork type quartz veinlets, which are rich in disseminated pyrite *(fig. 3d.)*

As well as the QMGPO is connected with an intermineral-hydrothermal breccia (XHT, *fig. 3f.*). The breccia is clast supported and the clasts are from the intermineral stock, proven by the stockwork quartz veinlets which cease on the boundary of the clasts *(fig. 3g.)*.The late porphyry stock in the studied zone is the fine grained porphyry (FGPO, *fig. 3i.*) underwent an earlier potassic alteration overprinted by a sericite-chlorite alteration and locally caused brecciation of the earlier intrusions (FGPO-XHT, *fig. 3h, j.*).The host rock of the porphyry phases is a magmatic breccia (MXH). The MXH is older than the porphyry stocks and is underwent propylitic alteration. The MXH is matrix supported and monomictic. The matrix and the clasts are cogenetic. The difference between the matrix and clasts is only the degree of the crystallization *(fig. 3k.)*.

4. Preliminary results of the fluid inclusion study

Fluid inclusion study was done on the quartz of the A2-type veinlets, as those veins contain appropriate host minerals and well preserved fluid inclusion assemblages. During the fluid inclusion petrography, four types of fluid inclusions were identified: (1) halite-bearing polyphase fluid inclusions (S_H+L+V), (2) fluid inclusions with other solid phase (S+L+V), (3) two phase liquid+vapor containing, vapor rich and liquid rich inclusions (L+V), (4) two phase (L+V) fluid inclusions arranged in plains. Types 1-3 occur as primary inclusions, thus suggesting an inhomogeneous parent fluid, i. e. a boiling system, while type 4 is a secondary generation. As the trapping of the primary fluid inclusion happened heterogeneously from an inhomogeneous system, the homogenisation temperatures (Th) of the aqueous liquid rich inclusions correspond to the formation temperature (Diamond, 2003). The measurements done on the inclusions with V=10 area% were taken into consideration.

Based on the results, the formation temperatures of the (L+V) inclusions cover a wide range (140-280 °C) while the (L+V+halite) inclusions homogenized at temperatures > 350 °C. The calculated salinities form two well distinguishable groups (0.5-5 NaCl equiv. wt% in L+V inclusions and~33 NaCl equiv. wt% in L+V+halite inclusions). The low homogenization temperatures and low salinity values in aqueous inclusions appear in the late-stage porphyry veining (Kouzmanov et al., 2012).

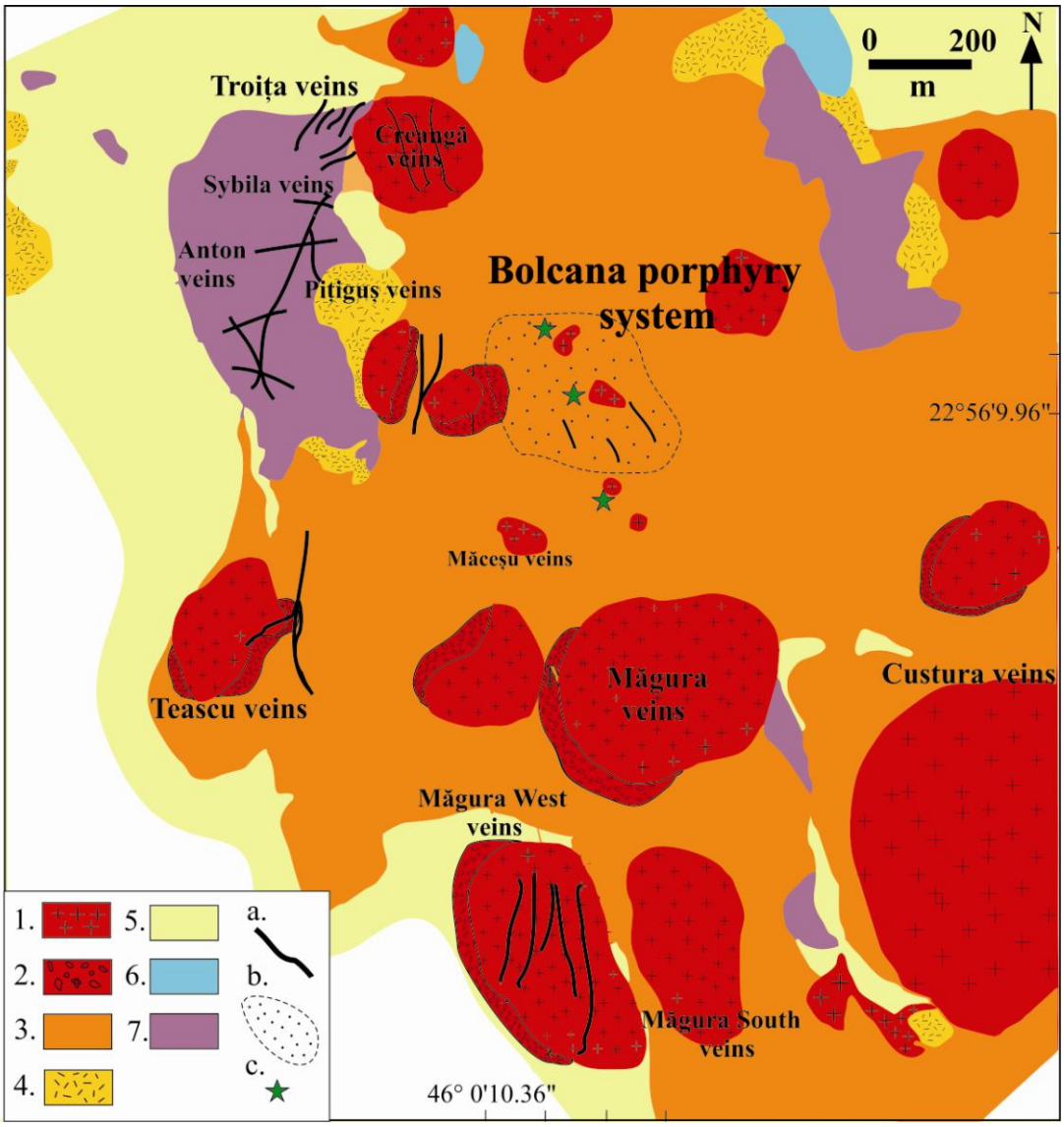

Fig. 1. The simplified geology map of the Bolcana-Troița-Măgura-Teascu ore district with the location of sampled drill holes (after DevaGold S.A. and Cardon et al., 2008). Lithology legend: 1) Miocene diorites (subvolcanic necks and dykes), 2) Breccias, 3) Miocene andesitic lavaflows, 4) Miocene andesitic pyroclastics, 5) Paleocene Almașu Mare Formation, 6) Mesozoic reef limestone, 7) Mesozoic ophiolites, a) mineralization in veins, b) disseminated mineralization, c) drill holes.

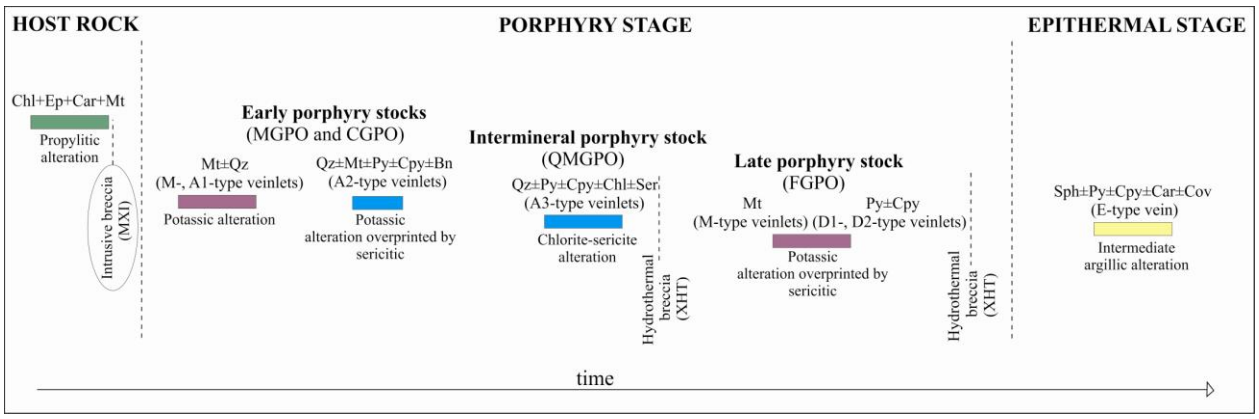

Fig. 2. Time relationship between the main porphyry and epithermal ore stages, magmatic stocks, hydrothermal veining and alterations in the studied part of the Bolcana ore prospect. Abbreviations: Chl-chlorite, Ep-epidote, Car-carbonate, Mt-magnetite, Qz-quartz, Py-pyrite, Cpy-chalcopyrite, Bn-bornite, Ser-sericite, Sph-sphalerite, Cov-covellin.

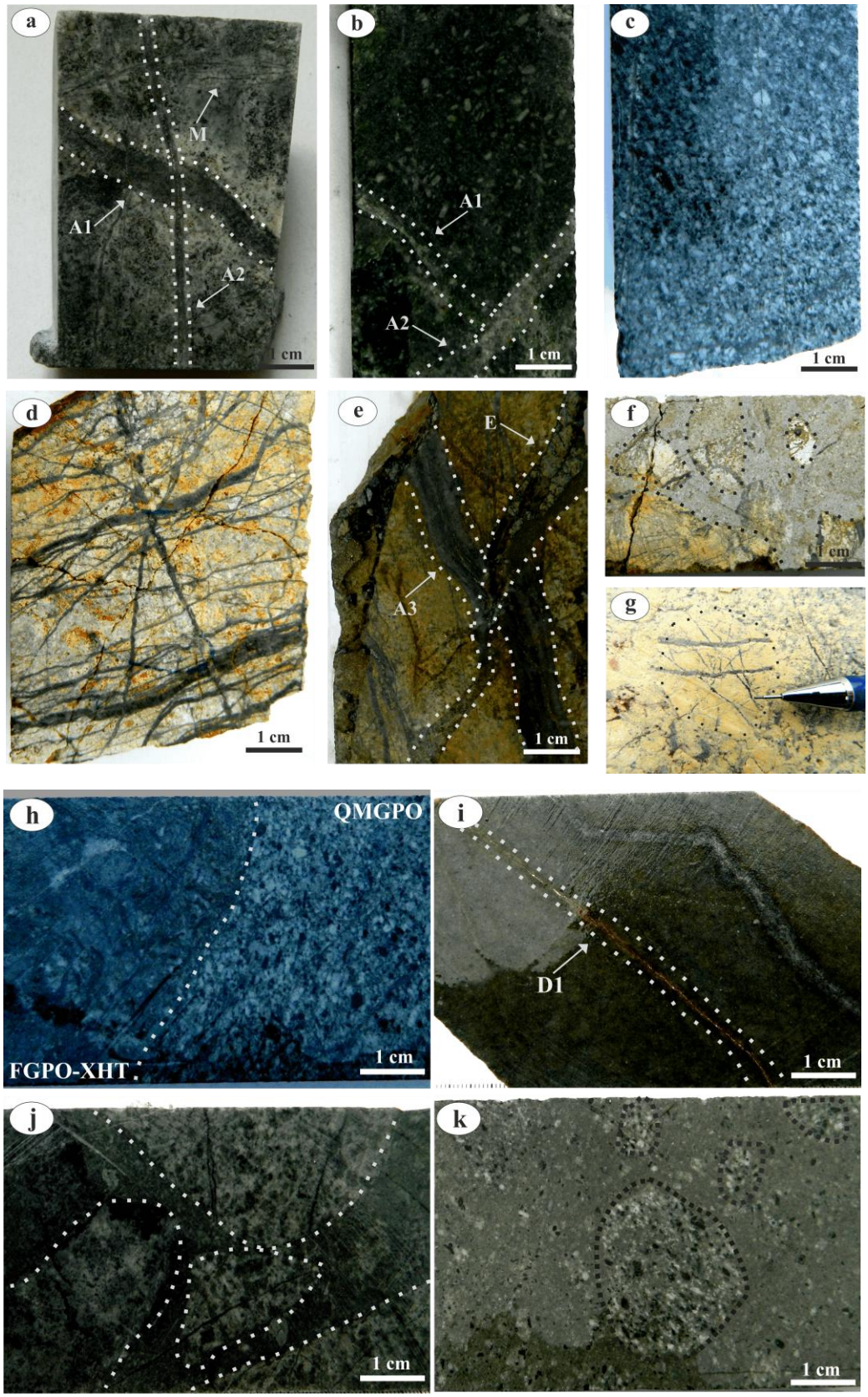

Fig. 3. Macroscopic features of the different porphyry stocks, hydrothermal alterations and the veins types observed in the studied part of the Bolcana ore prospect: **a** - MGPO with M1-, A1-, A2-veinlets; **b** - CGPO with A1-, A2-veinlets; **c** - QMGPO; **d** - QMGPO with argillic alteration and stockwork veinlets; **e** - E-type vein in the QMGPO; **f** - XHT; **g** - Clast of the XHT; **h** - The contact zone between the QMGPO and the FGPO-XHT; **i** - FGPO with D1-type veinlets; **j** - FGPO-XHT; **k** - magmatic breccia (host rock).

The hematite in the inclusions proven by the Raman spectroscopy suggests the magmatic origin and oxidizing character of the mineralizing fluids (Henley et al., 1984). The presence of $CaSO_4$ as a solid phase in polyphase fluid inclusions shows of the oxidizing character of the fluids and that the magma was saturated in sulphur (Lickfold et al., 2003). The CO_2 is a dominant component of the vapor phase after the boiling event (Webster et al., 2007).

5. Conclusions

As a conclusion, the studied part of the Bolcana porphyry Cu-Au mineralization is hosted by successive coalescent porphyry phases, breccias and related hydrothermal alterations.

Considering the time relationships, there are two early porphyry stocks which underwent potassic alteration overprinted by sericite(-chlorite) alteration. The intermineral porphyry stock was affected by a moderate sericite alteration. The late porphyry stock underwent a potassic alteration overprinted by a sericite-chlorite alteration and locally caused brecciation. Locally the intermineral porphyry underwent an intermediate argillic alteration and in this part an intermineral-hydrothermal breccia occurs, too. The host rock of the intrusion is a magmatic breccia with propylitic alteration. Six porphyry veinlet types and a superimposing epithermal type vein were also identified.

As a preliminary result of the fluid inclusion study, a boiling phenomena was identified in the relatively low temperature (140-280°C) A2-type veins. Temperatures of < 320 °C occur in late-stage porphyry-related veinlets, where the dominant inclusions are the low-to-intermediate salinity aqueous type, and hypersaline liquid inclusions assemblages that are produced by successive boiling of magmatic fluids with decreasing of pressure and temperature (Simmons et al., 1997).

As a result of the Raman spectroscopy, the oxidizing character and the sulphur-saturation of the mineralizing fluids is suggested. The hydrothermal alteration types observed in the magmatic phases together with the occurrence of intermediate argillic type alteration zones suggest that the studied part represents most likely a shallow zone of a porphyry mineralization.

6. Acknowledgements

Special thanks to all colleagues at Department of Mineralogy (ELTE), F. Kristály (University of Miskolc) and all the fellows at DevaGold Company. The work was supported by the Balassi Institute fellowship program and the Baross Gábor Program of the National Research and Technology Agency (NKTH), Hungary. Helpful suggestions and comments on an earlier version of the extended abstract by an anonymous reviewer are deeply appreciated.

7. References

Arancibia, O. N., and Clark, A. H. 1996. Early magnetite-amphibole-plagioclase alteration-mineralization in the Island Copper porphyry copper-gold-molybdenum deposit, British Columbia: Economic Geology, v. 91, p. 402−438.

Cardon, O., Mayer, A. S. A., Sausse, J., Milu, V., Chauvet, A., Leroy, J. L., Lespinasse, M., Udubașa, S. 2005. Connexion porphyre cuprifère-épithermaux de type low-sulfidation: analyse structurale et représentation 3D du secteur de Bolcana, Monts Apuseni, Roumanie, Comptes Rendus Geoscience, v. 337, p. 824-831.

Cardon, O., Reisberg, L., Mayer, A. S. A., Leroy, J., Milu, V., Zimmermann, C. 2008. Re-Os systematics of pyrite from the Bolcana porphyry copper deposit, Apuseni Mountains, Romania, Economic Geology, v. 103, p. 1695-1702.

Cioacă, M. E. 2011. Fluid evolution in the Bolcana ore deposit, Metaliferi Mountains (Romania), Carpathian Journal of Earth and Environmental Sciences, v. 6, no. 2., p. 215-224.

Diamond, L., W. 2003. Systematics of H_2O inclusions, In: Fluid inclusions: Analysis and Interpretation, Mineralogical Association of Canada Short Course Series, v. 32., p. 55-79.

Gustafson, L. B., and Hunt, J. P. 1975. The porphyry copper deposit at El Salvador, Chile: Economic Geology, v. 70, p. 857−912.

Henley, R., W., Truesdell, A., H., Barton, P., B. 1984. Fluid-mineral equilibria in hydrothermal systems, Economic Geology, v. 1., 99-112.

Kouzmanov, K., Pokrovski, G. 2012. Hydrothermal Controls on Metal Distribution in Porphyry Cu (-Mo-Au) Systems, Society of Economic Geologists, Inc. Special Publication 16, pp. 573–618.

Lickfold, V., Cooke, D., R., Smith, S., G., Ullrich, T., D. 2003. Endeavour copper-gold porphyry deposits, Northparkes, New South Wales: Intrusive history and fluid evolution, Economic Geology, v. 98., p. 1607-1636.

Milu, V., Leroy, J. L., Piantone, P. 2003. The Bolcana Cu-Au ore deposits (Metaliferi Mountains, Romania): first data on the alteration and related mineralisation, Comptes Rendus Geoscience, v. 335, p. 671-680.

Neubauer, F., Lips, A., Kouzmanov, K., Lexa, J., Ivăşcanu, P. 2005. Subduction slab detachment and mineralization: The Neogene in the Apuseni Mountains and Carpathians, Ore Geology Reviews, p. 14.

Sillitoe, R., H. 2010. Porphyry copper systems: Economic Geology, v. 105., p. 3-41.

Simmons, S. F., and Browne, P. R. L. 1997. Saline fluid inclusions in sphalerite from the Broadlands-Ohaaki geothermal system: A coincidental trapping of fluids boiled toward dryness: Economic Geology, v. 92, p. 485–489.

Webster, J., D., Mandeville, C., W. 2007. Fluid immiscibility in volcanic environments, Reviews in Mineralogy and Geochemistry, v. 65., p. 313-362.

Rom. J. Mineral Deposits, vol. 87 (2014), No. 1, p. 105-108

THE TEASCU EPITHERMAL GOLD DEPOSIT (METALIFERI MOUNTAINS): FIRST DATA ON THE ALTERATION AND MINERALIZATION

Laura TUŞA[1]*, Călin G. TĂMAŞ[1], Paul IVĂŞCANU[2], Zsolt KULCSAR[2], Laurenţiu IGNA[2]**

[1] Department of Geology, Babeş-Bolyai University, Cluj-Napoca; * *laura.tusa@yahoo.com*
[2] DevaGold S.A., Str. Principală, 89 C, Certeju de Sus ; ** *paul.ivascanu@eu.eldoradogold.com*

Abstract
Teascu epithermal ore deposit is a low-to intermediate sulphidation gold deposit, located approximately 20 km north from Deva. The mineralization is hosted by Hondol-Săcărâmb andesites as well as Badenian sedimentary rocks. Three hydrothermal pulses have been identified in the analyzed samples, of which, the second one is the most important and it is represented by Au-bearing quartz-pyrite veinlets. Four main alteration types have been identified: phyllic, argillic, propylitic and silicic. The variations in mica crystallinity identified by PIMA analyses suggest the rapid cooling of the hydrothermal system outwards from the main channel flow and suggest the possibility of identifying an ore shoot at greater depth.

Key words: Au epithermal ore deposit, hydrothermal alteration, Metaliferi Mountains, Romania.

1. Introduction

The Teascu epithermal gold deposit is located in the southern part of Apuseni Mountains, more precisely in the Brad-Săcărâmb metallogenetic district, where Miocene calc-alkaline intrusive and volcanic units host numerous porphyry Cu-Au and epithermal Au-Ag ± Pb-Zn deposits/mineralizations (Neubauer et al., 2005). The basement of the area consists of middle Jurassic-Lower Cretaceous ophiolites and Lower Cretaceous rhyolites (Băiţa rhyolites) (Milu et al., 2003) overlain by Badenian sedimentary formations: gravels, sands and silty clays. The Teascu epithermal gold deposit is located in the central-eastern part of the Troiţa-Măgura volcanic structure. The deposit is hosted by Săcărâmb-Hondol andesites and by Badenian sedimentary rocks situated below the andesite lava flows. The K-Ar age of Săcărâmb-Hondol andesites ranges between 10-12 Ma (Roşu et al., 1997; Pécskay et al., 2006). The genesis of Brad-Săcărâmb basin and associated ore deposits/mineralizations was controlled by NW-SE transtensional faults (Neubauer et al., 2005). The same structural setting controlled the epithermal fluid flow paths within Teascu area.

2. Materials and methods

The present study is based on more than 50 samples selected from six exploration drill cores performed during the exploration program run by Deva Gold S.A. in Teascu license perimeter. The studied drill cores are located as follows: two in the northern part, three in the central zone and one in the southern part of the mineralization halo. The samples were originally situated at depth between 80 and 300 meters.

Optical microscopic studies (transmitted and reflected light) were done in order to obtain preliminary data on mineralogy, petrography and hydrothermal alterations. X-ray diffraction (XRD) analyses on whole rock and on selected clay mineral fraction (random and oriented samples) were performed with a Bruker D8 Advanced XRD device, with a Co anticathode (λ = 1.79026 Å) running at a voltage of 35 kV, a current intensity of 40 mA and a scanning time of 200 ms. These investigations facilitated the identification of the clay minerals occurring in Teascu hydrothermal alteration zones.

Infrared spectroscopy analyses (PIMA) were performed in the field with a LabSpec 2600 Portable Vis/NIR Spectrometer with the spectral resolution of 3 nm @ 700 nm, 6 nm @ 1400/2100 nm, sampling interval of 1.377 nm @ 350-1050 nm, 2 nm @ 1000-2500, and a scanning time of 100 milliseconds.

3. Results

3.1. Petrography

The petrograpic investigations were firstly done macroscopically on the selected drill cores (Fig. 1) and were followed by transmitted light microscopy observations in thin sections. Macroscopic and microscopic observations confirm that the host rocks for the gold mineralization in Teascu area are

represented by amphibole-bearing andesites, as well as phreatomagmatic, hydrothermal and tectonic breccias. Sedimentary sequences, *i.e.* gravels, sands and silty clays located underneath andesites and/or brecciated andesites, may sometimes host minor mineralization due to the deposition of hydrothermal cement (quartz, sulfides) within vugs becoming thus mineralized conglomerates, sandstones and siltstones.

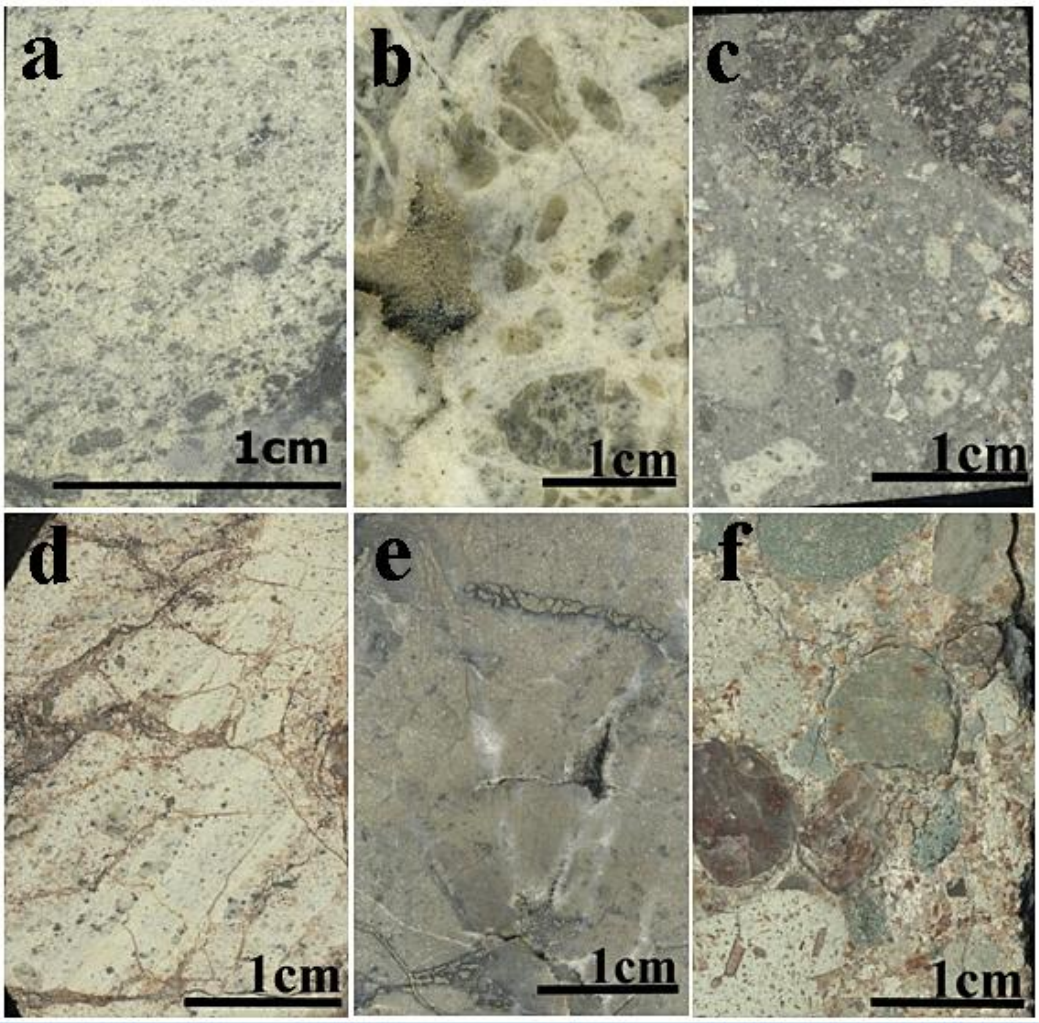

Fig. 1. Macroscopic view of different rocks from Teascu deposit: a-amphibole bearing andesite, b-hydrothermal breccia with quartz cement and andesitic fragments, c-phreatomagmatic polymictic breccia, d- brecciated andesite, e-mineralized siltstone, f-conglomerate with andesite, quartzite and ophiolite fragments.

3.2. Mineralization

Teascu is an epithermal gold ore deposit developed mostly as veinlet systems/stockworks in Hondol-Săcărâmb andesite lava flows. The flow of the mineralizing fluid was channeled by NW-SE fractures, by the contact between the sedimentary rocks and andesite lava flows as well as by the high porosity of some sedimentary sequences, *e.g.*, gravels. Quantitative geochemical analysis suggested that only the gold mineralization is economically relevant while other commodities *i.e.* Ag, Cu, Pb, Zn, Mo are not relevant, their grades being close to their abundance in the Earth's crust.

The mineralization is represented by base metal sulfides, with pyrite being the most abundant one, with subordinate marcasite, sphalerite and galena. Native gold was observed in quartz gangue and is presumed to occur as minute grains in pyrite as well. The highest gold grades occur in the samples with well-developed quartz-pyrite veinlets. XRD analyses combined with grade reports on the same samples indicate that the pyrite within high Au grade intervals possess an arsenian character. The native gold-bearing veins are mostly associated with quartz gangue, but in some cases carbonate gangue may also be present.

Based on grade results combined with preliminary microscopic observations and cross-cutting relationships, three hydrothermal pulses have been identified in the analyzed samples, each of these being represented by a specific mineral association:

1) disseminated pyrite and pyrite massive veins with very minor quartz gangue (Fig. 2-c);
2) quartz-pyrite-native gold veinlets (Fig. 2-a,b);
3) marcasite and final pyrite (barren) (Fig. 2-d).

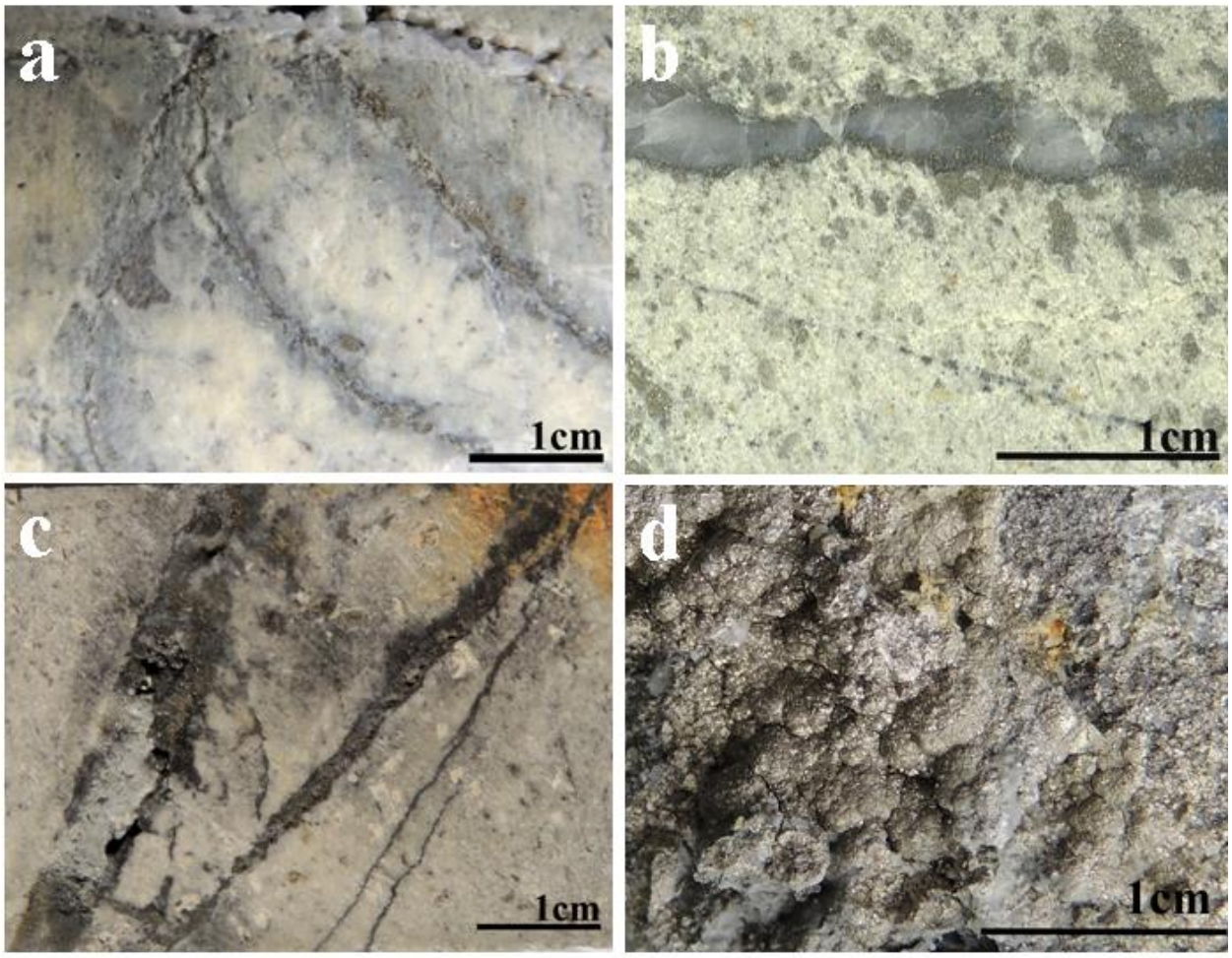

Fig. 2. Macroscopic view of core samples from Teascu deposit with different mineralization types: a-quartz-pyrite veinlets and related perifilonian silicification and phyllic alteration of the andesite host rock; b-quartz-pyrite veinlets and related phyllic alteration of the andesite host rock; c-pyrite veins (barren) and veinlets hosted by altered andesite; d- quartz-pyrite massive vein overprinted by marcasite.

3.3. Hydrothermal alteration types and zonality

The hydrothermal alterations have been studied by transmitted light microscopy and XRD on oriented clay fractions. The nomenclature of the alteration zones is according to Meyer and Hemley (1967). The main alteration zones identified so far in Teascu system are the phyllic, argillic and propylitic ones. Local silicification was also noticed associated with quartz veining. The phyllic alteration is defined by the following minerals: phengite, illite, and interlayered illite-smectite (montmorillonite), chlorite, quartz and pyrite. The argillic mineral assemblage from Teascu is represented by illite, montmorillonite, kaolinite and calcite. The propylitic alteration is characterized mostly by chlorite and calcite.

PIMA portable infrared spectroscopy was used in the field with the purpose of rapid identification of the hydrothermal alterations, the alteration halos and the variations of the temperature within the hydrothermal system. PIMA measurements also allowed pointing out mica crystallinity. The high values of mica crystallinity are correlated with high temperature hydrothermal fluids while low values of mica crystallinity are correlated with low temperature hydrothermal fluids. Based on these correlations it was possible to trace the spatial distribution of the mineralizing fluids' temperatures in one of the studied corridors which is delineated by two surface drillings. The results obtained so far suggest

the rapid cooling of the hydrothermal system outwards from the main channel flow and also on the main flow direction.

4. Conclusions

The present level of knowledge of the mineralization and the alterations from Teascu ore deposit suggests that this deposit is a low to intermediate sulphidation gold deposit. The mineralization is mostly hosted by andesites, hydrothermal, phreatomagmatic and tectonic breccias, but it is also hosted by sedimentary formations such as siltstones and conglomerates. Highest gold grades are found in the quartz-pyrite (arsenian pyrite) veinlets, which are associated with phyllic alteration. PIMA, XRD and grade results obtained so far suggest the possibility to identify an ore shoot at greater depth, correlated with the mineralized zone identified at present.

Acknowledgements

N. Har and T. Tămaş (Babeş-Bolyai University, Cluj-Napoca) are thanked for the help with the XRD analysis. Deva Gold S.A. is thanked for their support during the study: access in the field and to the drill cores, quantitative geochemical analysis.

References

Alderton, D. H. M., Fallick, A. E., 2000. The nature and genesis of gold-silver-tellurium mineralization in the Metaliferi Mountains of western Romania. Econ. Geology, 95, 495-515.

Meyer, C., Hemley, J.J., 1967. Wallrock alteration. In: Barnes, H.L. (ed), Geochemistry of hydrothermal ore deposits. New York, Holt, Rinehart and Wilson, p. 166-235.

Milu, V., Leroy, J. L., Piantone, P., 2003. The Bolcana Cu–Au ore deposit (Metaliferi Mountains, Romania): first data on the alteration and related mineralisation. Comptes Rendus Geoscience, 335(8), 671-680.

Neubauer, F., Lips, A., Kouzmanov, K., Lexa, J., Ivăşcanu, P., 2005. Subduction slab detachment and mineralization: The Neogene in the Apuseni Mountains and Carpathians, Ore Geology Reviews, p. 14.

Pécskay, Z., Lexa, J., Szakacs, A., Seghedi, I., Balogh, K., Konecny, V., Zelenka, T., Kovacs, M., Poka, T., Fulop, A., Marton, E., Panaiotu, C., Cvetkovic, V., 2006. Geochronology of Neogene magmatism in the Carpathian arc and intra-Carpathian area. Geologica Carpathica 57, 6, 511.

Roşu E., Pecskay Z., Ştefan A., Popescu G., Panaiotu C., Panaiotu C. E. (1997) The evolution of the Neogene Volcanism in the Apuseni Mountains (Romania): constraints from new K – Ar data. Geologica Carpatica, 48, 6, 353 – 359, Bratislava.

Rom. J. Mineral Deposits, vol. 87 (2014), No. 1, p. 109-112

PRELIMINARY MINERALOGICAL AND PETROGRAPHICAL INVESTIGATIONS ON MUNCELUL MIC DEPOSIT, POIANA RUSCĂ MOUNTAINS, ROMANIA

Alexandru LĂZĂREAN[1]*, Paul IVĂŞCANU[2], Horia POPESCU[2], Călin TĂMAŞ[1]**

[1]Department of Mineralogy, Babeş-Bolyai University, 1, M. Kogălniceanu Str., Cluj-Napoca, Romania; **alex.lazarean@yahoo.com*
[2]Deva Gold S.A., 89C, Principală Str., Certeju de Sus, Romania; ***paul.ivascanu@eu.eldoradogold.com*

Abstract: As part of the student summer internship program field work has been conducted and the current abstract summarize the initial findings focusing on geological setting of the Muncelul Mic ore deposit, located in north-eastern part of Poiana Ruscă Mountains, Romania. Surface and drill core samples of ore and host rock were collected and investigated in Department of Mineralogy, Babes-Bolyai University, Cluj-Napoca with optical microscopy (transmitted and reflected light) and X-ray diffractometry. The deposit was formed by the discharge of a high temperature seawater-dominated hydrothermal fluid during contemporaneous Devonian volcanism and metamorphosed during Variscan orogeny. The main host for mineralization is represented by meta-volcanic rocks dominated by quartz, feldspar, muscovite, chlorite and opaque minerals and subordinately by graphite schists, chlorite-sericite schists and quartzites. Massive, semi-massive and disseminated ore is dominated by sphalerite. Galena is the second most abundant ore mineral and is accompanied by pyrite, chalcopyrite, malachite and tetrahedrite. Muncelul Mic deposit represented historically an important source of Pb, Zn and, to a lesser extent, Cu, Au, Ag and the current exploration activity may lead to a better understanding of this ore deposit.

Keywords: Poiana Ruscă Massif, Muncelul Mic, sulphide ore, metamorphism, mineralogy

1. Introduction

Two major tectonic units occur in Poiana Ruscă Mountains, namely the meso-metamorphic unit in the south and the epi-metamorphic unit in the north (Kräutner et al., 1969). Muncelul Mic ore deposit (Fig. 1) is located in the north-eastern part of the epimetamorphic unit (Padeş series) and is hosted by meta-volcanic rocks, precisely alkali-feldspar metarhyolites of Lower Carboniferous age (Kräutner 1963 and 1996). The host rocks metamorphic sequences are known as Leşnic formation and represent the upper part of the Padeş series.

The first documents regarding the Muncelul Mic ore deposit belong to Unverricht (1857) concerning mainly the oxidation zones of ore deposit. An exploration program conducted by *Trustul de prospecţiuni, explorări şi deschideri de mine noi* (TPEDMN – Prospecting trust for exploration and new mine opening - Bucharest) started in 1951. The industrial mining activity at Muncelul Mic started in 1962. The resources identified at that time were estimated at 6.500 million tons ore (Gurău, 1974). Mining operations were suspended in 1997 and a new exploration program was recently initiated by Eldorado Gold Corporation.

2. Geological setting

The original magmatic units of Poiana Ruscă Mountains comprise a magmatic activity with two magmatic cycles, an early alkaline and a final silicic one (Kräutner, 1963; 1996). The first magmatic cycle was divided in two phases by the above mentioned author as follows: *i*) extrusive rocks (basic metatuffs) without metallogenetic activity; and *ii*) extrusive ± intrusive rocks (basic meta-tuffs subordinate acid meta-tuffs and lava flow) with related iron ore deposits, *e.g.* (Teliuc, Ghelar, Vadu Dobrii, Ruşchiţa, Valea Negrii). The second magmatic cycle was divided in two phases: *i*) extrusive rocks (acid metatuffs subordinate basic metatuffs); and *ii*) intrusive rocks (metarhyolites dikes) and associated sulfides ore deposits from Muncelul Mic, Veţel and Dobra.

The Muncelul Mic Pb-Zn ore deposit is composed of lenses, stratiform bodies as well as disseminated ores which altogether are partly mobilized along Variscan schistosity which metamorphosed the ore deposit and its host rocks.

Muncelul Mic ore deposit comprises Pb-Zn ore bodies associated with E-W and NW-SE trending metarhyolite dykes and sills. These dykes crosscut a metamorphic sequence composed of metagraywackes, metasandstones, metasiltites and marbles, which form Lower Carboniferous Padeş Group (Kräutner, 1972). The paragenesis of metapelitic and metapsamitic units indicate a temperature of

about 450°C for the metamorphism. The intergrowth of albite and orthoclase, produced by breakdown of high temperature volcanic Na-K feldspars, corresponds to a temperature below 500°C (Kräutner, 1996). These values indicate a moderate to high temperature and low pressure regional metamorphic facies. The most common types of crystalline host rocks are represented by graphite schists, chlorite-sericite schists, quartzite schists, metarhyolites.

3. Materials and methods

The surface exploration allowed the identification of the main rock types outcropping in Muncelul Mic area. Several waste dumps were visited in order to identify other rocks occurring only in the underground works as well as Pb-Zn ore fragments. The most representative samples were later on studied by optical microscopy (transmitted and reflected light) and X-ray diffraction (XRD). The XRD analyses made on whole rock samples were performed with a Bruker D8 Advanced XRD device, with a Co anticathode (λ = 1.79026 Å) running at a voltage of 35 kV, a current intensity of 40 mA and a scanning time of 200 ms.

4. Results

Site visits, field mapping, selective sampling as well as macroscopic observations, optical microscopy and spectral investigations allowed us to further characterize the rocks and ore types from Muncelul Mic. The current work summarizes the initial findings and set the stage for a more in-depth re-evaluation of Muncel genesis and economic potential.

4.1. Rock types

The metarhyolites from Muncelul Mic area are dominated by quartz, feldspars, muscovite, chlorite and opaque minerals (Fig. 1a). XRD analyses indicate that the feldspar is represented by albite, which occurs as white porfiroblasts 5-10 mm across, disposed parallel with the schistosity. Quartzite (Fig. 1b) with some phyllosilicate-rich layers (muscovite and chlorite) hosts minor mineralization as thin layers of sphalerite and galena situated randomly within mica-rich sequences, along quartz-micas layers as well as within quartzite sequences. Graphite schists consist mainly of quartz, graphite and sericite. Within graphite schists, the quartz appears frequently as centimeter scale boudins (Fig. 1c). Chlorite schists occur subordinately in Muncelul Mic area and, beside quartz, chlorite and sericite and, rarely, epidote grains have been observed under microscope.

4.2. Mineralization

According to Gurău (1974), Muncelul Mic ore deposit shows three stages of evolution of the mineralization:

1. Alternative accumulations of terigenous and volcanogenic material. During the post-volcanic evolution, hydrothermal fluids penetrated through the stratification planes and generated hydrothermal mineralization.
2. The mineralization and the host rocks were folded during thrust and fold tectonics that affected the Poiana Ruscă massif post mineralization.
3. Disjunctive deformations are represented by fissure folding and cleveage shearing.

Due to the geologic evolution mentioned above, the mineralization from Muncelul Mic occurs as boudins, centimetric stripes and impregnations. Boudins and stripes alternate with the host rocks and follow the initial stratification of host rock.

The examined samples contain mostly base metal sulfides, *i.e.* sphalerite, galena, pyrite, chalcopyrite and tetrahedrite. The gangue minerals associated with the sulfide-rich layers are represented by quartz, carbonates, chlorite, feldspars, and sericite.

As concerns the ore minerals relationships, the microscope investigation shows that sphalerite is usually associated with galena or with pyrite and represent the most common ore mineral. Galena and pyrite occur in lesser amount as compared with sphalerite, and frequently appear as inclusions in sphalerite. Chalcopyrite has a minor occurrence and, through oxidation, forms malachite. Tetrahedrite was only rarely observed as minute inclusions in sphalerite.

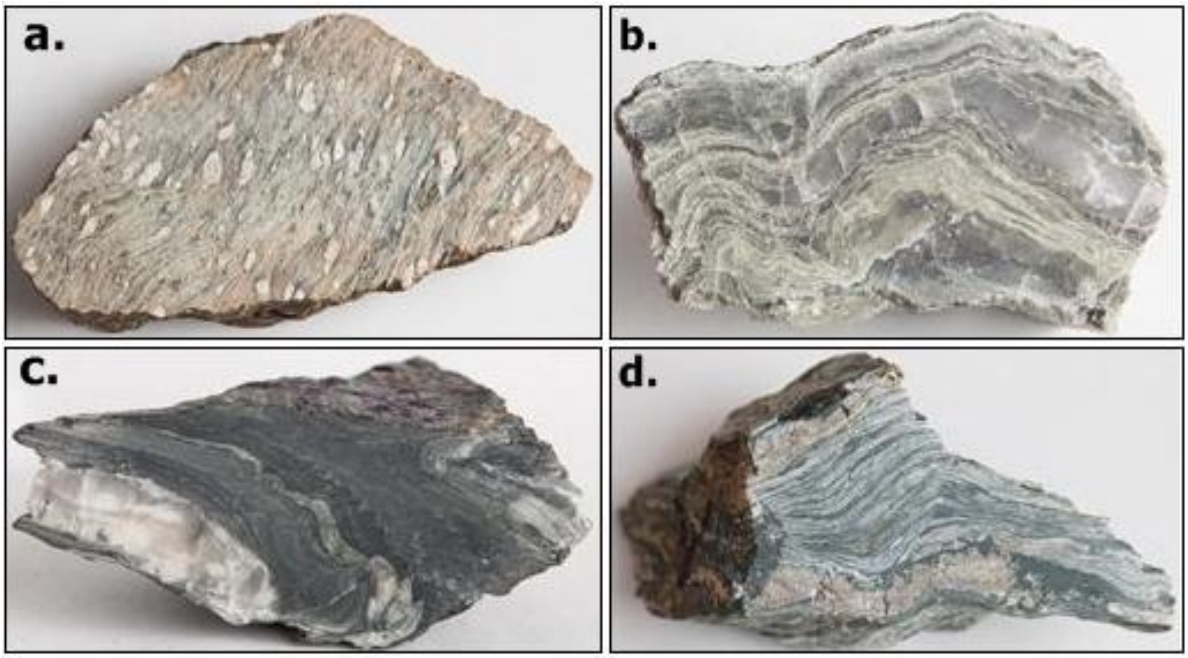

Fig.1. Different rock types occurring in Muncelul Mic area: a) metarhyolite with foliation wrapped around albite porphyroblasts; b) quartzite with thin layers of micas and sulfides; c) graphite schist with quartz boudins; d) chlorite schists with minor mineralization. The width of the images is about 10 cm for each sample (polished slices).

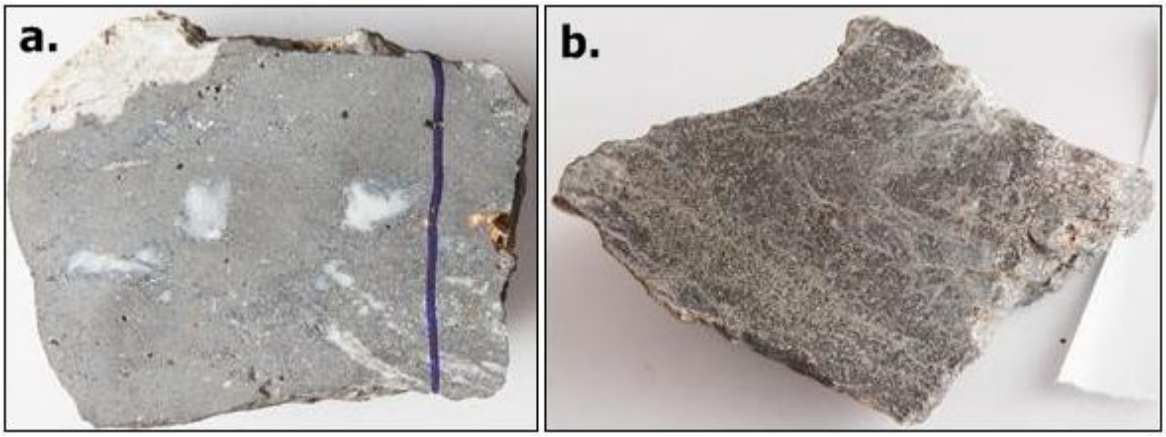

Fig.2. Polished slices of massive ore from Muncelul Mic deposit: a) sphalerite dominated ore with galena and rare pyrite and quartz gangue; b) deformed ore with pyrite and subordinate sphalerite and galena. The width of the images is 15 cm for 2a and 7 cm for 2b.

5. Conclusions and remarks

Muncelul Mic ore deposit is considered the result of a metamorphic remobilization and deformation of an earlier VMS (Volcanogenic Massive Sulfide) deposit. The massive ore is related to metavolcanics rocks, especially metarhyolites, but the ore is also hosted by graphite schists, chlorite-sericite schists and quartzites.

During the metamorphism, the mineralization and the host rock was folded, and, as a result, the mineralization appears as stripes, boudins and impregnations that follow the schistosity. The mineralogical assemblage of the ore consists of sphalerite, galena, pyrite, chalcopyrite, and tetrahedrite. Malachite occurs as secondary mineral.

The integration of these initial findings with observations from the ongoing exploration programs (trace geochemistry, microprobe, structural modeling and mineral zonation) will improve the understanding of Muncelul Mic deposit and potentially support developing a more robust genetic model.

6. Acknowledgements

N. Har (Mineralogy Department, University Babeş-Bolyai, Cluj Napoca) is thanked for the help during the XRD analysis. Deva Gold S.A. / Eldorado Gold Corporation staff is thanked for their support during the study.

References

Gurău, A., 1974. Structural geology and genetic study of polymetallic ore deposit from Muncelul Mic, north-eastern part of Poiana Ruscă crystalline massif. PhD Thesis, UniversityBabeş-Bolyai, Cluj Napoca, pp. 287-302.

Kräutner, H., 1963. Sulphide ore from Muncelul Mic (Poiana Ruscă). Carpatho-Balkan Geological Association, V Congress, Bucharest, Romania, 97-111.

Kräutner, H., 1996. Genetic Models for Variscan ore deposits in the Romanian Carpathians. In P. Grecula (Ed.) - Variscan metallogeny in the alpine orogenic belt. Mineralia Slovaca - Monography, Bratislava, 109-128.

Kräutner, H., Krautner, F., Mureşan, G., Mureşan, M., 1969. Stratigraphy, Evolution of Magmatism, Metamorphism and Tectonics of the Crystalline Formations in the Epimetamorphic Unit of the Poiana Ruscă Massif. Anuarul Comitetului de Stat al Geologiei, 37, 179-233.

Kräutner, H., Mureşan, M., Iliescu, V., Mânzatu, S., Vîjdea, E., Tănăsescu, A., Ioncică, M., Andăr, A., Anastase, Ş., 1972. Epimetamorphic Devonian-Lower Carboniferous from the Poiana Ruscă Mountains. Dări de seamă ale şedinţelor, LIX, 43-44.

- continued from the front cover -

Paulina HÎRTOPANU, Robert J. FAIRHURST
Mineralogy of the Grădiştea de Munte rare element minerals occurrence, Sebeş Mts., South Carpathians, Romania. Part I: oxides and carbonates **53**

Paulina HÎRTOPANU, Robert J. FAIRHURST
Mineralogy of the Grădiştea de Munte rare element minerals occurrence, Sebeş Mts., South Carpathians, Romania. Part II: phosphates and silicates **57**

Ingrid TURISOVÁ, Tomáš ŠTRBA, Peter ANDRÁŠ, Štefan ASCHENBRENNER
Floristic composition on the abandoned copper heaps in Central Slovakia **61**

Giuseppe BUCCHERI, Peter ANDRÁŠ, Maria Luisa ASTOLFI, Silvia CANEPARI, Mara CIUCCI, Alessandra MARINO
Heavy metal contamination in water at Libiola abandoned copper mine, Italy **65**

Paulina HÎRTOPANU, Sorin Silviu UDUBAŞA
Detailed mineralogy of blastfurnace slag samples from Galaţi metalurgical plant, Romania **71**

Teodor VELEA, Andreea MITU, Andreea GRĂDINARU, Georgiana MOISE, Luminiţa MARA, Cornel FRAŢILĂ, Mihai GHIŢĂ, Valentin DRĂGUŢ
Research on methods of treating mine water generated from exploitation of Roşia Poieni, Romania..... **75**

Ioan PINTEA
Magmatic and hydrothermal features of the fluid and melt inclusions from the quartz xenoliths, fragments and phenocrysts from Săpânţa Valley (Igniş Mountains, Romania) **79**

Igor V. CHERNYSHEV, Vladimir A. KOVALENKER, Andrei CHUGAEV, Gheorghe DAMIAN, Floarea DAMIAN, Luisa Elena IATAN, Ioan SEGHEDI
New high-precision lead isotope analyses of galena from Romanian ore districts and a review **83**

Olga Yu. PLOTINSKAYA, Gheorghe DAMIAN, Floarea DAMIAN
Sphalerite assemblages and composition in the Baia Mare region, Eastern Carpathians, Romania (preliminary data) **87**

Ioan SEGHEDI, Zoltan PÉCSKAY, Paraschiva ONESCU
Petrography, geochemistry and geochronology of selected samples from two Banatite intrusions near Gladna Montană, Poiana Ruscă Mountains, Romania **91**

Călin G. TĂMAŞ, Béatrice CAUUET, Jean MILOT
Mineralogy of precious metals ore from Les Fouilloux Gaul mine, Limousin (France) from metals traceability perspective **95**

Réka DÉNES, István MÁRTON, Gabriella B. KISS, Paul IVĂŞCANU, Zsolt VERESS
Additional data regarding the petrography and geochemistry of the magmatic phases and hydrothermal vein types from Bolcana porphyry Cu-Au mineralization (Apuseni Mts., Romania) **99**

Laura TUŞA, Călin G. TĂMAŞ, Paul IVĂŞCANU, Zsolt KULCSAR, Laurenţiu IGNA
The Teascu epithermal gold deposit (Metaliferi Mountains): first data on the alteration and mineralization **105**

Alexandru LĂZĂREAN, Paul IVĂŞCANU, Horia POPESCU, Călin TĂMAŞ
Preliminary mineralogical and petrographical investigations on Muncelul Mic deposit, Poiana Ruscă Mountains, Romania **109**